

# Regulation of the Spindle Checkpoint by Mad2 Binding Proteins

by

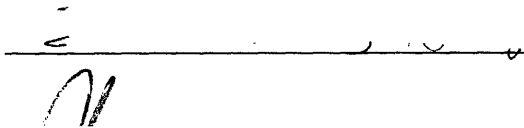
Robert S. Hagan  
A.B. Biochemical Sciences  
Harvard College, 1998


SUBMITTED TO THE DEPARTMENT OF BIOLOGY  
IN PARTIAL FULFILLMENT OF THE REQUIREMENTS FOR THE DEGREE OF

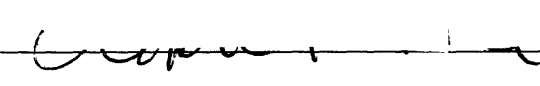
DOCTOR OF PHILOSOPHY IN BIOLOGY  
AT THE  
MASSACHUSETTS INSTITUTE OF TECHNOLOGY

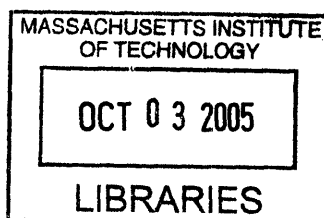
SEPTEMBER 2005

© 2005 Massachusetts Institute of Technology. All rights reserved.

Signature of Author:  \_\_\_\_\_  
Department of Biology  
September 4, 2005

Certified by:  \_\_\_\_\_  
Peter K. Sorger  
Professor of Biology and Biological Engineering  
Thesis Supervisor

Accepted by:  \_\_\_\_\_  
Stephen P. Bell  
Professor of Biology  
Chairman, Committee for Graduate Students



# Regulation of the Spindle Checkpoint by Mad2 Binding Proteins

by

Robert S. Hagan

Submitted to the Department of Biology on September 4, 2005  
in Partial Fulfillment of the Requirements  
for the Degree of Doctor of Philosophy in Biology

## Abstract

The spindle checkpoint ensures the fidelity of chromosome segregation by delaying anaphase until all sister chromatids form proper bipolar attachments to the mitotic spindle. Spindle checkpoint proteins localize to unattached or maloriented kinetochores in mitosis and generate a signal that prevents dissolution of sister chromatid cohesion. Checkpoint signaling requires binding of Mad2 to the checkpoint protein Mad1 and Cdc20, a subunit of the Anaphase Promoting Complex. We have characterized the interactions of human Mad2 with Mad1, Cdc20, and CMT2, a checkpoint inhibitor. Cdc20 and Mad1 form competitive high affinity complexes through contacts in the peptide binding cleft of Mad2, while CMT2 binds noncompetitively to the closed conformation of the Mad2 C-terminus. I propose a model by which conformation-specific binding of CMT2 silences Mad2 signal generation.

The requirement for active checkpoint inhibition in mitosis is not known. We examined the role of CMT2 in mitosis by fixed- and live-cell microscopy. CMT2 localizes to kinetochores in a Mad2-dependent manner and forms ternary complexes with Mad1-Mad2 and Cdc20-Mad2 *in vivo*. Surprisingly, CMT2 is required for completion of mitosis even in the absence of spindle damage. I show that CMT2 opposes Mad2 function at kinetochores and in the cytosol and propose that active silencing of the Mad2-dependent checkpoint is required for completion of mammalian mitosis.

Thesis Supervisor: Peter K. Sorger

Title: Professor of Biology, Professor of Biological Engineering

## ACKNOWLEDGEMENTS

My first thanks are to Peter – he has overseen this work through more twists and turns than either of us could have predicted, and he has remained a sounding board and an inspiration throughout. During my alternating episodes of manic enthusiasm and morose depression, he would always take the opposite tack and point me back in the right direction. He created an environment in which no experiment or approach is impossible or unthinkable, and as I leave the lab I hope that I will take with me a piece of that mindset. I will always be grateful for his advice.

Many thanks to Frank Gertler and Mike Yaffe, who served on my committee from beginning to end, overlooked my occasional disorganization, and provided helpful input and encouragement. Despite their better instincts, they always chose to treat me as a colleague rather than a student, and it is our intense discussions in hallways, at retreats, and over beers that I will remember the most. I must also thank David Housman and Randy King, who graciously agreed to serve on my thesis committee and actually read this work in its entirety. Their input has been invaluable in transforming this into a finished product.

I got hooked on the Sorger lab while working with Max Dobles and Ken Kaplan late at night with Steve Earle cranked all the way up. They taught me what I needed to go forward, and for that I will always owe them. Aurora Burds, Chris Espelin, and Kim Simons are members of the old guard who have been with me to share the laughs and groans. Special thanks go to my classmates and trenchmates, John Albeck and Stephanie Xie – we've been plugging away for a long time and it's beginning to look like we'll make it. I must also thank Emily Gillett and Jess Tytell, both for plugging away with us and for actually reading my thesis – I'll see you guys across the river. Finally, a big thanks to Bree Aldridge and Irina Shapiro for help with math and microscopy and for putting up with my occasional hazing – I swear, it was for your benefit.

I must thank a large number of postdocs who assisted my research and provided an example for my next step in science. Patrick Meraldi helped me get my head on straight and turned me on to cell biology; without him this work would have floundered. Viji Draviam put up with my constant forgetfulness with the microscope, never accepted anything but the best science, and had a smile and laugh at every hour of the day. Suzanne Gaudet deserves extra thanks for her encouragement and commiseration, her truly broad knowledge of science, and her giggling at my jokes. Andrew McAinsh was a constant source of enthusiasm and humor, a sounding board for my ideas, and a damn good bloke. Peter De Wulf was an excellent and intense foxhole companion in our bay for many years and never let me take any of this process too seriously. Finally, I must thank Mike Cardone, Ulrike Nielsen, Heather Hess, and Kate Leitermann for their help along the way.

Many other people at MIT contributed to this work directly or indirectly. Isaac Manke, Andy Elia, and Mustafa Unlu all helped me figure out the protein part of it. Joe Loureiro, Sean Milton, and the Beer Hour crew helped me figure out the non-protein part.

Margaret White came and talked to me every day and I will never forget her friendship and advice.

I am more grateful to my friends than they would ever accept. Doug Rubinson, Rita Khodosh, Sam Ng, Rahul Kohli, Jean-Marc Gauguet – you guys were my anchor, my example, and my buoy. Leah Blasiak saw me through the writing of this thesis; to her, I am grateful for everything. I am thankful to Rob Eikel, John Smith, Bill Evans, and Joe Geraci for their loyal and uncompromising friendship over the years.

Finally, I must thank my family – Mom, Dad, Emily, and Carey. You put me in the position to pursue whatever dream I chose, and without your love and support I would not have been able to finish it. It is my hope that this has made you proud.

## **Table of Contents**

<b>Title Page</b> .....	1
<b>Abstract</b> .....	2
<b>Acknowledgements</b> .....	3
<b>Chapter 1 – The Spindle Checkpoint</b> .....	6
<b>Chapter 2 – Conformation-specific binding of Mad2 by spindle checkpoint proteins Mad1, Cdc20, and CMT2</b> .....	73
<b>Chapter 3 - Negative regulation of the mammalian spindle checkpoint by CMT2 is required for completion of mitosis</b> .....	125
<b>Chapter 4 – Conclusions and Future Directions</b> .....	172
<b>Appendix – Hagan and Sorger, 2005</b> .....	200

## **Chapter 1**

### **The Spindle Checkpoint**

## **1.1 Introduction: Mitosis, Genomic Stability, and the Spindle Checkpoint**

A critical problem for the dividing eukaryotic cell is to ensure that its progeny receive exactly one copy of every chromosome. Chromosome segregation, the process by which a duplicated genome is equally partitioned into daughter cells, requires that sister chromatid pairs form bipolar attachments to opposite ends of the mitotic spindle. Because these attachments form through a stochastic search-and-capture mechanism, the time required for spindle assembly and complete chromosome attachment may vary widely from cell to cell. The spindle checkpoint ensures that the dissolution of sister chromatic cohesion, and hence entry into anaphase and chromosome disjunction, does not occur until the last chromosome pair has become properly attached to the spindle. In this way, the irreversible steps of cell-cycle progression are made dependent on an error-checking mechanism. This chapter examines the mechanistic details of the spindle checkpoint and compares them with other cell cycle checkpoints.

Because mitotic chromosomes can be visualized by light microscopy, their complex movements have been studied by cytologists for over a century. Even before Thomas Hunt Morgan demonstrated that chromosomes were the objects of genetic transmission, their role in the pathobiology of human disease was suspected. Theodor Boveri and Walter Sutton both noted the abnormal chromosome complement of tumor cells compared to normal neighboring cells. In the intervening century, the association of aneuploidy and tumorigenesis has been firmly established. Because genome instability drives tumorigenesis (Hanahan and Weinberg, 2000; Kinzler and Vogelstein, 1996), we must ask whether errors of chromosome segregation contribute to or result from cellular

transformation. However, the contribution of spindle checkpoint failure to human cancer is not yet known, and thus there is an urgent need to understand the mechanistic workings of the checkpoint.

## **1.2 Cell cycle checkpoints**

Cell division requires that several key tasks – genome duplication, chromosome segregation, and cytokinesis – occur with both high fidelity and in the proper order. To ensure that each phase does not begin until the previous step is completed free of errors, and to render movement between phases unidirectional and irreversible, phase-specific cyclins associate with cyclin-dependent kinases (Cdks) to drive progression through the cell cycle (Nigg, 2001). Cyclin binding activates Cdks and in many cases directs their substrate specificity. In metazoans, complexes of Cdk2 with either cyclin E or cyclin A coordinate the G1/S transition and DNA replication (Hinchcliffe et al., 1999; Meraldi et al., 1999). Once this is complete, Cdk1/cyclin B complexes orchestrate mitotic events such as nuclear envelope breakdown (NEB), Golgi fragmentation, centrosome separation, chromosome condensation, and spindle assembly (Murray, 2004). Cdk1/cyclin B also phosphorylates and regulates the anaphase promoting complex, or cyclosome (APC/C). APC/C, a multisubunit ubiquitin ligase, drives the metaphase-anaphase transition by directing the tagging and proteolysis of securin, thus allowing the dissolution of sister chromatid cohesion (Cohen-Fix et al., 1996; Visintin et al., 1997). The events of late mitosis and mitotic exit require the timely and complete inactivation of Cdk1 and destruction of cyclin B, which is itself ubiquitinated by Cdc20-directed APC/C. Proteolytic destruction of specific cyclin pools extinguishes their activity completely and



irreversibly, moving the cell cycle forward in a ratchet-like manner. In this way, while cyclin-dependent kinases and the ubiquitination machinery mutually regulate each other, allowing the coupled, oscillating waves of kinase activity and proteolysis to order the events of mitosis (Peters, 1999).

### **1.2.1 Formal definition of a checkpoint**

While phase-specific cyclin activity and regulated proteolysis confer the order of cell division events, cell cycle checkpoints render the transition between phases sensitive to the completion of key cellular tasks and the presence of errors. The canonical checkpoint was defined by Weinert and Hartwell in a genetic screen for *S. cerevisiae* mutants with an impaired response to DNA damage (Weinert and Hartwell, 1988). After irradiation with X-rays, wildtype yeast cells arrest in G2 and do not enter mitosis until genome damage has been resolved. Mutants in the *RAD9* gene fail to arrest, enter mitosis, and show decreased viability after irradiation. Notably, loss of Rad9p does not alter cell cycle progress or cell viability in the absence of DNA damage, and *rad9* mutants survive irradiation if mitosis is prolonged by treatment with nocodazole, a microtubule depolymerizing agent (Hartwell and Weinert, 1989; Weinert and Hartwell, 1989). These results suggested that the function of Rad9p is not to repair DNA damage but to delay entry into mitosis until after DNA repair has occurred. Thus, early models defined checkpoints as cell cycle subroutines that monitor but do not participate in the underlying cell division process. Formally, a minimal checkpoint is thought to consist of a sensor, which detects underlying errors; a transducer, which relays and perhaps amplifies the sensed signal; and an effector, which halts the cell cycle until damage has

been repaired. In reality, these tasks may rely on shared components, and crosstalk or feedback between them may exist. Additionally, checkpoints may possess a shutoff step to ensure that prolonged cell cycle arrest following repair does not impair the health of a cell.

Since the *RAD* screen, cell cycle checkpoints that monitor multiple DNA structural lesions, replication fork progress, unreplicated DNA, spindle position, and chromosome segregation in mitosis and meiosis have been identified (Bartek et al., 2004; Yang et al., 1997; Zhou and Elledge, 2000). While many elements of cell cycle checkpoints are conserved throughout evolution, further characterization of yeast and metazoan checkpoints has modified the classical model in two broad ways. First, it has become clear that many checkpoints not only alter the cell cycle but also actively regulate the appropriate response, i.e. repair or apoptosis. For example, budding yeast Rad24p participates in both DNA double strand break (DSB) repair and cell cycle arrest (Aylon and Kupiec, 2003). Second, while classical checkpoint genes are nonessential in yeast because they do not contribute to core processes, genetic deletion of homologous genes in higher metazoans has proven lethal (Basu et al., 1999; Brown and Baltimore, 2003; Dobles et al., 2000; Kitagawa and Rose, 1999). At least three non-exclusive models can explain these findings. First, the lesions monitored by such checkpoints occur in nearly every cell cycle in higher organisms and thus checkpoint activity is made necessary by the frequency of its use; unlike with Rad9p, a basal level of activity exists in the absence of an exogenous insult. Second, any given checkpoint is not active in every cell cycle, but the survival of a multicellular organism can be compromised by checkpoint failure in a few cells or at specific stages of development. Third, a checkpoint protein in higher

organisms may participate in the underlying repair process or contribute directly to cell cycle progression. Metazoan checkpoint proteins often have more complex multidomain structures than their yeast homologs and serve to integrate arrest and repair functions.

The requirement for cell cycle checkpoints in the fitness of multicellular organisms is illustrated by their frequent disruption in hereditary and acquired cancers. The study of familial cancer syndromes led to the identification of the Fanconi anemia, BRCA, and NBS families, and inherited mutations in p53 and the Chk kinases have been detected in Li-Fraumeni syndrome (McDonald and El-Deiry, 2001; Zhivotovsky and Kroemer, 2004). Disruption or mutation of these genes leads to the accumulation of genetic lesions and decoupling of the appropriate apoptotic response. The resulting cell can execute the movements of mitosis unaware of or powerless to respond to the genomic damage it is accumulating.

### **1.3 Chromosome segregation, the spindle, and kinetochores**

Eukaryotic cells rely on a self-assembling array of microtubules (MTs) known as the spindle to effect chromosome segregation. Microtubules emanate from microtubule organizing centers (MTOCs) called spindle pole bodies (in yeast) or centrosomes (in metazoans) and form attachments with the cell cortex and with anti-parallel MTs from the opposite pole. In addition, microtubules attach to chromosomes by binding to the kinetochore, a massive multiprotein complex that assembles on centromeric DNA. Correct genome partitioning requires that the kinetochores of a joined pair of sister chromatids form bipolar spindle attachments; that is, the two kinetochores must attach to

MTs radiating from opposite ends of the cell. Microtubules undergo periods of rapid assembly and disassembly that allow them to scan the volume of the cell randomly (Mitchison and Kirschner, 1984; Mitchison and Kirschner, 1985). Kinetochore-MT capture thus happens in a stochastic rather than directed or ordered fashion, allowing errors of both orientation and timing. Before describing the error-sensing mechanism of the spindle checkpoint, I will describe the relevant details of the mitotic spindle and the kinetochore.

### **1.3.1 The Mitotic Spindle**

Microtubule dynamicity directs spindle assembly and contributes to the forces necessary for chromosome segregation. Microtubules are hollow filaments approximately 25nm in diameter (Amos and Klug, 1974). Each tubule forms from the parallel association of 13 linear tubulin protofilaments, which in turn form from the GTP-dependent polymerization of  $\alpha\beta$ -tubulin heterodimers (Weisenberg and Deery, 1976). The asymmetry of the tubulin heterodimer imposes directionality on the microtubule.  $\alpha$ -tubulin subunits are exposed at the more stable minus end of the microtubule and tend to be buried in MTOCs.  $\beta$ -tubulin subunits are exposed at the less stable, dynamically growing plus end of the microtubule.

Microtubule plus ends undergo periods of rapid growth and shrinkage, termed “dynamic instability” (Allen and Borisy, 1974; Mitchison and Kirschner, 1984). While both  $\alpha$ - and  $\beta$ -tubulin bind GTP, only  $\beta$ -tubulin can hydrolyze and exchange GTP and GDP (Desai and Mitchison, 1997; Spiegelman et al., 1977). GTP occupancy controls tubulin polymerization, as only GTP-bound  $\alpha\beta$ -tubulin can be added to the plus end.

Because polymerization drives GTP hydrolysis, the majority of  $\beta$ -tubulin in a protofilament is GDP-bound. Preventing GTP hydrolysis by newly incorporated heterodimers may prevent depolymerization, thereby “capping” or stabilizing a protofilament. In this way, control of GTP hydrolysis by microtubule associated proteins (MAPs) contributes to microtubule dynamics. In addition, microtubules undergo catastrophe (a rapid transition from growth to shrinkage) and rescue (a sudden switch from shrinkage to growth). The interplay between polymerization, rescue, and catastrophe determines the dynamic nature of microtubules and allows them to generate variable force at the plus end (Rieder and Salmon, 1998). Microtubule dynamics increase drastically upon entry into mitosis, with polymerization and catastrophe rates increasing 5- to 10-fold (Belmont et al., 1990; Mitchison, 1986; Schulze and Kirschner, 1986; Verde et al., 1992). This increase in overall MT turnover allows the spindle to probe the cytoplasm for chromosomes more efficiently. In addition, microtubule dynamics provides some of the force required for movement of unattached kinetochores in prophase and prometaphase and for chromosome segregation in anaphase (Dogterom and Yurke, 1997; Inoue and Salmon, 1995; Rieder and Salmon, 1994). Motor proteins and MAPs also contribute to force generation both directly and by crosslinking microtubules and regulating their dynamicity (Hunter and Wordeman, 2000; Rogers et al., 2004; Sharp et al., 2000).

### **1.3.2 The Kinetochores**

Kinetochores are the focal point for the critical processes of the metaphase-anaphase transition: microtubule attachment, spindle checkpoint activation, sister

chromatid separation, and anaphase force generation. First identified cytologically as the primary chromosomal constriction, these complexes assemble on centromeric DNA in S phase (McCarroll and Fangman, 1988). Budding yeast centromeres were identified as genetic loci required for stable chromosome transmission (Clarke and Carbon, 1980; Cottarel et al., 1989), and an extensive body of work has shown that each of the 16 *S. cerevisiae* chromosomes contains a single, well-conserved 125bp sequence that is necessary and sufficient for centromeric function in both mitosis and meiosis (Sullivan et al., 2001). Electron microscopy, genetic screens, and biochemical reconstitution have shown that yeast kinetochores have at least three distinct regions: a DNA-binding layer, a microtubule-binding layer, a linker layer between them. While schematically simple, this single microtubule-DNA linking apparatus requires over 60 known proteins (De Wulf et al., 2003). The DNA-binding components of the yeast kinetochore, including the CBF3 complex, Cbf1p, and the histone variant Cse4p, makes sequence-specific contacts with regions of the point centromeres. The linker layer contains several discrete subcomplexes that are essential for kinetochore function but do not exhibit DNA- or MT-binding activity. The MT-binding layer is known to contain both MAPs and motors of the kinesin-like protein (KLP) family, and these proteins contribute to microtubule capture, tension generation, and poleward movement (Cheeseman et al., 2004). Electron microscopy reveals that budding yeast kinetochores bind and stabilize a single microtubule that is sufficient for segregation (Winey et al., 1995).

The centromeres of metazoans and even *Schizosaccharomyces pombe* are far more complex and are defined not by specific kinetochore-nucleating sequences but by heterochromatin structure. *S. pombe* centromeres span 40-100kbp and are characterized

by a non-conserved core sequence flanked by large inverted repeats, all of which is necessary for centromere function (Cleveland et al., 2003). Human centromeres range from 0.3-5Mbp and contain 1500-30,000 copies of tandemly repeated 171bp  $\alpha$ -satellite sequence (Clarke, 1998) These centromeres are characterized by the deposition of proteins such as CENP-A and CENP-C, homologs of *S. cerevisiae* Cse4p and Mif2, respectively (Meluh et al., 1998), and the resulting heterochromatin may persist and mark the site for the next cell cycle. Ablation or spontaneous deletion of centromeres results in neocentromere formation elsewhere on the same chromosome, and these neocentromeres are competent for chromosome transmission (Amor et al., 2004; Amor and Choo, 2002; Saffery et al., 2000). Interestingly, these  $\alpha$ -satellite arrays contain interspersed regions of CENP-A and histone H3, suggesting that they may consist of modular subunits, each of which attaches to a single microtubule (Vafa and Sullivan, 1997; Zinkowski et al., 1991). An important functional difference between budding yeast and higher eukaryotes is that while *S. cerevisiae* kinetochores attach to a single microtubule (Winey et al., 1995), *S. pombe* and metazoan kinetochores bind 15-30 MTs, suggesting that attachment may result from stages of capture, recruitment, maturation, and force generation (Brinkley and Cartwright, 1971; Rieder, 1982). Despite the added complexity of centromeres and kinetochores in higher eukaryotes relative to *S. cerevisiae*, metazoan kinetochores maintain the basic ultrastructural organization of a linker layer between DNA- and MT-binding layers (Blower et al., 2002).

While the genetic and epigenetic components of centromere formation appear largely conserved in metazoans, centromere location on chromosomes is not. Mouse centromeres are situated in a subtelomeric region of each chromosome and are hence

termed telocentric. *C. elegans* chromosome are holocentric and attach microtubules along the entire length of mitotic chromosomes (Albertson and Thomson, 1982). As a result, comparative genomic analysis has shown that *C. elegans* lacks obvious homologs of many yeast or mammalian kinetochore proteins, and the homologs that can be identified are often strikingly divergent when compared to nearer neighbors such as *Drosophila*. *C.elegans* appears to have evolved novel kinetochore and checkpoint proteins to deal with the unusual structural, geometric, and regulatory consequences of regulating microtubule attachment and centromere cohesion along the length of its chromosomes rather than at a specific region (Dernburg, 2001; Murray and Marks, 2001)

### **1.3.3 Kinetochore-Microtubule interactions**

The early stages of kinetochore-microtubule interaction differ between yeast and higher organisms. Because *S. cerevisiae* undergo a closed mitosis without nuclear envelope breakdown, centromeres remain associated with spindle pole body (SPB) microtubules throughout the cell cycle. Budding yeast centromeres replicate early in S phase (McCarroll and Fangman, 1988), and upon entry into M phase sister chromatid pairs associate with one SPB until bipolar attachment is achieved and the equalized forces cause them to congress (Goshima and Yanagida, 2000). Because the time required for bipolar attachment varies between chromosomes, sister pairs may oscillate dynamically between the poles as incorrect attachments form and are corrected. Upon attachment, centromere pairs come under tension and separate transiently but remain attached until the onset of anaphase (He et al., 2000). Metazoan centromeres replicate late in S phase and cannot form MT attachments until after NBD and spindle assembly in



prometaphase (Cleveland et al., 2003). As in yeast, mature kinetochore-MT attachments result in centromere stretching, equalized interkinetochore forces, and congression to the metaphase plate. Improperly attached or untensed kinetochores localize near the centrosome or “float” away from the spindle axis until capture occurs.

Multiple types of improper kinetochore-microtubule interactions have been observed *in vivo*, among them amphitelic, monotelic, syntelic, and merotelic attachment. Amphitelic chromosome pairs form bipolar attachments in which the two associated kinetochores attach to microtubules from the two opposing centrosomes (Figure 1.1). Because each kinetochore is attached to only one centrosome, and the centrosomes are at opposite ends of the spindle, forces on such a chromatid pair rapidly equalize and the pair congresses to the metaphase plate. These amphitelic attachments do not activate the spindle checkpoint and are permissive for progression into anaphase. Monotelic (or mono-oriented) attachment, which is typical of early prometaphase, occurs when only one of two paired kinetochores is captured by the spindle; this chromosome will experience pulling forces from only one end of the cell and thus will localize to that pole until the other kinetochore undergoes capture by MTs from the opposing pole. Chromosomes can also form syntelic attachments in which both kinetochores in a pair bind to microtubules emanating from the same pole. Under physiological conditions,

Figure 1.1

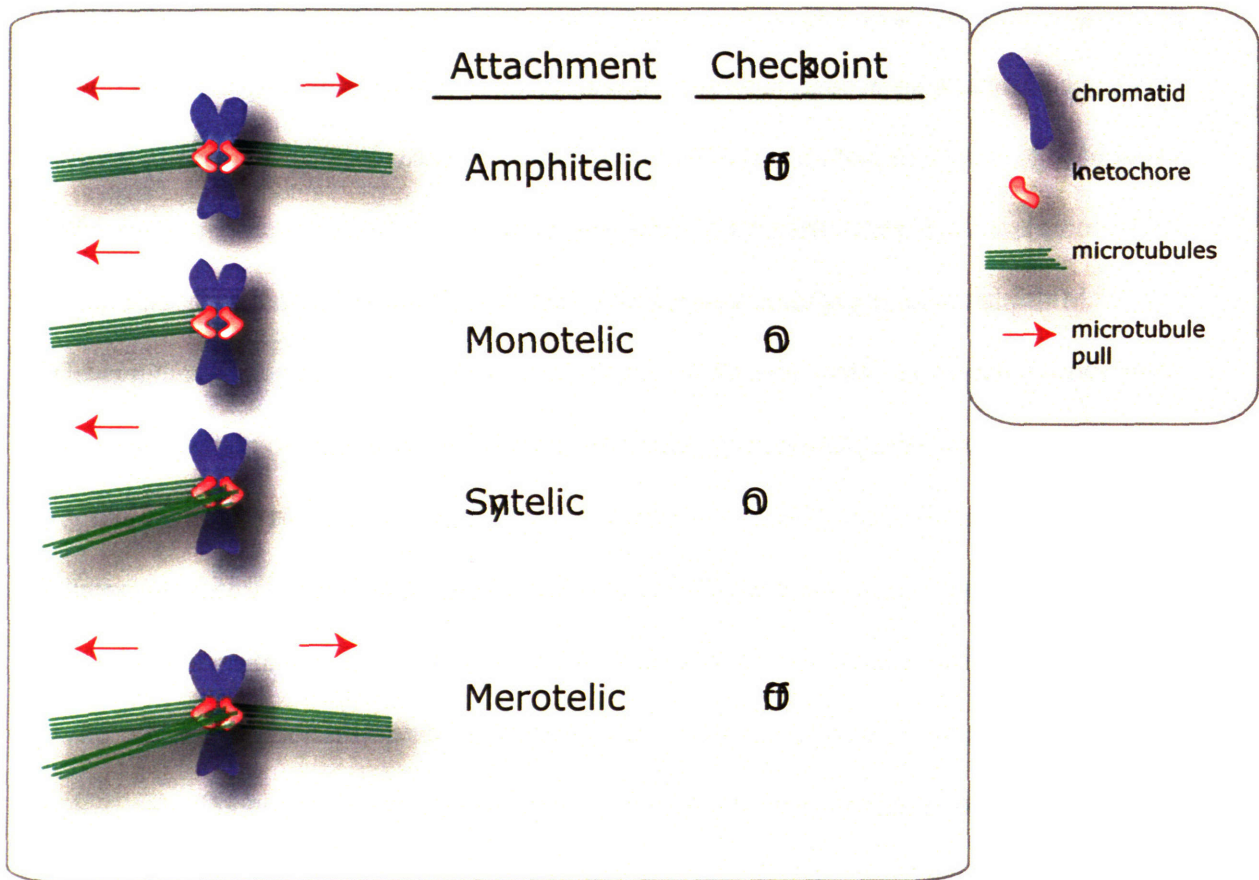


**Figure 1.1: Kinetochore-Microtubule attachments**

Proper bipolar orientation occurs when a sister chromatid pair forms an amphitelic attachment with microtubules from opposite ends of the cell. In monotelic attachment, one kinetochore remains unattached to microtubules. In syntelic attachment, both kinetochores bind microtubules emanating from the same pole and tension is not established. In merotelic attachment, one kinetochore of a pair is stably bound to microtubules from both poles, preventing proper segregation even though the checkpoint is inactivated.

both syntelic and monotelic kinetochores efficiently activate the spindle checkpoint and arrest cell cycle progression (Rieder et al., 1995; Rieder et al., 1994; Sluder et al., 1997).

Merotelic attachment occurs when a single kinetochore within a sister pair becomes attached to both spindle poles (Figure 1.1). Often the sister kinetochore is attached to one pole as well, and such attachments do not activate the spindle checkpoint because both kinetochores are attached and tension is generated. This state occurs commonly when centrosome separation is delayed until after NBD (Cimini et al., 2001; Kapoor et al., 2000). After loss of sister cohesion, a merotelic chromatid may fail to segregate and lag behind at the metaphase plate because it experiences equal pulling forces from both poles. Lagging merotelic chromosomes occur frequently in tissue culture cells (Rieder and Maiato, 2004) and provide an attractive mechanism for chromosome instability because they are not sensed by the canonical spindle checkpoint and the resulting lesion – gain or loss of a single chromosome – is milder than gross aneuploidy or polyploidy and thus is less likely to prove fatal to the daughter cell.

## **1.4 The spindle checkpoint**

### **1.4.1 Discovery of the spindle checkpoint**

Cells cannot enter anaphase until the spindle has been assembled and all chromosome pairs have formed bipolar attachment. Due to the stochastic process of microtubule search-and-capture, however, the time required to attach the last kinetochore pair may vary widely from cell to cell. Even before the formal definition of cell cycle checkpoints, several lines of evidence suggested that anaphase entry might be controlled

by some interaction between chromosomes and the spindle. In the late 1950s, work performed in preying mantid spermatocytes demonstrated that a single unpaired X chromosome led to a permanent meiotic arrest, the first demonstration that chromosomes actively regulate the cell cycle (Callan and Jacobs, 1957). Zirkle observed that focal irradiation of the metaphase spindle dislodged chromosomes from the metaphase plate and delayed anaphase onset drastically (Zirkle, 1970). Finally, the development of anti-microtubule compounds led to the observation that budding yeast cells whose spindles are disrupted by drugs such as nocodazole or benomyl or by temperature-sensitive tubulin mutations undergo cell cycle arrest with large buds and an undivided nucleus (Fuchs and Johnson, 1978; Huffaker et al., 1988; Jacobs et al., 1988). Similar effects were observed in mammalian cells treated with the chemotherapeutic agent taxol (Zieve et al., 1980).

These observations led directly to isolation of the canonical spindle checkpoint genes in two genetic screens for budding yeast mutants whose cell cycle progression is resistant to anti-microtubule drugs. Li and Murray screened for *S. cerevisiae* mutants that did not form colonies after continuous growth on low-dose benomyl plates (Li and Murray, 1991). These mitotic arrest-deficient mutants were named *MAD1*, *MAD2*, and *MAD3*. A second screen for mutants that fail to arrest after only 20 hours of growth on high-dose benomyl yielded the budding uninhibited by benzimidazole mutants, *BUB1*, *BUB2*, and *BUB3* (Hoyt et al., 1991). None of the canonical BUB or MAD genes are essential in budding yeast, though *bub1* $\Delta$  and *bub3* $\Delta$  cells have a slow growth phenotype that eventually may be overcome in culture by compensating mutations (Hoyt et al., 1991; Roberts et al., 1994). In addition, *mad* and *bub* mutants exhibit high rates of spontaneous chromosome loss when grown under normal conditions (Li and Murray,

1991; Warren et al., 2002). Subsequent work has shown that the MAD1-3, BUB1, and BUB3 genes are the canonical members of a checkpoint, commonly called the spindle checkpoint or spindle assembly checkpoint (SAC), that monitors kinetochore-microtubule attachment and the establishment of tension across kinetochore pairs before entry into anaphase. BUB2, in comparison, participates in a checkpoint that links mitotic exit to spindle position (Bardin and Amon, 2001; Bardin et al., 2000; Hu and Elledge, 2002). The sections below discuss in detail the genes and proteins of the spindle checkpoint.

#### **1.4.2 Checkpoint gene families**

Following the initial discovery and cloning of the six MAD and BUB genes, the number of genes found to function in the spindle assembly checkpoint has continued to expand. The majority of these genes exhibit strong conservation from yeast to humans, though certain important features of checkpoint signaling appear restricted to higher eukaryotes. The essential budding yeast kinase MPS1 was shown to be required for both spindle pole body (SPB) duplication and arrest in response to nocodazole (Lauze et al., 1995; Weiss and Winey, 1996). Homologs of Mad1, Mad2, Bub1, Bub3, and Mps1 were subsequently discovered in higher organisms (Musacchio and Hardwick, 2002). No mammalian Mad3 exists, but a protein kinase containing homology to both Mad3p and Bub1p has been identified in metazoans and named Bub-related 1, or BubR1 (Taylor et al., 1998). A regulatory subunit of budding yeast protein phosphatase 2A, Cdc55p, is required for maintenance of checkpoint arrest; *cdc55* mutants cannot prevent inhibitory phosphorylation of the cell cycle regulator Cdc28p and exit mitosis despite spindle

damage (Minshull et al., 1996; Wang and Burke, 1997). Treatment of human cells or *Xenopus laevis* egg extracts with nocodazole activates the MAP kinase p38, and pharmacologic inhibition of p38 or ERK2 impairs nocodazole arrest in *Xenopus* embryos (Minshull et al., 1994; Takenaka et al., 1997; Takenaka et al., 1998). CENPE is a plus end-directed kinesin-like motor that localizes to kinetochores, is required for checkpoint function, and may activate BubR1 kinase activity (Abrieu et al., 2000; Wood et al., 1997; Yen et al., 1991). The budding yeast kinase Ipl1p and its mammalian homolog Aurora B regulate the turnover of incorrect kinetochore-MT attachments and may contribute to the sensing of decreased interkinetochore tension (Biggins and Murray, 2001; Tanaka et al., 2002). A complex of the Rough Deal (ROD) and Zeste-white 10 (ZW10) proteins is required for checkpoint signaling in yeast and mammals and may assist in recruiting dynein and the Mad proteins to kinetochores (Chan et al., 2000; Kops et al., 2005). The relationships of these proteins in the spindle checkpoint is summarized in Figure 1.2 and discussed in more depth below.

A critical common feature of the diverse spindle checkpoint proteins is their localization to kinetochores in mitosis. Mad2 was the first checkpoint protein to be observed at kinetochores (Chen et al., 1996; Li and Benezra, 1996), and similar localization patterns were observed for the other Mad, Bub, and Mps1 proteins (Vigneron et al., 2004). Because budding yeast nuclei and spindles are so small and undergo a closed mitosis, the kinetochore localization of yeast checkpoint proteins was not characterized until the development of more precise microscopic methods (Gillett et al., 2004). Notably, while all known checkpoint proteins transit through kinetochores in mitosis, their localization is

Figure 1.2

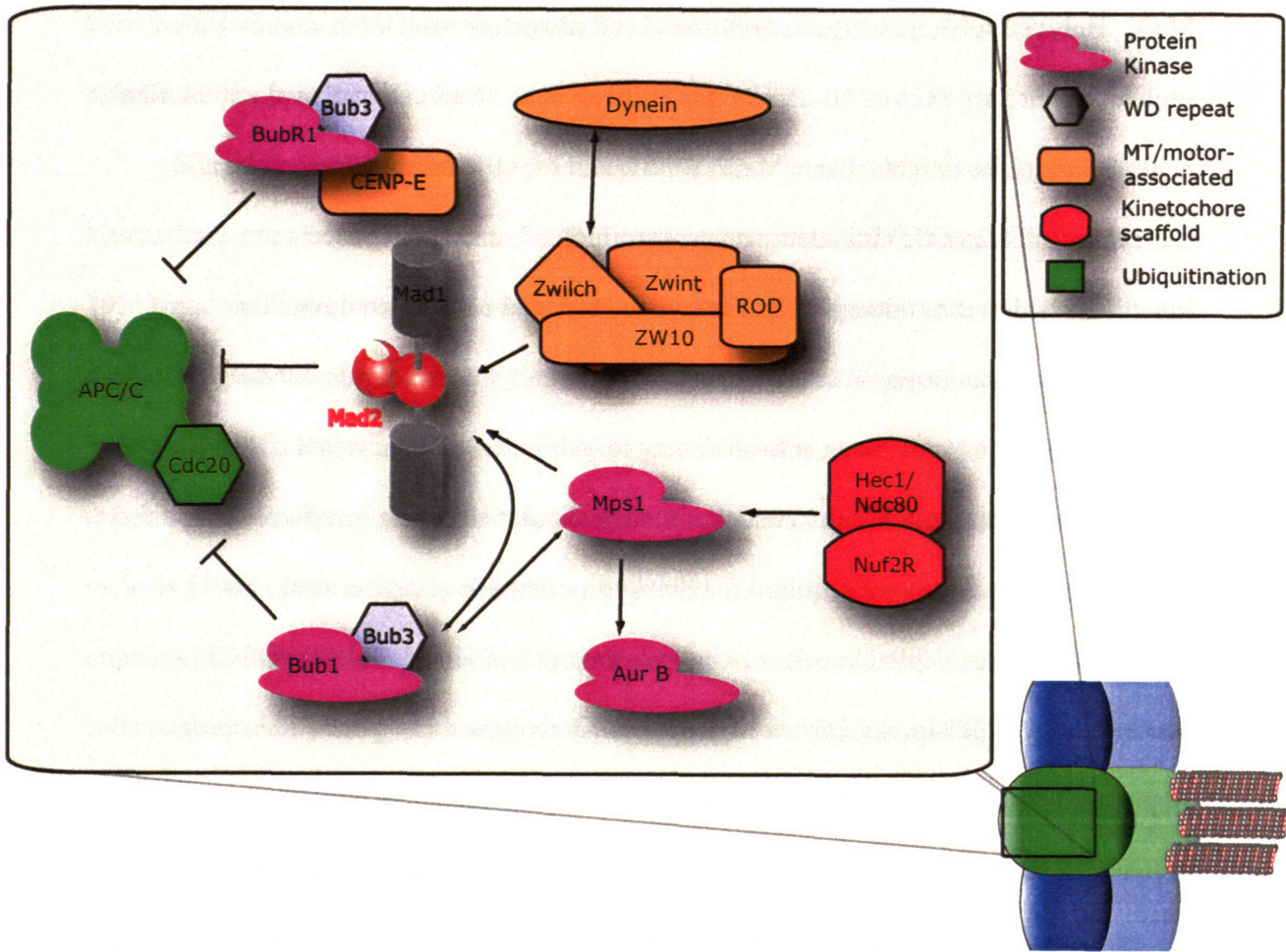


**Figure 1.2: The spindle checkpoint proteins**

Spindle checkpoint proteins bind to unattached kinetochores via the Hec1/Nuf2R complex. Upstream signaling from Mps1, dynein, and the RZZ complexes are required for localization of Mad and Bub complexes. Activated Mad2, BubR1/Bub3, and Bub1 inhibit Cdc20 directly and in combination, thus preventing ubiquitination of securin and anaphase entry.

neither identical nor static. While Mad1 and Bub1 remain stably bound to kinetochores, Mad2, BubR1, Bub3, and Mps1 rapidly bind and dissociate from kinetochores with replenishment half-lives of 10-25 seconds (Howell et al., 2000; Howell et al., 2004; Shah et al., 2004). Late in metaphase, Mad2, Mad1, and Mps1 leave the kinetochore and relocalize to the spindle and centrosomes. Bub1, Bub3, and BubR1 levels on kinetochores decrease noticeably but do not fall below the detection limit. This relocalization is proposed to silence the checkpoint, but it does not rule out the possibility that checkpoint proteins, once activated, may remain active in the cytosol ((Howell et al., 2001). The critical role of the kinetochore in checkpoint signaling is reflected in the fact that intact kinetochores are required for checkpoint function (Gardner et al., 2001). Indeed, deletion or depletion of core kinetochore proteins such as Ndc80p/HEC1, Nuf2p/Nuf2R, Spc24p, Spc25p, or Mis6p/CENP-I abrogates the spindle checkpoint, likely because under such conditions Mad and Bub proteins do not bind kinetochores (Liu et al., 2003; Martin-Lluesma et al., 2002; Meraldi et al., 2004).

### **1.4.3 Checkpoint inputs**

What molecular or ultrastructural lesion does the spindle checkpoint sense to ensure the fidelity of chromosome segregation? While signals could in theory emanate from any part of the mitotic machinery, including the spindle and the centrosomes, cytologic experiments suggest that kinetochores are the focus of both sensing and signal generation. Careful monitoring of PtK1 cells showed that, while the time between nuclear envelope breakdown and anaphase ranged from 23 minutes to many hours, anaphase robustly began  $23 \pm 1$  minute after capture of the last unattached kinetochore



(Rieder et al., 1994). Models of checkpoint activation have thus traditionally focused on two characteristics of kinetochore bipolarity: microtubule occupancy at kinetochores and tension across paired centromeres.

The classical tension model proposed that proper attachment of metaphase kinetochore pairs occurs when they are subject to equal poleward forces (McIntosh, 1991), and untensed or relaxed kinetochore pairs generate a signal that arrests the cell cycle. This model allows for a single relaxed kinetochore pair to signal above the background of many attached pairs. Early evidence for this model came from elegant experiments in preying mantid spermatocytes. These cells arrest for many hours in meiosis I when there is an unpaired X chromosome. Li and Nicklas applied tension to unpaired X chromosomes by pulling on them with a microneedle and observed that such cells initiate anaphase approximately one hour later (Li and Nicklas, 1995). Application of tension also decreased kinetochore phosphorylation as measured by staining for the multi-protein 3F3/2 phosphoepitope (Cyert et al., 1988; Gorbsky and Ricketts, 1993; Li and Nicklas, 1997). Following on these cytologic studies, Stern and Murray exploited budding yeast *cdc6* mutants to study cells in which kinetochores can attach to microtubules without exerting tension. Cdc6p is an initiator of DNA replication, and *cdc6* mutants enter mitosis with unreplicated chromosomes (Piatti et al., 1995). Without sister chromatids, kinetochores become attached and mono-oriented in mitosis and cause a spindle checkpoint-dependent delay before entering anaphase, suggesting that the checkpoint is sensing lack of tension rather than microtubule binding (Stern and Murray, 2001). Important caveats exist for the experiments on which the tension model is based, blurring the distinction between tension and attachment. Most critically, tension is

known to stabilize microtubule binding, so it is difficult to distinguish between the mechanical aspect of tension and its role in promoting cooperative binding of microtubules to kinetochores (King and Nicklas, 2000; Nicklas and Koch, 1969; Nicklas and Ward, 1994; Rieder and Alexander, 1990). The classic “glass needle experiment” was performed in invertebrate meiosis and may reflect different sensing functions between meiosis and mitosis. Concurrently, the time scale of mitotic exit in that experiment is consistent with the possibility that the exogenously tensed chromosome recruited MTs before anaphase ensued. The suggestion that the 3F3/2 phosphoepitope is an indicator of attachment, tension, or checkpoint arrest has been hampered by the discovery that in some species it stains kinetochores regardless of attachment status even into anaphase (Waters et al., 1996). It is not clear that the kinetochores of unreplicated chromosomes, such as those in *cdc6* cells, are functionally equivalent to replicated kinetochores. Finally, recent experiments with engineered dicentric minichromosomes in budding yeast suggest that tension inherently implies attachment (Dewar et al., 2004).

Does the spindle assembly checkpoint sense kinetochore-microtubule attachment rather than tension across kinetochore pairs? Cytologic studies in PtK1 cells demonstrated that a single unattached kinetochore is sufficient to engage the checkpoint (Ault et al., 1991; Ault and Rieder, 1992), and subsequent ablation of the unattached kinetochore by laser irradiation leads to anaphase onset (Rieder et al., 1995). In fact, spermatocytes in which all chromosomes have been removed execute anaphase and cytokinesis (Zhang and Nicklas, 1996). A powerful argument for the monitoring of attachment comes from checkpoint protein localization studies. In higher eukaryotes, Mad, Bub, and other checkpoint proteins localize to kinetochores in late prophase and

prometaphase, before microtubule attachment occurs, and this localization is enhanced by treatment with high doses of spindle poisons that prevent tubulin polymerization (Chen et al., 1996; Jablonski et al., 1998; Taylor and McKeon, 1997; Vigneron et al., 2004). In mono-attached pairs, Bub1, Bub3, and Mad2 become asymmetrically enriched on the unattached or more weakly attached kinetochore (Chen et al., 1996; Martinez-Exposito et al., 1999; Taylor et al., 2001; Waters et al., 1998). Equally instructive have been experiments in which PtK1 or HeLa cells are treated with sufficiently low doses of taxol or vinblastine to inhibit microtubule dynamics (and thus tension) but not destroy microtubule attachment. Under these conditions, Mad2 and Bub3 do not relocalize to kinetochores, suggesting that they are not responsive to tension sensing when kinetochores are microtubule-bound (Waters et al., 1998).

The subtle differences in Mad and Bub protein localization during metaphase or after exposure to certain spindle poisons has led to the proposal that the spindle checkpoint consists of two parallel pathways: sensing of microtubule occupancy at kinetochores by Mad2 and sensing of tension on kinetochores by BubR1 (Skoufias et al., 2001). However, this separation of attachment and tension is based on experiments from a wide range of organisms, often combining details from meiosis and mitosis, and with critical assumptions about the uniformity of response to drug application (Rieder and Maiato, 2004). Given the difficulty in disentangling tension and attachment experimentally, it remains possible that they are in fact two manifestations of the same phenomenon. In maize, Mad2 appears to sense tension in meiosis I and occupancy in mitosis (Yu et al., 1999). This may reflect geometric differences in the orientation of meiotic and mitotic kinetochores. Mitotic kinetochore pairs are held in close apposition

in prometaphase, and attachment of one kinetochore to a pole may orient its partner to face the other pole, thus drastically reducing the likelihood of syntelic attachment. In mitosis, therefore, attachment of both members of a pair may be sufficient to ensure tension. Homologous chromosomes in meiosis I are held together by chiasmata and the four kinetochores in a homologous pair may orient with a greater degree of freedom than a mitotic pair (Lew and Burke, 2003). In this case, homologous pairs are more likely to form syntelic or other incorrect attachments, and sensing of tension may confer a higher degree of accuracy. Thus, many of the differences that are attributed to attachment and tension may in fact reflect different requirements for proper kinetochore-microtubule interactions in different cells, species, or developmental stages.

#### **1.4.4 Outputs of the spindle assembly checkpoint**

Spindle checkpoint activation arrests the cell cycle by inhibiting the multisubunit ubiquitin ligase known as the Anaphase Promoting Complex, or cyclosome (APC/C). APC/C directs the metaphase-anaphase transition and mitotic exit by tagging substrates with polyubiquitin chains, thus targeting them for proteolysis by the 26S proteasome (Glotzer et al., 1991; Hershko et al., 1991). Orderly cell cycle progression requires that pools of critical substrates are tagged for proteolysis and rapidly destroyed in coordinated waves rather than in a continuous stream. As a result, APC/C activation occurs through regulated association with specificity factors that link the ligase and substrate rather than by direct association with substrates as they become available, as is the case for other ubiquitin ligases such as the SCF complex. Two WD proteins direct APC/C activity in budding yeast: Cdc20p directs entry into anaphase and Cdh1p controls mitotic exit

(Schwab et al., 1997; Visintin et al., 1997). APC/C<sup>Cdc20</sup> ubiquitinates cyclin A and B, but non-degradable cyclin mutants arrest yeast cells in telophase, after the arrest observed in *cdc20* mutants, suggesting that they are not the critical substrates for anaphase entry (Holloway et al., 1993; Surana et al., 1993). The critical substrate was found to be Pds1p/securin, a protein that prevents the activation of the protease Esp1p/separase (Yamamoto et al., 1996a; Yamamoto et al., 1996b). Because separase degrades members of the cohesin complex and leads to separation of sister chromatids, the destruction of securin and ensuing activation of separase are the final triggering events of anaphase.

Spindle checkpoint activation leads to the inhibition of Cdc20 and its homologs by several different mechanisms. A major landmark in checkpoint biology was the discovery that Mad2 binds Cdc20 *in vivo* and inhibits APC/C<sup>Cdc20</sup> *in vitro* (Fang et al., 1998; Hwang et al., 1998; Kim et al., 1998). Budding yeast *cdc20* mutants that cannot interact with Mad2p cannot arrest in the presence of spindle poisons, suggesting that this interaction is critical for checkpoint activation (Schott and Hoyt, 1998). These findings were followed by the discovery that Mad3p co-immunoprecipitates with Cdc20, and BubR1 can directly bind and inhibit APC/C<sup>Cdc20</sup> independent of Mad2 (Hardwick et al., 2000; Tang et al., 2001; Wu et al., 2000). While Mad3/BubR1 and Mad2 each inhibit Cdc20, several lines of evidence suggest that they may work together. In both budding yeast and mammalian cells, Mad2 and Mad3/BubR1 copurify with Bub3 and Cdc20 in a large mitotic checkpoint complex, or MCC (Fraschini et al., 2001a; Sudakin et al., 2001). BubR1 and Mad2 inhibit APC/C<sup>Cdc20</sup> synergistically *in vitro* (Fang, 2002), and in fission yeast Mad3p is required for the arrest caused by overexpression of Mad2p (Millband and Hardwick, 2002). While Bub1 does not participate in the larger checkpoint complexes,

human Bub1 phosphorylates Cdc20 *in vitro* (Tang et al., 2004a). Phosphorylated Cdc20 does not efficiently activate APC/C *in vitro*, and mutation of all Cdc20 phosphoacceptor sites to alanine renders it dominant negative to checkpoint function in HeLa cells. These results implicate Bub1 as a direct catalytic inhibitor of APC/C. Thus, at least four possible Cdc20 inhibitors can be found among the canonical spindle checkpoint genes: Bub1, Bubr1/Mad3p, Mad2, and the MCC complex. Because these checkpoint proteins exist in multiprotein complexes with mutual interdependencies for function and localization, it is difficult to order them in a linear or epistatic pathway. The following sections discuss in more detail the components of the spindle checkpoint.

#### **1.4.5 Mad1, Mad2, and Cdc20**

Mad1 and Mad2 form the nucleus of a dynamic stoichiometric inhibitor of Cdc20. Mad1 and Mad2 form a stable complex throughout the cell cycle in yeast and metazoans, and this complex is required for checkpoint activity (Chen et al., 1999; Jin et al., 1998). Upon checkpoint activation, Mad2 also binds to and inhibits Cdc20. Crystallographic analysis has revealed that Mad1 is a homodimeric coiled-coil protein, while Mad2 is a small  $\alpha\beta$ -sandwich (Sironi et al., 2002). Mad2 and Mad1 form a 2:2 tetramer in which the C-terminal tail of Mad2 wraps around an exposed intercoil region of Mad1 and refolds into the main  $\beta$ -sheet of Mad2, thus encircling Mad1 like a safety belt (Figure 1.3).

Figure 1.3

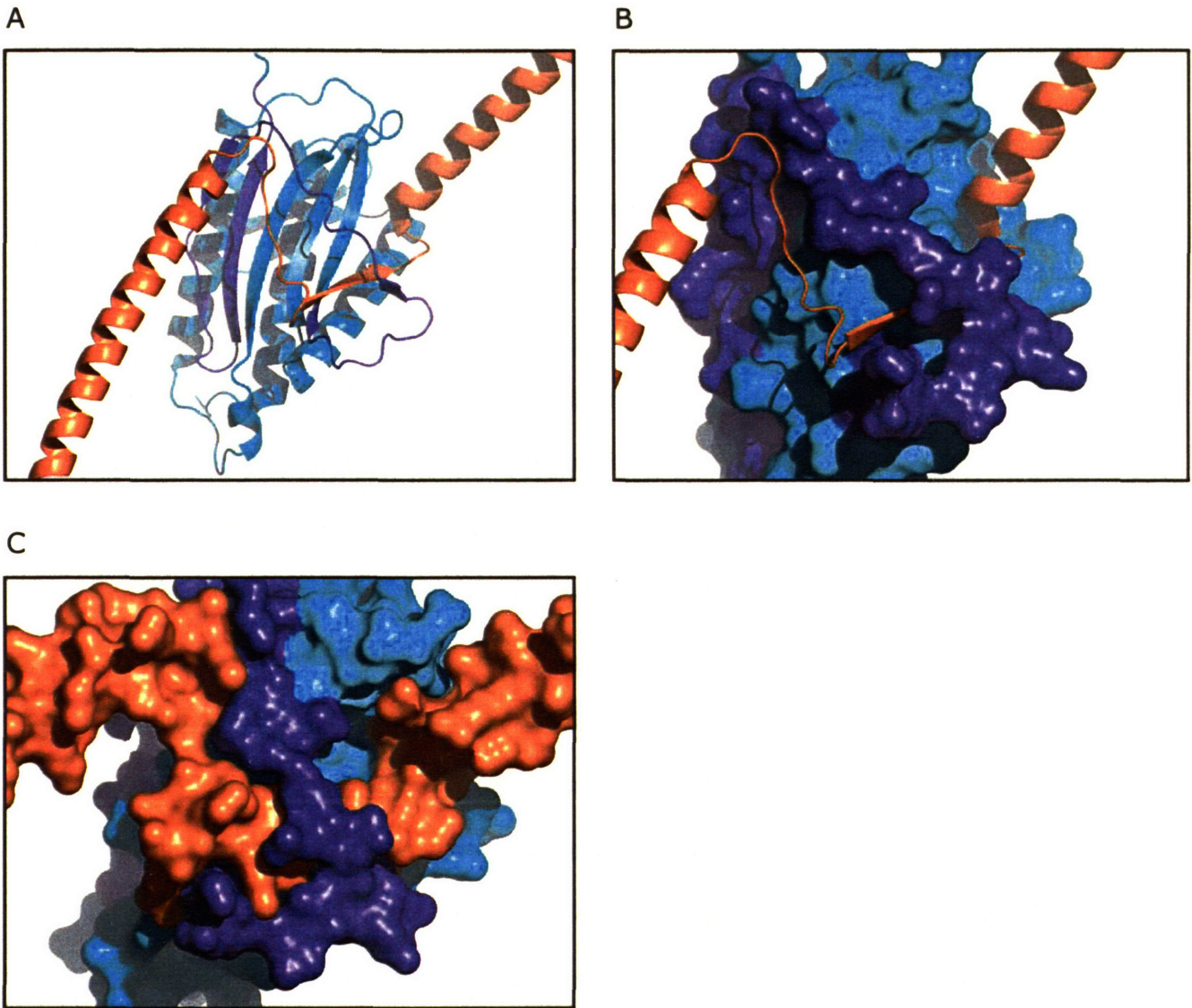


**Figure 1.3: Mad1-Mad2 structure**

Mad2 binds and encloses Mad1 with a safety belt mechanism. Ribbon (A) and surface (B, C) diagrams of the Mad1-Mad2 crystal structure of Sironi et al (Sironi et al., 2002) were generated in PyMOL. The C-terminal tail of Mad2 (dark blue) encloses an inter-coil section of Mad1 (orange) and inserts into the body of Mad2 (cyan).

In solution, Mad2 adopts at least two distinct folds that represent the open and closed tail conformations, referred to as O-Mad2 and C-Mad2 (Luo et al., 2004). The open and closed conformers are stable and interconvert spontaneously with extremely slow kinetics. However, while bacterially expressed Mad2 can be separated chromatographically into O- and C-Mad2, only O-Mad2 is detected upon purification from nocodazole-arrested HeLa cells. This is surprising given that NMR analysis suggests that Mad2 also adopts the closed conformation upon binding to Cdc20, and this complex is known to exist in HeLa cells. However, because of the difficulty of expressing and purifying Cdc20, structural analysis has been confined to complexes of Mad2 with short Cdc20 fragments that lack the large C terminal WD domain. Binding of full length Cdc20 may induce structural rearrangements in Mad2 that are not yet known. The likelihood that Mad1 and Cdc20 compete for Mad2 binding is seemingly at odds with the observation in budding yeast that Mad1 is required genetically for binding of Mad2 to Cdc20. However, this requirement has not been documented in higher eukaryotes and may result from different levels of basal checkpoint signaling in yeast versus metazoans.

Interphase Mad1 is saturated with Mad2, and these complexes localize to nuclear pore complexes in budding yeast and the nuclear periphery in metazoans (Campbell et al., 2001; Iouk et al., 2002). Upon entry into M phase, Mad1/Mad2 localizes to kinetochores, though the bulk of Mad1-free Mad2 remains cytosolic. FRAP experiments reveal that the Mad1-bound pool of Mad2 remains stably bound to Mad1, while the cytosolic pool undergoes rapid cycles of kinetochore binding and dissociation (Howell et al., 2000; Howell et al., 2004; Shah et al., 2004). This cycling or “kinetochore flux” of



Mad2 is believed to occur through an unusual heterotypic homodimerization in which O-Mad2 from the cytosolic pool binds C-Mad2 bound to Mad1 at kinetochores. Mad2 mutants lacking 10 residues from the extreme C terminus (Mad2 $\Delta$ C) cannot complete tail closure and thus remain locked in the open state, while full length Mad2 bound to fragments of Mad1 or Cdc20 remain in the closed state. Using these approximations of the open and closed state, it has been shown *in vitro* that O-Mad2 can bind to C-Mad2-Mad1 and C-Mad2-Cdc20, but neither O-Mad2 nor C-Mad2 can self-associate. Mad2 mutants that cannot dimerize do not localize to kinetochores when transiently expressed in HeLa cells and act as dominant negative inhibitors of the checkpoint. The Mad2-Mad2-Mad1 structure is not known and is the focus of intense investigation.

Mad1p is a phosphoprotein in budding yeast, and checkpoint activation results in hyperphosphorylation that requires the kinase Mps1p. While Mps1p is presumed to phosphorylate Mad1p, this activity has not been reconstituted *in vitro*, and hyperphosphorylated Mad1 has not been observed in higher eukaryotes. The phosphorylation status of Mad2 is equally uncertain. Phosphorylation of four serines in the Mad2 tail upon nocodazole arrest has been reported, and mutation of these residues to mimic phosphorylation abrogated the *in vivo* binding of Mad2 to Mad1, Cdc20, and the APC/C subunits Cdc16 and Cdc27 (Wassmann et al., 2003). However, this modification of Mad2 has not been reported elsewhere.

While most features of Mad2-Mad1 signaling are conserved from yeast to mammals, higher eukaryotes appear to have adapted Mad2 to other purposes. A Mad2-like protein known as Mad2B or Mad2L2 exists in frogs and mammals and functions to inhibit Cdh1 late in mitosis (Cahill et al., 1999; Chen and Fang, 2001; Pflieger et al.,

2001). Human Mad2B is 48% similar and 26% identical to human Mad2 in the conserved regions. Two notable areas of divergence are at positions 133-134 of Mad2, which mediate Mad2 dimerization, and the C terminal 35 residues of Mad2, which perform tail closure and thus control binding to Mad1 and Cdc20. These differences suggest that Mad2B may be unable to dimerize or bind Mad1 or Cdc20. Human Mad2B binds and inhibits Cdh1 but not Cdc20, while *Xenopus* Mad2B inhibits both Cdc20 and Cdh1 *in vitro* (Chen and Fang, 2001; Pflieger et al., 2001). One speculative explanation for this divergence is that Mad2B arose as a result of duplication of the Mad2 locus and has become progressively more specific for Cdh1 inhibition throughout evolution. Far from being a mere oddity, the existence of Mad2B points to the notion that the yeast and mammalian spindle checkpoints share most of their components but connect them differently.

While Mad1 and Mad2 are nonessential in yeast, Mad2 is essential in higher eukaryotes. Deletion of Mad2 in mice results in embryonic lethality, while loss of function mutants of either Mad1/*mdf-1* or Mad2/*mdf-2* are embryonic lethal in *C. elegans* (Dobles et al., 2000; Kitagawa and Rose, 1999). However, it is notable that both mouse and worm embryos execute numerous rounds of cell division before succumbing to high levels of apoptosis. Mice that are heterozygous for Mad2 develop lung papillary adenocarcinoma very late in life, suggesting that Mad2 is a haploinsufficient tumor suppressor (Michel et al., 2001). Complete RNAi knockdown of Mad2 abrogates checkpoint response to nocodazole and causes HeLa cells to degrade cyclin B and securin soon after nuclear envelope breakdown (Meraldi et al., 2004; Michel et al., 2004). These cells enter anaphase before chromosomes fully condense and align, resulting in a

catastrophic mitosis, multinucleation, and cell death. Strikingly, Mad1 knockdown prevents checkpoint arrest in nocodazole but does not lead to premature anaphase in unperturbed cells, pointing to a role for Mad2 in constraining Cdc20 activity early in mitosis, thus setting a default delay in mitotic timing apart from checkpoint function (Martin-Lluesma et al., 2002).

What is required for Mad2 and Mad1 to localize to kinetochores? An extensive set of experiments has examined checkpoint protein localization in the context of RNAi of a variety of both checkpoint and kinetochore proteins (Rieder and Maiato, 2004; Vigneron et al., 2004). Because checkpoint proteins exist in several overlapping complexes with mutual interdependencies, it is difficult to order their functions in a linear or epistatic pathway. While results differ slightly between systems, it seems clear that Mad2 localization is a final effector step in the pathway, requiring Mad1, Bub1, BubR1, Mps1, Bub3, Aurora B, CENP-E, and the kinetochore Hec1/Nuf2r. Mad1 localization requires the Hec1/Nuf2r complex as well as Bub1. In addition, Mad1 interacts directly or indirectly with Bub1, BubR1, and another mitotic kinase Nek2A, and phosphorylation of BubR1 in mitosis requires Mad1 (Brady and Hardwick, 2000; Chen, 2002; Lou et al., 2004). While the details of all these interactions remain to be clarified, Mad1 may be considered to function as a kinetochore scaffold for recruiting and activating several components of the checkpoint, most notably Mad2.

#### **1.4.6 Mad3/BubR1 and MCC**

The mammalian serine-threonine kinase BubR1 and its yeast homolog Mad3p, which lacks the kinase domain, are checkpoint effectors that inhibit Cdc20 alongside

Mad2, but the details of Mad3/BubR1 function and biochemistry are not as well understood. Several important parallels exist between Mad2 and Mad3/BubR1. Mad3/BubR1 exists in a stable, stoichiometric complex throughout the cell cycle with Bub3 (Taylor et al., 1998). BubR1/Mad3 mutants whose Bub3-binding region is deleted do not localize to prometaphase kinetochores. BubR1 and Bub3 cycle through kinetochores with rapid kinetics like Mad2 (Howell et al., 2004). Deletion of BubR1 in flies and mice is embryonic lethal, and BubR1 depletion leads to early anaphase entry, loss of nocodazole arrest, and catastrophic mitosis similar to Mad2 RNAi (Basu et al., 1999; Meraldi et al., 2004; Wang et al., 2004a). Mad3p, BubR1, and kinase-deficient BubR1 all bind Cdc20 independent of Mad2 and inhibit APC/C *in vitro*. Finally, Mad3p/BubR1 participates with Mad2 and Bub3 in the larger MCC complex throughout the cell cycle (Fraschini et al., 2001b; Sudakin et al., 2001). The function and regulation of MCC as a whole is not known. MCC purified from interphase, mitotic, and checkpoint-active cells is equally potent at inhibiting APC/C *in vitro*, suggesting that APC/C sensitivity to regulation by the checkpoint varies over the cell cycle.

Is BubR1/Mad3 simply another Cdc20 inhibitor that acts parallel to Mad2?

Several clues suggest that BubR1 plays a subtly different role in sensing kinetochore status and effecting checkpoint arrest. In addition to Bub3, BubR1 also forms a stoichiometric complex with CENP-E, a kinesin-like motor that is not found in MCC (Abrieu et al., 2000; Yao et al., 2000). Because CENP-E is a motor protein that localizes to kinetochores and can bind microtubules, it is an attractive candidate for sensing the state of tension between kinetochores and the spindle. CENP-E binding stimulates BubR1 activity, which is in turn required for Mad2 to localize to kinetochores (Mao et

al., 2003). Surprisingly, CENP-E kinetochore localization in *Xenopus* extracts requires the BubR1 kinase domain but not kinase activity, suggesting that CENP-E may directly bind and stimulate the BubR1 kinase analogous to cyclin-Cdk activation (Weaver et al., 2003). This suggests a model in which localization of BubR1 to kinetochores recruits CENP-E independent of phosphorylation. Upon binding, CENP-E activates BubR1 kinase activity, leading to phosphorylation of unknown substrates that promote Mad2 localization and checkpoint activation. BubR1 kinase activity is then silenced either by MT attachment or the establishment of tension, perhaps via a tension-dependent conformational change in CENP-E. The idea that BubR1 responds to tension rather than attachment is discussed in section 1.4.3 and rests largely on the finding that BubR1 persists, albeit in lower amounts, on attached kinetochores in late prometaphase and metaphase, while Mad2 and Mad1 do not. In mono-attached kinetochore pairs, Bub1 and Mad2 become enriched at the unattached kinetochore while BubR1 is present equally on both.

Unlike Mad2, BubR1 is proposed to have both catalytic checkpoint activating and non-catalytic APC/C inhibitory activities. The addition of a Bub1-like kinase domain to Mad3 during evolution suggests that BubR1 may have acquired functions in addition to Mad3-like checkpoint signaling, and these functions may have evolved as both kinetochores and kinetochore-microtubule attachment became more complex. Because both the structural mode of APC/C<sup>Cdc20</sup> inhibition by BubR1/Mad3p and the relevant substrates of BubR1 kinase remain unknown, significant further investigation is required. Additionally, while it is known that BubR1 binds and dissociates from kinetochores with the same kinetics as Mad2, it is not known whether they cycle as monomers, as members

of a complex, or as members of separate complexes. Finally, the difficulty of assaying BubR1 kinase or non-kinase activity has prevented researchers from determining whether active BubR1 exists in the cytosol or is confined to kinetochores.

Does BubR1 possess non-checkpoint functions? Careful analysis of BubR1 RNAi cells suggests that BubR1 may actively regulate kinetochore-microtubule attachment (Lampson and Kapoor, 2005). Mammalian BubR1, along with Bub1, binds to and phosphorylates the tumor suppressor Adenomatous Polyposis Coli (Apc), and mouse embryonic stem cells harboring Apc mutations lose chromosomes at elevated rates (Fodde et al., 2001; Kaplan et al., 2001). Truncated Apc mutants abrogate the nocodazole arrest, and studies in BubR1<sup>+/-</sup> ApcMin<sup>+/-</sup> mice suggest that decreased BubR1 expression exacerbates the tumor phenotype of ApcMin<sup>+/-</sup> mice (Rao et al., 2005; Tighe et al., 2004). Remarkably, mice bearing a BubR1 hypomorph allele that causes progressively decreased expression do not develop tumors but instead exhibit genomic instability and a profound accelerated aging phenotype (Baker et al., 2004). These mice develop infertility, suggesting that the stoichiometric functions of BubR1 are absolutely required for meiosis. The pleiotropic effects of BubR1 mutation are just as profound in the heritable human disorder mosaic variegated aneuploidy, in which recessive BubR1 mutations lead to growth retardation, microcephaly, and childhood cancer (Hanks et al., 2004). Because BubR1/Mad3p is a point of divergence between the checkpoints of yeast and higher organisms, it presents a fascinating opportunity to study how basic cell biology is manifested at the level of tissue and organism.

#### **1.4.7 Bub1: a multifunctional checkpoint kinase**

Like BubR1, Bub1 is a multifunctional serine-threonine kinase that inhibits Cdc20 directly. Bub1 can directly inhibit Cdc20 *in vitro* by phosphorylating several sites in the Cdc20 N-terminus (Tang et al., 2004a). The contribution of Bub1 kinase activity to checkpoint activation remains unclear due to conflicting data. The highly atypical Bub1 kinase domain is strongly conserved from yeast to man but is not required for checkpoint activity in budding yeast and some *Xenopus* egg extract activities (Sharp-Baker and Chen, 2001; Warren et al., 2002). In other *Xenopus* experiments, Bub1 kinase activity enhances the efficiency of checkpoint arrest in response to weaker stimuli such as a single unattached kinetochore, suggesting that it may be required for amplification of checkpoint signal (Chen, 2004).

As with BubR1, Bub3 binds to Bub1 and appears to act as an adaptor protein that localizes Bub1 to kinetochore. In some systems, the Bub1-Bub3 interaction is required for Bub1 kinetochore localization, while in others Bub3 requires Bub1 (Sharp-Baker and Chen, 2001; Taylor et al., 1998). Bub1 localizes to kinetochores in very early prophase, before BubR1 or Mad2. Unlike Mad2 or BubR1, Bub1 binds statically to kinetochores and does not shuttle to the cytoplasm. Because Bub1 resides at kinetochores and is required for the localization of BubR1, CENP-E, CENP-F, Mad1, and Mad2 (Johnson et al., 2004; Sharp-Baker and Chen, 2001), Bub1 appears, like Mad1, to act as a scaffold for activation of other checkpoint effectors. Bub1 may interact with Mad1 in budding yeast (Brady and Hardwick, 2000), but they do not co-fractionate and this interaction has not been detected in other organisms.

Disagreement exists on the effect of Bub1 depletion in human cells. While RNAi of Bub1 RNAi does not lead to premature anaphase like RNAi of BubR1 or Mad2, it has been reported to inactivate the checkpoint (Meraldi and Sorger, 2005; Tang et al., 2004a), activate the checkpoint by causing defects in chromosome attachment (Tang et al., 2004b), and have no effect on checkpoint activation (Johnson et al., 2004). Despite these disagreements, it is clear that mammalian Bub1 is required for proper chromosome congression and attachment in addition to a checkpoint signaling role. Several possible models may explain these findings, including direct interaction with Apc or indirect interaction with CENP-E via BubR1, but strong evidence points to an interaction between Bub1 and the Shugoshin/Sgo1 protein. Shugoshin family members were discovered in flies and yeast for their role in maintaining centromeric cohesion in meiosis by protecting specialized meiosis-specific cohesin complexes from proteolysis by separase (Katis et al., 2004; Kerrebrock et al., 1992; Kitajima et al., 2004; Marston et al., 2004; Rabitsch et al., 2004). In higher eukaryotes and fission yeast, shugoshin also maintains centromeric cohesion in mitosis, and loss of Sgo proteins leads to a loss of tension and mitotic delay or arrest (Marston et al., 2004; Salic et al., 2004). Bub1 is required in fission yeast and mammals for Sgo localization to kinetochores, and cells depleted of either Bub1 or Sgo appear to undergo premature centromere separation (Kitajima et al., 2005; Tang et al., 2004b). The phenotype of Bub1 RNAi in human cells may be explained by partial knockdown effects; strong but incomplete RNAi may deplete Bub1 levels below the threshold required for Sgo1 localization (i.e. by stoichiometric binding to Bub1) but above the threshold required for spindle checkpoint activation (i.e. by catalytic kinase



activity). Presently, no interaction between Bub1 and Sgo has been demonstrated. It remains critical to determine whether Bub1 binds or phosphorylates Sgo.

Bub1 mutations have been found in a subset of colorectal and pancreatic cancers that exhibit chromosome instability and impaired spindle checkpoints (Cahill et al., 1998; Hempen et al., 2003). Like BubR1, Bub1 binds and phosphorylates the tumor suppressor Apc, but the significance of this interaction is not known (Kaplan et al., 2001).

Therefore, a causal link between Bub1 and cancer development remains to be established.

### **Other checkpoint genes: Mps1, Aurora B, and ROD/Zw10/Zwilch**

MPS1 was identified as a checkpoint gene shortly after the classic MAD and BUB screens, but little is known about its function. Mps1 is a serine-threonine kinase like the Bubs and simple overexpression of Mps1p in budding yeast causes a metaphase arrest that requires Mad and Bub proteins but, strangely, not functional kinetochores (Fraschini et al., 2001b; Poddar et al., 2004). Budding yeast MPS1 is also required for spindle pole duplication, but this function is clearly absent in the fission yeast homolog Mph1. RNAi depletion of Mps1 in mammals abrogates the checkpoint as expected, but conflicting reports exist on whether Mps1 overexpression drives centrosome duplication. Mps1 is also required for wound healing in zebrafish and hypoxia response in *Drosophila* embryos (Fischer et al., 2004; Poss et al., 2002). While chemical genetic analysis has begun to dissect the contribution of budding yeast Mps1p to both spindle assembly (Jones et al., 2005) and tension monitoring (Dorer et al., 2005), the checkpoint substrates of Mps1 in both yeast and mammals remain unknown. As mentioned previously, budding yeast MPS1 is required for Mad1p hyperphosphorylation during benomyl arrest, but this

interaction is not known to be direct and has not been observed in other systems. Budding yeast Mps1p does phosphorylate the SPB components Spc110p, Spc42p, and Spc98p (Castillo et al., 2002; Friedman et al., 2001; Pereira et al., 1998), but illumination of Mps1 checkpoint function awaits the identification of relevant checkpoint substrates.

Another serine-threonine kinase, Aurora B, has been implicated in assisting spindle checkpoint response to loss of tension at kinetochores. Aurora B and its yeast homolog Ipl1p exist in a tight complex with the chromosomal passenger protein survivin/Bir1p and the inner centromere protein INCENP/Sli15p. Aurora B/Ipl1p is not required for metaphase arrest following kinetochore-microtubule detachment, but it is required for arrest when attached kinetochores are not under tension, such as taxol treatment in mammalian cells or cohesion or replication mutants in yeast (Biggins and Murray, 2001; Ditchfield et al., 2003; Tanaka et al., 2002). Ipl1p destabilizes kinetochore-microtubule attachments that do not result in tension generation, and inhibition of Aurora kinase activity with a small molecule shows that the Aurora kinases (which include Aurora A and C) are required for correction of attachment that is not bipolar (Hauf et al., 2003). Thus, the function of Aurora B/Ipl1p in sensing tension is not clear: checkpoint deficiency in Aurora/Ipl1 impaired cells might result from an inability to *create* detachment by clearing microtubules from kinetochores that are not under tension. The Aurora kinases are the subject of intense scrutiny because of their frequent amplification and overexpression in a variety of human cancers (Bischoff et al., 1998; Taylor et al., 2004).

While Mps1 and the Aurora/Ipl1 complexes are conserved between yeast and mammals, at least one complex required for checkpoint function appears limited to

higher eukaryotes. Each member of the Rough Deal (ROD)/Zeste-white 10 (Zw10)/Zwilch or RZZ complex is required for checkpoint activation in nocodazole, and the complex is collectively required for kinetochore localization of Mad1 and Mad2 (Buffin et al., 2005; Karess, 2005; Scaerou et al., 1999). Intriguingly, the role of ROD and Zw10 in the checkpoint was first discovered by their requirement for kinetochore localization of dynein, which may function to deplete Mad1 and Mad2 from kinetochores during checkpoint inactivation (Scaerou et al., 2001; Starr et al., 1998). How the RZZ complex influences Mad1 and Mad2 localization is not known, as direct interactions between them have not been detected and neither Mad1 nor Mad2 fractionates with the large, 700kD RZZ complex. However, RZZ complexes in syncytial *Drosophila* embryos cycle through kinetochores with the same kinetics as Mad2 and BubR1, suggesting that they are positioned for sensing kinetochore status in the same way (Basto et al., 2004). The RZZ complex has the distinction of being the only checkpoint complex in which mutations are frequently detected in human cancers (Wang et al., 2004b). Coupled with their non-conservation throughout evolution, this observation suggests that the RZZ complex may have evolved as an additional layer of regulation atop the ancient “core” checkpoint proteins.

### **1.5 Checkpoint inactivation**

How can a cell arrested in mitosis by the spindle checkpoint resume progression into anaphase once all kinetochores finally achieve proper bipolar attachment and tension? Given the multiplicity of proven and potential APC/C inhibitors, it seems

unlikely that checkpoint silencing could occur by a single mechanism. One possibility is that the absence of unattached or untensed kinetochores simply halts generation of the “wait anaphase” signal, and any existing signal decays passively until it falls below the threshold required for Cdc20 inhibition. While this idea is attractive in its simplicity, it predicts that the time to recover from arrest will vary widely between cells with qualitatively or quantitatively different checkpoint-engaging lesions. Measuring and comparing time differences in anaphase entry after checkpoint shutoff has proven difficult in mammalian cells because of the reliance on microtubule poisons as tools for activating the checkpoint. These drugs accumulate to wildly different levels in different cell types and persist within cells for varying times after washout (Rieder and Maiato, 2004). Furthermore, drugs such as nocodazole and taxol are often applied at doses that activate stress response kinases and pathways and thus affect cell cycle progression differently than, for example, kinetochore protein RNAi. In addition, common population-based assays such as FACS or immunoblotting do not give as precise measurements of anaphase entry kinetics as do single cell assays. Thus, while it remains possible that passive decay of checkpoint signal leads to variable kinetics of mitotic exit, there is little data to argue for passive checkpoint inactivation in higher eukaryotes. In comparison, the classic PtK1 experiments described in section 1.4.3 found that anaphase ensued with a precise, robust time lag of  $23 \pm 1$  minutes after the final attachment event regardless of the length of time spent in prometaphase. The essentiality of the checkpoint and the kinetochore localization of checkpoint proteins in every mitosis argue strongly for a default “on” state in metazoans, while in yeast the checkpoint is “off” until activated by a lesion.

In budding yeast, it has been proposed that cells can pass the metaphase-anaphase transition without APC/C activation. Mutation of the phosphatase Cdc55p allows inhibitory phosphorylation of the cyclin-dependent kinase Cdc28p, and adaptation to prolonged spindle checkpoint arrest occurs when Cdc28 activity falls and cells enter anaphase without degrading cyclin B (Minshull et al., 1996; Rudner and Murray, 1996). Cdc28p activity also activates APC/C<sup>Cdc20</sup> in yeast directly, suggesting that improper Cdc28p activity or loss of Cdc55p could bypass spindle checkpoint signaling (Rudner et al., 2000; Rudner and Murray, 2000). Because adaptation occurs only after prolonged drug arrest, it may not reflect physiological checkpoint silencing, and this phenomenon has not been observed in cells other than budding yeast.

If the checkpoint is not bypassed by direct APC/C inactivation, it might be turned off actively by displacement of checkpoint proteins from the kinetochore. An elegant mechanism for silencing might involve simple competition between microtubules and checkpoint complexes for the same binding site on kinetochores. Because of the interdependency of checkpoint proteins for kinetochore localization, their many binding interactions, and the synergy of BubR1 and Mad2 activities *in vitro*, displacing these complexes into the cytoplasm may extinguish further signal generation, though it may not suffice to silence already active complexes or re-activate inhibited Cdc20.

Two candidate checkpoint inhibitors have been identified by yeast two-hybrid screens for checkpoint protein interactors. Breast cancer specific gene 1, BCSG1, binds to BubR1 and may promote its degradation by the 26S proteasome (Gupta et al., 2003). However, the function of BCSG1 in either checkpoint inactivation or mitotic progression has not been established. Another protein, CMT2, was identified as a Mad2 interactor.

In the following section I discuss relevant details of CMT2's discovery and present for the first time data from public genome resources regarding the CMT2 locus and CMT2 expression.

### **1.5.1 Identification of CMT2**

CMT2 was identified in a two-hybrid screen for human Mad2 binding proteins (Habu et al., 2002). CMT2 lacks obvious homologs in budding or fission yeast, and sequence analysis does not reveal known domains. CMT2 levels in synchronized HeLa cells were low or absent in interphase, increased in S phase, and decreased late in the subsequent M phase. CMT2 immunoprecipitates with Mad2 in late mitosis, but debate exists over whether CMT2-Mad2 binding competes with or coincides with Cdc20 Mad2 binding (Habu et al., 2002; Xia et al., 2004). Overexpression of CMT2 causes a slight decrease in the mitotic index of cell populations arrested in nocodazole, suggesting that CMT2 can silence a strongly activated checkpoint. Depletion of CMT2 by antisense oligonucleotides leads to apoptosis following a very transient delay in anaphase onset as measured by FACS. CMT2 in these studies was observed in nucleoplasmic speckles in mitosis and at the spindle midzone in anaphase and telophase. The authors proposed that CMT2 acts by a "handoff" mechanism in which Mad2 is transferred from Cdc20 to CMT2, thus allowing APC/C activation. Because cells treated with CMT2 antisense progressed normally until metaphase and undergo apoptosis only in the presence of an assembled spindle, the authors inferred that CMT2 also functions to suppress apoptosis late in mitosis. In a subsequent study, the same authors examined the effect of CMT2 RNAi on HeLa cells and found mild impairment of checkpoint release by population

FACS assay (Xia et al., 2004). In this study, CMT2 and Cdc20 bound Mad2 simultaneously, and CMT2 binding to Mad2-Cdc20 was sufficient for APC/C activation. Thus, neither the basic function of CMT2 nor the details of its mechanism are clear. In addition, the basic biology, expression, and conservation of CMT2 are not known.

### 1.5.2 Characterization of CMT2

Human CMT2 maps to chromosome 6p21.1, a region notable for its frequent amplification and translocation in human cancers (Figure 1.4A). Northern blots performed by the Kasuza cDNA Project using the EST probe KIAA0110, which encodes human CMT2, revealed that CMT2 mRNA is expressed ubiquitously, with enrichment in testis, colon, and skeletal muscle (Figure 1.4B). Searches for CMT2 homologues by iterative protein psiBLAST revealed broad but surprising species conservation. CMT2 gene homologs are present in the genomes of mammals, birds, fish, insect, and plants but noticeably absent from nematodes and yeast (Figure 1.5A). As discussed above, *C. elegans* possess holocentric chromosomes and have novel or highly divergent kinetochore and checkpoint proteins. BLAST searches also revealed a second CMT2-like protein in both mice and humans, which we term CMT2B. Human CMT2B is predicted to be a 3' splice variant of hCMT2 but has not been detected experimentally (data not shown). Mouse CMT2B differs from mmCMT2 throughout its sequence, and reverse translation of mmCMT2B does not map to any locus in current builds of the mouse genome, suggesting that the database mmCMT2B sequence may contain errors.

Comparison of CMT2 protein sequences reveals three highly conserved regions, termed CR1-3 (Figure 1.5B and 1.6A).

Figure 1.4

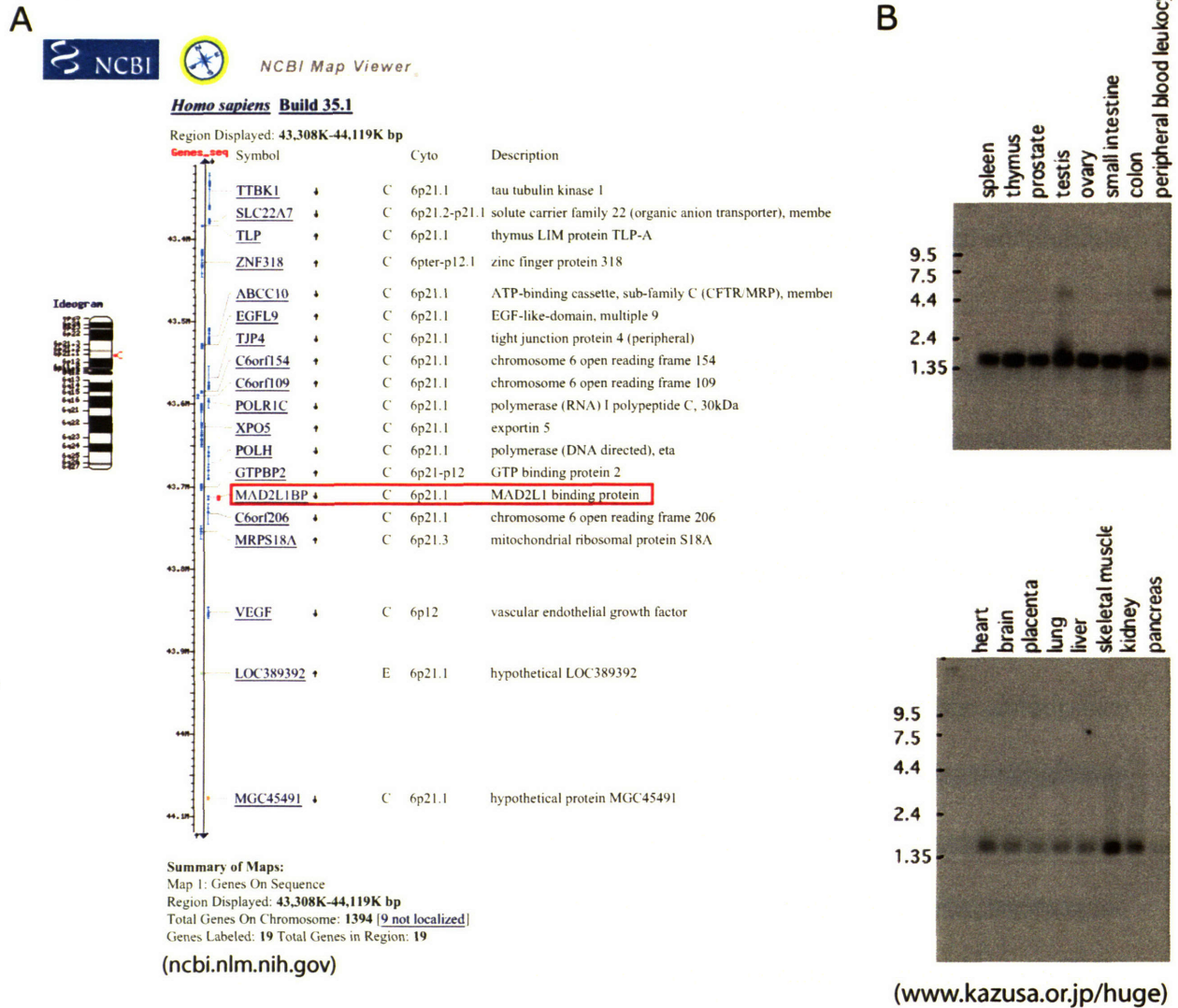
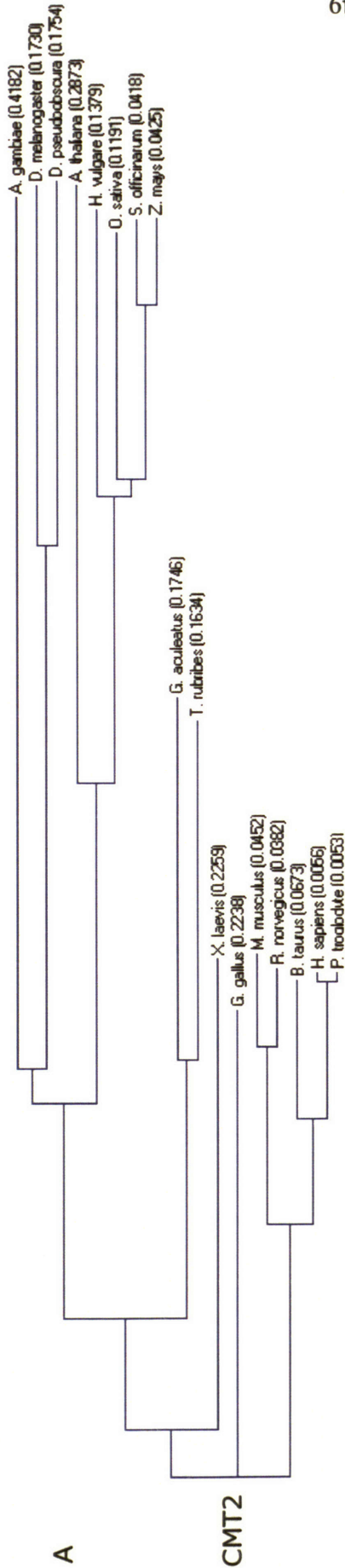


**Figure 1.4: Genomic locus and expression of CMT2**

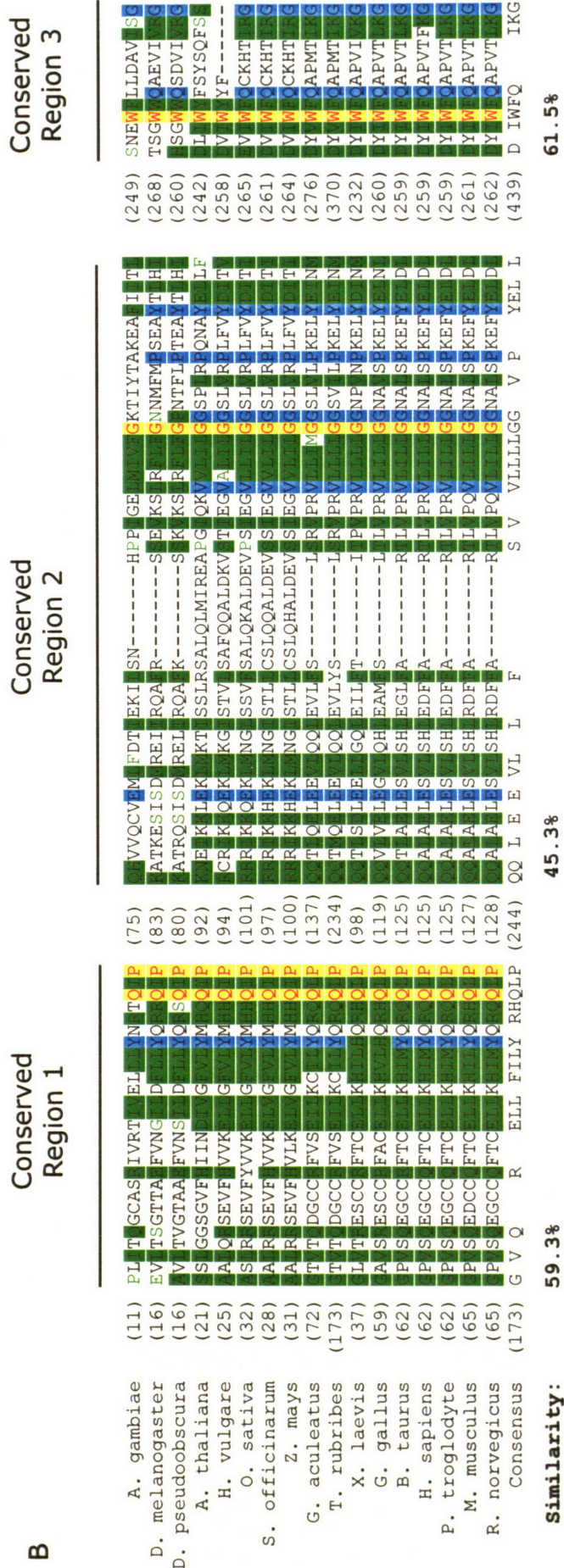
(A) The genomic of human CMT2 at chromosome 6p21.1 as visualized by the NCBI Map Viewer ([www.ncbi.nlm.nih.gov](http://www.ncbi.nlm.nih.gov)). The sequence is oriented such that the 6p telomere is at the top and the centromere is at the bottom. CMT2, listed as MAD2L1BP, is highlighted (red). Neighboring genes are depicted at their relative positions. (B) Tissue expression of CMT2. Human EST KIAA0110, which encodes CMT2, was used as a Northern blot probe against mRNA samples from a panel of 16 adult human tissues. This data is from the public dataset at [www.kazusa.or.jp/huge](http://www.kazusa.or.jp/huge).



Figure 1.5



49

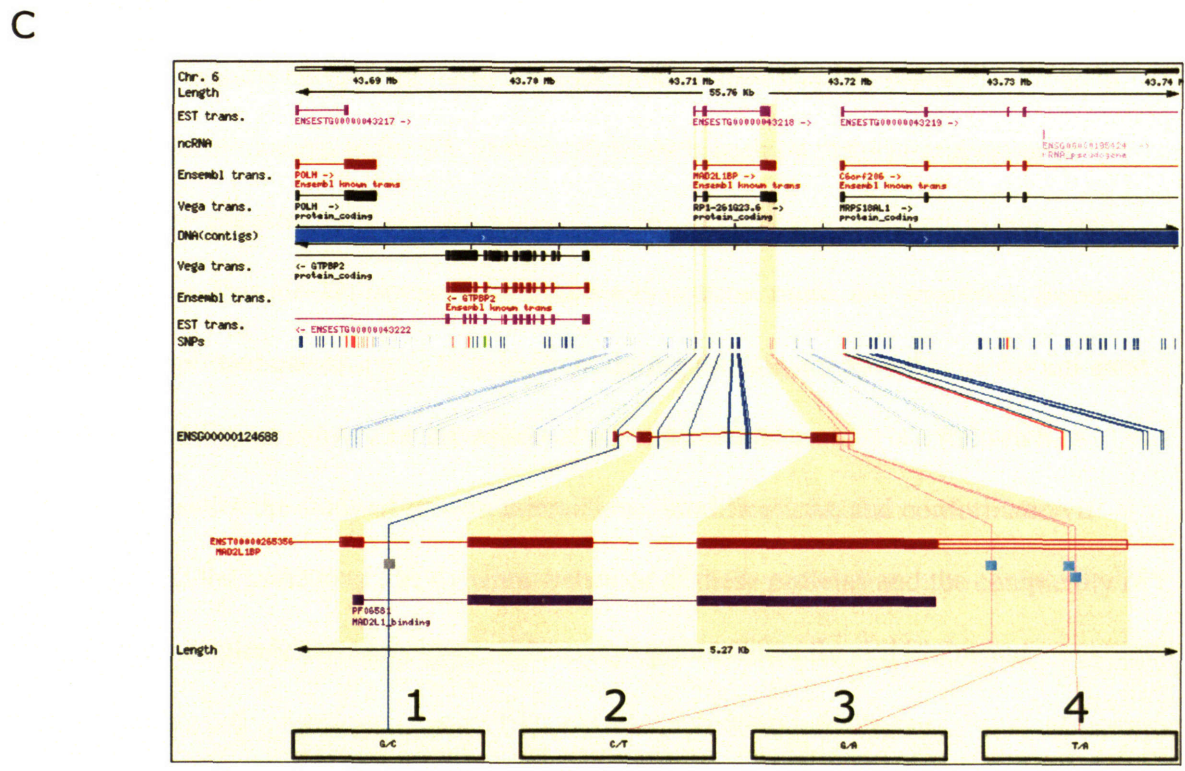
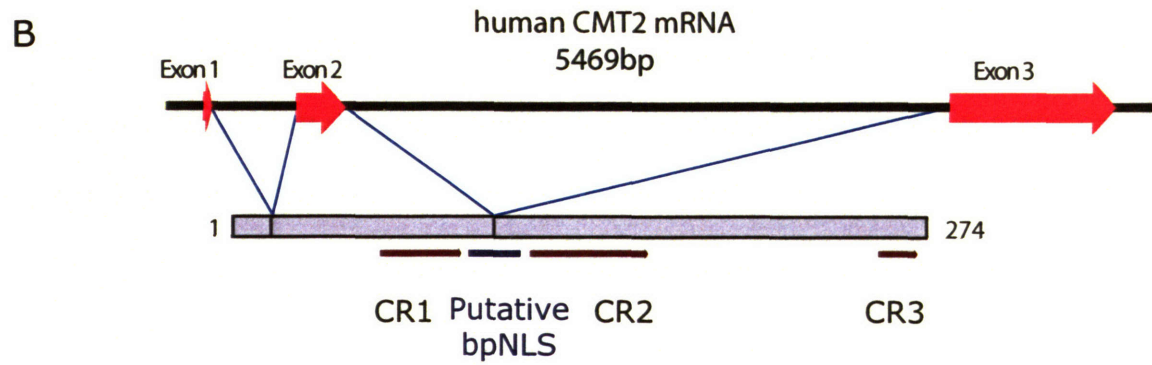
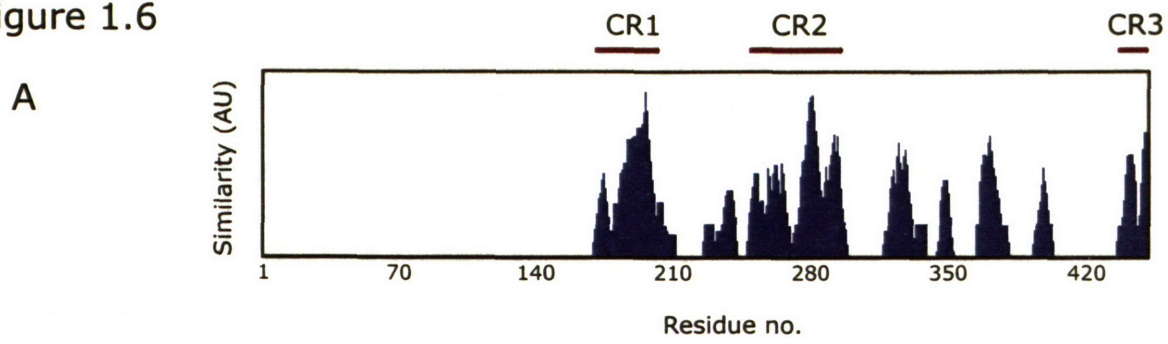


(11) PL T GCAS IVRT EL N T Q P (75) V V Q C V M F D T E K I S N ----- H P P G E K T I Y T A K E A I T (249) S N E W L L D A V S C  
 (16) EV TSGTTA FVNG D F I Y Q Q P (83) A T K E S I S D R E I R Q A R ----- S E K S R G N N M F M S E A Y T H (268) T S G W C A E V I S C  
 (16) V TVGTAA FVNS D F I Y Q S Q P (80) A T R Q S I S D R E L R Q A K ----- S K K S R G N T F L T E A Y T H (260) S G W C S D V I S C  
 (21) S G S G V F I I N G V Y M Q P (92) E F K L E K K T S S L R S A L Q L M I R E A P G Q K V G G S P F R Q N A Y L F (242) L W F S Y S Q F S  
 (25) A Q S E V F V V K G V Y M Q P (94) C R K Q E K N G S T V S A F Q Q A L D K V T E G V A G G S L R E L F V Y T (258) V W Y F -----  
 (32) S R S E V F Y V V K G V Y M Q P (101) R K Q E K N G S S V S A L Q K A L D E V F S E G V G G S L R E L F V Y T (265) V W C K H T S C  
 (28) A R S E V F V V K G V Y M Q P (97) R K H E K N G S T L C S L Q Q A L D E V S E G V G G S L R E L F V Y T (261) V W C K H T S C  
 (31) A R S E V F V L K G V Y M Q P (100) R K H E K N G S T L C S L Q H A L D E V S E G V G G S L R E L F V Y T (264) V W C K H T S C  
 (72) T T D G C C F V S K C Y Q Q P (137) T Q L E E Q Q E V L S ----- L R P R V M G S L I E K E L Y N (276) Y W C A P M T S C  
 (173) T T D G C C F V S K C Y Q Q P (234) T Q L E E Q Q E V L S ----- L R P R V M G S V I E K E L Y N (370) Y W C A P M T S C  
 (37) L T E S C C F T C K E Y Q Q P (98) V T S L E E L G Q E I L T ----- I P P R V I G G N P N E K E L Y N (232) Y W C A P V I S C  
 (59) A S E S C C F A C K E Y Q Q P (119) V V L E G Q H E A M S ----- L L P R V S G N A S E K E L Y N (260) Y W C A P V T S C  
 (62) P S E G C C F T C K E Y Q Q P (125) T A L E S S H E G L A ----- R L P R V I G N A S E K E F Y D (259) Y W C A P V T S C  
 (62) P S E G C C F T C K E Y Q Q P (125) A A L E S S S H E D F A ----- R L P R V I G N A S E K E F Y D (259) Y W C A P V T F S C  
 (62) P S E G C C F T C K E Y Q Q P (125) A A L E S S S H E D F A ----- R L P R V I G N A S E K E F Y D (259) Y W C A P V T S C  
 (65) P S E D C C F T C K E Y Q Q P (127) A A L E S S S H R D F A ----- R L P Q V I G G N A S E K E F Y D (261) Y W C A P V T S C  
 (65) P S E D C C F T C K E Y Q Q P (128) A A L E S S S H R D F A ----- R L P Q V I G G N A S E K E F Y D (262) Y W C A P V T S C  
 (173) G V Q R E L L F I L Y R H Q L P (244) Q Q L E E V L L F S V V L L L L G G V P Y E L L I K G (439) D I W F Q I K G

**Figure 1.5: Evolutionary conservation of CMT2**

(A) Phylogenetic tree analysis of CMT2 protein sequences from 17 eukaryotic species. Numbers indicate relative distance from the consensus sequence. (B) Alignment and consensus of conserved regions 1-3 from 17 CMT2 sequences. Yellow indicates completely conserved residues. Blue indicates blocks of conservation. Green indicates blocks of similarity. Light green type indicates weak similarity. Phylogenetic analysis and alignments were performed using the AlignX program of the Vector NTi software suite.

Figure 1.6



ID	class	alleles	ambiguity	chr pos	SNP type
1 <a href="#">rs11755829</a>	snp	G/C	S	643711692	INTRONIC
2 <a href="#">rs7106</a>	snp	C/T	Y	643716364	3' UTR
3 <a href="#">rs1804066</a>	snp	G/A	R	643716529	3' UTR
4 <a href="#">rs1799726</a>	snp	T/A	W	643716543	3' UTR

**Figure 1.6 CMT2 domain structure, splicing, and SNPs**

(A) Similarity levels over the aligned length of CMT2 protein sequences from 17 eukaryotic species. Numbering is based on the consensus sequence from alignments generated in Figure 1.5. The low degree of similarity in consensus residues 1-160 are due to the unusually long N-terminus of *T. rubribes* CMT2. (B) Splicing of human CMT2 mRNA and CMT2 protein domain structure. The putative bipartite NLS at positions 99-116 was reported by Habu et al. (C) Single nucleotide polymorphisms (SNPs) in human CMT2 genomic sequence. SNPs deposited in the NCBI Genome Build 35.1 are imposed on the human CMT2 mRNA and genomic locus.

At the extreme C terminus CR3 (human residues 259-272) is the most highly conserved, with 61.5% similarity over 17 species. CR1 (human 62-88, 59.3%) and CR2 (human 125-169, 45.3%) are less conserved. By comparison, the predicted bipartite NLS (human 99-116) shows no conservation (4.2% similarity). The human CMT2 locus at 6p21.1 contains three exons (Figure 1.6B), with conserved regions clustering in exons 2 and 3. The amino termini of CMT2 homologs show little sequence conservation, and certain species such as *T. rubribes* (fugu) contain much longer amino terminal sequences. Human genome databases contain evidence of four single nucleotide polymorphisms (SNPs), all of which are in non-coding regions (Figure 1.6C).

## 1.6 Conclusion

The spindle checkpoint poses a unique biochemical and cell biological problem. A brief, critical moment in the life of the cell depends both on the proper sensing of complex moving structures and the proper coupling of mechanical signals to cell cycle progression. This mechanism must be exquisitely precise, rapid, and sensitive. Because the transcriptional machinery is largely silent during mitosis, the spindle checkpoint must be mediated almost entirely by the action of proteins. As a result, it is a field rich in opportunities for the study of protein interactions, modifications, and conformational changes. At the same time, the dynamic behavior of these proteins and the complexity of chromosome-spindle interactions provide many opportunities for cell biological exploration.

Much progress has been made by combining the power of yeast genetics with the high-resolution imaging of mammalian cells, allowing the identification and early

characterization of the canonical checkpoint proteins. However, comparison of yeast and mammals has exposed the differences in their spindle checkpoints that overlie their commonalities. As the field moves forward, the pressing questions fall into two broad categories.

First, at a biochemical and structural level, what are the mechanisms by which spindle checkpoint proteins localize to the kinetochore, interact with each other, and transduce the “wait anaphase” signal? Many of the molecules involved were identified more than a decade ago but still have not been assigned a clear function. Mad2 is the most intensively studied of the checkpoint proteins, yet new Mad2 functions continue to be found and new mechanisms for its action proposed. In chapter 2 of this thesis I focus on the interaction of Mad2 with different classes of binding proteins and discuss a new model for Mad2 binding, activation, and regulation.

Second, given the increased complexity of the spindle checkpoint in metazoans, what are the consequences of checkpoint dysfunction in mammals? The differences between mammalian and yeast checkpoints likely stem from the added complexity of metazoan centromeres and kinetochore-microtubule interactions, but they are likely reinforced by the deleterious effects of chromosome missegregation in multicellular organisms. The connection between the spindle checkpoint and tumorigenesis remains unclear, but existing work suggests that cancer rarely, if ever, results from simple mutation or deletion of checkpoint genes. Less simplistic models of checkpoint dysfunction must necessarily consider metazoan-specific aspects of checkpoint signaling such as checkpoint gene transcription, apoptosis following checkpoint arrest or chromosome missegregation, and checkpoint silencing. The question of how an active

checkpoint is inactivated in human cells remains unanswered. In chapter 3 of this thesis I examine the role of CMT2 in opposing Mad2 function and propose a model for CMT2 function at kinetochores and in the cytosol. Finally, in chapter 4, I discuss a new cooperative model of checkpoint activation and propose further avenues of research.

## References

- Abrieu, A., Kahana, J. A., Wood, K. W., and Cleveland, D. W. (2000). CENP-E as an essential component of the mitotic checkpoint in vitro. *Cell* *102*, 817-826.
- Albertson, D. G., and Thomson, J. N. (1982). The kinetochores of *Caenorhabditis elegans*. *Chromosoma* *86*, 409-428.
- Allen, C., and Borisy, G. G. (1974). Structural polarity and directional growth of microtubules of *Chlamydomonas* flagella. *J Mol Biol* *90*, 381-402.
- Amor, D. J., Bentley, K., Ryan, J., Perry, J., Wong, L., Slater, H., and Choo, K. H. (2004). Human centromere repositioning "in progress". *Proc Natl Acad Sci U S A* *101*, 6542-6547.
- Amor, D. J., and Choo, K. H. (2002). Neocentromeres: role in human disease, evolution, and centromere study. *Am J Hum Genet* *71*, 695-714.
- Amos, L., and Klug, A. (1974). Arrangement of subunits in flagellar microtubules. *J Cell Sci* *14*, 523-549.
- Ault, J. G., DeMarco, A. J., Salmon, E. D., and Rieder, C. L. (1991). Studies on the ejection properties of asters: astral microtubule turnover influences the oscillatory behavior and positioning of mono-oriented chromosomes. *J Cell Sci* *99 ( Pt 4)*, 701-710.
- Ault, J. G., and Rieder, C. L. (1992). Chromosome mal-orientation and reorientation during mitosis. *Cell Motil Cytoskeleton* *22*, 155-159.
- Aylon, Y., and Kupiec, M. (2003). The checkpoint protein Rad24 of *Saccharomyces cerevisiae* is involved in processing double-strand break ends and in recombination partner choice. *Mol Cell Biol* *23*, 6585-6596.
- Baker, D. J., Jeganathan, K. B., Cameron, J. D., Thompson, M., Juneja, S., Kopecka, A., Kumar, R., Jenkins, R. B., de Groen, P. C., Roche, P., and van Deursen, J. M. (2004). BubR1 insufficiency causes early onset of aging-associated phenotypes and infertility in mice. *Nat Genet* *36*, 744-749.
- Bardin, A. J., and Amon, A. (2001). Men and sin: what's the difference? *Nat Rev Mol Cell Biol* *2*, 815-826.
- Bardin, A. J., Visintin, R., and Amon, A. (2000). A mechanism for coupling exit from mitosis to partitioning of the nucleus. *Cell* *102*, 21-31.
- Bartek, J., Lukas, C., and Lukas, J. (2004). Checking on DNA damage in S phase. *Nat Rev Mol Cell Biol* *5*, 792-804.



- Basto, R., Scaerou, F., Mische, S., Wojcik, E., Lefebvre, C., Gomes, R., Hays, T., and Karess, R. (2004). In vivo dynamics of the rough deal checkpoint protein during *Drosophila* mitosis. *Curr Biol* *14*, 56-61.
- Basu, J., Bousbaa, H., Logarinho, E., Li, Z., Williams, B. C., Lopes, C., Sunkel, C. E., and Goldberg, M. L. (1999). Mutations in the essential spindle checkpoint gene *bub1* cause chromosome missegregation and fail to block apoptosis in *Drosophila*. *J Cell Biol* *146*, 13-28.
- Belmont, L. D., Hyman, A. A., Sawin, K. E., and Mitchison, T. J. (1990). Real-time visualization of cell cycle-dependent changes in microtubule dynamics in cytoplasmic extracts. *Cell* *62*, 579-589.
- Biggins, S., and Murray, A. W. (2001). The budding yeast protein kinase *Ipl1/Aurora* allows the absence of tension to activate the spindle checkpoint. *Genes Dev* *15*, 3118-3129.
- Bischoff, J. R., Anderson, L., Zhu, Y., Mossie, K., Ng, L., Souza, B., Schryver, B., Flanagan, P., Clairvoyant, F., Ginther, C., *et al.* (1998). A homologue of *Drosophila aurora* kinase is oncogenic and amplified in human colorectal cancers. *Embo J* *17*, 3052-3065.
- Blower, M. D., Sullivan, B. A., and Karpen, G. H. (2002). Conserved organization of centromeric chromatin in flies and humans. *Dev Cell* *2*, 319-330.
- Brady, D. M., and Hardwick, K. G. (2000). Complex formation between *Mad1p*, *Bub1p* and *Bub3p* is crucial for spindle checkpoint function. *Curr Biol* *10*, 675-678.
- Brinkley, B. R., and Cartwright, J., Jr. (1971). Ultrastructural analysis of mitotic spindle elongation in mammalian cells in vitro. Direct microtubule counts. *J Cell Biol* *50*, 416-431.
- Brown, E. J., and Baltimore, D. (2003). Essential and dispensable roles of ATR in cell cycle arrest and genome maintenance. *Genes Dev* *17*, 615-628.
- Buffin, E., Lefebvre, C., Huang, J., Gagou, M. E., and Karess, R. E. (2005). Recruitment of *Mad2* to the kinetochore requires the *Rod/Zw10* complex. *Curr Biol* *15*, 856-861.
- Cahill, D. P., da Costa, L. T., Carson-Walter, E. B., Kinzler, K. W., Vogelstein, B., and Lengauer, C. (1999). Characterization of *MAD2B* and other mitotic spindle checkpoint genes. *Genomics* *58*, 181-187.
- Cahill, D. P., Lengauer, C., Yu, J., Riggins, G. J., Willson, J. K., Markowitz, S. D., Kinzler, K. W., and Vogelstein, B. (1998). Mutations of mitotic checkpoint genes in human cancers. *Nature* *392*, 300-303.
- Callan, H. G., and Jacobs, P. A. (1957). The meiotic process in *Mantis religiosa* L. males. *J Genet* *55*, 200-217.

Campbell, M. S., Chan, G. K., and Yen, T. J. (2001). Mitotic checkpoint proteins HsMAD1 and HsMAD2 are associated with nuclear pore complexes in interphase. *J Cell Sci* *114*, 953-963.

Castillo, A. R., Meehl, J. B., Morgan, G., Schutz-Geschwender, A., and Winey, M. (2002). The yeast protein kinase Mps1p is required for assembly of the integral spindle pole body component Spc42p. *J Cell Biol* *156*, 453-465.

Chan, G. K., Jablonski, S. A., Starr, D. A., Goldberg, M. L., and Yen, T. J. (2000). Human Zw10 and ROD are mitotic checkpoint proteins that bind to kinetochores. *Nat Cell Biol* *2*, 944-947.

Cheeseman, I. M., Niessen, S., Anderson, S., Hyndman, F., Yates, J. R., 3rd, Oegema, K., and Desai, A. (2004). A conserved protein network controls assembly of the outer kinetochore and its ability to sustain tension. *Genes Dev* *18*, 2255-2268.

Chen, J., and Fang, G. (2001). MAD2B is an inhibitor of the anaphase-promoting complex. *Genes Dev* *15*, 1765-1770.

Chen, R. H. (2002). BubR1 is essential for kinetochore localization of other spindle checkpoint proteins and its phosphorylation requires Mad1. *J Cell Biol* *158*, 487-496.

Chen, R. H. (2004). Phosphorylation and activation of Bub1 on unattached chromosomes facilitate the spindle checkpoint. *Embo J* *23*, 3113-3121.

Chen, R. H., Brady, D. M., Smith, D., Murray, A. W., and Hardwick, K. G. (1999). The spindle checkpoint of budding yeast depends on a tight complex between the Mad1 and Mad2 proteins. *Mol Biol Cell* *10*, 2607-2618.

Chen, R. H., Waters, J. C., Salmon, E. D., and Murray, A. W. (1996). Association of spindle assembly checkpoint component XMad2 with unattached kinetochores. *Science* *274*, 242-246.

Cimini, D., Howell, B., Maddox, P., Khodjakov, A., Degrossi, F., and Salmon, E. D. (2001). Merotelic kinetochore orientation is a major mechanism of aneuploidy in mitotic mammalian tissue cells. *J Cell Biol* *153*, 517-527.

Clarke, L. (1998). Centromeres: proteins, protein complexes, and repeated domains at centromeres of simple eukaryotes. *Curr Opin Genet Dev* *8*, 212-218.

Clarke, L., and Carbon, J. (1980). Isolation of a yeast centromere and construction of functional small circular chromosomes. *Nature* *287*, 504-509.

Cleveland, D. W., Mao, Y., and Sullivan, K. F. (2003). Centromeres and kinetochores: from epigenetics to mitotic checkpoint signaling. *Cell* *112*, 407-421.

- Cohen-Fix, O., Peters, J. M., Kirschner, M. W., and Koshland, D. (1996). Anaphase initiation in *Saccharomyces cerevisiae* is controlled by the APC-dependent degradation of the anaphase inhibitor Pds1p. *Genes Dev* *10*, 3081-3093.
- Cottarel, G., Shero, J. H., Hieter, P., and Hegemann, J. H. (1989). A 125-base-pair CEN6 DNA fragment is sufficient for complete meiotic and mitotic centromere functions in *Saccharomyces cerevisiae*. *Mol Cell Biol* *9*, 3342-3349.
- Cyert, M. S., Scherson, T., and Kirschner, M. W. (1988). Monoclonal antibodies specific for thiophosphorylated proteins recognize *Xenopus* MPF. *Dev Biol* *129*, 209-216.
- De Wulf, P., McAinsh, A. D., and Sorger, P. K. (2003). Hierarchical assembly of the budding yeast kinetochore from multiple subcomplexes. *Genes Dev* *17*, 2902-2921.
- Dernburg, A. F. (2001). Here, there, and everywhere: kinetochore function on holocentric chromosomes. *J Cell Biol* *153*, F33-38.
- Desai, A., and Mitchison, T. J. (1997). Microtubule polymerization dynamics. *Annu Rev Cell Dev Biol* *13*, 83-117.
- Dewar, H., Tanaka, K., Nasmyth, K., and Tanaka, T. U. (2004). Tension between two kinetochores suffices for their bi-orientation on the mitotic spindle. *Nature* *428*, 93-97.
- Ditchfield, C., Johnson, V. L., Tighe, A., Ellston, R., Haworth, C., Johnson, T., Mortlock, A., Keen, N., and Taylor, S. S. (2003). Aurora B couples chromosome alignment with anaphase by targeting BubR1, Mad2, and Cenp-E to kinetochores. *J Cell Biol* *161*, 267-280.
- Dobles, M., Liberal, V., Scott, M. L., Benezra, R., and Sorger, P. K. (2000). Chromosome missegregation and apoptosis in mice lacking the mitotic checkpoint protein Mad2. *Cell* *101*, 635-645.
- Dogterom, M., and Yurke, B. (1997). Measurement of the force-velocity relation for growing microtubules. *Science* *278*, 856-860.
- Dorer, R. K., Zhong, S., Tallarico, J. A., Wong, W. H., Mitchison, T. J., and Murray, A. W. (2005). A Small-Molecule Inhibitor of Mps1 Blocks the Spindle-Checkpoint Response to a Lack of Tension on Mitotic Chromosomes. *Curr Biol* *15*, 1070-1076.
- Fang, G. (2002). Checkpoint protein BubR1 acts synergistically with Mad2 to inhibit anaphase-promoting complex. *Mol Biol Cell* *13*, 755-766.
- Fang, G., Yu, H., and Kirschner, M. W. (1998). The checkpoint protein MAD2 and the mitotic regulator CDC20 form a ternary complex with the anaphase-promoting complex to control anaphase initiation. *Genes Dev* *12*, 1871-1883.

Fischer, M. G., Heeger, S., Hacker, U., and Lehner, C. F. (2004). The mitotic arrest in response to hypoxia and of polar bodies during early embryogenesis requires *Drosophila* Mps1. *Curr Biol* 14, 2019-2024.

Fodde, R., Kuipers, J., Rosenberg, C., Smits, R., Kielman, M., Gaspar, C., van Es, J. H., Breukel, C., Wiegant, J., Giles, R. H., and Clevers, H. (2001). Mutations in the APC tumour suppressor gene cause chromosomal instability. *Nat Cell Biol* 3, 433-438.

Fraschini, R., Beretta, A., Lucchini, G., and Piatti, S. (2001a). Role of the kinetochore protein Ndc10 in mitotic checkpoint activation in *Saccharomyces cerevisiae*. *Mol Genet Genomics* 266, 115-125.

Fraschini, R., Beretta, A., Sironi, L., Musacchio, A., Lucchini, G., and Piatti, S. (2001b). Bub3 interaction with Mad2, Mad3 and Cdc20 is mediated by WD40 repeats and does not require intact kinetochores. *Embo J* 20, 6648-6659.

Friedman, D. B., Kern, J. W., Huneycutt, B. J., Vinh, D. B., Crawford, D. K., Steiner, E., Scheiltz, D., Yates, J., 3rd, Resing, K. A., Ahn, N. G., *et al.* (2001). Yeast Mps1p phosphorylates the spindle pole component Spc110p in the N-terminal domain. *J Biol Chem* 276, 17958-17967.

Fuchs, D. A., and Johnson, R. K. (1978). Cytologic evidence that taxol, an antineoplastic agent from *Taxus brevifolia*, acts as a mitotic spindle poison. *Cancer Treat Rep* 62, 1219-1222.

Gardner, R. D., Poddar, A., Yellman, C., Tavormina, P. A., Monteagudo, M. C., and Burke, D. J. (2001). The spindle checkpoint of the yeast *Saccharomyces cerevisiae* requires kinetochore function and maps to the CBF3 domain. *Genetics* 157, 1493-1502.

Gillett, E. S., Espelin, C. W., and Sorger, P. K. (2004). Spindle checkpoint proteins and chromosome-microtubule attachment in budding yeast. *J Cell Biol* 164, 535-546.

Glotzer, M., Murray, A. W., and Kirschner, M. W. (1991). Cyclin is degraded by the ubiquitin pathway. *Nature* 349, 132-138.

Gorbsky, G. J., and Ricketts, W. A. (1993). Differential expression of a phosphoepitope at the kinetochores of moving chromosomes. *J Cell Biol* 122, 1311-1321.

Goshima, G., and Yanagida, M. (2000). Establishing biorientation occurs with precocious separation of the sister kinetochores, but not the arms, in the early spindle of budding yeast. *Cell* 100, 619-633.

Gupta, A., Inaba, S., Wong, O. K., Fang, G., and Liu, J. (2003). Breast cancer-specific gene 1 interacts with the mitotic checkpoint kinase BubR1. *Oncogene* 22, 7593-7599.

Habu, T., Kim, S. H., Weinstein, J., and Matsumoto, T. (2002). Identification of a MAD2-binding protein, CMT2, and its role in mitosis. *Embo J* 21, 6419-6428.

- Hanahan, D., and Weinberg, R. A. (2000). The hallmarks of cancer. *Cell* *100*, 57-70.
- Hanks, S., Coleman, K., Reid, S., Plaja, A., Firth, H., Fitzpatrick, D., Kidd, A., Mehes, K., Nash, R., Robin, N., *et al.* (2004). Constitutional aneuploidy and cancer predisposition caused by biallelic mutations in BUB1B. *Nat Genet* *36*, 1159-1161.
- Hardwick, K. G., Johnston, R. C., Smith, D. L., and Murray, A. W. (2000). MAD3 encodes a novel component of the spindle checkpoint which interacts with Bub3p, Cdc20p, and Mad2p. *J Cell Biol* *148*, 871-882.
- Hartwell, L. H., and Weinert, T. A. (1989). Checkpoints: controls that ensure the order of cell cycle events. *Science* *246*, 629-634.
- Hauf, S., Cole, R. W., LaTerra, S., Zimmer, C., Schnapp, G., Walter, R., Heckel, A., van Meel, J., Rieder, C. L., and Peters, J. M. (2003). The small molecule Hesperadin reveals a role for Aurora B in correcting kinetochore-microtubule attachment and in maintaining the spindle assembly checkpoint. *J Cell Biol* *161*, 281-294.
- He, X., Asthana, S., and Sorger, P. K. (2000). Transient sister chromatid separation and elastic deformation of chromosomes during mitosis in budding yeast. *Cell* *101*, 763-775.
- Hempfen, P. M., Kurpad, H., Calhoun, E. S., Abraham, S., and Kern, S. E. (2003). A double missense variation of the BUB1 gene and a defective mitotic spindle checkpoint in the pancreatic cancer cell line Hs766T. *Hum Mutat* *21*, 445.
- Hershko, A., Ganoth, D., Pehrson, J., Palazzo, R. E., and Cohen, L. H. (1991). Methylated ubiquitin inhibits cyclin degradation in clam embryo extracts. *J Biol Chem* *266*, 16376-16379.
- Hinchcliffe, E. H., Li, C., Thompson, E. A., Maller, J. L., and Sluder, G. (1999). Requirement of Cdk2-cyclin E activity for repeated centrosome reproduction in *Xenopus* egg extracts. *Science* *283*, 851-854.
- Holloway, S. L., Glotzer, M., King, R. W., and Murray, A. W. (1993). Anaphase is initiated by proteolysis rather than by the inactivation of maturation-promoting factor. *Cell* *73*, 1393-1402.
- Howell, B. J., Hoffman, D. B., Fang, G., Murray, A. W., and Salmon, E. D. (2000). Visualization of Mad2 dynamics at kinetochores, along spindle fibers, and at spindle poles in living cells. *J Cell Biol* *150*, 1233-1250.
- Howell, B. J., McEwen, B. F., Canman, J. C., Hoffman, D. B., Farrar, E. M., Rieder, C. L., and Salmon, E. D. (2001). Cytoplasmic dynein/dynactin drives kinetochore protein transport to the spindle poles and has a role in mitotic spindle checkpoint inactivation. *J Cell Biol* *155*, 1159-1172.

Howell, B. J., Moree, B., Farrar, E. M., Stewart, S., Fang, G., and Salmon, E. D. (2004). Spindle checkpoint protein dynamics at kinetochores in living cells. *Curr Biol* *14*, 953-964.

Hoyt, M. A., Totis, L., and Roberts, B. T. (1991). *S. cerevisiae* genes required for cell cycle arrest in response to loss of microtubule function. *Cell* *66*, 507-517.

Hu, F., and Elledge, S. J. (2002). Bub2 is a cell cycle regulated phospho-protein controlled by multiple checkpoints. *Cell Cycle* *1*, 351-355.

Huffaker, T. C., Thomas, J. H., and Botstein, D. (1988). Diverse effects of beta-tubulin mutations on microtubule formation and function. *J Cell Biol* *106*, 1997-2010.

Hunter, A. W., and Wordeman, L. (2000). How motor proteins influence microtubule polymerization dynamics. *J Cell Sci* *113 Pt 24*, 4379-4389.

Hwang, L. H., Lau, L. F., Smith, D. L., Mistrot, C. A., Hardwick, K. G., Hwang, E. S., Amon, A., and Murray, A. W. (1998). Budding yeast Cdc20: a target of the spindle checkpoint. *Science* *279*, 1041-1044.

Inoue, S., and Salmon, E. D. (1995). Force generation by microtubule assembly/disassembly in mitosis and related movements. *Mol Biol Cell* *6*, 1619-1640.

Iouk, T., Kerscher, O., Scott, R. J., Basrai, M. A., and Wozniak, R. W. (2002). The yeast nuclear pore complex functionally interacts with components of the spindle assembly checkpoint. *J Cell Biol* *159*, 807-819.

Jablonski, S. A., Chan, G. K., Cooke, C. A., Earnshaw, W. C., and Yen, T. J. (1998). The hBUB1 and hBUBR1 kinases sequentially assemble onto kinetochores during prophase with hBUBR1 concentrating at the kinetochore plates in mitosis. *Chromosoma* *107*, 386-396.

Jacobs, C. W., Adams, A. E., Szaniszló, P. J., and Pringle, J. R. (1988). Functions of microtubules in the *Saccharomyces cerevisiae* cell cycle. *J Cell Biol* *107*, 1409-1426.

Jin, D. Y., Spencer, F., and Jeang, K. T. (1998). Human T cell leukemia virus type 1 oncoprotein Tax targets the human mitotic checkpoint protein MAD1. *Cell* *93*, 81-91.

Johnson, V. L., Scott, M. I., Holt, S. V., Hussein, D., and Taylor, S. S. (2004). Bub1 is required for kinetochore localization of BubR1, Cenp-E, Cenp-F and Mad2, and chromosome congression. *J Cell Sci* *117*, 1577-1589.

Jones, M. H., Huneycutt, B. J., Pearson, C. G., Zhang, C., Morgan, G., Shokat, K., Bloom, K., and Winey, M. (2005). Chemical genetics reveals a role for Mps1 kinase in kinetochore attachment during mitosis. *Curr Biol* *15*, 160-165.

Kaplan, K. B., Burds, A. A., Swedlow, J. R., Bekir, S. S., Sorger, P. K., and Nathke, I. S. (2001). A role for the Adenomatous Polyposis Coli protein in chromosome segregation. *Nat Cell Biol* 3, 429-432.

Kapoor, T. M., Mayer, T. U., Coughlin, M. L., and Mitchison, T. J. (2000). Probing spindle assembly mechanisms with monastrol, a small molecule inhibitor of the mitotic kinesin, Eg5. *J Cell Biol* 150, 975-988.

Karess, R. (2005). Rod-Zw10-Zwilch: a key player in the spindle checkpoint. *Trends Cell Biol*.

Katis, V. L., Galova, M., Rabitsch, K. P., Gregan, J., and Nasmyth, K. (2004). Maintenance of cohesin at centromeres after meiosis I in budding yeast requires a kinetochore-associated protein related to MEI-S332. *Curr Biol* 14, 560-572.

Kerrebrock, A. W., Miyazaki, W. Y., Birnby, D., and Orr-Weaver, T. L. (1992). The *Drosophila* mei-S332 gene promotes sister-chromatid cohesion in meiosis following kinetochore differentiation. *Genetics* 130, 827-841.

Kim, S. H., Lin, D. P., Matsumoto, S., Kitazono, A., and Matsumoto, T. (1998). Fission yeast Slp1: an effector of the Mad2-dependent spindle checkpoint. *Science* 279, 1045-1047.

King, J. M., and Nicklas, R. B. (2000). Tension on chromosomes increases the number of kinetochore microtubules but only within limits. *J Cell Sci* 113 Pt 21, 3815-3823.

Kinzler, K. W., and Vogelstein, B. (1996). Lessons from hereditary colorectal cancer. *Cell* 87, 159-170.

Kitagawa, R., and Rose, A. M. (1999). Components of the spindle-assembly checkpoint are essential in *Caenorhabditis elegans*. *Nat Cell Biol* 1, 514-521.

Kitajima, T. S., Hauf, S., Ohsugi, M., Yamamoto, T., and Watanabe, Y. (2005). Human Bub1 defines the persistent cohesion site along the mitotic chromosome by affecting Shugoshin localization. *Curr Biol* 15, 353-359.

Kitajima, T. S., Kawashima, S. A., and Watanabe, Y. (2004). The conserved kinetochore protein shugoshin protects centromeric cohesion during meiosis. *Nature* 427, 510-517.

Kops, G. J., Kim, Y., Weaver, B. A., Mao, Y., McLeod, I., Yates, J. R., 3rd, Tagaya, M., and Cleveland, D. W. (2005). ZW10 links mitotic checkpoint signaling to the structural kinetochore. *J Cell Biol* 169, 49-60.

Lampson, M. A., and Kapoor, T. M. (2005). The human mitotic checkpoint protein BubR1 regulates chromosome-spindle attachments. *Nat Cell Biol* 7, 93-98.

- Lauze, E., Stoelcker, B., Luca, F. C., Weiss, E., Schutz, A. R., and Winey, M. (1995). Yeast spindle pole body duplication gene *MPS1* encodes an essential dual specificity protein kinase. *Embo J* 14, 1655-1663.
- Lew, D. J., and Burke, D. J. (2003). The spindle assembly and spindle position checkpoints. *Annu Rev Genet* 37, 251-282.
- Li, R., and Murray, A. W. (1991). Feedback control of mitosis in budding yeast. *Cell* 66, 519-531.
- Li, X., and Nicklas, R. B. (1995). Mitotic forces control a cell-cycle checkpoint. *Nature* 373, 630-632.
- Li, X., and Nicklas, R. B. (1997). Tension-sensitive kinetochore phosphorylation and the chromosome distribution checkpoint in praying mantid spermatocytes. *J Cell Sci* 110 ( Pt 5), 537-545.
- Li, Y., and Benezra, R. (1996). Identification of a human mitotic checkpoint gene: *hsMAD2*. *Science* 274, 246-248.
- Liu, S. T., Hittle, J. C., Jablonski, S. A., Campbell, M. S., Yoda, K., and Yen, T. J. (2003). Human CENP-I specifies localization of CENP-F, MAD1 and MAD2 to kinetochores and is essential for mitosis. *Nat Cell Biol* 5, 341-345.
- Lou, Y., Yao, J., Zereshki, A., Dou, Z., Ahmed, K., Wang, H., Hu, J., Wang, Y., and Yao, X. (2004). NEK2A interacts with MAD1 and possibly functions as a novel integrator of the spindle checkpoint signaling. *J Biol Chem* 279, 20049-20057.
- Luo, X., Tang, Z., Xia, G., Wassmann, K., Matsumoto, T., Rizo, J., and Yu, H. (2004). The Mad2 spindle checkpoint protein has two distinct natively folded states. *Nat Struct Mol Biol* 11, 338-345.
- Mao, Y., Abrieu, A., and Cleveland, D. W. (2003). Activating and silencing the mitotic checkpoint through CENP-E-dependent activation/inactivation of BubR1. *Cell* 114, 87-98.
- Marston, A. L., Tham, W. H., Shah, H., and Amon, A. (2004). A genome-wide screen identifies genes required for centromeric cohesion. *Science* 303, 1367-1370.
- Martinez-Exposito, M. J., Kaplan, K. B., Copeland, J., and Sorger, P. K. (1999). Retention of the BUB3 checkpoint protein on lagging chromosomes. *Proc Natl Acad Sci U S A* 96, 8493-8498.
- Martin-Lluesma, S., Stucke, V. M., and Nigg, E. A. (2002). Role of Hec1 in spindle checkpoint signaling and kinetochore recruitment of Mad1/Mad2. *Science* 297, 2267-2270.



- McCarroll, R. M., and Fangman, W. L. (1988). Time of replication of yeast centromeres and telomeres. *Cell* 54, 505-513.
- McDonald, E. R., 3rd, and El-Deiry, W. S. (2001). Checkpoint genes in cancer. *Ann Med* 33, 113-122.
- McIntosh, J. R. (1991). Structural and mechanical control of mitotic progression. *Cold Spring Harb Symp Quant Biol* 56, 613-619.
- Meluh, P. B., Yang, P., Glowczewski, L., Koshland, D., and Smith, M. M. (1998). Cse4p is a component of the core centromere of *Saccharomyces cerevisiae*. *Cell* 94, 607-613.
- Meraldi, P., Draviam, V. M., and Sorger, P. K. (2004). Timing and checkpoints in the regulation of mitotic progression. *Dev Cell* 7, 45-60.
- Meraldi, P., Lukas, J., Fry, A. M., Bartek, J., and Nigg, E. A. (1999). Centrosome duplication in mammalian somatic cells requires E2F and Cdk2-cyclin A. *Nat Cell Biol* 1, 88-93.
- Meraldi, P., and Sorger, P. K. (2005). A dual role for Bub1 in the spindle checkpoint and chromosome congression. *Embo J* 24, 1621-1633.
- Michel, L., Diaz-Rodriguez, E., Narayan, G., Hernando, E., Murty, V. V., and Benezra, R. (2004). Complete loss of the tumor suppressor MAD2 causes premature cyclin B degradation and mitotic failure in human somatic cells. *Proc Natl Acad Sci U S A* 101, 4459-4464.
- Michel, L. S., Liberal, V., Chatterjee, A., Kirchwegger, R., Pasche, B., Gerald, W., Dobles, M., Sorger, P. K., Murty, V. V., and Benezra, R. (2001). MAD2 haplo-insufficiency causes premature anaphase and chromosome instability in mammalian cells. *Nature* 409, 355-359.
- Millband, D. N., and Hardwick, K. G. (2002). Fission yeast Mad3p is required for Mad2p to inhibit the anaphase-promoting complex and localizes to kinetochores in a Bub1p-, Bub3p-, and Mph1p-dependent manner. *Mol Cell Biol* 22, 2728-2742.
- Minshull, J., Straight, A., Rudner, A. D., Dernburg, A. F., Belmont, A., and Murray, A. W. (1996). Protein phosphatase 2A regulates MPF activity and sister chromatid cohesion in budding yeast. *Curr Biol* 6, 1609-1620.
- Minshull, J., Sun, H., Tonks, N. K., and Murray, A. W. (1994). A MAP kinase-dependent spindle assembly checkpoint in *Xenopus* egg extracts. *Cell* 79, 475-486.
- Mitchison, T., and Kirschner, M. (1984). Dynamic instability of microtubule growth. *Nature* 312, 237-242.
- Mitchison, T. J. (1986). The role of microtubule polarity in the movement of kinesin and kinetochores. *J Cell Sci Suppl* 5, 121-128.

- Mitchison, T. J., and Kirschner, M. W. (1985). Properties of the kinetochore in vitro. II. Microtubule capture and ATP-dependent translocation. *J Cell Biol* 101, 766-777.
- Murray, A. W. (2004). Recycling the cell cycle: cyclins revisited. *Cell* 116, 221-234.
- Murray, A. W., and Marks, D. (2001). Can sequencing shed light on cell cycling? *Nature* 409, 844-846.
- Musacchio, A., and Hardwick, K. G. (2002). The spindle checkpoint: structural insights into dynamic signalling. *Nat Rev Mol Cell Biol* 3, 731-741.
- Nicklas, R. B., and Koch, C. A. (1969). Chromosome micromanipulation. 3. Spindle fiber tension and the reorientation of mal-oriented chromosomes. *J Cell Biol* 43, 40-50.
- Nicklas, R. B., and Ward, S. C. (1994). Elements of error correction in mitosis: microtubule capture, release, and tension. *J Cell Biol* 126, 1241-1253.
- Nigg, E. A. (2001). Mitotic kinases as regulators of cell division and its checkpoints. *Nat Rev Mol Cell Biol* 2, 21-32.
- Pereira, G., Knop, M., and Schiebel, E. (1998). Spc98p directs the yeast gamma-tubulin complex into the nucleus and is subject to cell cycle-dependent phosphorylation on the nuclear side of the spindle pole body. *Mol Biol Cell* 9, 775-793.
- Peters, J. M. (1999). Subunits and substrates of the anaphase-promoting complex. *Exp Cell Res* 248, 339-349.
- Pfleger, C. M., Salic, A., Lee, E., and Kirschner, M. W. (2001). Inhibition of Cdh1-APC by the MAD2-related protein MAD2L2: a novel mechanism for regulating Cdh1. *Genes Dev* 15, 1759-1764.
- Piatti, S., Lengauer, C., and Nasmyth, K. (1995). Cdc6 is an unstable protein whose de novo synthesis in G1 is important for the onset of S phase and for preventing a 'reductional' anaphase in the budding yeast *Saccharomyces cerevisiae*. *Embo J* 14, 3788-3799.
- Poddar, A., Daniel, J. A., Daum, J. R., and Burke, D. J. (2004). Differential kinetochore requirements for establishment and maintenance of the spindle checkpoint are dependent on the mechanism of checkpoint activation in *Saccharomyces cerevisiae*. *Cell Cycle* 3, 197-204.
- Poss, K. D., Wilson, L. G., and Keating, M. T. (2002). Heart regeneration in zebrafish. *Science* 298, 2188-2190.
- Rabitsch, K. P., Gregan, J., Schleiffer, A., Javerzat, J. P., Eisenhaber, F., and Nasmyth, K. (2004). Two fission yeast homologs of *Drosophila* Mei-S332 are required for chromosome segregation during meiosis I and II. *Curr Biol* 14, 287-301.

- Rao, C. V., Yang, Y. M., Swamy, M. V., Liu, T., Fang, Y., Mahmood, R., Jhanwar-Uniyal, M., and Dai, W. (2005). Colonic tumorigenesis in BubR1<sup>+/-</sup>ApcMin<sup>+</sup> compound mutant mice is linked to premature separation of sister chromatids and enhanced genomic instability. *Proc Natl Acad Sci U S A* *102*, 4365-4370.
- Rieder, C. L. (1982). The formation, structure, and composition of the mammalian kinetochore and kinetochore fiber. *Int Rev Cytol* *79*, 1-58.
- Rieder, C. L., and Alexander, S. P. (1990). Kinetochores are transported poleward along a single astral microtubule during chromosome attachment to the spindle in newt lung cells. *J Cell Biol* *110*, 81-95.
- Rieder, C. L., Cole, R. W., Khodjakov, A., and Sluder, G. (1995). The checkpoint delaying anaphase in response to chromosome monoorientation is mediated by an inhibitory signal produced by unattached kinetochores. *J Cell Biol* *130*, 941-948.
- Rieder, C. L., and Maiato, H. (2004). Stuck in division or passing through: what happens when cells cannot satisfy the spindle assembly checkpoint. *Dev Cell* *7*, 637-651.
- Rieder, C. L., and Salmon, E. D. (1994). Motile kinetochores and polar ejection forces dictate chromosome position on the vertebrate mitotic spindle. *J Cell Biol* *124*, 223-233.
- Rieder, C. L., and Salmon, E. D. (1998). The vertebrate cell kinetochore and its roles during mitosis. *Trends Cell Biol* *8*, 310-318.
- Rieder, C. L., Schultz, A., Cole, R., and Sluder, G. (1994). Anaphase onset in vertebrate somatic cells is controlled by a checkpoint that monitors sister kinetochore attachment to the spindle. *J Cell Biol* *127*, 1301-1310.
- Roberts, B. T., Farr, K. A., and Hoyt, M. A. (1994). The *Saccharomyces cerevisiae* checkpoint gene BUB1 encodes a novel protein kinase. *Mol Cell Biol* *14*, 8282-8291.
- Rogers, G. C., Rogers, S. L., Schwimmer, T. A., Ems-McClung, S. C., Walczak, C. E., Vale, R. D., Scholey, J. M., and Sharp, D. J. (2004). Two mitotic kinesins cooperate to drive sister chromatid separation during anaphase. *Nature* *427*, 364-370.
- Rudner, A. D., Hardwick, K. G., and Murray, A. W. (2000). Cdc28 activates exit from mitosis in budding yeast. *J Cell Biol* *149*, 1361-1376.
- Rudner, A. D., and Murray, A. W. (1996). The spindle assembly checkpoint. *Curr Opin Cell Biol* *8*, 773-780.
- Rudner, A. D., and Murray, A. W. (2000). Phosphorylation by Cdc28 activates the Cdc20-dependent activity of the anaphase-promoting complex. *J Cell Biol* *149*, 1377-1390.

- Saffery, R., Irvine, D. V., Griffiths, B., Kalitsis, P., and Choo, K. H. (2000). Components of the human spindle checkpoint control mechanism localize specifically to the active centromere on dicentric chromosomes. *Hum Genet* *107*, 376-384.
- Salic, A., Waters, J. C., and Mitchison, T. J. (2004). Vertebrate shugoshin links sister centromere cohesion and kinetochore microtubule stability in mitosis. *Cell* *118*, 567-578.
- Scaerou, F., Aguilera, I., Saunders, R., Kane, N., Blottiere, L., and Karess, R. (1999). The rough deal protein is a new kinetochore component required for accurate chromosome segregation in *Drosophila*. *J Cell Sci* *112 ( Pt 21)*, 3757-3768.
- Scaerou, F., Starr, D. A., Piano, F., Papoulas, O., Karess, R. E., and Goldberg, M. L. (2001). The ZW10 and Rough Deal checkpoint proteins function together in a large, evolutionarily conserved complex targeted to the kinetochore. *J Cell Sci* *114*, 3103-3114.
- Schott, E. J., and Hoyt, M. A. (1998). Dominant alleles of *Saccharomyces cerevisiae* CDC20 reveal its role in promoting anaphase. *Genetics* *148*, 599-610.
- Schulze, E., and Kirschner, M. (1986). Microtubule dynamics in interphase cells. *J Cell Biol* *102*, 1020-1031.
- Schwab, M., Lutum, A. S., and Seufert, W. (1997). Yeast Hct1 is a regulator of Clb2 cyclin proteolysis. *Cell* *90*, 683-693.
- Shah, J. V., Botvinick, E., Bonday, Z., Furnari, F., Berns, M., and Cleveland, D. W. (2004). Dynamics of centromere and kinetochore proteins; implications for checkpoint signaling and silencing. *Curr Biol* *14*, 942-952.
- Sharp, D. J., Rogers, G. C., and Scholey, J. M. (2000). Microtubule motors in mitosis. *Nature* *407*, 41-47.
- Sharp-Baker, H., and Chen, R. H. (2001). Spindle checkpoint protein Bub1 is required for kinetochore localization of Mad1, Mad2, Bub3, and CENP-E, independently of its kinase activity. *J Cell Biol* *153*, 1239-1250.
- Sironi, L., Mapelli, M., Knapp, S., De Antoni, A., Jeang, K. T., and Musacchio, A. (2002). Crystal structure of the tetrameric Mad1-Mad2 core complex: implications of a 'safety belt' binding mechanism for the spindle checkpoint. *Embo J* *21*, 2496-2506.
- Skoufias, D. A., Andreassen, P. R., Lacroix, F. B., Wilson, L., and Margolis, R. L. (2001). Mammalian mad2 and bub1/bubR1 recognize distinct spindle-attachment and kinetochore-tension checkpoints. *Proc Natl Acad Sci U S A* *98*, 4492-4497.
- Sluder, G., Thompson, E. A., Miller, F. J., Hayes, J., and Rieder, C. L. (1997). The checkpoint control for anaphase onset does not monitor excess numbers of spindle poles or bipolar spindle symmetry. *J Cell Sci* *110 ( Pt 4)*, 421-429.

- Spiegelman, B. M., Penningroth, S. M., and Kirschner, M. W. (1977). Turnover of tubulin and the N site GTP in Chinese hamster ovary cells. *Cell* *12*, 587-600.
- Starr, D. A., Williams, B. C., Hays, T. S., and Goldberg, M. L. (1998). ZW10 helps recruit dynactin and dynein to the kinetochore. *J Cell Biol* *142*, 763-774.
- Stern, B. M., and Murray, A. W. (2001). Lack of tension at kinetochores activates the spindle checkpoint in budding yeast. *Curr Biol* *11*, 1462-1467.
- Sudakin, V., Chan, G. K., and Yen, T. J. (2001). Checkpoint inhibition of the APC/C in HeLa cells is mediated by a complex of BUBR1, BUB3, CDC20, and MAD2. *J Cell Biol* *154*, 925-936.
- Sullivan, B. A., Blower, M. D., and Karpen, G. H. (2001). Determining centromere identity: cyclical stories and forking paths. *Nat Rev Genet* *2*, 584-596.
- Surana, U., Amon, A., Dowzer, C., McGrew, J., Byers, B., and Nasmyth, K. (1993). Destruction of the CDC28/CLB mitotic kinase is not required for the metaphase to anaphase transition in budding yeast. *Embo J* *12*, 1969-1978.
- Takenaka, K., Gotoh, Y., and Nishida, E. (1997). MAP kinase is required for the spindle assembly checkpoint but is dispensable for the normal M phase entry and exit in *Xenopus* egg cell cycle extracts. *J Cell Biol* *136*, 1091-1097.
- Takenaka, K., Moriguchi, T., and Nishida, E. (1998). Activation of the protein kinase p38 in the spindle assembly checkpoint and mitotic arrest. *Science* *280*, 599-602.
- Tanaka, T. U., Rachidi, N., Janke, C., Pereira, G., Galova, M., Schiebel, E., Stark, M. J., and Nasmyth, K. (2002). Evidence that the Ipl1-Sli15 (Aurora kinase-INCENP) complex promotes chromosome bi-orientation by altering kinetochore-spindle pole connections. *Cell* *108*, 317-329.
- Tang, Z., Bharadwaj, R., Li, B., and Yu, H. (2001). Mad2-Independent inhibition of APCCdc20 by the mitotic checkpoint protein BubR1. *Dev Cell* *1*, 227-237.
- Tang, Z., Shu, H., Oncel, D., Chen, S., and Yu, H. (2004a). Phosphorylation of Cdc20 by Bub1 provides a catalytic mechanism for APC/C inhibition by the spindle checkpoint. *Mol Cell* *16*, 387-397.
- Tang, Z., Sun, Y., Harley, S. E., Zou, H., and Yu, H. (2004b). Human Bub1 protects centromeric sister-chromatid cohesion through Shugoshin during mitosis. *Proc Natl Acad Sci U S A* *101*, 18012-18017.
- Taylor, S. S., Ha, E., and McKeon, F. (1998). The human homologue of Bub3 is required for kinetochore localization of Bub1 and a Mad3/Bub1-related protein kinase. *J Cell Biol* *142*, 1-11.

Taylor, S. S., Hussein, D., Wang, Y., Elderkin, S., and Morrow, C. J. (2001). Kinetochore localisation and phosphorylation of the mitotic checkpoint components Bub1 and BubR1 are differentially regulated by spindle events in human cells. *J Cell Sci* *114*, 4385-4395.

Taylor, S. S., and McKeon, F. (1997). Kinetochore localization of murine Bub1 is required for normal mitotic timing and checkpoint response to spindle damage. *Cell* *89*, 727-735.

Taylor, S. S., Scott, M. I., and Holland, A. J. (2004). The spindle checkpoint: a quality control mechanism which ensures accurate chromosome segregation. *Chromosome Res* *12*, 599-616.

Tighe, A., Johnson, V. L., and Taylor, S. S. (2004). Truncating APC mutations have dominant effects on proliferation, spindle checkpoint control, survival and chromosome stability. *J Cell Sci* *117*, 6339-6353.

Vafa, O., and Sullivan, K. F. (1997). Chromatin containing CENP-A and alpha-satellite DNA is a major component of the inner kinetochore plate. *Curr Biol* *7*, 897-900.

Verde, F., Dogterom, M., Stelzer, E., Karsenti, E., and Leibler, S. (1992). Control of microtubule dynamics and length by cyclin A- and cyclin B-dependent kinases in *Xenopus* egg extracts. *J Cell Biol* *118*, 1097-1108.

Vigneron, S., Prieto, S., Bernis, C., Labbe, J. C., Castro, A., and Lorca, T. (2004). Kinetochore localization of spindle checkpoint proteins: who controls whom? *Mol Biol Cell* *15*, 4584-4596.

Visintin, R., Prinz, S., and Amon, A. (1997). CDC20 and CDH1: a family of substrate-specific activators of APC-dependent proteolysis. *Science* *278*, 460-463.

Wang, Q., Liu, T., Fang, Y., Xie, S., Huang, X., Mahmood, R., Ramaswamy, G., Sakamoto, K. M., Darzynkiewicz, Z., Xu, M., and Dai, W. (2004a). BUBR1 deficiency results in abnormal megakaryopoiesis. *Blood* *103*, 1278-1285.

Wang, Y., and Burke, D. J. (1997). Cdc55p, the B-type regulatory subunit of protein phosphatase 2A, has multiple functions in mitosis and is required for the kinetochore/spindle checkpoint in *Saccharomyces cerevisiae*. *Mol Cell Biol* *17*, 620-626.

Wang, Z., Cummins, J. M., Shen, D., Cahill, D. P., Jallepalli, P. V., Wang, T. L., Parsons, D. W., Traverso, G., Awad, M., Silliman, N., *et al.* (2004b). Three classes of genes mutated in colorectal cancers with chromosomal instability. *Cancer Res* *64*, 2998-3001.

Warren, C. D., Brady, D. M., Johnston, R. C., Hanna, J. S., Hardwick, K. G., and Spencer, F. A. (2002). Distinct chromosome segregation roles for spindle checkpoint proteins. *Mol Biol Cell* *13*, 3029-3041.

Wassmann, K., Liberal, V., and Benezra, R. (2003). Mad2 phosphorylation regulates its association with Mad1 and the APC/C. *Embo J* *22*, 797-806.

- Waters, J. C., Chen, R. H., Murray, A. W., and Salmon, E. D. (1998). Localization of Mad2 to kinetochores depends on microtubule attachment, not tension. *J Cell Biol* *141*, 1181-1191.
- Waters, J. C., Skibbens, R. V., and Salmon, E. D. (1996). Oscillating mitotic newt lung cell kinetochores are, on average, under tension and rarely push. *J Cell Sci* *109 (Pt 12)*, 2823-2831.
- Weaver, B. A., Bonday, Z. Q., Putkey, F. R., Kops, G. J., Silk, A. D., and Cleveland, D. W. (2003). Centromere-associated protein-E is essential for the mammalian mitotic checkpoint to prevent aneuploidy due to single chromosome loss. *J Cell Biol* *162*, 551-563.
- Weinert, T., and Hartwell, L. (1989). Control of G2 delay by the rad9 gene of *Saccharomyces cerevisiae*. *J Cell Sci Suppl* *12*, 145-148.
- Weinert, T. A., and Hartwell, L. H. (1988). The RAD9 gene controls the cell cycle response to DNA damage in *Saccharomyces cerevisiae*. *Science* *241*, 317-322.
- Weisenberg, R. C., and Deery, W. J. (1976). Role of nucleotide hydrolysis in microtubule assembly. *Nature* *263*, 792-793.
- Weiss, E., and Winey, M. (1996). The *Saccharomyces cerevisiae* spindle pole body duplication gene MPS1 is part of a mitotic checkpoint. *J Cell Biol* *132*, 111-123.
- Winey, M., Mamay, C. L., O'Toole, E. T., Mastronarde, D. N., Giddings, T. H., Jr., McDonald, K. L., and McIntosh, J. R. (1995). Three-dimensional ultrastructural analysis of the *Saccharomyces cerevisiae* mitotic spindle. *J Cell Biol* *129*, 1601-1615.
- Wood, K. W., Sakowicz, R., Goldstein, L. S., and Cleveland, D. W. (1997). CENP-E is a plus end-directed kinetochore motor required for metaphase chromosome alignment. *Cell* *91*, 357-366.
- Wu, H., Lan, Z., Li, W., Wu, S., Weinstein, J., Sakamoto, K. M., and Dai, W. (2000). p55CDC/hCDC20 is associated with BUBR1 and may be a downstream target of the spindle checkpoint kinase. *Oncogene* *19*, 4557-4562.
- Xia, G., Luo, X., Habu, T., Rizo, J., Matsumoto, T., and Yu, H. (2004). Conformation-specific binding of p31(comet) antagonizes the function of Mad2 in the spindle checkpoint. *Embo J* *23*, 3133-3143.
- Yamamoto, A., Guacci, V., and Koshland, D. (1996a). Pds1p is required for faithful execution of anaphase in the yeast, *Saccharomyces cerevisiae*. *J Cell Biol* *133*, 85-97.
- Yamamoto, A., Guacci, V., and Koshland, D. (1996b). Pds1p, an inhibitor of anaphase in budding yeast, plays a critical role in the APC and checkpoint pathway(s). *J Cell Biol* *133*, 99-110.

- Yang, S. S., Yeh, E., Salmon, E. D., and Bloom, K. (1997). Identification of a mid-anaphase checkpoint in budding yeast. *J Cell Biol* *136*, 345-354.
- Yao, X., Abrieu, A., Zheng, Y., Sullivan, K. F., and Cleveland, D. W. (2000). CENP-E forms a link between attachment of spindle microtubules to kinetochores and the mitotic checkpoint. *Nat Cell Biol* *2*, 484-491.
- Yen, T. J., Compton, D. A., Wise, D., Zinkowski, R. P., Brinkley, B. R., Earnshaw, W. C., and Cleveland, D. W. (1991). CENP-E, a novel human centromere-associated protein required for progression from metaphase to anaphase. *Embo J* *10*, 1245-1254.
- Yu, H. G., Muszynski, M. G., and Kelly Dawe, R. (1999). The maize homologue of the cell cycle checkpoint protein MAD2 reveals kinetochore substructure and contrasting mitotic and meiotic localization patterns. *J Cell Biol* *145*, 425-435.
- Zhang, D., and Nicklas, R. B. (1996). 'Anaphase' and cytokinesis in the absence of chromosomes. *Nature* *382*, 466-468.
- Zhivotovsky, B., and Kroemer, G. (2004). Apoptosis and genomic instability. *Nat Rev Mol Cell Biol* *5*, 752-762.
- Zhou, B. B., and Elledge, S. J. (2000). The DNA damage response: putting checkpoints in perspective. *Nature* *408*, 433-439.
- Zieve, G. W., Turnbull, D., Mullins, J. M., and McIntosh, J. R. (1980). Production of large numbers of mitotic mammalian cells by use of the reversible microtubule inhibitor nocodazole. Nocodazole accumulated mitotic cells. *Exp Cell Res* *126*, 397-405.
- Zinkowski, R. P., Meyne, J., and Brinkley, B. R. (1991). The centromere-kinetochore complex: a repeat subunit model. *J Cell Biol* *113*, 1091-1110.
- Zirkle, R. E. (1970). Ultraviolet-microbeam irradiation of newt-cell cytoplasm: spindle destruction, false anaphase, and delay of true anaphase. *Radiat Res* *41*, 516-537.



## **Chapter 2**

### **Conformation-specific Binding of Mad2 by Spindle Checkpoint Proteins**

#### **Mad1, Cdc20, and CMT2**

## 2.1 Abstract

The spindle assembly checkpoint monitors kinetochore-microtubule interactions in mitosis to prevent errors of chromosome segregation. Mad and Bub checkpoint proteins localize to unattached or maloriented chromosomes and generate a signal that delays anaphase onset until all chromosomes achieve bipolar attachment. This signal is transmitted to Cdc20, an essential activator of the anaphase promoting complex. Mad2 plays a critical role in checkpoint signaling through its association with partner proteins such as Mad1, Cdc20, and the recently-discovered CMT2 protein. In this paper, we compare directly the association of Mad2 with its binding partners and show that whereas Mad1, Cdc20, and other Mad2 interactors compete with each other with each for binding to a single site on Mad2, CMT2 binding is non-competitive. Mad1 and Cdc20 constitute a class of high affinity interactors that contact the Mad2 peptide-binding cleft. CMT2 selectively binds the closed conformation of the Mad2 C-terminal tail. As a consequence, ternary complexes containing Mad2, CMT2 and either Mad1 or Cdc20 can form. Based on the Mad2 crystal structure, we propose that CMT2 inhibits Mad2 function by capping the Mad2 homodimerization surface.

## 2.2 Introduction

The spindle assembly checkpoint constitutes a signal transduction system that makes the dissolution of sister chromatid cohesion dependent on correct kinetochore-microtubule binding (Chan and Yen, 2003; Cleveland et al., 2003; Hoyt, 2001; Lew and Burke, 2003; Musacchio and Hardwick, 2002). Spindle checkpoint genes were first isolated in *S. cerevisiae* and are highly conserved among eukaryotes (Hoyt et al., 1991; Li and Murray, 1991). During prometaphase in animal cells, Mad1, Mad2, BubR1, Bub1, Bub3 and Mps1 accumulate to high levels on kinetochores and then dissociate as microtubule attachments form. Mad and Bub proteins remain bound to the kinetochores of unattached and maloriented chromosomes, however, and maintain mitotic arrest until spindle assembly is complete (Hoffman et al., 2001). Checkpoint activation leads to the inhibition of Cdc20, an essential activator of the anaphase promoting complex/cyclosome (APC/C<sup>Cdc20</sup>). APC/C<sup>Cdc20</sup> is a multi-subunit ubiquitin ligase that targets cyclin B, securin and a variety of other proteins for destruction at the metaphase-anaphase transition (Nasmyth, 2002; Peters, 2002). Mad2 and BubR1 can be co-purified as part of a large mitotic checkpoint complex (MCC) and the two proteins appear to function together in Cdc20 regulation (Sudakin et al., 2001). Thus, we can think of kinetochores as the input to the spindle checkpoint pathway and activated Mad2 and BubR1 as the output.

Despite intense study, the mechanisms of checkpoint signals generation at kinetochores and propagation through the cell to regulate APC/C<sup>Cdc20</sup> remain poorly understood. Of particular interest are the activation of Mad2 at kinetochores and the Mad2-dependent inhibition of Cdc20. Dissection of Mad2 activity has proven difficult due to its multiple binding partners and dynamic localization. In cells with an activated

checkpoint, Mad2 is found both on kinetochores and in the cytosol. FRAP experiments show that Mad2 cycles between kinetochore-associated and cytosolic pools with a half-life of 25 sec., although a subset of Mad2 also remains stably kinetochore-bound (Howell et al., 2000). A considerable body of data suggests that the formation of Mad2-Mad1 and Mad2-Cdc20 complexes is essential for Mad2 trafficking and checkpoint signaling. Mad1 lies upstream of Mad2 in the checkpoint pathway (Chen et al., 1999; Chen et al., 1998; Luo et al., 2002), is highly concentrated at kinetochores (Chen et al., 1998) and, at least in yeast and frogs, is required for the formation of Mad2-Cdc20 complexes (Chung and Chen, 2002; Hwang et al., 1998). In contrast to Mad1 and Mad2, Cdc20 and APC are found at multiple locations in cells such as the kinetochore, spindle, and spindle poles (Kallio et al., 2002). Thus, it is generally assumed that checkpoint signaling involves the Mad1-dependent activation of Mad2 at kinetochores followed by Mad2's dissociation from kinetochores and re-association with cytoplasmic Cdc20.

Structural analysis of Mad2 shows that it has two meta-stable conformations that interconvert on a time scale of hours in the absence of bound ligand (Luo et al., 2004). These are referred to as “open” (O-Mad2) and “closed” (C-Mad2). The formation of the closed conformation of Mad2, which is facilitated by Mad1 and Cdc20 binding, involves a major rearrangement of the Mad2 C-terminal tail (Luo et al., 2002; Sironi et al., 2002). Crystallography of Mad1-Mad2 co-complexes reveals that Mad1 binds within a cleft in Mad2 and that tail closure creates a “safety belt” locking Mad1 in place (Sironi et al., 2002). NMR analysis suggests a similar mode of binding for Cdc20 (Luo et al., 2002), although it remains unclear how closely the large multi-component checkpoint complexes found in cells correlate with Mad2 binding activities observed for purified proteins. A

paradox of these structural findings is that they involve Mad1-Mad2 and Mad2-Cdc20 complexes whose half-life of 16 hours or more is much greater than the half-life of the checkpoint signal (which shuts off in cells within minutes of chromosome-microtubule binding (Rieder et al., 1994)) or the 25 sec required for Mad2 to cycle between kinetochore and cytosolic pools (Howell et al., 2000). The high affinity with which Mad2 binds to Mad1 and Cdc20 seems incompatible with dissociation from one protein and re-association with the other, and even if this were possible, it is not clear how an activated state could be transmitted from Mad1 to Cdc20. One possibility is that Mad2 might be covalently modified. Phosphorylation of Mad2 has been detected in human cells (although not in yeast) and is proposed to block binding to both Mad1 and Cdc20 rather than to transmit a signal (Wassmann et al., 2003). A second possibility is that Mad2 signaling might involve a switch between the two Mad2 conformations, which have been shown to have different potencies as Cdc20 inhibitors (Luo et al., 2004). A third possibility is that Mad2 might bind to a protein other than Mad1 and Cdc20 and formation of this complex might be involved in signal transmission.

Recent work points to a variation on this third possibility that is somewhat counterintuitive: the extra Mad2-binding protein is Mad2 itself. De Antoni et al have shown that Mad2 undergoes selective heterotypic homodimerization in which open Mad2 (O-Mad2) can dimerize with closed, ligand-bound Mad2 (C-Mad2), but neither conformer can self-associate (De Antoni et al., 2005). Mutation of two residues, R133A and Q134A, abrogates Mad2 dimerization, and such mutants cannot localize to kinetochores *in vivo*, presumably because they cannot bind Mad1-C-Mad2 complexes. De Antoni et al propose that Mad2 dimerization serves to enrich O-Mad2 at kinetochores,

thus positioning it for Cdc20 binding when the checkpoint becomes active. They propose that, in theory, heterotypic Mad2 dimerization could also be nucleated on C-Mad2-Cdc20 complexes in the cytoplasm, thus providing a platform for signal amplification. If correct, this model of Mad2 complex assembly would resolve the apparent paradox of stable kinetochore complexes and rapid exchange of Mad2 between the kinetochore and the cytosol. However, if O-Mad2 activation is nucleated on C-Mad2 complexes, which are known to exist throughout the cell cycle (Iouk et al., 2002; Poddar et al., 2005; Shah et al., 2004), it remains unclear how either generation of active Mad2 or amplification of Mad2 signal is made sensitive to kinetochore-microtubule attachment. Furthermore, neither Mad2 dimerization nor its rapid cycling through kinetochores has been observed in yeast, suggesting that they may not be necessary for some aspects of Mad2 checkpoint function. Finally, Mad2 is not sufficient for checkpoint activity in the absence of other checkpoint effectors such as BubR1, which may act synergistically (Sudakin et al., 2001). The work of De Antoni et al in identifying an intermediate step in checkpoint activation calls into question the exact molecular composition of the “wait anaphase” signal. BubR1 and Mps1 cycle through kinetochores with kinetics similar to Mad2 (Howell et al., 2004; Shah et al., 2004) and it remains to be seen how Mad2 dimerization relates to formation of a larger checkpoint complex such as MCC.

CMT2 has recently been shown to be an additional Mad2 binding partner in higher eukaryotes. It has been proposed that CMT2 negatively regulates the checkpoint by competing with Cdc20 for Mad2 binding at the metaphase to anaphase transition (Habu et al., 2002). However, it is not known whether CMT2 binds to Mad2 in the same manner as Mad1 and Cdc20 and its precise roles in regulating mitotic regulation remain

unclear. In this chapter, we investigate the biochemistry of interactions between Mad2 and its binding partners, focusing particularly on CMT2. We demonstrate that short peptides in Mad1 and Cdc20 bind with high affinity to Mad2 in a manner that requires pocket and tail residues, but that CMT2 interacts with Mad2 in a fundamentally different manner that is not competitive with Mad1 or Cdc20. This different binding mode also manifests itself as a difference in function that is described in the following chapter: while Mad1 and Cdc20 act to maintain cell cycle signaling, CMT2 antagonizes it, apparently by associating with and inactivating the Mad2 closed conformer.

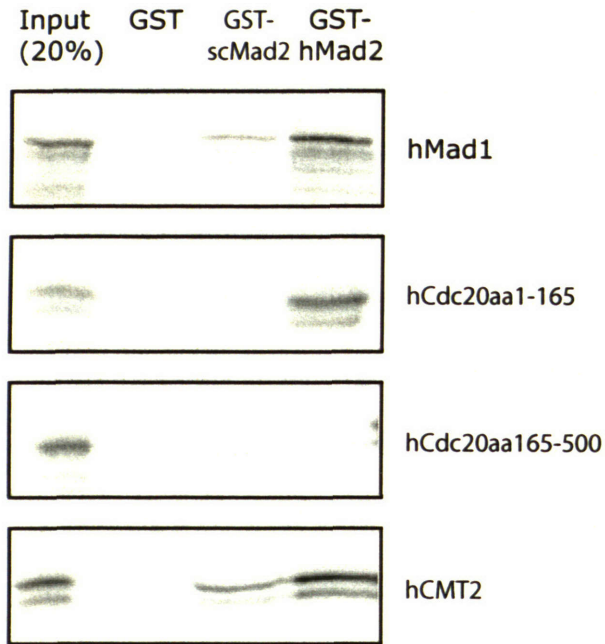
## **2.3 RESULTS**

### **2.3.1 Identification of Mad2-binding regions in Mad1 and Cdc20**

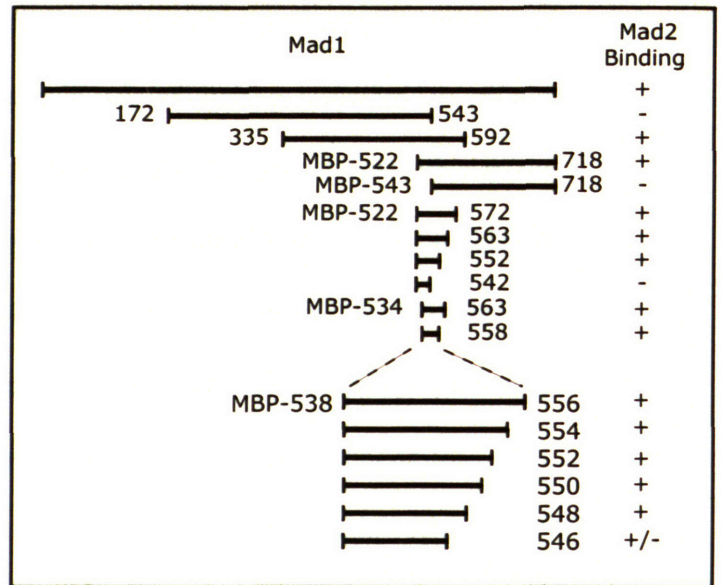
As a first step in dissecting interactions between Mad2 and its binding partners, we mapped the sequences in Mad1 and Cdc20 required for Mad2 association. Mad2 has been shown to bind stably to a 100 residue fragment of Mad1 (Sironi et al., 2002) and to the N-terminal 153 residues of Cdc20 (Zhang and Lees, 2001). Mutations near positions 205-210 of budding yeast Cdc20 and 131 of fission yeast Cdc20 (Slp1) abrogate Mad2 association and disrupt checkpoint control (Hwang et al., 1998; Kim et al., 1998). However, Mad2 residues required for Mad2-Mad1 and Mad2-Cdc20 interaction have not been determined experimentally. Indeed, one recent structural analysis relied on phage display to find short tight-binding Mad2 peptides (Luo et al., 2002). We therefore examined the ability of *in vitro* translated fragments of Mad1, Cdc20, and CMT2 to bind bacterially expressed GST-Mad2 in a simple pull-down assay (Figure 2.1A). Both hMad1 and hCdc20 exhibit striking species-specificity and bind well to hMad2 but poorly to *S.*

Figure 2.1

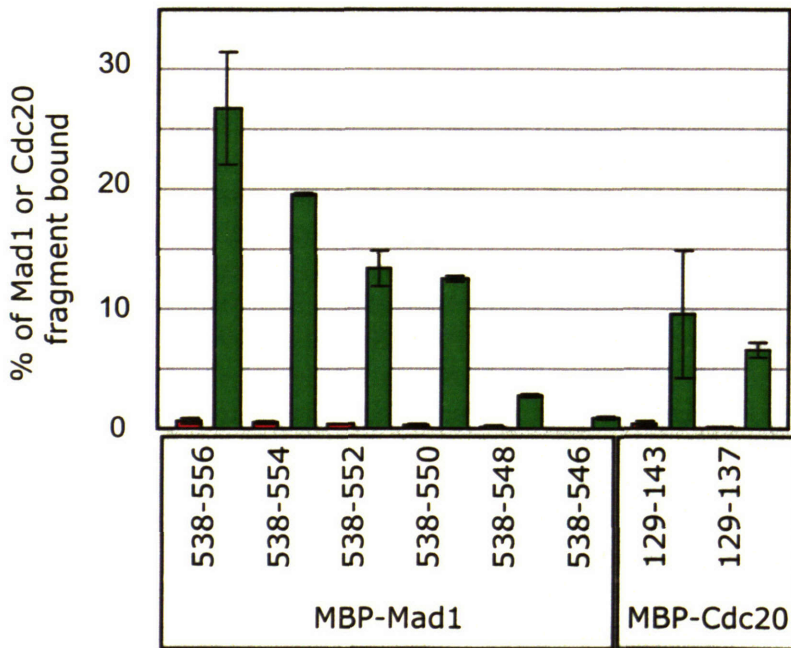
A



B



C



Immobilized: **GST-scMad2** or **GST-hMad2**

binding region length (aa):

19 17 15 13 11 9 15 9

D

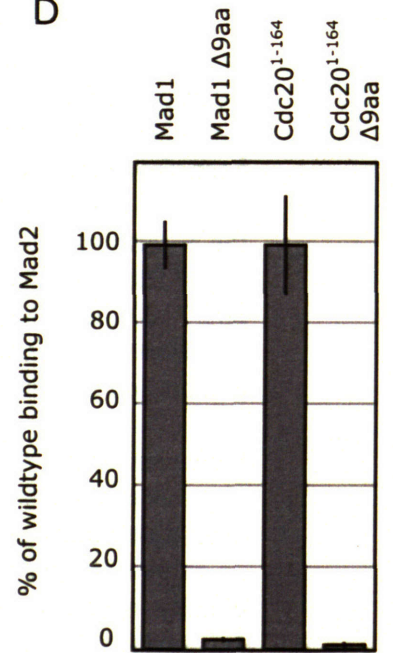




**Figure 2.1: Mapping Mad2 binding interactions**

(A) hMad1, hCMT2, hCdc20<sup>1-165</sup>, and hCdc20<sup>165-500</sup> were <sup>35</sup>S-labeled by *in vitro* translation and incubated with GST, GST-scMad2, or GST-hMad2. After centrifugation and washing, bound proteins were quantitated following SDS-PAGE and autoradiography. The input lane represents 20% of the total labeled protein in the binding reaction. (B) Schematic of Mad1 mapping experiments. *In vitro* translated Mad1 fragments corresponding to the indicated sequences were analyzed by pull-down as described in (A). Fragments of 200 residues or less were translated as fusions to maltose binding protein (MBP) to ease detection on gels. (C) Short Mad1 and Cdc20 fragments bind Mad2. Mad1 and Cdc20 fragments spanning the indicated residues were fused to MBP and binding to yeast (y) or human (h) Mad2 was assayed as in (A). Graph indicates mean and range of two independent experiments. (D) Nine residue motifs in both Mad1 and Cdc20 are required for Mad2 binding. Full length Mad1, Mad1 $\Delta$ 9 lacking residues 541-549, Cdc20<sup>1-164</sup> and Cdc20<sup>1-164</sup>  $\Delta$ 9 lacking residues 129-137 were examined in pull-down assays as described in (A). Binding to non-deleted proteins was set at 100% in both cases. Error bars show the range of two independent experiments.

*cerevisiae* Mad2, while hCMT2 binds nearly equally to yeast and human Mad2. Under these assay conditions, a deletion series identified a nine residue Mad1 sequence (positions 538-546) as the sole Mad2-binding sequence in Mad1 (Figure 2.1B and 2.1C and data not shown). Similar truncation analysis of Cdc20 limited its Mad2-binding activity to a 9aa region in the amino terminus (Figure 2.1A and 2.1C). When these nine residue regions were deleted from full-length Mad1 and Cdc20, binding to Mad2 was abolished (Figure 2.1D). Significant truncation of CMT2 from either the N- or C-terminus also abrogated Mad2 binding (data not shown and M. Mapelli, personal communication).

### **2.3.2 Refinement and characterization of the Mad2-binding motif**

When a peptide array comprising successive 20 residue peptides spanning Mad1 positions 538-546 was probed with *in vitro* translated Mad2, two tight-binding peptides were identified (Figure 2.2A). Similar array analysis of human Cdc20 12mers identified a sequence centered on position 130 as sufficient for high affinity Mad2 association (Figure 2.2B). When an array of peptides carrying point mutations in the tightest binding Cdc20 peptide was probed with recombinant Mad2, Cdc20 positions 129-133 were found to be critical for Mad2 association (Fig 2.2C). Combining mapping data and sequence analysis of Mad1 and Cdc20 from fourteen different species results in an overall consensus Mad2-binding sequence of (K/R)(I/V)(I/V/L)X $\phi$ XXXP (Figure 2.2D and E and Supplemental Figure 2.1).

Synthetic peptides containing this consensus motif were assayed for Mad2 binding by surface plasmon resonance (SPR) and found to have non-ideal Langmuir

Figure 2.2

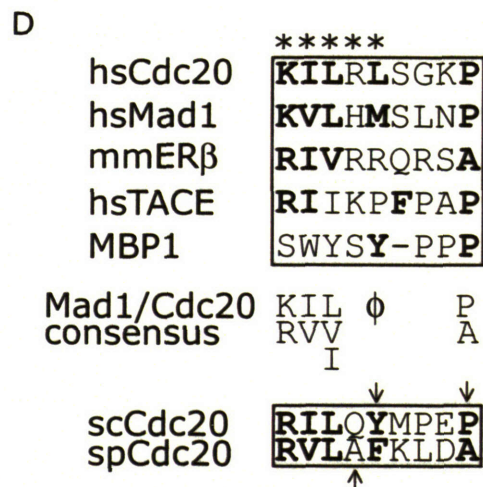
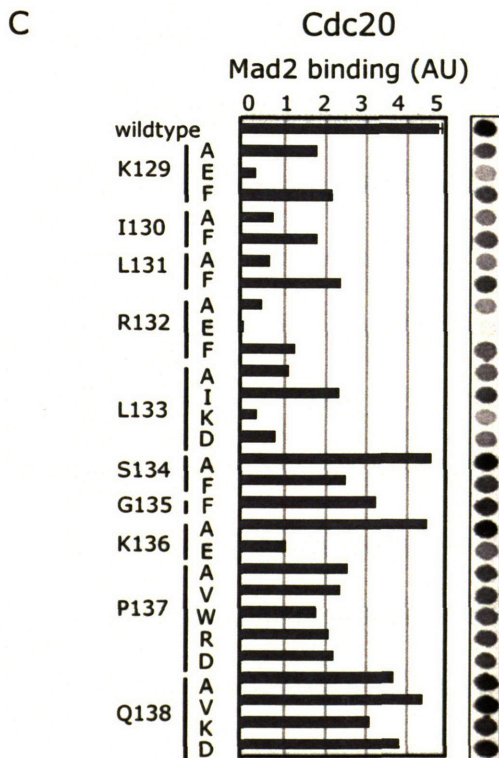
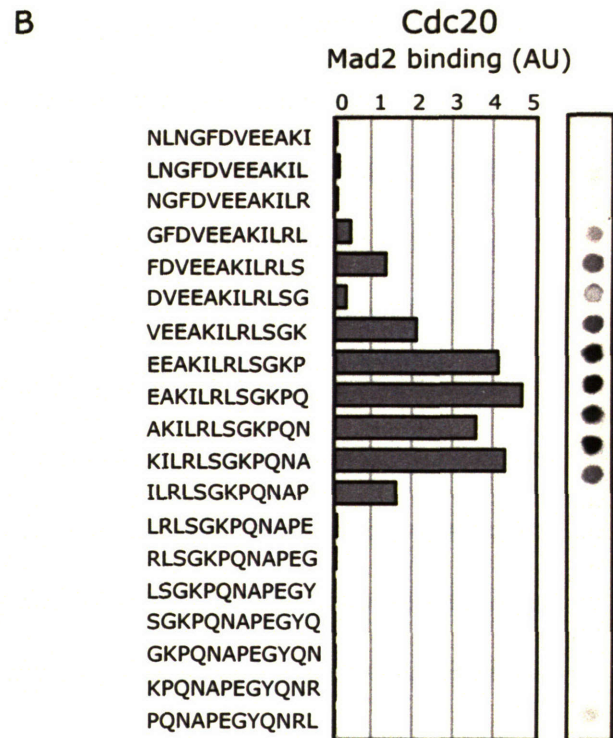
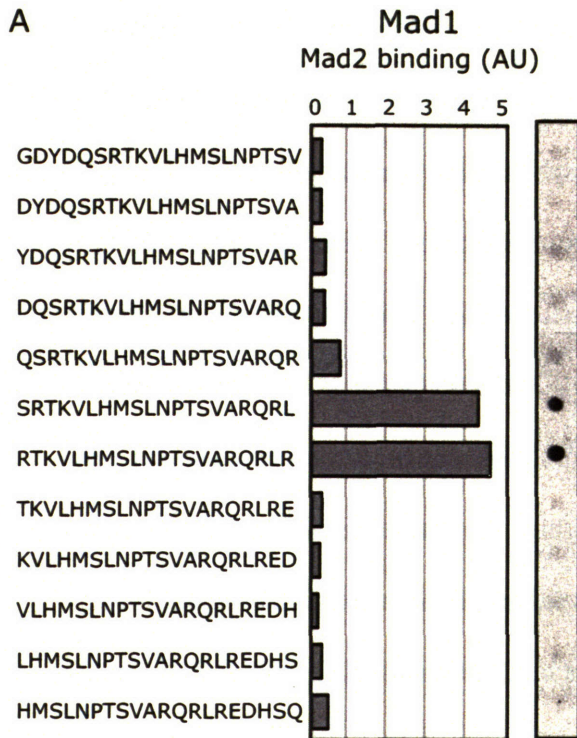


**Figure 2.2:** Refinement of the Mad2-binding motif

(A) Successive 20-residue Mad1 peptides spanning the region 532-562 and synthesized on a nitrocellulose membrane were probed for Mad1 binding using <sup>35</sup>S-labeled Mad2 translated *in vitro*. Filters were scanned on a PhosphorImager for quantitation. Bars indicate Mad2 binding activity for each peptide spot in arbitrary units. (B) As in (A), successive 12 residue peptides from Cdc20 residues 119-148 were synthesized on filters and probed with <sup>35</sup>S-labeled Mad2. (C) Synthetic 12-residue Cdc20 (127-138) peptides representing wild-type (EAKILRLSGKPQ) and mutated sequences were spotted and probed with <sup>35</sup>S-labeled Mad2 as in (C). (D) Alignment of the minimal Mad2 binding motif from several proteins. Asterisks indicate residues whose mutation abrogates Mad2 association *in vivo*; bold text denotes residues that conform to the Mad2-binding consensus. Arrows indicate the position of known checkpoint-defective mutants in budding yeast. See Table 1 for further details. (E) Graphical depiction of the relative contribution of each residue in the optimal Mad2-binding motif from all known Cdc20 and Mad1 homologs, human TACE, and human ERβ. Graphic was generated using the WebLogos program.

association and dissociation kinetics suggestive of a conformational change (data not shown). To estimate the affinity of Mad2 for a 25-residue Mad1 peptide, Mad2 was immobilized and probed with Mad1 peptide that had been pre-bound to titrated Mad2 (Figure 2.3A), giving an approximate  $K_d$  of 25nM. Isothermal titration calorimetry (ITC) with bacterially expressed Mad2 showed high affinity binding ( $K_d$  of 20-40 nM; Figure 2.3B and Table 2.1) to 20-25 residue peptides and to internal peptides as short as nine residues ( $K_d$  of 80 nM for Mad1 KVLHMSLNP). From these data we conclude that a short nine residue epitopes at Mad1<sup>541-549</sup> and Cdc20<sup>129-137</sup> are necessary and sufficient for tight Mad2 binding.

With this consensus sequence we identified by inspection putative Mad2-binding sequences in other Mad2 partners of unknown physiological significance, the estrogen receptor ER $\beta$  and the metalloprotease TACE/ADAM17 (Nelson et al., 1999; Poelzl et al., 2000). Peptide array and mutant analysis (Supplemental Figure 2.2) revealed that these sequences were indeed the sites of Mad2 interaction and that both mER $\beta$  and TACE bind to Mad2 in manner similar to Mad1 and Cdc20. Scanning the human genome with an optimized consensus motif revealed a wide array of putative Mad2 binding proteins which are summarized in Table 2.2. Cdc20 possesses a second putative Mad2 binding site in its WD domain, but this domain does not exhibit measurable Mad2 binding (Figure 2.1A) and likely is constrained within the tight WD fold. In contrast, even low stringency searches with the Mad2 consensus sequence did not reveal any evidence of a second Mad2 binding site in human Mad1, confirming our mapping data. Moreover, no potential Mad2 binding sites were found in CMT2, implying that CMT2 might bind to Mad2 in a different manner than Mad1 and Cdc20.

Figure 2.3

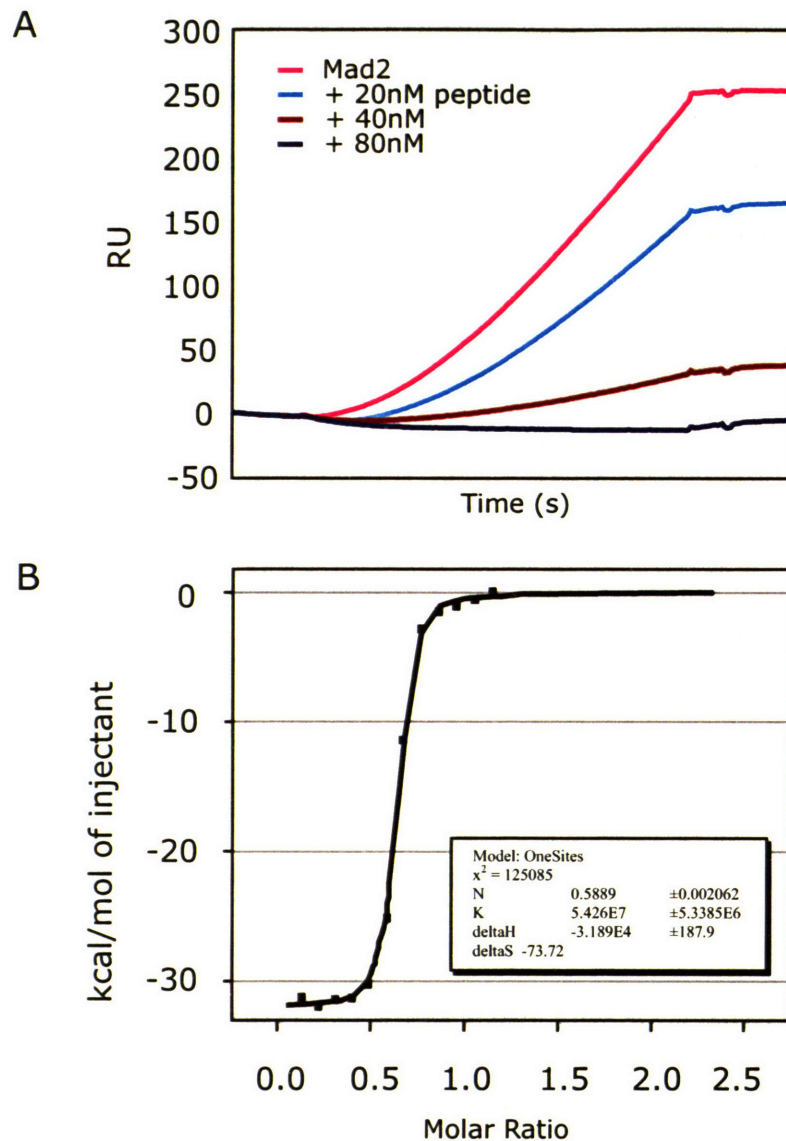


**Figure 2.3:** A Mad1<sup>534-558</sup> peptide binds Mad2 with high affinity

(A) Synthetic Mad1<sup>534-558</sup> was immobilized on BIAcore sensor chips (BIAcore International SA, Neuchatel, Switzerland). Recombinant Mad2 was pre-incubated with indicated concentrations of Mad1<sup>534-558</sup> peptide and then passed over Mad1<sup>534-558</sup>-coupled surfaces. Binding was followed by surface plasmon resonance. (B) Calorimetric analysis of Mad1<sup>534-558</sup>-Mad2 binding. Mad1<sup>534-558</sup> peptide was injected with mixing into a solution of Mad2 and evolved enthalpies were measured. Graph shows evolved enthalpies fit with the standard model data for a single binding site.

Table 2.1

Table I: Affinities of Mad2-peptide complexes by ITC

Protein	Residues		$K_d$ (nM)	Source
Mad1	534-558	DYDQSRTKVLHMSLNPTSVARQLR	18.4±1.83	1
	539-557	RTKVLHMSLNPTSVARQLR	36.7±20.0	1
	541-549	<b>GSGKVLHMSLNPGSG</b>	82.6±18.9	1
	523-550	EAQLERRALQGDYDQSRTKVLHMSLNPT	270	2
	540-551	TKVLHMSLNPTS	ND	1
Cdc20	124-138	DVEEAKILRLSGKPKQ	28.4±7.74	1
	127-141	EAKILRLSGKPKQNAPEGYQNR	15.6±3.71	1
	129-137	<b>GSGKILRLSGKPKGSG</b>	36.5±8.94	1
	129-147	KILRLSGKPKQNAPEGYQNR	42.7±7.03	1
	118-138	LNLNGFDVEEAKILRLSGKPKQ	100	3
	127-137	EAKILRLSGKPKQ	3600	4
TACE	723-734	SVRIKPFPAPO	ND	
mER $\beta$	180-191	GYRIVRRQRSAS	ND	
MBP1		SWYSYPPQRAV	90	2
MBP2		DARIIKLPVPKP	ND	

(1) This study

(2) De Antoni et al., 2004 (submitted)

(3) Sironi et al., 2002

(4) Luo et al., 2002

Residues in bold were added as spacers for the terminal charges.

Table 2.2 – Mad2-binding motifs in human proteins

Protein name	Accession no.	Code	Mad2-binding domain	Description
Mad1	Q9Y6D9	MDL1_HUMAN	221 - 229: KIIIVedIP	Spindle checkpoint protein
Cdc20	Q5JU4	Q5JU4_HUMAN	129 - 137: KILFLsgKP	APC/C subunit
			445 - 453: RVLsltmsP	
TACE/ADAM17	P78536	ADA17_HUMAN	725 - 733: RIIFKFPaP	A disintegrin and metalloproteinase domain 17; TNF-alpha converting enzyme; TNF-alpha convertase
Cdh1/Hct1	Q9UM11	FZR_HUMAN	445 - 453: RVLyLamsP	Fizzy-related protein homolog (Fzr) (Cdh1/Hct1 homolog) (hCDH1) (CDC20-like protein 1)
APC1/Tsg24	Q9H1A4	ANCI_HUMAN	245 - 253: KIVFLntdP	Anaphase promoting complex subunit 1 (APC1) (Cyclosome subunit 1) (Protein Tsg24) (Mitotic checkpoint regulator)
CDC2L5	Q14004	CD2L5_HUMAN	873 - 881: KVIltlwyRP 1241 - 1249: RILeltpEP	Cell division cycle 2-like protein kinase
CDC2L7	Q9NYY4	CD2L7_HUMAN	895 - 903: KVIltlwyRP	Cell division cycle 2-related protein kinase 7
CDK6	Q00534	CDK6_HUMAN	230 - 238: KILdVlgIP	Cell division protein kinase 6
CDK9	P50750	CDK9_HUMAN	188 - 196: RVVtLwyRP	Cell division protein kinase 9
PPP2R1A	P30153	2AAA_HUMAN	484 - 492: KVLamsqDP	Serine/threonine protein phosphatase 2A, 65 kDa regulatory subunit A, alpha isoform; Medium tumor antigen-associated 61 kDa protein
PPP2R1B	P30154	2AAB_HUMAN	497 - 505: KVLWmandP	Serine/threonine protein phosphatase 2A, 55 kDa regulatory subunit B, gamma isoform
PPP2R2C	Q9Y2T4	2ABG_HUMAN	47 - 55: RVVlFqreP	Serine/threonine protein phosphatase 2A, 55 kDa regulatory subunit B, gamma isoform
PPP3CA	Q08209	P2BA_HUMAN	16 - 24: RVVkAvpFP	Serine/threonine protein phosphatase 2B catalytic subunit, alpha isoform
PPP3CB	P16298	P2BB_HUMAN	25 - 33: RVVkAvpFP	Serine/threonine protein phosphatase 2B catalytic subunit, beta isoform
PPP3CC	P48454	P2BC_HUMAN	13 - 21: RVLkAvpFP	Serine/threonine protein phosphatase 2B catalytic subunit, gamma isoform
PPM1B	O75688	PP2CB_HUMAN	340 - 348: RILSAenIP	Protein phosphatase 2C beta isoform
Rad17	O75943	RAD17_HUMAN	221 - 229: KIILVedIP	Cell cycle checkpoint protein RAD17
PR/PGR	P06401	PRGR_HUMAN	919 - 927: KIAGmvpK	Progesterone receptor
ROD	P50748	KNTC1_HUMAN	726 - 734: KVLAPeLiP	Kinetochores-associated protein 1 (Rough deal homolog) (hRod) (HSROD)
KIF13B	Q9NQ8	KI13B_HUMAN	873 - 881: KIIfqAtgIP	Kinesin-like protein KIF13B (Kinesin-like protein GAKIN)
Cdc20-like 2	Q86Y32	Q86Y32_HUMAN	487 - 495: RVLhLalsP	CDC20-like protein form 2
Cdc20-like 3	Q86Y31	Q86Y31_HUMAN	449 - 457: RVLhLalsP	CDC20-like protein form 3
Cdc14C	Q8NCT2	Q8NCT2_HUMAN	156 - 164: RIIfEgdtP	CDC14C protein
MKP-7	Q9BY84	DUS16_HUMAN	25 - 33: KVLILdsrP	Dual specificity protein phosphatase 16; MKP-7
CSEIL	P55060	CAS_HUMAN	601-609: KLIlavsknP	Chromosome segregation 1-like protein



### **2.3.3 Binding of Mad2 to CMT2 is noncompetitive with Cdc20 and Mad1**

To determine directly whether the manner of CMT2 binding to Mad2 differs from that of Mad1 and Cdc20, binding competition studies were performed. Bacterially-expressed GST-Mad2 was incubated sequentially with peptides from Mad1 or Cdc20 or control peptides and then with *in vitro* translated human Mad1, Cdc20 or CMT2. Mad2-bound proteins were then isolated by centrifugation and quantified on gels. The pull-down experiments were reproducible, although 6 hour binding reactions were not representative of true equilibrium binding states for 20 nM interactions. Using pull-downs, we observed that Cdc20-Mad2 binding was reduced 10 to 20-fold in the presence of excess Mad1 or Cdc20 peptide as compared to a scrambled control peptide (Figure 2.4A). Similarly, Mad1-Mad2 binding was reduced by an excess of either Mad1 or Cdc20 peptide (Fig 2.4B). For reasons that are not clear, a tight-binding Cdc20 peptide was less effective as an inhibitor of Mad1-Mad2 binding than an equal affinity Mad1 peptide. This phenomenon was reproducible and may reflect the non-equilibrium conditions of the competition assay. Importantly, the observed cross-competition between Mad1 and Cdc20 peptides confirms the expectation from sequence analysis that the two proteins bind to a common site on Mad2. This competition is not affected by immobilization of Mad2 on a solid support, as peptides also compete for Mad2 binding in solution as assayed by native gel electrophoresis (Supplemental Figure 2.4A and 2.4B). In contrast, the binding of CMT2 to Mad2 was not affected by the presence of excess Mad1 or Cdc20 peptides (Fig 2.4C). Thus, CMT2 binds to Mad2 in a fashion that is not competitive with Mad1 and Cdc20.

Figure 2.4

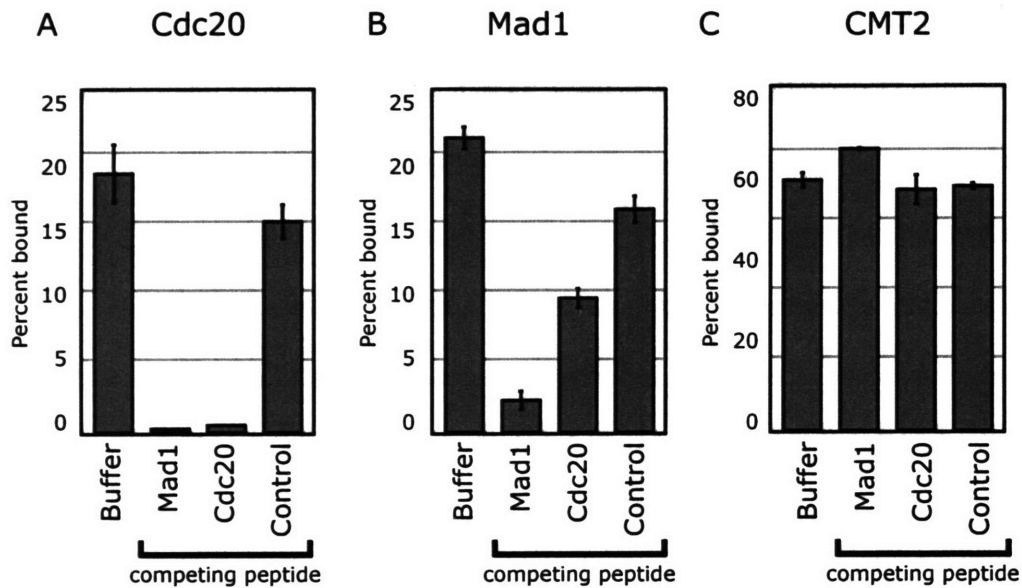


**Figure 2.4:** Mad1 and Cdc20 binding peptides do not compete with CMT2 for Mad2 binding. Purified GST-Mad2 on beads was preincubated overnight with buffer, Mad1 peptide (534-558), Cdc20 peptide (129-147), or a scrambled Mad1 control peptide and then mixed for 6 hours with *in vitro* translated (A) Cdc20, (B) Mad1, or (C) CMT2 and pull-downs performed as described in Figure 1. Bars indicate percentage of co-precipitated *in vitro* translated protein; error bars show the range of two independent experiments.

### 2.3.4 CMT2 binds the Mad2 C-terminal tail

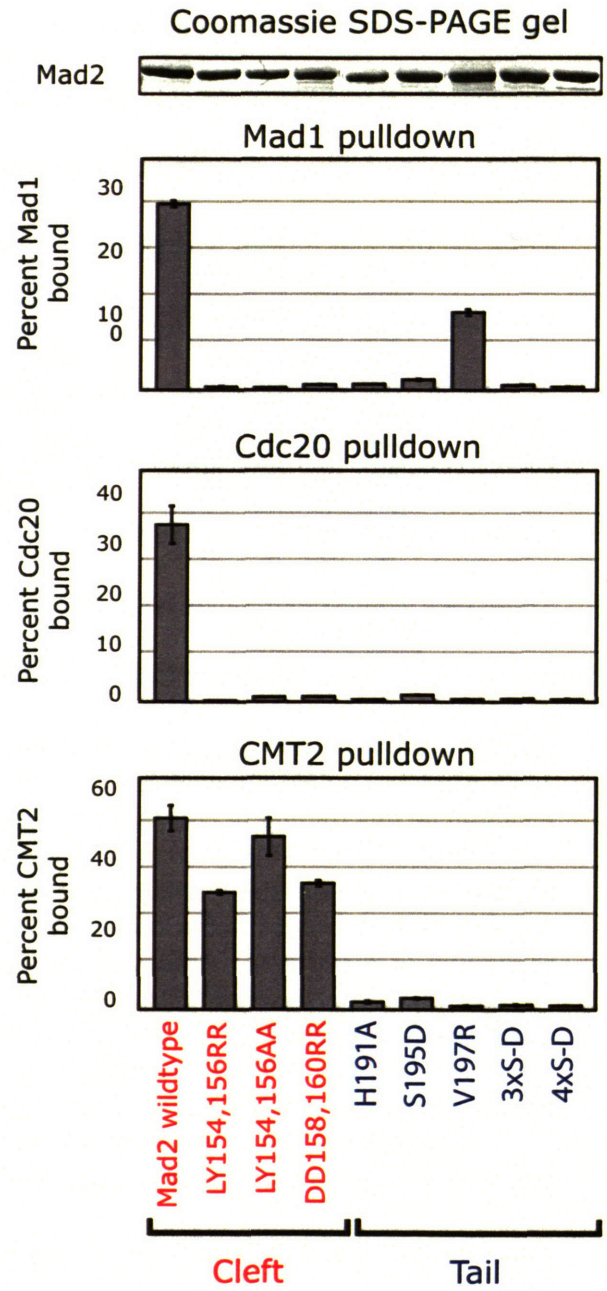
As a different approach to probing interactions involving Mad2, we constructed point mutations in Mad2 surface residues thought to play a role in Mad1 binding. Structurally, these mutations comprise two distinct classes: cleft mutations lying in the Mad2 peptide-binding sheet and tail mutations lying in the C-terminus of the protein and along the  $\beta$ -strand formed when the C-terminal tail closes back over the binding cleft to form the “safety belt” (Figure 2.5A). Eight mutant Mad2 proteins were expressed in *E. coli*, purified to homogeneity and analyzed in parallel for binding to Mad1, Cdc20 and CMT2 (Figure 2.5B). Both cleft and tail mutations in Mad2 were observed to abrogate binding to Mad1 and Cdc20, consistent with predictions from the Mad1-Mad2 structure. These data suggest that it may be possible to identify Mad2 mutations that discriminate between binding to Mad1 and Cdc20. V197R, for example, binds moderately well to Mad1 but not at all to Cdc20 in a pull-down assay. It will be necessary, however, to recapitulate this finding *in vivo* to determine its utility in dissecting the mechanisms of checkpoint signaling. Importantly, three double-mutations in the cleft exhibited clear separation-of-function in that they bound well to CMT2 and poorly or not at all to Mad1 or Cdc20. In contrast, H191A, S195D and V197R, which lie in the tail of Mad2, abolished binding to CMT2 as well as to Mad1 and Mad2. We conclude from these data and from competition experiments that, unlike Mad1 and Cdc20, CMT2 does not bind to Mad2 by inserting into the cleft but by contacting either the C-terminal tail or regions whose structure are affected by tail positioning. Conformational changes in the Mad2 C-terminal tail are responsible for switching Mad2 between open and closed states, and this conformational switch may direct CMT2 binding.

Figure 2.5

A



B



**Figure 2.5:** Mad2-CMT2 binding involves the Mad2 C terminus but not the peptide-binding cleft. **(A)** Mad2 mutants in the tail (blue) or cleft (red) residues of Mad2. Yellow backbone depicts the Mad2-binding portion of Mad1 from Sironi et al (Sironi et al., 2002). **(B)** Binding of wildtype or mutant GST-Mad2 to Mad1, Cdc20, or CMT2 translated *in vitro* was assessed using a pull-down assay as described in Figure 1. Bars indicate percentage of co-precipitated protein; error bars show the range of two independent experiments. Mad2 pseudophosphorylation mutants S195D, 3xS-D, and 4xS-D are named following the convention of Wassmann (Wassmann et al., 2003). 3xS-D incorporates mutations at positions S178, S185, and S195, all of which lie in the Mad2 tail. 4xS-D has an additional mutation at S170 in the overlying safety belt. Equal loading of GST-Mad2 mutants was ensured by quantitation of mutant proteins on SDS-PAGE gels followed by Coomassie staining.

### 2.3.5 Formation of ternary CMT2 complexes *in vitro*

The cross-competition and mutant analysis described above strongly suggests that CMT2 binds to Mad2 in a distinct fashion from Mad1 and Cdc20. If this is true, then it should be possible to form ternary complexes involving CMT2, Mad2 and either Mad1 or Cdc20. To test this idea, gel filtration chromatography was used to analyze the hydrodynamic properties of various complexes assembled *in vitro* from recombinant proteins and protein fragments. Bacterially-expressed Mad2 eluted from a Superdex 75 column as a dimer (Figure 2.6A), while CMT2 eluted from the same column in a position consistent with a monomer. The behavior of Mad2 under these conditions has been analyzed in detail previously and reflects the existence of an equilibrium between open and closed Mad2 states and between monomeric and dimeric forms (De Antoni et al., 2005; Luo et al., 2004; Sironi et al., 2001). When CMT2 and Mad2 were mixed and then subjected to column analysis, all of the CMT2 and a fraction of the Mad2 co-eluted at an apparent molecular weight larger than Mad2 dimer and consistent with a 1:1 Mad2:CMT2 complex (Figure 2.6A, lower panel fractions 2-8). The fraction of Mad2 that did not bind CMT2 (lower panel fractions 9-10) may represent a conformer pool that is not competent for CMT2 binding. This pool elutes at the Mad2 monomer size and suggests that CMT2 binding dissociates the C-Mad2-O-Mad2 dimer into a Mad2-CMT2 dimer and a Mad2 monomer. Similar dimer dissociation is observed with binding of synthetic peptides to recombinant Mad2 (Figure 2.6D red trace, Supplemental Figure 2.4E) and is consistent with the idea that single Mad2 conformers cannot homodimerize (De Antoni et al., 2005). This suggests that in this *in vitro* context CMT2 is binding to either C-Mad2 or O-Mad2, but not to both or to a Mad2 dimer.

Figure 2.6

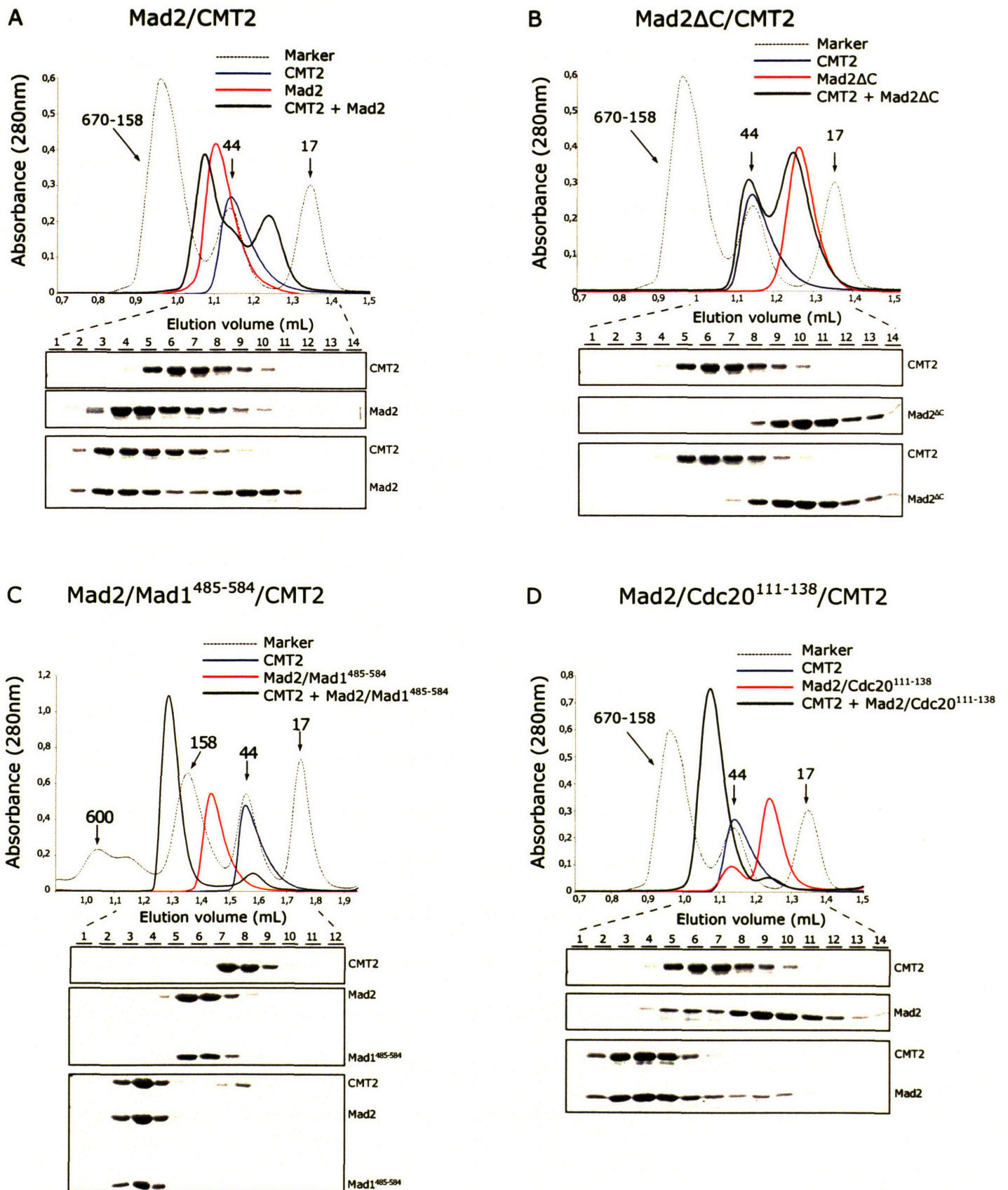


**Figure 2.6:** Formation of ternary complexes involving CMT2, Mad2, Mad1 and Cdc20

Size exclusion chromatography of complexes containing Mad2, CMT2 and other proteins on Superdex 75 (A, B, C) or Superdex 200 (D). In each panel, column traces are shown above and Coomassie-stained SDS-PAGE gels of successive fractions are shown below. Colored traces represent the elution of profile of individual components and the heavy black trace represents the elution profiles of mixtures following 1 hr of incubation at room temperature. Molecular weight markers are shown as a dotted line. Experiments were performed with CMT2 alone and CMT2 mixed with (A) wild-type Mad2, (B) a Mad2 $\Delta$ C mutant lacking the C-terminal tail, (C) Mad2 co-expressed with Mad1<sup>485-584</sup>, or (D) Mad2 Cdc20 bound to Cdc20 (111-138) peptide.



Because O-Mad2 and C-Mad2 cannot be distinguished chromatographically, we tested the ability of CMT2 to bind a conformation-specific Mad2 mutant. Mad2 $\Delta$ C lacks C-terminal residues 196-205, does not bind Mad1 or Cdc20, and exerts a dominant negative effect on checkpoint activation in nocodazole (Luo et al., 2000; Luo et al., 2002). Mad2 $\Delta$ C did not shift CMT2 into a higher molecular weight form (Figure 2.5B), suggesting that CMT2 specifically requires an intact Mad2 tail for binding.

Peptide fragments of Mad1 and Cdc20 do not compete with CMT2 for Mad2 binding (Figure 2.4C). While it is possible that CMT2 forms ternary complexes with Mad2 and either Cdc20 or Mad1, it is also possible that CMT2 either actively displaces Mad2 ligands (Habu et al., 2002) or stabilizes Mad2 in a conformation that promotes peptide release. To test whether a ternary complex can form with Mad1, recombinant CMT2 was mixed with Mad2 that had been co-expressed with a 100-residue fragment of Mad1 (co-expression of Mad2 with Mad1<sup>485-584</sup> is necessary for solubility; Sironi et al. 2002). Gel filtration revealed formation of a species that eluted more rapidly than either CMT2 or Mad2- Mad1<sup>485-584</sup> alone and represented a single large complex containing all three proteins (Fig 2.5C). When eluted fractions were analyzed by SDS-PAGE and Coomassie staining, stoichiometric amounts of each protein were observed, suggestive of a 1:1:1 or 2:2:2 complex.. To investigate whether a triple complex could also assemble between CMT2, Mad2 and Cdc20, Cdc20 peptide in excess was added to CMT2 and Mad2. All of the Mad2 and CMT2 were observed to shift into a single large species (Figure 2.5D). Under the conditions used here, Mad2 is known to bind avidly to Cdc20 peptide and we presume that CMT2-Mad2 association is increased in the presence of peptide because Mad2 is driven into a closed conformation (see discussion for details).

We conclude from these data that stable Mad1-Mad2-CMT2 and Cdc20-Mad2-CMT2 ternary complexes can assemble from recombinant proteins and that CMT2 must therefore bind to the closed conformation of Mad2 regardless of ligand occupancy.

## 2.4 DISCUSSION

Here we report a biochemical analysis of interactions between the spindle checkpoint protein Mad2 and three binding partners known to play a role in mitotic regulation: Mad1, Cdc20 and CMT2. We establish that Mad2 binds to these three proteins in two distinct ways. Peptides as short as 9 residues derived from Mad1, a protein which lies upstream of Mad2 in the checkpoint signaling pathway, and Cdc20, a downstream protein, compete with each other for binding to a common site on Mad2. High resolution structural analysis has shown that this binding involves interactions between Mad2 and peptide ligands within a defined cleft, as well as a major structural rearrangement of Mad2 from an open into a closed conformation (Luo et al., 2002; Sironi et al., 2002). In the closed conformation, the C-terminal tail moves over the cleft (forming a “safety belt”) and blocks ligand release. Proteins such as TACE and ER $\beta$ , which make tight complexes with Mad2 of unknown physiological significance, also bind in the Mad2 cleft. In contrast, we find that CMT2 binds to Mad2 in a distinct fashion that is not competitive with Mad1 and Cdc20 but appears to be selective for the closed Mad2 conformation. As a consequence, stable triple complexes comprising Mad2-CMT2-Mad1 or Mad2-CMT2-Cdc20 can form. RNAi and over-expression studies described in chapter 3 establish that the structural distinction between Mad1/Cdc20-Mad2 and CMT2

–Mad2 binding reflects a distinct role for CMT2 as a repressor of Mad2-mediated spindle checkpoint signaling *in vivo*.

#### **2.4.1 Binding of Mad2 to Mad1, Cdc20 and CMT2**

Because the checkpoint signal is “transmitted” in some manner from Mad1 to Cdc20, an obvious question is whether Mad2 binds identically to its target sequence in these two proteins. It has been proposed that Mad2 might be channeled from Mad1 to Cdc20 (Luo et al., 2002; Luo et al., 2004; Sironi et al., 2002), although the mechanisms behind such exchange remain obscure. De Antoni et al suggest that binding of an additional O-Mad2 molecule to C-Mad2-Mad1 primes and positions O-Mad2 for binding to Cdc20. Structural analysis establishes that residues along an extended cleft in Mad2 are responsible for sequence-selective binding to extended peptide motifs in Mad1 and Cdc20. However, some controversy remains whether the short sequences implicated in binding by structural analysis are really sufficient for high-affinity association of Mad1 and Cdc20 to Mad2; one recent structural analysis, for example, relied on phage display to find high-affinity Mad2-binding peptides (Luo et al., 2002). It has been suggested that Mad1-Mad2 binding may be stabilized either by Mad1 dimerization or by Mad1 sequence elements outside the Mad2-binding region, although this has been difficult to interpret due to asymmetry of the two Mad1-Mad2 units in the crystal structure (Sironi et al., 2002). The peptide-based analysis in this chapter, in addition to mutagenesis and ITC data, establishes conclusively that short nonamer peptides from Mad1 and Cdc20 are both necessary and sufficient for high affinity Mad2 binding with a  $K_d \sim 20\text{-}40$  nM. In addition, we show that no other sequence in Mad1 is sufficient for binding Mad2. This

supports the assertion that Mad2 dimerization is responsible for formation of an O-Mad2-C-Mad2-Mad1 complex and not a second Mad2 binding site on Mad1 (DeAntoni et al., 2005). As expected, the mutation of Mad2 residues along the cleft involved in Mad1 and Cdc20 binding abrogates association *in vitro* (Figures 2.5 and 2.7A and B). Short Mad1 and Cdc20 peptides also compete with each other for binding to Mad2 (Supplemental Figure 2.4A) whereas peptides mutated at contact positions lack Mad2 binding activity. Moreover, when Mad2-binding nonamers in Cdc20 and Mad1 are aligned from the fourteen species for which they are available, a clear consensus can be derived - ((K/R)(I/V)(I/V/L)X $\phi$ XXXP - representing a refinement of a previously described consensus (Sironi et al., 2002)).

In the Mad2-Mad1 crystal structure, residues 1-5 of the binding nonamer are overlaid by the Mad2 safety belt and participate in  $\beta$ -augmentation with strand  $\beta_6$  of Mad2, largely via backbone interactions. The next three positions bulge out from Mad2 and are followed by a proline that serves to orient the ensuing Mad1 helix for a homodimeric coiled-coil interaction. Our mutagenesis of the Cdc20 nonamer complements the analysis of Mad1 by Sironi and colleagues, who saw stringent requirements at positions one, three, and five of the nonamer. The motif-ending proline contributes only weakly to the affinity of short peptides, as all classes of substitution cause a two-fold decrease in binding (Figure 2.2C). In contrast, other positions in the nonamer are less selective and tolerate certain substitutions but show more marked decreases in Mad2 binding. Notably, this proline is conserved in Mad1 and Cdc20 in the vast majority of surveyed species (Supplemental Figure 2.2). The substitution of alanine in *S. pombe* Slp1 and human TACE, for example, suggests that if helix or domain

orientation is the major function at this position, a flexible linker may substitute in contexts where there is not a nearby bulky structure such as a coiled-coil. It should be noted that reducing the Mad2-peptide interaction to its barest minimum may result in more stringent selection than would occur in a full-length protein. For example, the Mad1-Mad1 homodimer interaction may stabilize the binding of Mad2, as mutations in the coiled-coil interface appear to influence Mad2 binding indirectly despite the lack of Mad2 contacts at that site. A clearer understanding of Mad1's contribution to Mad2 activation will require crystallographic characterization of the O-Mad2 bound to the C-Mad2-Mad1 core.

#### **2.4.2 Phosphorylation of the Mad2 tail**

Wassmann et al have reported that up to four serines in the C-terminal tail of Mad2 are phosphorylated in nocodazole-arrest HeLa cells (Wassmann et al., 2003). When transiently expressed, Mad2 mutants in which these serines are replaced by aspartic acid fail to interact with Mad1 or APC/C and act as dominant negatives with regard to checkpoint function. However, it is not clear if these mutants fold correctly *in vivo* and in yeast it is not known if they are imported into the nucleus. Wassmann et al suggest that rapid phosphorylation and dephosphorylation cycles of Mad2 allow it to dissociate from Mad1 and bind Cdc20, despite the fact that S195 on Mad1-bound closed Mad2 is not accessible for phosphorylation. We show that mutation of one (S195), three, or four serines to aspartic acid in the Mad2 C terminus abrogates binding to Mad1, Cdc20, and CMT2 (Figure 2.5B). Both classes of Mad2 interactors require tail closure for binding, and CMT2 binds selectively to C-Mad2 regardless of whether the Mad2

ligand cleft is occupied (Xia et al., 2004). Because S195 is not solvent exposed in the C-Mad2 conformer as mentioned, it seems likely that pseudophosphorylation mutants instead represent “always open” mutants similar to the well-studied Mad2 $\Delta$ C truncation mutant. Indeed, *in vivo* studies describe similar behavior for Mad2 tail S-D and  $\Delta$ C mutants; both abrogate the checkpoint in a dominant-negative fashion and fail to bind Mad1 or APC/C (De Antoni et al., 2005; Wassmann et al., 2003). While the localization of Mad2 S-D mutants was not determined, Mad2 $\Delta$ C localizes to kinetochores by associating with Mad1-bound endogenous C-Mad2. How do “always open” mutants inhibit checkpoint function? Presumably, because they are able to dimerize with Mad1-bound C-Mad2, they accumulate at kinetochores and prevent the binding of cytosolic O-Mad2, thus preventing the formation of Mad2-Cdc20 complexes. Such a scenario might occur on cytosolic C-Mad2-Cdc20 complexes as well.

### **2.4.3 Binding to Non-checkpoint proteins**

Despite its well established role in mitotic progression, Mad2 has multiple other binding partners, including including a hormone receptor (ER $\beta$ ), a transmembrane metalloprotease (TACE/ADAM17), a growth factor receptor (insulin receptor, IR), a cytokine receptor (GM-CSFR), and a ubiquitin-like protein (FAT10) (Liu et al., 1999; Nelson et al., 1999; O'Neill et al., 1997; Poelzl et al., 2000; Takeda et al., 2001). What is the significance, if any, of these interactions? Because Mad2 is expressed throughout interphase, it might have “moonlighting” functions in other pathways (Jeffery, 2003). The Mad2-binding motif in TACE is adjacent to proline-rich sequences, suggesting that Mad2 may negatively regulate TACE binding by SH3 domain proteins (Nelson et al.,

1999). Levels of Mad2-IR interaction were inversely proportional to insulin stimulation, suggesting that insulin signaling displaces Mad2 from IR in anticipation of mitogenesis following a pro-growth signal (O'Neill et al., 1997). Strikingly, Mad2 does not associate with the IR-related IGF1R, and IR possesses an obvious Mad2-binding motif (RILSFYYSP) in the carboxy-terminal region necessary for Mad2-binding. Human MAD2 maps to a genomic locus associated with insulin resistance (Krishnan et al., 1998), suggesting that alteration of Mad2 expression might affect IR signaling. However, neither FAT10 nor GM-CSFR contain obvious Mad2-binding motifs and thus perhaps interact with Mad2 via a different binding mode like CMT2. Another is that non-mitotic proteins may sequester Mad2 to reduce the effective concentration in the cell when it is not required and release it during mitosis. A similar situation has been proposed in budding yeast, where Mad1p and Mad2p associate with nuclear pore complexes. This association may control import of Cdc20 into the nucleus in early mitosis (Iouk et al., 2002), and release of Mad2 from yeast nuclear pore complexes is necessary for checkpoint activation (Quimby et al., 2005). Thus, establishment of sequestered pools at the cell and nuclear periphery may enable the early mitotic Mad2 function to be rapidly established immediately upon nuclear envelope breakdown. A final possibility is that these receptors are involved in the spindle checkpoint. Our finding that both TACE and mER $\beta$  bind the same site of Mad2 that binds Mad1 and Cdc20 is consistent with this hypothesis, although other interpretations are equally likely.

#### **2.4.4 Anatomy of Mad2**

The experiments shown here show that Mad1 and Cdc20, to a first approximation, bind to Mad2 in a similar (and competitive) manner. It is striking however, that when chordata or fungal Mad1 and Cdc20 sequences are analyzed on their own, Mad2-binding sites on Mad1 are found to be more similar to each other, and those on Cdc20 to each other, than Cdc20 sequences are to Mad1 sequences (Supplemental Figure 2.1A and B). These data hint at differential control over these two sets of interactions. In support of this, at least one mutant in the tail of Mad2 (V197R) shows partial separation of function in biochemical assays by binding more tightly to Mad1 than to Cdc20. Overall, we believe that available data supports a working model in which Mad1 and Cdc20 bind to Mad2 in a fundamentally similar manner. However, the data also warrant a direct search for separation-of-function binding mutants in Mad2, as well as a careful analysis of their biochemical and biological properties.

The most significant conclusion from our biochemical analysis is that CMT2 binds Mad2 in a fundamentally different fashion from Mad1 and Cdc20. Even low stringency sequence searches fail to uncover a potential Mad2-binding nonamer in CMT2. Mad1 and Cdc20 peptides do not compete with CMT2 for Mad2 binding, and stable triple complexes involving CMT2-Mad2-Mad1 or CMT2-Mad2-Cdc20 can be reconstituted *in vitro* and isolated *in vivo* (Chapter 3). Moreover, whereas mutants in the Mad2 binding cleft abolish binding by both Cdc20 and Mad1, they do not affect binding by CMT2, implying that CMT2 does not bind in the Mad2 cleft (Figure 2.7A and B). Why then, is the binding of CMT2 to Mad2 blocked by mutations in the Mad2 C-terminal tail? Perhaps CMT2 contacts the Mad2 tail by making sequence-specific contacts with residues H191, V197 and S195 such that their mutation interferes with CMT2-Mad2



complex formation. Alternatively, CMT2 might be selective for the closed conformation of Mad2, in which case the H191A, S195D, V197R mutations would exert their effects by preventing formation of the closed state. In weighing these possibilities, it is important to note that Mad1- and Cdc20-binding stabilize the closed Mad2 conformation and the existence of stable CMT-Mad2-Mad1 and CMT2-Mad2-Cdc20 complexes therefore demonstrates that CMT2 can bind Mad2 in the closed state (Luo et al., 2002; Luo et al., 2004; Sironi et al., 2002). Moreover, in the closed Mad2 conformation, the side chains of tail residues H191, S195, and V197 are buried in the interior of the protein, making it unlikely that they make stereo-selective contacts with CMT2 (Figure 2.7A and B). Thus, it seems likely that CMT2 binds selectively to the closed form of Mad2 via contacts outside the binding cleft. Consistent with this, a Mad2 fragment spanning residues 45-78 bound CMT2 in a two-hybrid screen (Habu et al., 2002). These residues form an alpha-helix and beta-turn that traverse the space between the cleft and residues R133 and Q134, which have been implicated in Mad2 dimerization (Figure 2.7C). We therefore propose that CMT2 binds to Mad2 in the closed conformation, perhaps in a manner that affects the ability of Mad2 to self-associate (Figure 7C). The closed and open conformations of Mad2 interconvert slowly in the absence of binding partners, however, and biochemical reconstitution suggests that CMT2 can bind not only to Mad1-Mad2 and Cdc20-Mad2 but also apo-Mad2 (Figure 2.1A).

#### **2.4.5 Implications for checkpoint control**

A significant mystery surrounds the mechanism by which Mad1-Mad2 binding at kinetochores generates a transmissible signal leading to the Mad2-dependent inhibition of

APC/C<sup>Cdc20</sup> throughout the cell. No covalent modifications of Mad2 have been found with the right properties to represent an activated state. However, the existence of two slowly inter-converting Mad2 conformers, an open apo state and closed state in which the safety belt is engaged, suggests that a conformational change might be involved in signaling (Luo et al., 2004). The closed conformation of Mad2 has been shown to be more potent in APC inhibition and is presumed to be the active form. The question therefore arises as to how conformational changes in Mad2 are regulated. Data in this chapter show that short peptides from Mad1 and Cdc20 bind tightly to Mad2 in a competitive fashion, consistent with earlier work using longer Mad1 and Cdc20 fragments (Luo et al., 2002; Sironi et al., 2002). The affinity of these interactions is such that exchange from Mad1 to Cdc20 on the time scale of checkpoint signaling, with or without preservation of conformational state, seems very unlikely (at least in the absence of as-yet undiscovered catalysts) and we have been unable to detect rapid exchange events either in the presence or absence of CMT2 (unpublished observations). Thus, it is surprising that Mad2 cycles on and off kinetochores with a half-life of 25 seconds (Howell et al., 2000) given that kinetochore binding requires Mad1 (Chen et al., 1998). We have found no evidence for a second lower-affinity Mad2 binding site on Mad1 or Cdc20, supporting the idea that the exchangeable pool of Mad2 on kinetochores binds to a Mad2-Mad1 complex (Sironi *et al.*, 2001) via Mad2-Mad2 dimer contacts (De Antoni et al., 2005). In the conformational signaling model, this freely exchanging Mad2 is presumed to carry the checkpoint signal. While the experiments in this chapter do not address this model directly, CMT2 binding to Mad2-Mad1 and Mad2-Cdc20 near the site of Mad2-Mad2 interaction should block the recruitment of additional Mad2,

extinguishing signal generation (Figure 2.7). Moreover, the binding of CMT2 to apo-Mad2 in the closed conformation should negatively regulate any Mad2 actively involved in signal transmission.

#### **2.4.6 Model for CMT2 inhibition of Mad2**

CMT2 must be able to inhibit Mad2, or “de-inhibit” Cdc20 in a ternary complex. By identifying Mad1-CMT2 ternary complexes, we beg the question of how CMT2 inhibits Mad2 when it is bound to Mad1 as well. Mad1-Cdc20 and Mad1-Mad2 binding are believed to be structurally similar, though Cdc20 may undergo conformational changes as well. We have shown that CMT2 binds selectively to the closed conformation of Mad2, and residues required for this binding are spatially apposed – though sequentially distant – to the region required for Mad2 dimerization. We suggest that CMT2 functions primarily to “cap” or occlude the Mad2 homodimerization site, thus preventing the association of O-Mad2 and C-Mad2. De Antoni et al suggest that Mad2 dimerization occurs both on the kinetochore and in the cytosol, but this remains to be established experimentally (De Antoni et al., 2005).

Xia et al show *in vitro* that a recombinant CMT2-Mad2-Cdc20 complex activates APC/C, suggesting that CMT2 somehow relieves the inhibitory effect of Mad2 on Cdc20 without dissociating them from each other (Xia et al., 2004). One possibility is that CMT2 binding causes Cdc20 to re-adopt an APC/C-activating conformation that is occluded in the Mad2-Cdc20 complex. However, little is known about the structure of Cdc20 or its mechanism of APC/C activation. Understanding the mechanism of Mad2

Figure 2.7

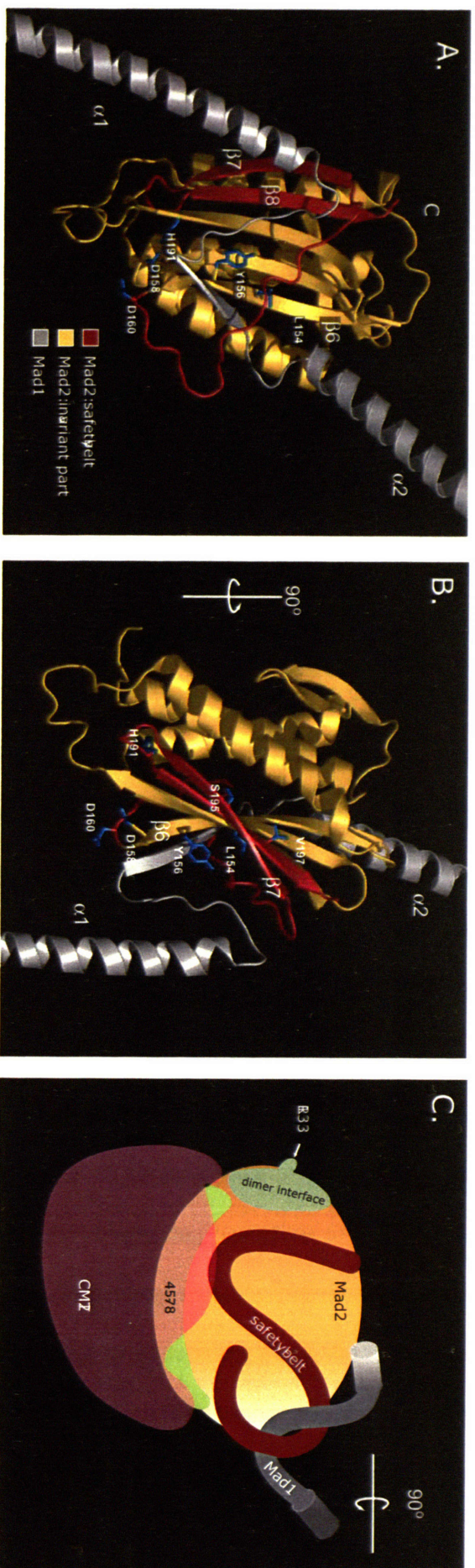


**Figure 2.7:** Structural model of Mad2 binding interactions

(A) and (B) depict the Mad1-Mad2 co-complex from Sironi et al (2002). The side chains of residues mutated in this work are shown in blue. (C) A speculative model of the CMT-Mad2 interaction. CMT2 (purple) is postulated to contact residues 45-78 (light green) which stretch from the Mad1 binding site to the Mad2 dimer interface (dark green) marked by R133. The CMT2 binding site is adjacent to and perhaps overlaps the closed conformation of the Mad2 tail (red).

inhibition requires structural characterization of CMT2 ternary complexes, as well as an understanding of post-translational modifications of CMT2, Cdc20, and APC/C.

#### **2.4.7 Summary and Conclusions**

We show that CMT2 forms a complex with the mitotic spindle checkpoint protein Mad2 that is biochemically distinct from previously known Mad2 complexes. Because previous Mad2 complexes were required for checkpoint activation, the existence of a second binding mode is consistent with CMT2's putative role as a checkpoint inactivator. We explore the cell biological implications of CMT2 complex formation in chapter 3. The results presented here beg several important questions. First, does CMT2 form complexes with Mad2 in the cytosol, at the kinetochore, or both? Does CMT2 cycle on and off of kinetochores with rapid kinetics, as does Mad2, or is its localization constrained by association with other proteins? Second, our biochemical data point to a model in which CMT2 binds selectively to closed Mad2 and prevents Mad2 dimerization. It will be important to map in detail the Mad2-CMT2 binding interface and to test whether CMT2 competes with O-Mad2 for binding to C-Mad2 complexes. Just as it remains unknown why Mad2 dimerization only occurs between two different Mad2 conformers, it is hard to envision how tail closure might control CMT2 binding. Does CMT2 form complexes with other checkpoint proteins? At the same time, the control of Mad2 tail opening and closing is unknown. Closed Mad2 complexes exist throughout the cell cycle, but it is not known if these complexes form passively with the slow kinetics of open-closed interconversion or if there is an active "Mad2-loading" activity. Finally, the relative contributions of the two ternary complexes discussed here,

Cdc20-Mad2-CMT2 and Mad1-Mad2-CMT2, to checkpoint activation and inactivation, remains to be understood. Mad2 and the spindle checkpoint proteins monitor complex, undefined cellular lesions in the crowded space of the mitotic spindle with very rapid resolution. Understanding this system will require a careful cytological study of its dynamic components as well as in-depth structural understanding of these protein complexes.

## **2.5 MATERIALS AND METHODS**

### **Generation of plasmids**

Mad2 was generated by PCR subcloning of an EST clone (Genbank ID R10991) into pGEX-6P-2 (Amersham Biosciences). CMT2 was PCR subcloned from IMAGE clone 321778 (ATCC). Plasmids encoding Cdc20 were the kind gift of J.-M. Peters. Plasmids encoding Mad1 were obtained from N. Pavletich and K.-T. Jeang, while constructs for TACE and ER $\beta$  were obtained from M. Mendelsohn and C. Blobel, respectively. The Mad2 and CMT2 cDNAs were subcloned into pEGFP-C1 (BD Biosciences Clontech). For expression in insect cells, CMT2 was subcloned into a pFASTBAC-derived vector from K. Kaplan. Mad2 mutants shown in Figure 4 were created by the QuickChange method (Stratagene). The cDNA for mRFP, a kind gift of R. Tsien, was fused to histone H2B in pCDNA3.1 (Invitrogen). All PCR-derived plasmids were confirmed by sequencing. The Mad2-Mad1 coexpression construct has been previously described (Sironi *et al.*, 2002).

### **Protein expression**

*Bacterial expression:* GST fusion proteins were expressed in BL21(DE3) or BL21 Codon Plus *E. coli* (Stratagene). Cells were resuspended in breakage buffer (50mM Hepes pH 8.0, 150mM NaCl, 2mM EDTA, 1mM DTT, 1mM PMSF, 10% glycerol) and the bacteria lysed by sonication. Lysates were clarified and incubated with glutathione sepharose beads (Amersham Pharmacia Biotech).

*Baculovirus expression:* The human CMT2 cDNA was subcloned into a modified pFastBac transfer vector (GIBCO-BRL) in frame with an N-terminal GST tag cleavable by PreScission protease (Amersham-Pharmacia Biotech). A GST-CMT2 baculovirus was used to infect Sf9 cells growing in suspension. Cells were harvested 72 hours post-infection and resuspended in lysis buffer (20 mM Tris-HCl pH 8, 0.15 M NaCl, 0.1 % Triton, 1 mM DTT, 0.5 mM EDTA and a tablet of protease inhibitor cocktail (Roche)). Cells were lysed by sonication and the extracts were clarified by centrifugation at 150,000g for 45 minutes at 4 °C. The supernatant was incubated with glutathione sepharose beads for 3 hours at 4 °C. After extensive washing in 20 mM Tris-HCl pH 8, 0.1 M NaCl, 1 mM DDT and 0.5 mM EDTA, beads were incubated overnight with PreScission protease for GST tag removal. The purity of the eluted CMT2 preparation was assessed by SDS-PAGE and the concentration determined by absorbance at 280nm. Procedures for the expression and purification of recombinant 6H-Mad2, 6H-Mad2<sup>ΔC</sup>, and Mad2-Mad1<sup>485-584</sup> have been described (Sironi et al. 2001; Sironi et al. 2002).

*In vitro translation:* Proteins were made *in vitro* using the TnT T7, TnT T3, and TnT T7 Quick for PCR systems (Promega). DNA templates for *in vitro* translation were made by two rounds of PCR amplification to add a T7 promoter to the 5' end, and to improve translational yield at least 12 bases were added 3' to the STOP codon. The 5'

added sequence includes 10 bases to improve translational yield, a T7 promoter, a BamHI site, a Kozak consensus sequence, and an HA epitope. Mutants shown in Figure 1D and Supplemental Figure 3 were generated by megaprimer PCR before *in vitro* translation.

### **Peptide synthesis**

Cdc20, TACE and ER $\beta$  peptides were synthesized on a PEG 500-modified cellulose membrane (AbiMed AC01-12, MIT Biopolymers Facility) via coupling to  $\beta$ -alanine residues. A membrane spotted with Mad1 peptides was obtained from Research Genetics. Membranes were moistened in MeOH, washed in TBST (25mM Tris pH8.0, 137mM NaCl, 13.4mM KCl, 0.1% Tween-20), and blocked overnight at 4°C in TBS-T with 2% BSA. *In vitro* translated, radiolabeled Mad2 was purified on a Sephadex G-25 spin column to remove unincorporated <sup>35</sup>S-methionine. Membranes were then washed in TBST and probed with 50 $\mu$ l Mad2 in 1.5-3ml TBST with 1% BSA for one hour at room temperature. Membranes were rinsed with TBST and washed in the following solutions: TBST, TBST with 0.5M NaCl, TBST with 0.5% Triton-X 100, and TBST. Dried membranes were exposed on a PhosphorImager and binding was quantitated using Molecular Dynamics software. Mad1 and Cdc20 peptides were synthesized by Biosynthesis, Inc (Lewisville, Texas) and the Center for Cancer Research BioPolymers Lab (MIT). A scrambled Mad1 peptide, GGCRVVS~~K~~LYARLTDNQRQMRPHLSTDS, was used as a control.

### **Binding Assays**



*Pull-down assays:* *In vitro* binding assays were performed with  $^{35}\text{S}$ -methionine labeled *in vitro*-translated protein and GST-fusion protein immobilized on glutathione sepharose beads (Pharmacia). After repeated washing in breakage buffer, beads were incubated with fusion protein lysates in the presence of 1% Triton X-100 at 4°C with gentle rocking for 2 hours. The beads were pelleted, washed with IP buffer (50mM Hepes pH 8.0, 150mM NaCl, 50mM  $\beta$ -glycerophosphate, 50mM NaF, 1mM EDTA, 10% glycerol, 1% Triton-X 100) and resuspended to a 50% slurry. Binding reactions were performed for 6 hours at 4°C in IP buffer with 1mM DTT. Beads were pelleted, washed 3 times in IP buffer, boiled in SDS loading buffer, and resolved by SDS-PAGE. Dried gels were exposed on a PhosphorImager (Molecular Dynamics). Signals from radiolabeled protein were quantified using Molecular Dynamics software.

*Isothermal Titration Calorimetry:* ITC measurements were carried out using a VP-ITC titration calorimeter (MicroCal, Inc). Peptides at a concentration of 30-200 $\mu\text{M}$  were injected into a solution of 5-20 $\mu\text{M}$  hMad2 in 150mM NaCl, 50mM Hepes pH 8.0 at 18°C. Binding isotherms were corrected for dilution enthalpies by subtraction of a blank titration of peptide into buffer and the corrected data were fitted using Origin software.

*Size exclusion chromatography:* 30 $\mu\text{g}$  of pure CMT2 was incubated for 1 hour at 20°C with equimolar amounts of Mad2, Mad2 $^{\Delta\text{C}}$  or Mad2-Mad1 $^{485-584}$  complex in binding buffer (20 mM Tris-HCl pH 8, 0.1 M NaCl, 1 mM DTT and 0.5 mM EDTA). To generate a Mad2-Cdc20 complex, 30 $\mu\text{g}$  of Mad2 was pre-incubated for 1 hour at 20°C with a 20-fold molar excess of a synthetic Cdc20 (111-138) peptide. An equimolar amount of CMT2 was then added, and after a new incubation of 1 hour at 20°C the reaction was resolved by size-exclusion chromatography. The incubation mixtures were separated on a

SMART FPLC system (Pharmacia) using Superdex S75 or Superdex S200 size-exclusion chromatography columns equilibrated with binding buffer. Eluted fractions were resolved by SDS-PAGE.

*Surface plasmon resonance:* All experiments were performed at 25°C on a Biacore 2000 (Biacore). Peptides were coupled to CM5 sensor chips with EDC and NHS according to the manufacturer's instructions. Roughly 4000-10000 RU of peptide were coupled per flow cell. Aliquots (20  $\mu$ L) of 20nM Mad2 in HEPES-buffered saline (HBS, 20mM HEPES pH 7.0, 150mM NaCl, 1mM EDTA pH 8.0) were preincubated with different concentrations of peptide before injection at a flow rate of 5 $\mu$ L/min. After binding, surfaces were washed, regenerated with 50mM glycine pH 2.2, and washed again. Binding data were interpreted using the BiaEvaluation 3.2 software (Biacore) and fit using a simple Langmuir interaction model.

### **Supplemental Material**

A phylogenetic analysis of Mad2 binding peptides can be found in Supplemental Figure 2.1. Peptide array analysis of Mad2-binding regions in TACE and ER $\beta$  is presented in Supplemental Figure 2.2. Characterization of Mad2 binding peptides in solution is presented in Supplemental Figure 2.3

### **2.8 Acknowledgements**

We thank the following people for the kind gift of reagents: K. Kaplan (UC Davis), C. Blobel (Sloan-Kettering Institute, New York), K.-T. Jeang (NIH, Bethesda), N. Pavletich (Memorial Sloan-Kettering Cancer Center, New York), J.-M. Peters (IMP, Vienna), and

M. Mendelsohn (Boston University). We also thank A. Elia for assistance with ITC and members of the Sorger and Musacchio labs for assistance and help with manuscript preparation. This work was funded by NIH grant CA84179 to P.K.S. Marina Mapelli contributed the chromatography data in Figure 2.4. Max Dobles contributed to the peptide array data in Figures 2.2 and Supplemental Figure 2.2.

## 2.7 References

- Chan, G. K., and Yen, T. J. (2003). The mitotic checkpoint: a signaling pathway that allows a single unattached kinetochore to inhibit mitotic exit. *Prog Cell Cycle Res* 5, 431-439.
- Chen, R. H., Brady, D. M., Smith, D., Murray, A. W., and Hardwick, K. G. (1999). The spindle checkpoint of budding yeast depends on a tight complex between the Mad1 and Mad2 proteins. *Mol Biol Cell* 10, 2607-2618.
- Chen, R. H., Shevchenko, A., Mann, M., and Murray, A. W. (1998). Spindle checkpoint protein Xmad1 recruits Xmad2 to unattached kinetochores. *J Cell Biol* 143, 283-295.
- Chung, E., and Chen, R. H. (2002). Spindle checkpoint requires Mad1-bound and Mad1-free Mad2. *Mol Biol Cell* 13, 1501-1511.
- Cleveland, D. W., Mao, Y., and Sullivan, K. F. (2003). Centromeres and kinetochores: from epigenetics to mitotic checkpoint signaling. *Cell* 112, 407-421.
- De Antoni, A., Pearson, C. G., Cimini, D., Canman, J. C., Sala, V., Nezi, L., Mapelli, M., Sironi, L., Faretta, M., Salmon, E. D., and Musacchio, A. (2005). The Mad1/Mad2 complex as a template for Mad2 activation in the spindle assembly checkpoint. *Curr Biol* 15, 214-225.
- DeAntoni, A., Sala, V., and Musacchio, A. (2005). Explaining the oligomerization properties of the spindle assembly checkpoint protein Mad2. *Philos Trans R Soc Lond B Biol Sci* 360, 637-647, discussion 447-638.
- Habu, T., Kim, S. H., Weinstein, J., and Matsumoto, T. (2002). Identification of a MAD2-binding protein, CMT2, and its role in mitosis. *Embo J* 21, 6419-6428.
- Hoffman, D. B., Pearson, C. G., Yen, T. J., Howell, B. J., and Salmon, E. D. (2001). Microtubule-dependent changes in assembly of microtubule motor proteins and mitotic spindle checkpoint proteins at PtK1 kinetochores. *Mol Biol Cell* 12, 1995-2009.
- Howell, B. J., Hoffman, D. B., Fang, G., Murray, A. W., and Salmon, E. D. (2000). Visualization of Mad2 dynamics at kinetochores, along spindle fibers, and at spindle poles in living cells. *J Cell Biol* 150, 1233-1250.
- Howell, B. J., Moree, B., Farrar, E. M., Stewart, S., Fang, G., and Salmon, E. D. (2004). Spindle checkpoint protein dynamics at kinetochores in living cells. *Curr Biol* 14, 953-964.
- Hoyt, M. A. (2001). A new view of the spindle checkpoint. *J Cell Biol* 154, 909-911.
- Hoyt, M. A., Totis, L., and Roberts, B. T. (1991). *S. cerevisiae* genes required for cell cycle arrest in response to loss of microtubule function. *Cell* 66, 507-517.

- Hwang, L. H., Lau, L. F., Smith, D. L., Mistrot, C. A., Hardwick, K. G., Hwang, E. S., Amon, A., and Murray, A. W. (1998). Budding yeast Cdc20: a target of the spindle checkpoint. *Science* 279, 1041-1044.
- Iouk, T., Kerscher, O., Scott, R. J., Basrai, M. A., and Wozniak, R. W. (2002). The yeast nuclear pore complex functionally interacts with components of the spindle assembly checkpoint. *J Cell Biol* 159, 807-819.
- Jeffery, C. J. (2003). Moonlighting proteins: old proteins learning new tricks. *Trends Genet* 19, 415-417.
- Kallio, M. J., Beardmore, V. A., Weinstein, J., and Gorbsky, G. J. (2002). Rapid microtubule-independent dynamics of Cdc20 at kinetochores and centrosomes in mammalian cells. *J Cell Biol* 158, 841-847.
- Kim, S. H., Lin, D. P., Matsumoto, S., Kitazono, A., and Matsumoto, T. (1998). Fission yeast Slp1: an effector of the Mad2-dependent spindle checkpoint. *Science* 279, 1045-1047.
- Krishnan, R., Goodman, B., Jin, D. Y., Jeang, K. T., Collins, C., Stetten, G., and Spencer, F. (1998). Map location and gene structure of the Homo sapiens mitotic arrest deficient 2 (MAD2L1) gene at 4q27. *Genomics* 49, 475-478.
- Lew, D. J., and Burke, D. J. (2003). The spindle assembly and spindle position checkpoints. *Annu Rev Genet* 37, 251-282.
- Li, R., and Murray, A. W. (1991). Feedback control of mitosis in budding yeast. *Cell* 66, 519-531.
- Liu, Y. C., Pan, J., Zhang, C., Fan, W., Collinge, M., Bender, J. R., and Weissman, S. M. (1999). A MHC-encoded ubiquitin-like protein (FAT10) binds noncovalently to the spindle assembly checkpoint protein MAD2. *Proc Natl Acad Sci U S A* 96, 4313-4318.
- Luo, X., Fang, G., Coldiron, M., Lin, Y., Yu, H., Kirschner, M. W., and Wagner, G. (2000). Structure of the Mad2 spindle assembly checkpoint protein and its interaction with Cdc20. *Nat Struct Biol* 7, 224-229.
- Luo, X., Tang, Z., Rizo, J., and Yu, H. (2002). The Mad2 spindle checkpoint protein undergoes similar major conformational changes upon binding to either Mad1 or Cdc20. *Mol Cell* 9, 59-71.
- Luo, X., Tang, Z., Xia, G., Wassmann, K., Matsumoto, T., Rizo, J., and Yu, H. (2004). The Mad2 spindle checkpoint protein has two distinct natively folded states. *Nat Struct Mol Biol* 11, 338-345.
- Musacchio, A., and Hardwick, K. G. (2002). The spindle checkpoint: structural insights into dynamic signalling. *Nat Rev Mol Cell Biol* 3, 731-741.

Nasmyth, K. (2002). Segregating sister genomes: the molecular biology of chromosome separation. *Science* 297, 559-565.

Nelson, K. K., Schlondorff, J., and Blobel, C. P. (1999). Evidence for an interaction of the metalloprotease-disintegrin tumour necrosis factor alpha convertase (TACE) with mitotic arrest deficient 2 (MAD2), and of the metalloprotease-disintegrin MDC9 with a novel MAD2-related protein, MAD2beta. *Biochem J* 343 Pt 3, 673-680.

Nomoto, S., Haruki, N., Takahashi, T., Masuda, A., Koshikawa, T., Fujii, Y., and Osada, H. (1999). Search for in vivo somatic mutations in the mitotic checkpoint gene, hMAD1, in human lung cancers. *Oncogene* 18, 7180-7183.

O'Neill, T. J., Zhu, Y., and Gustafson, T. A. (1997). Interaction of MAD2 with the carboxyl terminus of the insulin receptor but not with the IGFIR. Evidence for release from the insulin receptor after activation. *J Biol Chem* 272, 10035-10040.

Peters, J. M. (2002). The anaphase-promoting complex: proteolysis in mitosis and beyond. *Mol Cell* 9, 931-943.

Poddar, A., Stukenberg, P. T., and Burke, D. J. (2005). Two complexes of spindle checkpoint proteins containing Cdc20 and Mad2 assemble during mitosis independently of the kinetochore in *Saccharomyces cerevisiae*. *Eukaryot Cell* 4, 867-878.

Poelzl, G., Kasai, Y., Mochizuki, N., Shaul, P. W., Brown, M., and Mendelsohn, M. E. (2000). Specific association of estrogen receptor beta with the cell cycle spindle assembly checkpoint protein, MAD2. *Proc Natl Acad Sci U S A* 97, 2836-2839.

Quimby, B. B., Arnaoutov, A., and Dasso, M. (2005). Ran GTPase regulates Mad2 localization to the nuclear pore complex. *Eukaryot Cell* 4, 274-280.

Rieder, C. L., Schultz, A., Cole, R., and Sluder, G. (1994). Anaphase onset in vertebrate somatic cells is controlled by a checkpoint that monitors sister kinetochore attachment to the spindle. *J Cell Biol* 127, 1301-1310.

Shah, J. V., Botvinick, E., Bonday, Z., Furnari, F., Berns, M., and Cleveland, D. W. (2004). Dynamics of centromere and kinetochore proteins; implications for checkpoint signaling and silencing. *Curr Biol* 14, 942-952.

Sironi, L., Mapelli, M., Knapp, S., De Antoni, A., Jeang, K. T., and Musacchio, A. (2002). Crystal structure of the tetrameric Mad1-Mad2 core complex: implications of a 'safety belt' binding mechanism for the spindle checkpoint. *Embo J* 21, 2496-2506.

Sironi, L., Melixetian, M., Faretta, M., Prosperini, E., Helin, K., and Musacchio, A. (2001). Mad2 binding to Mad1 and Cdc20, rather than oligomerization, is required for the spindle checkpoint. *Embo J* 20, 6371-6382.

Sudakin, V., Chan, G. K., and Yen, T. J. (2001). Checkpoint inhibition of the APC/C in HeLa cells is mediated by a complex of BUBR1, BUB3, CDC20, and MAD2. *J Cell Biol* 154, 925-936.

Takeda, M., Dohmae, N., Takio, K., Arai, K., and Watanabe, S. (2001). Cell cycle-dependent interaction of Mad2 with conserved Box1/2 region of human granulocyte-macrophage colony-stimulating factor receptor common betac. *J Biol Chem* 276, 41803-41809.

Wassmann, K., Liberal, V., and Benezra, R. (2003). Mad2 phosphorylation regulates its association with Mad1 and the APC/C. *Embo J* 22, 797-806.

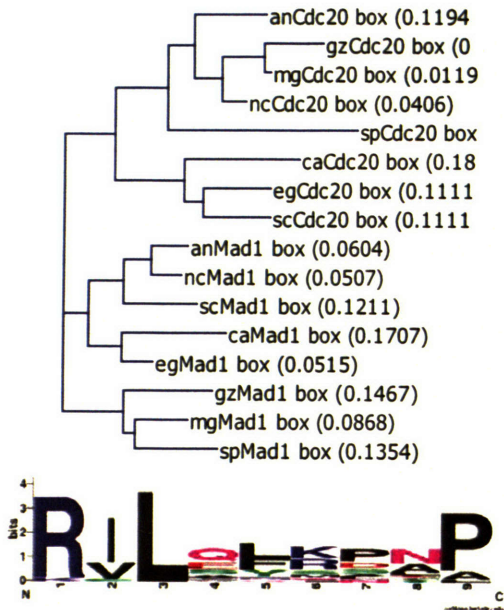
Xia, G., Luo, X., Habu, T., Rizo, J., Matsumoto, T., and Yu, H. (2004). Conformation-specific binding of p31(comet) antagonizes the function of Mad2 in the spindle checkpoint. *Embo J* 23, 3133-3143.

Zhang, Y., and Lees, E. (2001). Identification of an overlapping binding domain on Cdc20 for Mad2 and anaphase-promoting complex: model for spindle checkpoint regulation. *Mol Cell Biol* 21, 5190-5199.

# Supplemental Figure 2.1

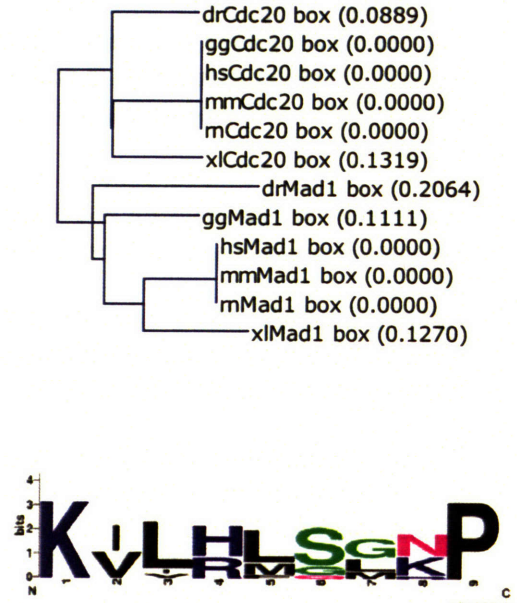
**A**

fungal Mad2 binding nonamers of Cdc20/Mad1



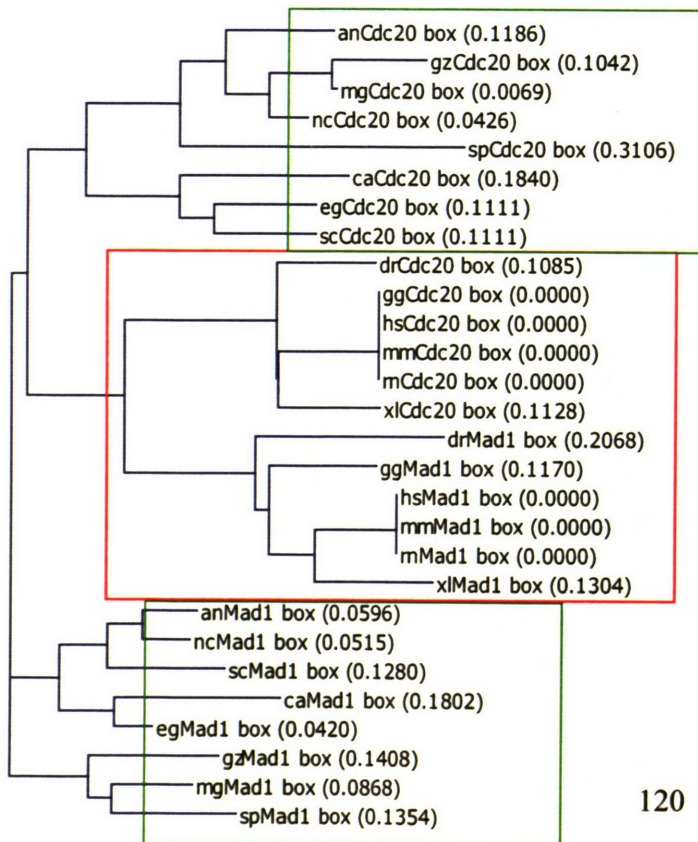
**B**

chordata Mad2 binding nonamers of Cdc20/Mad1



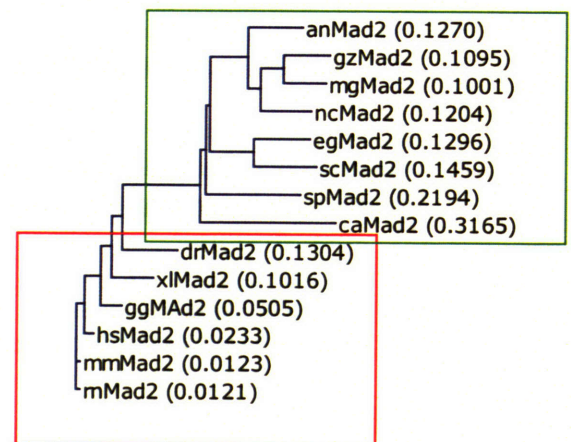
**C**

fungal and chordata Mad2 binding nonamers of Cdc20/Mad1



**D**

fungal and chordata Mad2

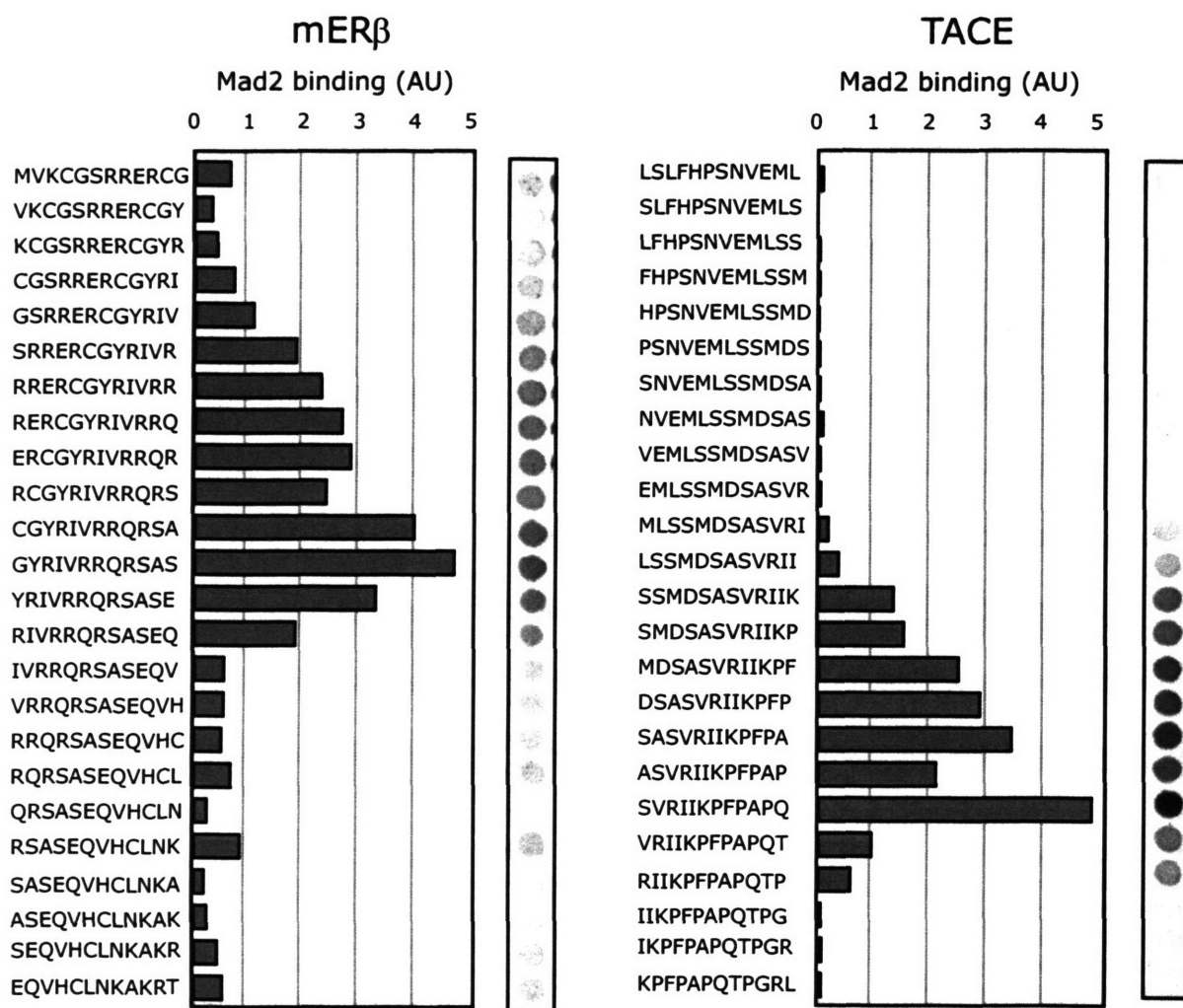




**Supplemental Figure 2.1:** Evolution of the Mad2 binding motif

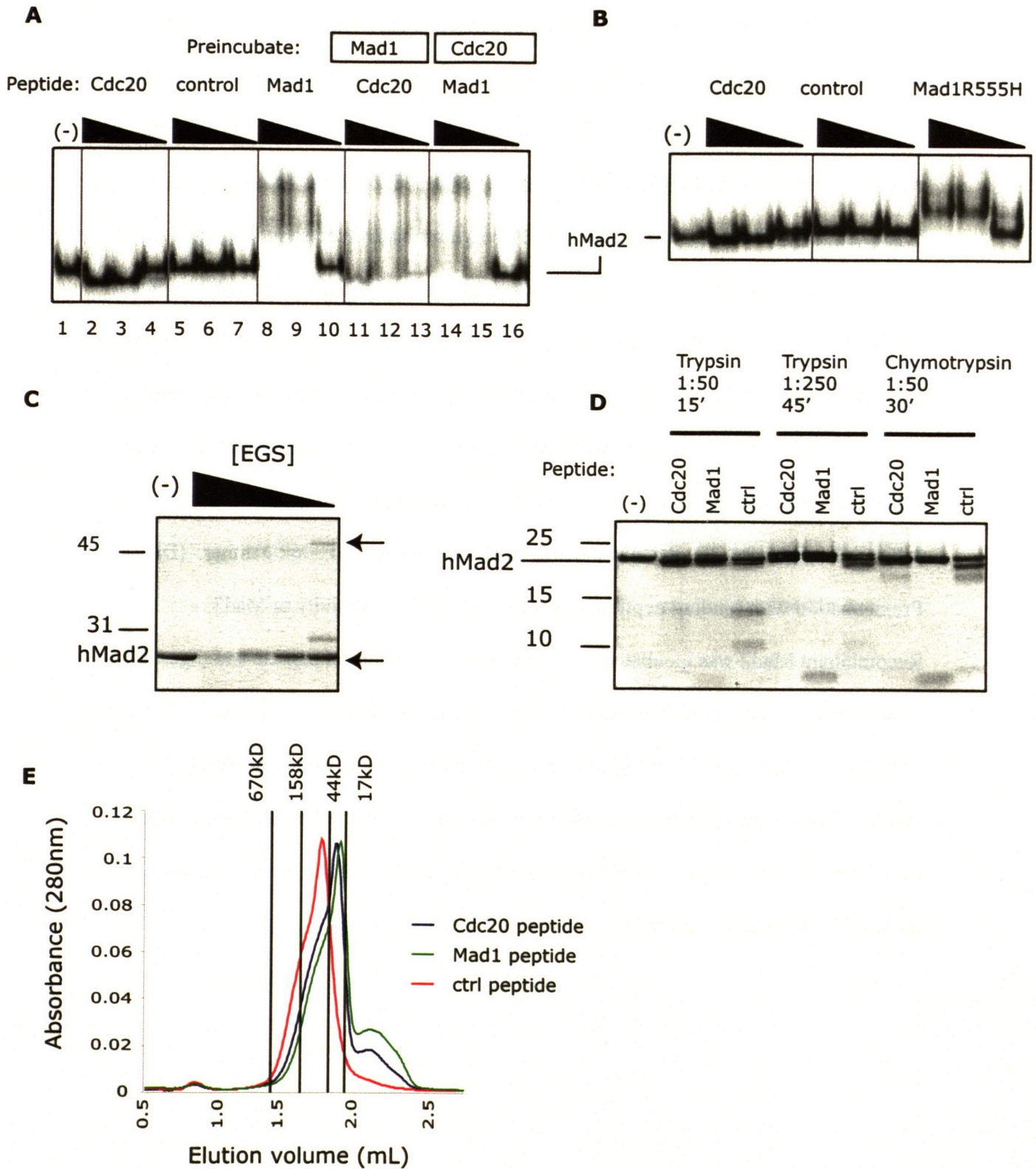
(A) Phylogenetic tree of Mad2-binding nonamers derived from Cdc20 and Mad1 in eight fungal species. Relative contributions at each position are depicted below as in Figure 2.2. (B) As in (A), phylogenetic tree of Mad2-binding nonamers from Cdc20 and Mad1 in six chordata. (C) Phylogenetic tree of combined fungal and chordata Mad2-binding nonamers. (D) Phylogenetic tree analysis of Mad2 sequences from fungal and chordate species. Trees were generated using the AlignX program in the Vector NTi software suite. Within the Mad2-binding consensus sequence in (C), chordata Cdc20 and Mad1 sequences (red boxes) are closer to each other than they are to their respective fungal counterparts (green boxes), mirroring the phylogenetic tree for Mad2 in (D) and suggestive of co-evolution among Mad2 and its binding motifs in both Mad1 and Cdc20.

## Supplemental Figure 2.2



**Supplemental Figure 2.2:** TACE and mERbeta contain Mad1/Cdc20-like Mad2 binding motifs. Successive 12 residue peptides from mERbeta (233-267) and TACE (705-739) were synthesized on filters and probed with radiolabeled Mad2 as in Figure 1 (A-C). Bars indicate Mad2 binding activity for each peptide in arbitrary units.

# Supplemental Figure 2.3



**Supplemental Figure 2.3:** Characterization of Mad2-binding peptides. **(A)** Mad1 and Cdc20 peptides compete for Mad2 binding in solution. Titrations of synthetic Cdc20, control, or Mad1 peptides were incubated with recombinant Mad2 before native gel electrophoresis and Coomassie staining (lanes 1-10). To test for competition, Mad2 was preincubated with 100  $\mu$ M Mad1 (lanes 11-13) or Cdc20 (lanes 14-16) peptide before titration of competing peptide. **(B)** A polymorphism detected in lung cancers does not alter Mad2 binding. A subset of human lung tumors possess the polymorphism Mad1R555H (Nomoto et al., 1999). As in (A), peptides from Cdc20 (lanes 2-4), control (5-7), and Mad1R555H were incubated with Mad2 and binding was assayed by native gel electrophoresis. **(C)** *In vitro* crosslinking demonstrates the existence of a Mad2 dimer. Recombinant Mad2 was crosslinked with EGS and reactions were quenched and subjected to SDS-PAGE. Arrows indicate ~23kD monomer and ~46kD dimer. **(D)** Preincubation with binding peptides alters the proteolytic sensitivity of Mad2. Recombinant Mad2 was incubated with Cdc20, Mad1, or control peptide and digested with trypsin or chymotrypsin as indicated. Reactions were quenched and resolved by SDS-PAGE. **(E)** Ligand binding converts Mad2 from dimer to monomer. Mad2 was incubated with Cdc20, Mad1, or control peptides and mixtures were subjected to size exclusion chromatography on a SMART Superdex 75 FPLC column. Protein was detected by absorbance at 280nm.

### **Chapter 3**

## **Negative Regulation of the Mammalian Spindle Checkpoint by CMT2 is Required for Completion of Mitosis**

### **3.1 Abstract**

The spindle assembly checkpoint links anaphase onset to the completion of chromosome-microtubule attachment. Checkpoint signaling begins when Mad and Bub proteins bind to kinetochores of unattached or maloriented chromosomes. Dynamic transit of Mad2 protein between the kinetochore and cytosol allows it to bind and inhibit Cdc20, an essential activator of the anaphase promoting complex. CMT2, a Mad2-binding protein, may control the rate of recovery from checkpoint arrest, but its full function and site of action are not known. We examine the role of CMT2 in mitosis by live- and fixed-cell microscopy and find that it localizes to kinetochores and the cytosol. Critically, CMT2 is required for exit from mitosis. CMT2-depleted cells arrest in metaphase, and their checkpoints remain active even though Mad and Bub proteins leave the kinetochore. We propose that, in contrast with previous models of checkpoint adaptation, mammalian cells cannot complete mitosis without actively silencing the Mad2-dependent spindle checkpoint.

### 3.2 Introduction

The spindle assembly checkpoint prevents chromosome segregation errors by linking the dissolution of sister chromatid cohesion to the formation of correct kinetochore-microtubule attachment (for reviews see (Chan and Yen, 2003; Cleveland et al., 2003; Hoyt, 2001; Lew and Burke, 2003; Musacchio and Hardwick, 2002)). Spindle checkpoint genes were first isolated in *S. cerevisiae* and are highly conserved among eukaryotes (Hoyt *et al.*, 1991; Li and Murray, 1991). The presence of unattached or maloriented chromosomes in prometaphase or metaphase initiates a signaling cascade among the Mad, Bub, and Mps1 protein families that converges on Cdc20, an essential regulator of the anaphase promoting complex/cyclosome (APC/C). Mad2 and BubR1 are the final effectors of Cdc20 inhibition and the three proteins can be co-purified in a large mitotic checkpoint complex, or MCC (Sudakin et al., 2001). Mad2, BubR1, and Cdc20 shuttle rapidly between the cytosol and kinetochores (Howell et al., 2000; Shah et al., 2004), and this dynamic localization is believed to be necessary for generation of the “wait anaphase” signal. Transient dimerization between the closed conformation of Mad2, which is stably bound to Mad1 at kinetochores, and the open, cytosolic conformation may promote formation of Mad2-Cdc20 complexes and APC/C inhibition leading to metaphase arrest (Shah et al., 2004). In addition, recent results suggest that the Mad2-BubR1-Cdc20 regulatory circuit may function to constrain APC activity early in mitosis (Meraldi et al., 2004), before the spindle checkpoint becomes active.

While much is known about the generation and transmission of spindle checkpoint activity, very little is known about how the checkpoint is extinguished once chromosomes become attached. Classic cytologic experiments showed that in PtK1 cells,

anaphase begins  $23 \pm 1$  minutes after the last chromosome pair becomes attached (Rieder et al., 1994). At least two models might explain this phenomenon. One possibility is that attachment of the last kinetochore ends active generation of a “wait anaphase” signal, and anaphase ensues once this signal decays sufficiently to allow Cdc20 and APC/C activation. In this scenario, the time required for anaphase onset reflects the time required for the active checkpoint signal to decay. This signal may be comprised of the individual activities of Mad2, Bub1, and BubR1/Mad3, as well as the synergistic activity of the larger MCC complex (Sudakin et al., 2001; Tang et al., 2004). A second possibility is that attachment of the last kinetochore is permissive for active inhibition of checkpoint activity and generation of a “go anaphase” signal. The former model fits well with classical conceptions of checkpoint signaling in which cell cycle checkpoints are not activated until the presence of a frank lesion (Hartwell and Weinert, 1989). The second model is consistent with the idea that the Mad2- and BubR1-dependent checkpoint is active in every mitosis in some organisms (Dobles et al., 2000; Kalitsis et al., 2000). In this case, a uniformity of anaphase-onset time would only result from passive decay if the pool of Cdc20-inhibiting signal was equally uniform from cell to cell. If there is variation in the *amount* of “wait anaphase” signal generated in otherwise unperturbed cells, then the time from attachment to anaphase should vary unless the signal is actively silenced. How might the checkpoint be actively silenced? One proposed mechanism suggests that bulk removal of checkpoint complexes from kinetochores to the spindle by a minus end-directed motor such as dynein could render the checkpoint insensitive to kinetochore status (Howell et al., 2001). The search for binding partners of known



checkpoint proteins has identified two putative checkpoint inhibitors: BSCG1, which binds BubR1 (Gupta et al., 2003), and CMT2, which binds Mad2.

CMT2 (“Cought by Mad2”) was identified as a Mad2 interactor in higher eukaryotes that accumulates in HeLa cells before mitosis and is degraded at the beginning of G1 (Habu et al., 2002). CMT2 was proposed to compete with Cdc20 for Mad2 binding, thus liberating Cdc20 and leading to anaphase onset (Habu et al., 2002). In contrast, other studies demonstrate that CMT2 forms a stable ternary complex with Mad2 and Cdc20 (Habu et al., 2002; Xia et al., 2004). These authors observed nucleoplasmic speckles of CMT2 in early mitosis and CMT2 on the spindle and at the midzone after metaphase. Fixed-cell assays suggested that RNAi depletion of CMT2 suppresses the rate of recovery from checkpoint arrest, causing a transient delay in mitotic exit after cells are released from nocodazole. These findings implicate in CMT2 in adaptation to prolonged checkpoint signaling (Minshull et al., 1996) but do not point to a role for CMT2 in unperturbed mitosis. We test the function of CMT2 by fixed- and live-cell methods and show that it is essential for mitotic progression. While canonical cell cycle checkpoints are dispensable error-monitoring pathways, we suggest that the metazoan spindle checkpoint is a fundamental subroutine of mitosis and active silencing of Mad2 is necessary for mitotic progression.

### **3.3 Results**

#### **3.3.1 CMT2 RNAi arrests cells in mitosis and opposes Mad2 function**

To probe the function of CMT2 *in vivo*, we tested a panel of siRNA duplexes targeted against the human CMT2 mRNA in HeLa cells. Two duplexes, CMT2-1 and

CMT2-3, caused an approximately 20- to 50-fold depletion of CMT2 in asynchronous cells by western blot (Figure 3.1A and data not shown). When cells were examined by light microscopy, CMT2 RNAi caused an increase in the mitotic index (21%) compared to control RNAi (5%, Figure 3.1B). Mad2 RNAi, which decreases the time spent in mitosis, decreased the mitotic index (4%) slightly as expected.

To examine the mitotic phenotype of CMT2 RNAi more closely, we transfected HeLa cells stably expressing Histone 2B-mRFP or Histone 2B-GFP with GFP-CMT2 plasmid or depleted the protein by RNAi. Control cells were transfected with GFP plasmid or a control Lamin A siRNA. The time of anaphase onset relative to nuclear breakdown (NBD; defined as T=0) was determined morphologically. Anaphase times in HeLa cells exhibit a characteristic skew-normal distribution with a modal peak time of anaphase onset of  $26 \pm 1.5$  min (Meraldi et al., 2004). All cells overexpressing GFP-CMT2 underwent abnormal and premature anaphase, with chromosome separation at T = 12 min, while overexpression of GFP alone had no effect (Figure 3.2A). GFP-CMT2 overexpression closely phenocopied Mad2 depletion by RNAi, which accelerates the overall timing of mitosis so that anaphase is highly premature with a peak onset of as little as T=12 min (Figure 3.2A). Both GFP-CMT2 and Mad2 RNAi cells executed anaphase with lagging and unattached chromosomes (Figure 3.2A). Conversely, CMT2-depleted cells arrested in metaphase with congressed chromosomes (Figure 3.2B). This arrest was robust, as 90% of the cells had not entered anaphase 45 minutes after NBD compared to only 8% of control cells, and the arrest lasted up to 6 hours or longer. This phenotype resembled that seen in overexpression of GFP-Mad2, in which over 60% of cells arrest in mitosis (Figure 3.2B). Thus, CMT2 and Mad2 have

## Figure 3.1

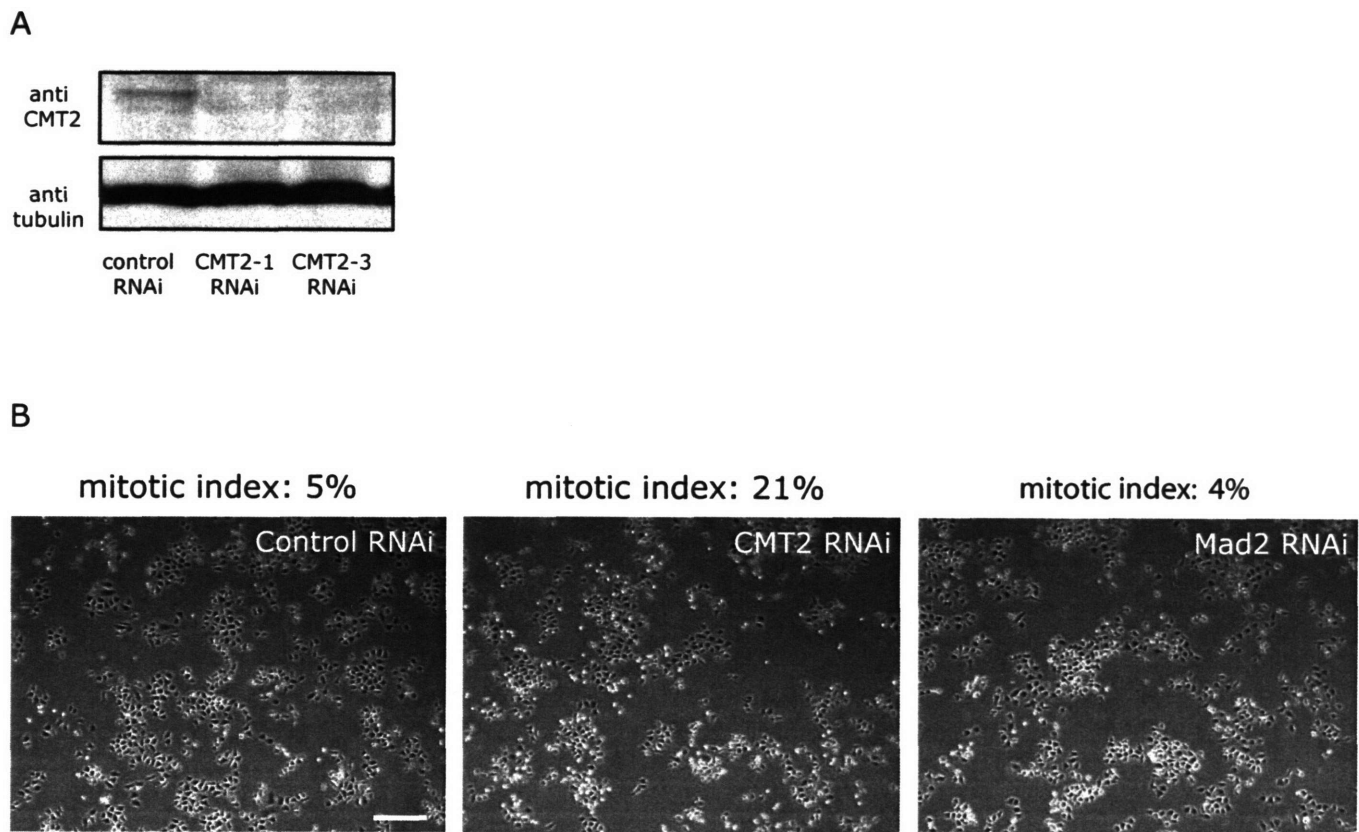


### Figure 3.1: CMT2 RNAi arrests cells in mitosis

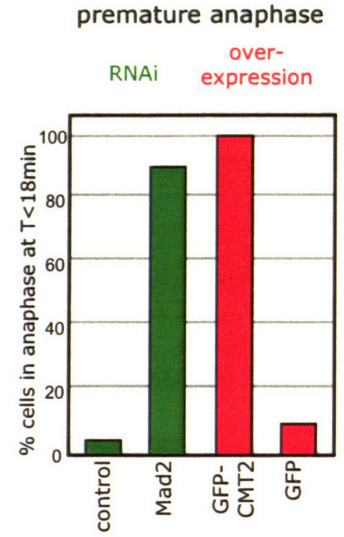
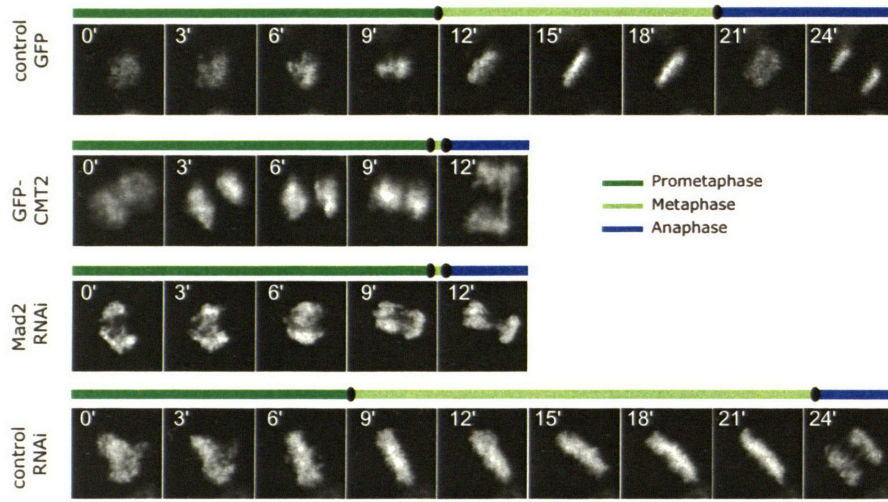
(A) Immunoblots of whole cell lysates from HeLa cells treated with siRNA against lamin A (negative control) or CMT2. Blots were probed with antibodies as indicated. (B)

Light microscopy images of HeLa cells transfected with siRNAs against CMT2,

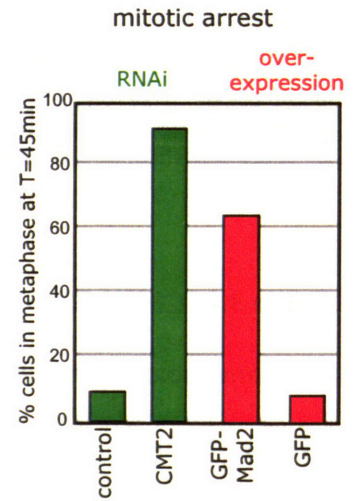
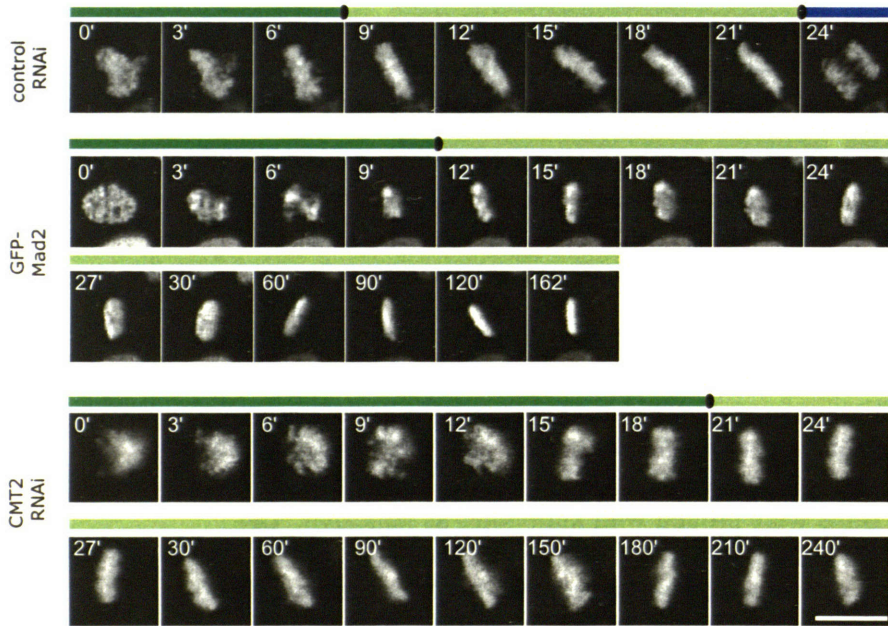
Mad2, or control. Mitotic index was assayed by rounding. Scale bar is 100 $\mu$ m.

Figure 3.2

A



B



C



**Figure 3.2: CMT2 regulates mitotic timing in unperturbed cells**

**(A)** CMT2 over-expression and Mad2 depletion cause errors in DNA segregation. HeLa Histone 2B-mRFP cells were transfected with GFP or GFP-CMT2 (top) and Histone 2B-GFP cells were transfected with Mad2 siRNA or control siRNA (bottom) and followed by time-lapse microscopy. The times represent minutes after NBD; scale bar, 10  $\mu$ m.

Graph shows fraction of cells undergoing premature anaphase, defined as chromosome segregation at  $T < 18$ min. Bars depict the mean of at least two experiments of at least 50

cells each (RNAi) or at least 5 cells each (overexpression). **(B)** CMT2 depletion and

Mad2 overexpression arrest cells in mitosis. As in (A), HeLa Histone 2B-GFP cells were transfected with CMT2 or control siRNA and HeLa Histone 2b-mRFP cells were

transfected with GFP-Mad2. Graph depicts fraction of cells arrested in mitosis, defined

as still in metaphase at  $T > 45$ min. **(C)** Immunoblots of whole cell lysates from HeLa cells

treated with siRNA against lamin A (negative control), CMT2, Mad2, and Mad1. Blots were probed with antibodies as indicated.

opposing effects on progression of unperturbed mitosis: excess CMT2 abrogates the checkpoint and accelerates mitosis while decreased CMT2 causes mitotic arrest.

### 3.3.2 Characterization of CMT2 RNAi arrest

We next sought to determine when in mitosis CMT2-depleted cells arrest. Immunofluorescence microscopy indicated that CMT2-depleted cells arrested in metaphase, with congressed chromosomes, high cyclin B levels and low cyclin A levels (Figure 3.3A). Previous studies suggested that CMT2 negatively regulates checkpoint signaling by binding to Mad2. However, it remains possible that CMT2 depletion damages the spindle or interferes with chromosome-microtubule attachment, causing a spindle checkpoint-dependent cell cycle arrest. To exclude this possibility, we examined two markers of chromosome-microtubule attachment: kinetochore tension and checkpoint protein localization. After chromosome congression, establishment of bipolar kinetochore-microtubule attachment results in centromere stretching from pulling forces (Shelby et al., 1996). Decreased or absent centromere stretching is indicative of defective or immature attachment. We measured interkinetochore distances in live, unfixed HeLa-CENP-B-GFP cells. Depletion of the human kinetochore protein hNuf2R to abolish attachment resulted in inter-kinetochore distances of  $0.6 \mu\text{m} \pm 0.2$  (Figure 3.3B). In contrast, inter-kinetochore distances in both control and CMT2-depleted cells averaged  $1.7 \mu\text{m} \pm 0.2$ . Chromosome congression was also normal in both control and CMT2 RNAi cells (Figure 3.2B and 3.3A).

We next monitored kinetochore-bound levels of Mad and Bub proteins by immunofluorescence. High levels of checkpoint proteins are found on unattached

Figure 3.3

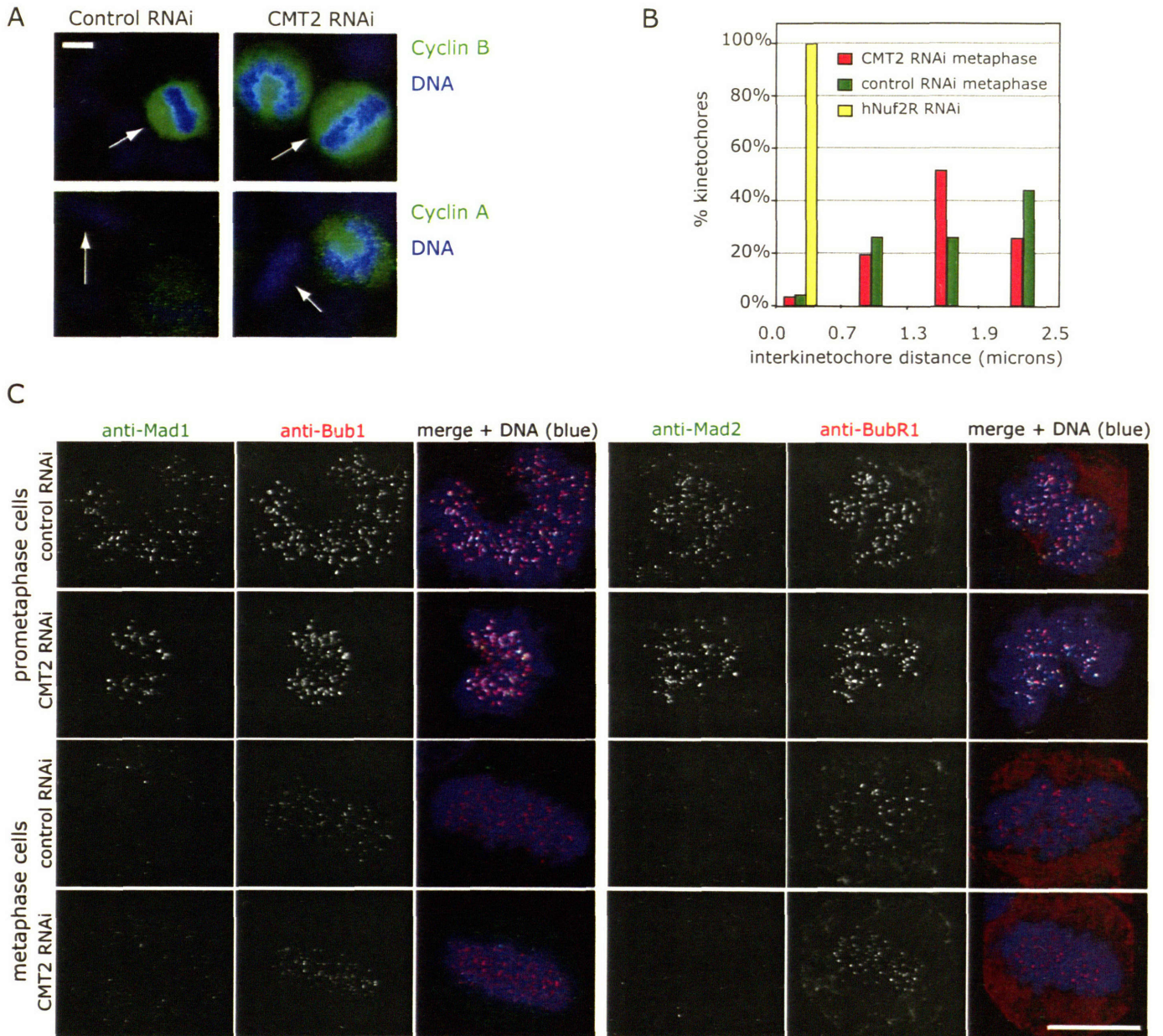


**Figure 3.3: CMT2 depletion arrests cells in a “checkpoint off” metaphase**

(A) Cells depleted of CMT2 arrest in mitosis. HeLa cells were treated with control or CMT2 siRNA and stained with DAPI (blue) and anti- cyclin B or anti-cyclin A (green).

(B) Kinetochores in CMT2-depleted cells are under tension. HeLa GFP-CENP-B cells were transfected with siRNAs against CMT2 or hNuf2R or a control and interkinetochore distances were measured in metaphase cells *in vivo* following 3D deconvolution microscopy. Distances were measured for 10 kinetochore pairs in each of 5 cells for each treatment.

(C) Checkpoint proteins localize normally in CMT2 depleted cells. HeLa cells depleted for CMT2 or Lamin A control were stained with DAPI (blue) and antibodies against the indicated checkpoint proteins (red and green). Scale bars are 10 $\mu$ m .

kinetochores during prometaphase and these levels fall as chromosomes bind microtubules during metaphase (Hoffman et al., 2001; Waters et al., 1998). However, high levels of Mad and Bub proteins remain associated with lagging and maloriented chromosomes, making immunofluorescence signals of checkpoint proteins at kinetochores a sensitive indicator of kinetochore-microtubule attachment status (Hoffman et al., 2001). When Mad1, Mad2, Bub1, and BubR1 and levels were compared in CMT2-depleted and control cells, levels of kinetochore-bound checkpoint proteins were indistinguishable (Figure 3.3C and Supplemental Figure 3.2). In both cases, Mad and Bub proteins were present at high levels in prometaphase and at significantly lower levels in metaphase. In CMT2-depleted metaphase cells, Mad2 had fully dissociated from kinetochores, implying that all chromosomes had made correct attachments to microtubules (Figure 3.3C). These experiments demonstrate that CMT2 is not required for the recruitment of checkpoint proteins to kinetochores or their subsequent dissociation in metaphase.

### **3.3.3 CMT2 localizes to kinetochores in a Mad2-dependent fashion**

To understand how CMT2 promotes anaphase entry, we next examined its subcellular localization. Previous studies conflict, stating that CMT2 may localize to either the nucleoplasm or the mitotic spindle (Habu et al., 2002; Xia et al., 2004). Using two different anti-CMT2 antibodies, we observed a dual localization pattern for CMT2 in HeLa cells: it was present on unattached kinetochores in prometaphase as determined by co-localization with CREST autoimmune serum and was also observed throughout the cytosol (Figure 3.4A). This localization pattern was specific, as two different siRNAs



Figure 3.4

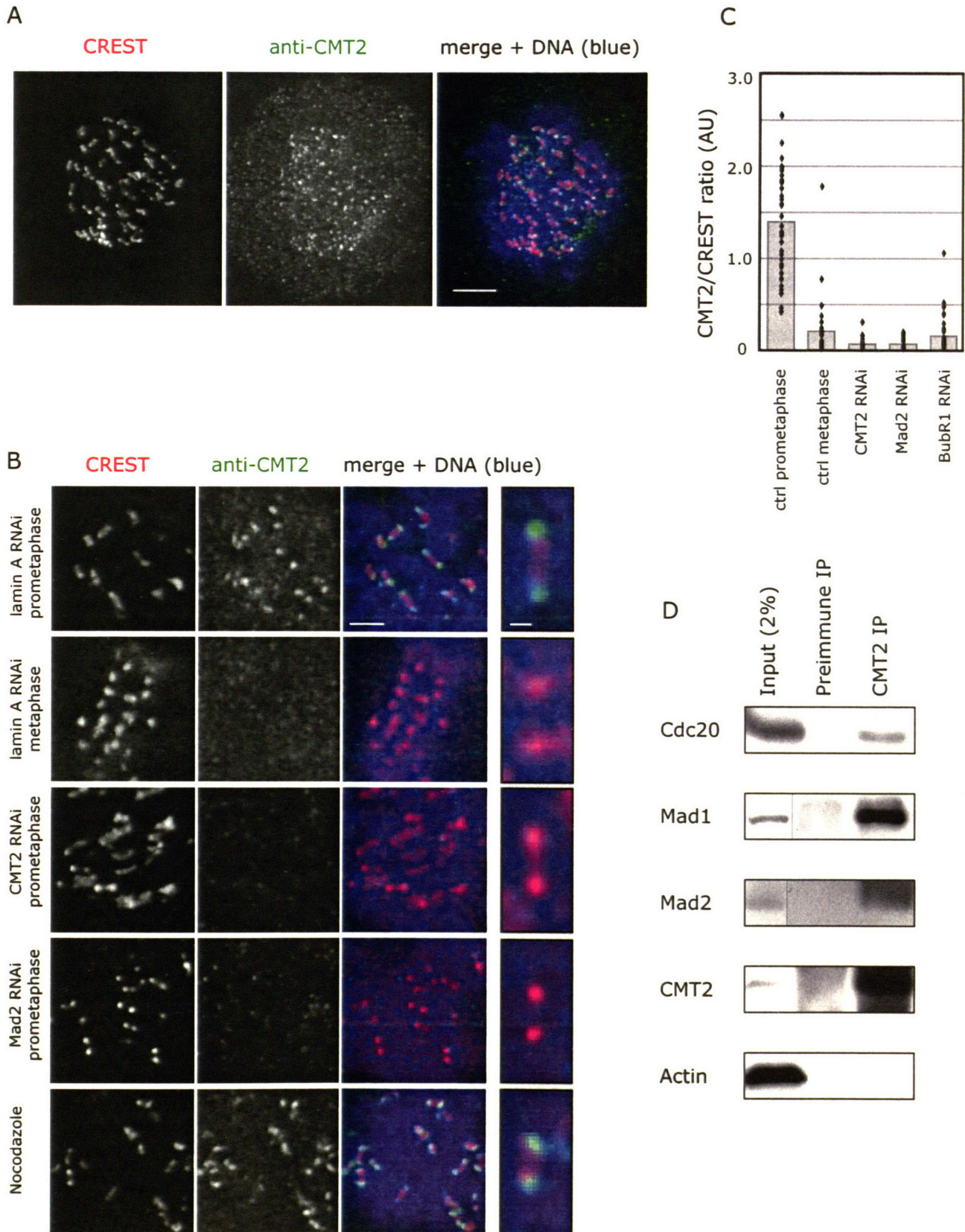


**Figure 3.4: CMT2 undergoes Mad2-dependent kinetochore localization**

(A) CMT2 localizes to kinetochores. HeLa cells were stained with DAPI, anti-CMT2, and CREST sera. Scale bar is 5 $\mu$ m. (B) CMT2 binds to kinetochores in prometaphase and requires Mad2. HeLa cells treated with the indicated siRNA were stained with DAPI, CREST, and anti-CMT2. Scale bar is 2.5 $\mu$ m. Indicative sister kinetochore pairs are magnified at right; scale bar is 0.5 $\mu$ m. (C) Quantitation of CMT2 loss from kinetochores. CMT2/CREST signal ratios from individual cells are plotted as dots; bars represent mean ratio values. (D) CMT2 forms ternary complexes with Mad1-Mad2 and Cdc20-Mad2 *in vivo*. Anti-CMT2 and pre-immune immunoprecipitates from nocodazole-arrested HeLa cells were resolved by SDS-PAGE and immunoblotting. Input lane represents 2% of protein used in IP.

against CMT2 strongly decreased both kinetochore and cytosolic staining (Figure 3.4B and C and Supplemental Figure 3.3). This pattern is reminiscent of Mad2, which exists both in a stably-bound pool at unattached kinetochores and a rapidly-cycling pool that shuttles between kinetochores and the cytosol. Because CMT2 binds Mad2, we investigated CMT2 localization in Mad2-depleted cells. Mad2 RNAi abrogated CMT2 levels on prometaphase kinetochores to an extent equal to CMT2 RNAi (Figure 3.4B and 3.4C). CMT2 is thus the first known protein whose kinetochore localization is Mad2 dependent (Vigneron et al., 2004). Like Mad2, CMT2 signal on kinetochores was high after nocodazole treatment, and in the absence of nocodazole decreased to nearly undetectable levels as kinetochores became attached and congressed on the metaphase plate (Hoffman et al., 2001); Figure 3.4B and 3.4C). The localization pattern we observe suggests that CMT2 may already interact with some population of Mad2 on kinetochores during prometaphase, when the checkpoint is still active. CMT2 is known to form ternary complexes with Mad2-Cdc20 in the cytosol, and we show in chapter 2 that CMT2 forms ternary complexes *in vitro* with Mad2-Mad1. To confirm that CMT2 participates in kinetochore-bound complexes, we immunoprecipitated CMT2 from nocodazole-arrested prometaphase cells and found that Mad2 and Cdc20 associated with CMT2 as expected (Fig 3.4D). Notably, Mad1 was present in CMT2 immunoprecipitates as well. While Mad2 and Cdc20 colocalize at kinetochores and in the cytosol, Mad1 is restricted to kinetochores in mitosis (Kallio et al., 1998; Shah et al., 2004). Thus, CMT2 localizes to kinetochores and forms stable ternary complexes with kinetochore checkpoint proteins.

As a final test of CMT2 localization, we transfected HEK 293 and HeLa cells with GFP-CMT2 and imaged them with fluorescence microscopy. In live, unfixed

interphase HEK 293 cells, GFP-CMT2 is confined to the nucleus (Figure 3.5A), suggesting that its putative bipartite NLS is functional. In live, unfixed HeLa Histone 2B-mRFP cells, bright kinetochore foci of GFP-CMT2 were visible in prometaphase (Figure 3.5B). Some GFP-CMT2 also remained in the mitotic cytoplasm. We observed a similar localization for transiently expressed GFP-Mad2 (Figure 3.5C). It is notable that in live prometaphase cells, GFP fusions of both CMT2 and Mad2 were visible on only a subset of kinetochores, unlike GFP-ZW10, which localize to every kinetochore (data not shown). For Mad2, this is believed to reflect the existence of stably- and dynamically-associated kinetochore populations of Mad2, (Shah et al., 2004), though it may also reflect failure of transiently-expressed protein to incorporate into pre-assembled complexes.

### **3.3.5 CMT2 RNAi arrest is spindle checkpoint dependent**

To determine if CMT2 RNAi arrest depends on the Mad2 checkpoint, we used the live-cell assay described above to observe HeLa Histone 2B-GFP cells co-depleted of CMT2 and other proteins by RNAi. Under these conditions,  $71 \pm 18\%$  of CMT2-depleted cells remained in mitosis 45 minutes after NBD, compared to  $11 \pm 8\%$  of control cells (Figure 3.2B and 3.6). As expected, depletion of Mad2 accelerated mitotic progression such that no Mad2 RNAi cells were observed in mitosis at  $T = 45$  minutes ( $0 \pm 0\%$ ). Co-depletion of Mad2 with CMT2 alleviated the arrest caused by CMT2 RNAi, with  $12 \pm 4\%$  of cells not yet in anaphase after 45 minutes, similar to control cells. Thus, Mad2 protein is required for cell cycle arrest in the absence of CMT2.

Figure 3.5

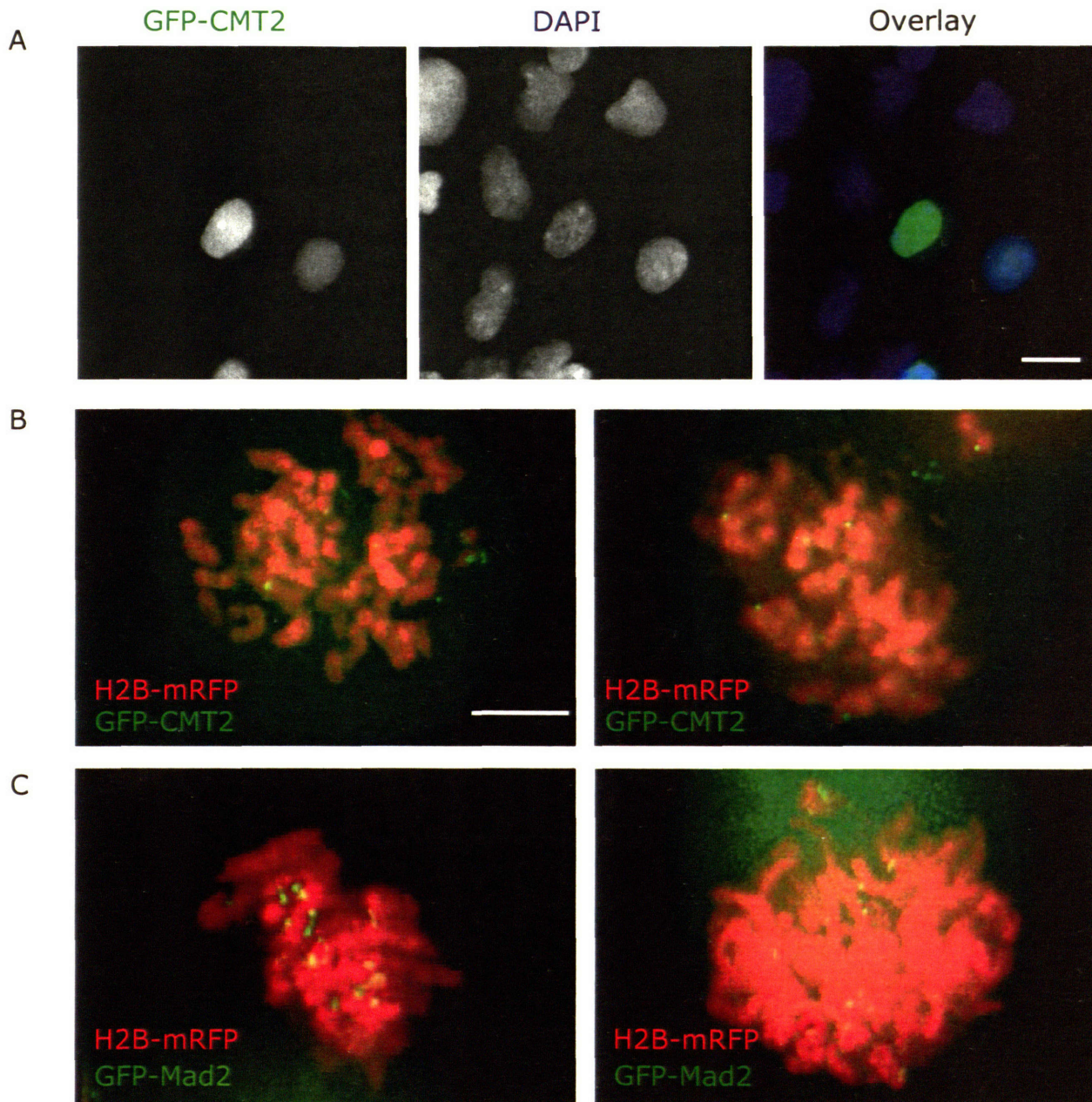


**Figure 3.5: GFP-CMT2 localizes to kinetochores in live cells**

(A) GFP-CMT2 is nuclear in interphase. HEK293 cells were transfected with GFP-CMT2, fixed, and stained with DAPI. Scale bar represents 5 $\mu$ m. (B) HeLa cells were cotransfected with Histone 2B-mRFP and either GFP-CMT2 (top) or GFP-Mad2 (bottom) and imaged by deconvolution microscopy. Scale bar represents 3 $\mu$ m.

We next asked whether CMT2 depletion arrest requires upstream proteins that generate the checkpoint signal or downstream checkpoint effectors. Mad1 and the kinetochore protein Nuf2R are required for Mad2 to bind kinetochores and thus provide a scaffold for checkpoint activation (Martin-Lluesma et al., 2002; Meraldi et al., 2004). BubR1 is a checkpoint effector that acts cooperatively with Mad2 to inhibit Cdc20 in solution (Fang, 2002; Tang et al., 2001). BubR1 RNAi phenocopied Mad2 RNAi, with cells progressing rapidly into anaphase and only  $1\pm 1\%$  remaining in metaphase at  $T = 45$  minutes (Figure 3.6). After co-depletion of BubR1 with CMT2,  $9\pm 8\%$  of cells remained in mitosis at  $T = 45$ , similar to Mad2-CMT2 co-depletion. However, cells co-depleted of CMT2 with either Mad1 ( $87\pm 18\%$ ) or Nuf2R ( $77\pm 7\%$ ) remained arrest in mitosis compared to cells depleted of only Mad1 ( $4\pm 3\%$ ) or Nuf2R ( $10\pm 4\%$ ). Thus, CMT2 depletion in a context where Mad2 cannot localize to kinetochores arrests cells in metaphase, suggesting that CMT2 is necessary to inhibit cytosolic Mad2.

### **3.3.6 CMT2 functions on and off kinetochores**

Does CMT2 also inhibit the generation of Mad2 signal on kinetochores? We examined more closely the mitotic kinetics of RNAi treated HeLa Histone 2B-GFP cells in order to probe on- and off-kinetochore Mad2 function. Cumulative frequency graphs showed that populations of control RNAi cells progressed from NBD to anaphase with a  $t_{1/2} = 21$  minutes (Figure 3.7A), and all cells entered anaphase by 30 minutes. The majority of CMT2 RNAi cells remained arrested for many hours or until photodamaged, though 38% of cells entered mitosis after 3 hours, perhaps reflecting heterogeneity of depletion. When cytoplasmic and kinetochore pools of Mad2 were both depleted by

Figure 3.6

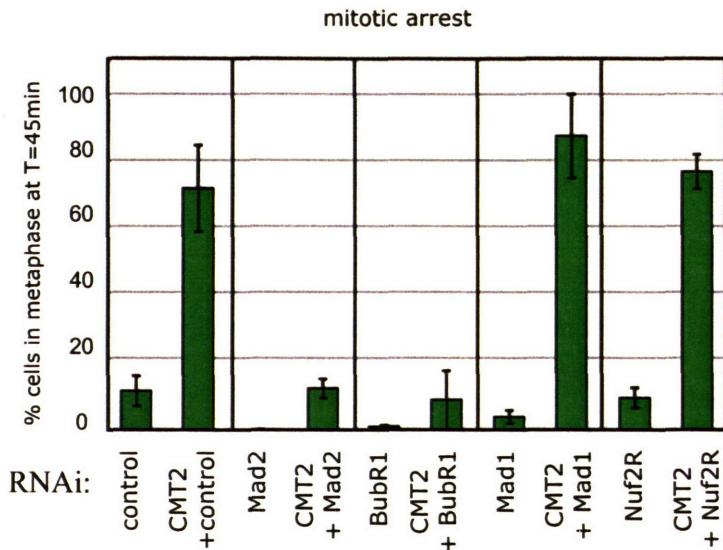


**Figure 3.6: CMT2 RNAi arrest requires checkpoint effectors and targets cytosolic Mad2**

HeLa HeLa Histone 2B-GFP cells were treated with siRNA and mitotic arrest was measured by live cell imaging as in Figure 1B. Graph depicts fraction of cells arrested in mitosis, defined as remaining in metaphase at T>45 minutes after NBD. Bars indicate mean and SEM of at least two independent experiments and at least 100 cells.

Mad2 RNAi, anaphase entry occurred with a half-life of 9 minutes. As was observed with mitotic arrest (Figure 3.6), BubR1 RNAi phenocopied Mad2 depletion, with extremely rapid kinetics of anaphase entry ( $t_{1/2} = 12$  minutes, Figure 3.7C). Mad1 RNAi, which displaces kinetochore Mad2, caused cells to enter anaphase with normal kinetics and a  $t_{1/2} = 20$  minutes (Figure 3.7A).

When cells were co-depleted of CMT2 and Mad2 by double RNAi, we observed a Mad2-like phenotype of accelerated mitosis ( $t_{1/2} = 11$  min, Figure 3.6 and 3.7B). Co-depletion of BubR1 with CMT2 also abrogated CMT2 RNAi arrest, with cells entering anaphase with wildtype-like kinetics ( $t_{1/2} = 21$  minutes, Figure 3.7C). When CMT2 was co-depleted with Mad1, anaphase  $t_{1/2}$  was 90 minutes and by 3 hours 80% of cells overcame metaphase arrest and entered anaphase (Figure 3.7B). This “leak through” phenotype may reflect the requirement for Mad1 to localize Mad2 to the kinetochore or it may reflect a specific genetic interaction between Mad1 and CMT2. Because the HEC1/Nuf2R complex is required for checkpoint proteins to localize to kinetochores, we therefore examined the mitotic behavior of Nuf2R and Nuf2R-CMT2 depleted cells. Nuf2R depletion did not alter anaphase entry significantly, with  $t_{1/2}$  of approximately 28 minutes (Figure 3.7D). Cells co-depleted of Nuf2R and CMT2 entered anaphase with slow, linear kinetics and a  $t_{1/2} = 70$  minutes.

Thus, co-depletion of CMT2 with checkpoint signal generators or effectors gives two separate sets of phenotypes. Checkpoint effectors such as BubR1 or Mad2 are absolutely required for metaphase arrest in the absence of CMT2. Co-depletion with Mad2 or BubR1 overcomes CMT2 RNAi arrest and cells enter anaphase before chromosomes become attached. In comparison, checkpoint signal generators such as



Figure 3.7

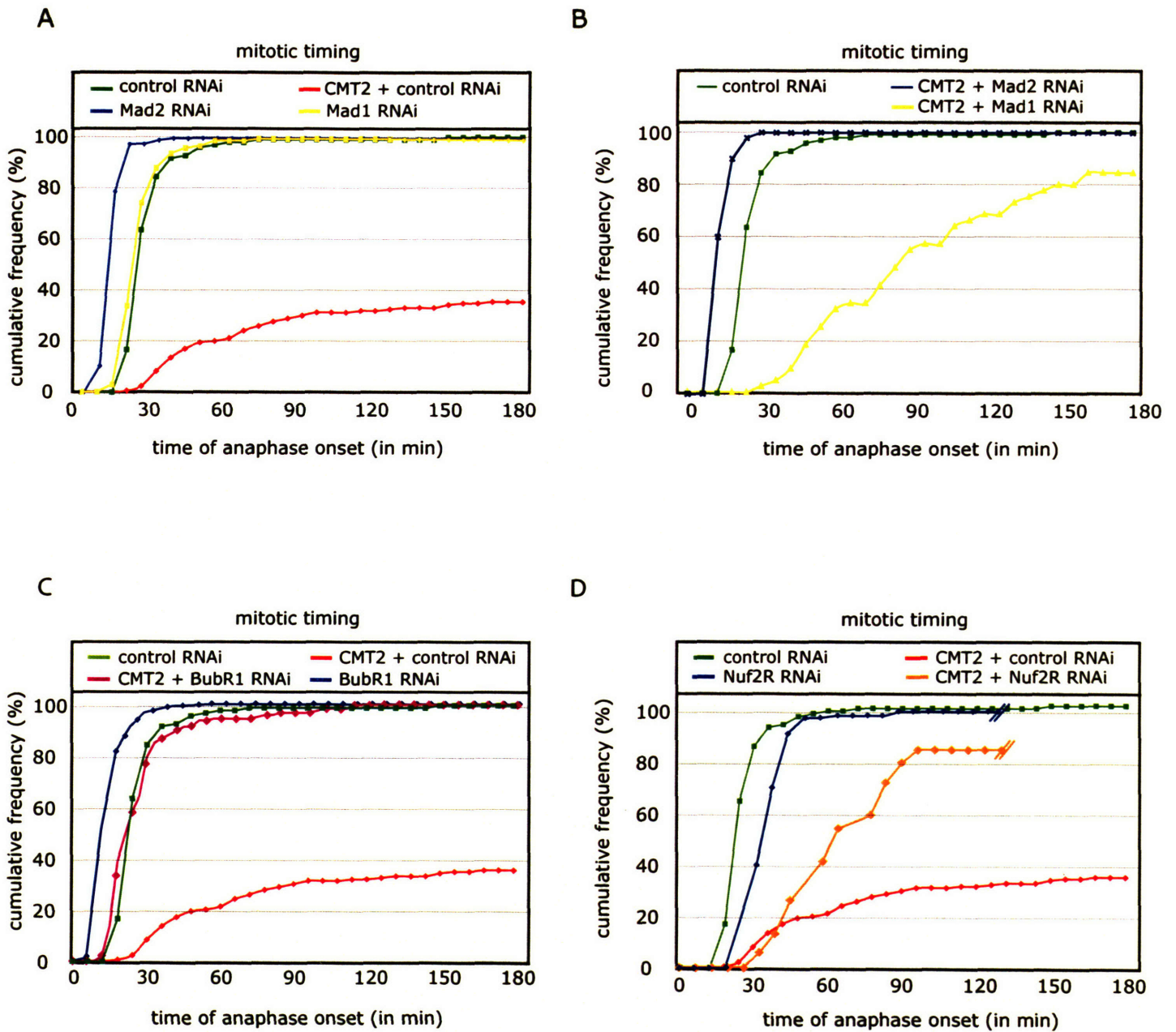


**Figure 3.7: Kinetic analysis of CMT2 depletion**

HeLa Histone 2B-GFP cells transfected with siRNA were followed in mitosis by live cell imaging as described above. Graphs depict the cumulative frequency of anaphase entry times, defined as time from nuclear breakdown to anaphase A.

Mad1 and Nuf2R are not required for CMT2 RNAi arrest and co-depleted cells enter anaphase, albeit with slow and heterogeneous kinetics..

### 3.4 Discussion

In this chapter we test the function of CMT2 *in vivo* and find that it is required for progression of HeLa cells through mitosis. Cells depleted of CMT2 cannot pass the metaphase-anaphase transition, and cells that overexpress CMT2 enter anaphase before all their chromosomes have time to attach to the spindle. Strikingly, cells lacking CMT2 arrest in metaphase with aligned, attached chromosomes and checkpoint protein localization consistent with a “checkpoint off” state. CMT2 and Mad2 have opposing effects on cell cycle progression, and we demonstrate for the first time that CMT2 drives cells into anaphase by targeting the Mad2/BubR1 checkpoint effector complex and not upstream checkpoint signals. Previous studies have detected CMT2 function only in the context of spindle damage provoked by anti-microtubule drugs (Habu et al., 2002; Xia et al., 2004). We show, in contrast, that a cell cannot enter anaphase until CMT2 silences the spindle checkpoint, consistent with findings that the spindle checkpoint is active in every cell cycle (Dobles et al., 2000; Meraldi et al., 2004; Michel et al., 2001).

The mechanism by which CMT2 opposes Mad2 function and allows Cdc20 activity is not yet known. We demonstrate for the first time that CMT2 localizes to prometaphase kinetochores and forms ternary complexes *in vivo* with the Mad1-Mad2 kinetochore complex. The interaction of Mad2 and CMT2 at the kinetochore suggests that CMT2 might inhibit the spindle checkpoint upon kinetochore-microtubule binding. We suggest that CMT2 is required for inhibiting Mad2 both at kinetochores and in the cytosol. Combined with biochemical data from chapter 2 and structural models of Mad2,

we propose a model in which CMT2 drives cell cycle progression both by stemming the flux of Mad2 through the kinetochore and by de-inhibiting Cdc20 in the cytosol. The work presented here supports the notion that CMT2 is a potent “off switch” for the spindle checkpoint and points to the urgency of identifying how that switch is flipped when kinetochore-microtubule binding is achieved.

### 3.4.1 Checkpoint activation and inactivation

What is the molecular nature of the active spindle checkpoint signal? At least three proteins are proposed as *direct* inhibitors of cell cycle progression: Bub1, BubR1, and Mad2. Recent work has shown that Bub1 can phosphorylate Cdc20 *in vitro* and inhibit APC/C<sup>Cdc20</sup> activation (Tang et al., 2004). Mutation of all phosphoacceptor residues on Cdc20 abrogates the checkpoint and causes premature anaphase. *In vitro*, BubR1 binds Cdc20 and inhibits APC/C both on its own and synergistically with Mad2 (Fang, 2002). However, it is not clear whether *in vivo* BubR1 acts independently or only with Mad2 in a larger mitotic checkpoint complex known as MCC. Careful quantitation of checkpoint complexes in yeast suggests that the BubR1 homolog Mad3 only associates with Cdc20 in conjunction with Mad2, while Mad2 associates with Cdc20 free of Mad3 (Poddar et al., 2005). Like Bub1, BubR1 is required for the kinetochore localization of other checkpoint proteins, and the very strong phenotype seen in BubR1 RNAi may reflect multiple roles in checkpoint assembly and activation (Chen, 2002). Considerable debate exists over the role of BubR1 kinase activity in checkpoint signaling. Kinase-inactive BubR1 mutants sustain checkpoint signaling in *Xenopus* egg extracts and *in vitro* APC/C activation assays, and budding yeast Mad3/BubR1, which clearly lacks a kinase

domain, binds Cdc20 (Chen, 2002; Tang et al., 2001). However, in other assays, impairment of BubR1 kinase activity prevents sustained arrest, implying that BubR1 may inhibit Cdc20 both stoichiometrically and catalytically (Kops et al., 2004; Weaver et al., 2003).

Mad2 cell cycle inhibitory activity appears to involve at least two components: Cdc20 binding and Mad2 dimerization. Cdc20 binding by Mad2 is believed to inhibit APC/C activation by sterically blocking access of Cdc20 either to APC/C or to Cdc20 substrates. Other “core” APC/C subunits such as Cdc27 and Cdc16 have been found in complex with Mad2-Cdc20, suggesting that Mad2-bound Cdc20 may bind APC/C without activating it (Kallio et al., 1998). However, these results differ between yeast and mammals and are further confused by the obvious molecular heterogeneity of APC/C complexes. Mad2 dimerization is proposed to promote checkpoint signaling by promoting flux of open Mad2 conformers (O-Mad2) through the kinetochore by dynamic association with closed (C-Mad2)-Mad1 complexes. However, neither Mad2 dimerization nor cycling through kinetochores has been observed in yeast. Furthermore, mere positioning of O-Mad2 at kinetochore sites cannot be sufficient for Cdc20-binding or checkpoint activation, as pools of O-Mad2 and Cdc20 co-exist in the cytosol without binding. Clearly, some other aspect of checkpoint signaling is required to render O-Mad2-Cdc20 interaction at kinetochores sensitive to the state of kinetochore-microtubule attachment (Hagan and Sorger, 2005). As with BubR1, the relative inhibitory roles of Mad2 alone and Mad2 bound to MCC have not been distinguished. Because CMT2 was originally identified as a Mad2 binding protein, we tested its ability to oppose Mad2 function. CMT2 overexpression mirrors Mad2 depletion (Figure 3.2), and Mad2

overexpression causes a similar, if perhaps weaker, metaphase arrest to CMT2 RNAi. CMT2 and Mad2 colocalize at kinetochores and in the cytoplasm, and Mad2 is required for the metaphase arrest caused by CMT2 RNAi.

If CMT2 specifically inhibits Mad2 function, why does loss of BubR1 overcome CMT2 RNAi arrest (Figure 3.6 and 3.7C)? One possibility is that BubR1 is absolutely required for APC/C inhibition in all contexts, and BubR1 RNAi is epistatic to CMT2 depletion or interference with Mad2 activity. This is consistent with the finding in fission yeast that Mad3p was required for the arrest caused by Mad2 overexpression (Millband and Hardwick, 2002). However, as this arrest did not require Mad1p, it may represent simple Cdc20 inhibition by Mad2p mass action and not true kinetochore-sensitive checkpoint signaling. A second possibility is that CMT2 interacts functionally, if not directly, with BubR1. Careful quantitation in budding yeast found all prometaphase Cdc20 in two complexes: a large pool of Mad2-Cdc20 and a small pool of MCC-Cdc20, which contains Mad2, Mad3, and Bub3 (Poddar et al., 2005). An analogous MCC complex containing BubR1 exists throughout metazoan cell cycles (Sudakin et al., 2001) but the existence of Mad2-free BubR1-Cdc20 has not been ruled out. This suggests a scenario in which Mad3/BubR1 is absolutely required for Cdc20 inhibition but functions *in vivo* solely in Mad2-containing complexes. Binding of CMT2 to Mad2-Cdc20 complexes enabled them to activate APC/C *in vitro* (Xia et al., 2004), but these experiments did not probe the involvement of BubR1 in APC/C activation. It therefore is necessary to compare quantitatively APC/C activity for CMT2-BubR1-Cdc20 and CMT2-Mad2-BubR1-Cdc20. If Mad2 and BubR1 do, in fact, inhibit Cdc20 cooperatively, then their negative regulation may occur in a cooperative or coupled fashion as well.

Attempts at finding BubR1-binding proteins have not identified CMT2 but it remains to be seen whether they interact indirectly. Clearly checkpoint inactivation cannot be well characterized without a more complete catalog of checkpoint inhibitory complexes and their mechanism of APC/C inhibition.

### **3.4.2 Mechanism of CMT2 function**

How and where does CMT2 inhibit Mad2? We show that CMT2, like Mad2, localizes to both the kinetochore and the cytosol, and that kinetochore localization requires Mad2. CMT2 depletion arrests the cell cycle, and this arrest is mediated by Mad2 (Figure 3.6 and 3.7A). Therefore, we use CMT2 RNAi arrest as a proxy for Mad2 activation to probe CMT2 function on and off kinetochores.

Kinetochore-dependent checkpoint signaling requires Nuf2R and Mad1 for formation of Mad1-Mad2 “core” complexes that promote cycling of cytosolic, open Mad2 through the kinetochore (De Antoni et al., 2005; Howell et al., 2004). In the absence of the Mad1/Nuf2R scaffold, a pool of active, cytoplasmic Mad2 is formed early in mitosis and inhibits Cdc20 (Meraldi et al., 2004). This Mad2 pool imposes a default delay before anaphase entry but is not sensitive to kinetochore-microtubule attachment. When we co-deplete CMT2 in this context of Mad1 or Nuf2R RNAi, metaphase arrest still occurs (Figure 3.6), providing strong evidence that CMT2 is required for silencing of off-kinetochore, cytosolic Mad2.

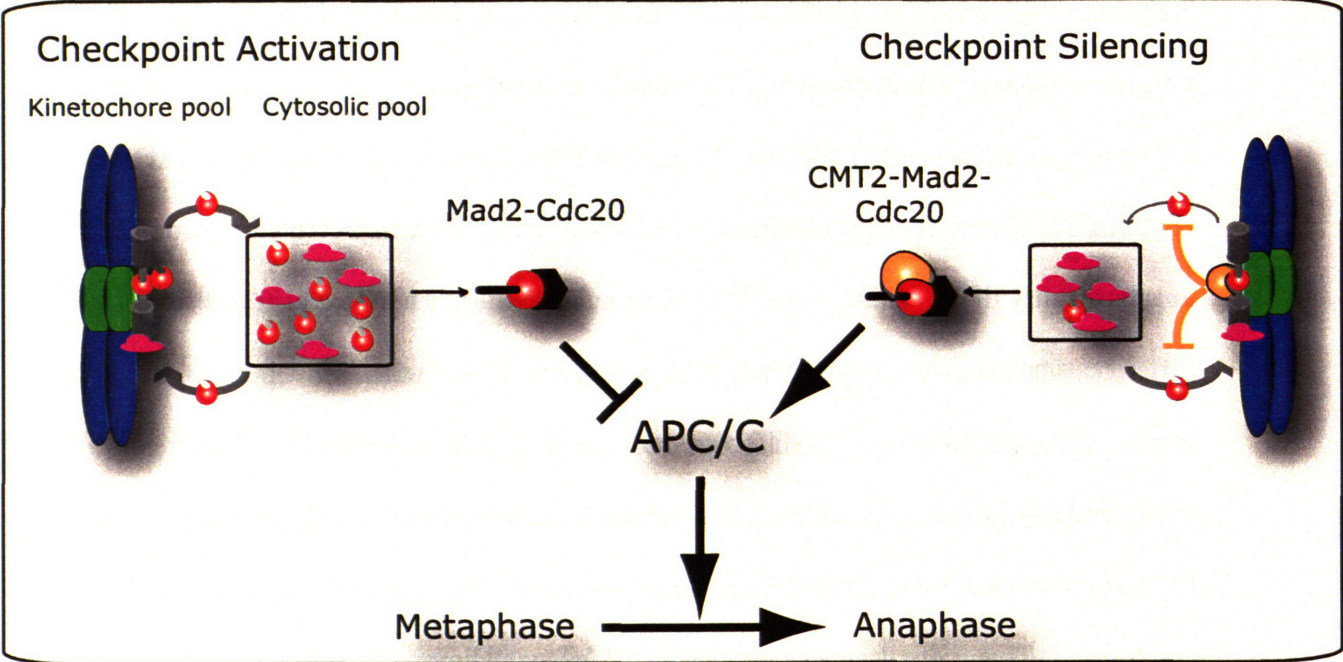
To ask whether CMT2 inhibits Mad2 at kinetochores, we closely examined the kinetics of anaphase entry to assess the size of the active Mad2 pool. In Mad1 or Nuf2R RNAi, the cytoplasmic Mad2 pool is not replenished from the kinetochore and anaphase

begins with a  $t_{1/2}$  of approximately 20 min, identical to control cells (Figure 3.7A and 3.8). When this Mad2 pool is freed from inhibition by co-depletion of CMT2, cells undergo prolonged a metaphase and most cells are effectively arrested, but this arrest is not as long-lived as in CMT2 RNAi. More than 80% of cells depleted of Mad1-CMT2 or Nuf2R-CMT2 enter anaphase within 3 hours after NBD. We interpret this variation of anaphase entry times, which range from 30 minutes to more than three hours, to reflect differences in the size of active Mad2 pool generated in early mitosis independent of Mad1. Without silencing by CMT2, this pool becomes inactive with a half-life of approximately 90 minutes. When CMT2 alone is depleted, the kinetochore-independent pool of active Mad2 is augmented by active Mad2 generated at the kinetochore. The resulting Mad2 activity is able to inhibit Cdc20 for many hours (Figures 3.2 and 3.7). We infer that the different kinetics of anaphase entry observed in CMT2 and Mad1/CMT2 RNAi reflects quantitatively different Cdc20-inhibition, strongly suggesting that CMT2 also inhibits Mad1-dependent Mad2 activity at the kinetochore. Further parsing of on- and off-kinetochore function of CMT2 will require location-specific probes and mutants of both CMT2 and Mad2.

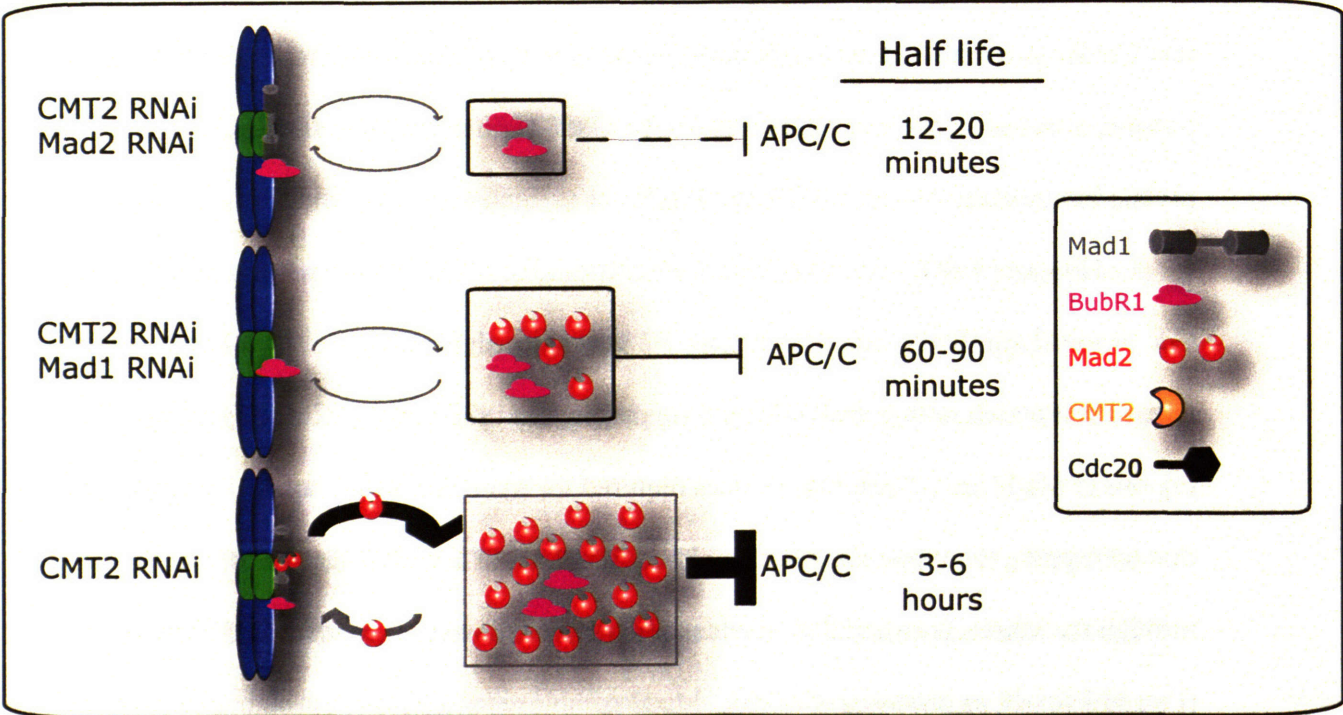
How can CMT2 inhibit cytosolic Cdc20-Mad2 as well as kinetochore-bound Cdc20-Mad2 and Mad1-Mad2? In chapter 2 we explored the ability of CMT2 to form ternary complexes with both Mad2 binding partners and showed that CMT2-binding regions in Mad2 are adjacent to residues required for Mad2 dimerization. We suggest that by capping the dimer interface on closed Mad2, CMT2 inhibits the flux of Mad2 through the kinetochore and thus silences signal generation at the Mad1-Mad2 complex (Figure 3.8). If, as proposed, Cdc20-C-Mad2 complexes also undergo dynamic

Figure 3.8

A



B





**Figure 3.8: A model of CMT2 function**

**(A)** CMT2 inhibits Mad2 by preventing dimerization and releasing inhibition of Mad2-bound Cdc20. Mad2 (red) cycles between a cytosolic pool and the kinetochore. Binding of Mad2 to Mad2-Mad1 at the kinetochore is required for generation of activity in the cytosol. Upon checkpoint silencing, CMT2 binds Mad2-Mad1 and the kinetochore and Mad2-Cdc20 in the cytosol. Kinetochore CMT2 inhibits Mad2 dimerization and prevents replenishment of the cytosolic pool. CMT2 binding to Mad2-Cdc20 renders the complex competent for APC/C activation. **(B)** Comparison of anaphase entry half-lives reveals a role for CMT2 at the kinetochore. When both CMT2 and Mad2 are depleted (top), APC/C inhibition is minimal and anaphase begins shortly after NBD. When Mad1 and CMT2 are depleted (middle), the cytosolic Mad2 pool that forms early in mitosis is not replenished from the kinetochore by a Mad1 complex. In the absence of inhibition by CMT2, this Mad2 activity remains active for 60-90 minutes. When CMT2 alone is depleted (bottom), a large pool of Mad2 activity is generated by kinetochore Mad2-Mad1 and is not inhibited by CMT2. APC/C remains inhibited for many hours.

association with O-Mad2 from the cytosol, CMT2 would be predicted to cap and inhibit this interaction as well (De Antoni et al., 2005; Hagan and Sorger, 2005). Very recent experiments show that purified CMT2 competes with O-Mad2 for Mad1-Mad2 binding *in vitro* (M. Mapelli, personal communication).

Does CMT2 inhibit both of Mad2's checkpoint activating activities? Xia et al show *in vitro* that CMT2 restores the ability of Mad2-bound Cdc20 to activate APC/C without displacing Mad2 (Xia et al., 2004). This striking result contradicts the common assumption that Mad2 inhibits Cdc20 by sequestration or steric hindrance and suggests that in the Cdc20-Mad2-CMT2 complex CMT2 can effectively de-inhibit Mad2-bound Cdc20. In the absence of structural insights into either APC/C<sup>Cdc20</sup> activation or Cdc20 inhibition by Mad2, it is difficult to envision how addition of CMT2 to the Cdc20-Mad2 complex relieves Cdc20 inhibition. CMT2 knockdown arrests cells with high cyclin B and low cyclin A (Figure 3.3A). Because cyclin A is a Cdc20 substrate, this result shows that CMT2 is not a general de-inhibitor of all mitotic Cdc20 (Dawson et al., 1995; Geley et al., 2001; Sigrist et al., 1995). One possibility is that CMT2-Cdc20-Mad2 complexes form in early mitosis but are incompetent for APC/C activation towards cyclin B and securin because of modification of CMT2, Cdc20, or APC/C. Both Cdc20 and APC/C are extensively modified in mitosis (Kotani et al., 1999; Rudner and Murray, 2000; Yudkovsky et al., 2000) and APC/C purified from interphase cells is insensitive to inhibition by MCC (Sudakin et al., 2001). A second possibility is that Cdc20 adopts multiple conformations, and both checkpoint sensitivity and APC/C activation are specific for Cdc20 conformers. We explore this possibility more fully in Chapter 4. The evidence presented here suggests that CMT2 inhibits Mad2 both at the kinetochore and in

the cytosol; understanding the mechanism of this impressive cell biological task will require further biochemical and structural study.

### **3.4.3 CMT2 localization and the assembly of checkpoint complexes**

Mitosis is a series of events in which complex mechanical tasks must be tightly coordinated. A common theme of mitosis, as well as classical signal transduction, is the regulated co-localization of interacting proteins. Two important aspects of checkpoint protein localization have informed models of the spindle checkpoint. First, all known metazoan spindle checkpoint proteins localize to kinetochores after nuclear envelope breakdown (Lew and Burke, 2003). In budding yeast, Bub proteins localize to kinetochores in every mitosis while Mad proteins appear to bind only to kinetochores that become detached (Gillett et al., 2004). This difference between yeast and metazoans likely reflects structural differences in spindle assembly between their closed and open mitoses. The second major aspect of checkpoint protein localization is their dynamicity: Mad2, Cdc20, Bub3, BubR1, and Mps1 bind, dissociate, and rebind unattached kinetochores with half-lives of 1-25 seconds, while Bub1, Mad1, and a population of Mad2 remain stably associated at kinetochores and do not cycle (Howell et al., 2004; Shah et al., 2004). Upon kinetochore attachment, Bub1 and BubR1 levels decrease but are still detectable, while all other checkpoint proteins leave the kinetochore and relocalize to the cytosol, spindle, and spindle poles (Taylor et al., 1998). What is the significance of checkpoint protein trafficking? Dynamic cycling of Mad2 and BubR1 between kinetochores and the cytosol is suspected to be critical for rapid sensing of kinetochore-microtubule occupancy, as well as for transmission and amplification of the

“wait anaphase” signal to the rest of the cell. Depletion of checkpoint proteins from kinetochores and relocalization to the spindle and poles in metaphase may contribute to silencing of the checkpoint signal.

If CMT2 negatively regulates Mad2, why does CMT2 bind to unattached kinetochores in prometaphase and nocodazole-treated cells (Figure 3.3 and 3.5) rather than to attached, silenced kinetochores? This observation suggests that checkpoint signaling is not a simple stepwise process, but that positive and negative regulators are recruited simultaneously to the point of attachment sensing. Indeed, no evidence exists to suggest that the kinetochore pool of a given checkpoint protein is homogenous; proteins may be modified, activated, or inactivated at kinetochores such that multiple forms of one protein are present on the same kinetochore. Thus CMT2 might bind to Mad2 on checkpoint active kinetochores either (1) without activating Cdc20 due to APC/C modification status (Kraft et al., 2003); (2) in insufficient amounts to silence the signal; or (3) concomitant with CMT2 modification that leaves CMT2 Mad2-bound but inactive for APC/C activation. We have begun gathering evidence of CMT2 modification by other checkpoint proteins that is consistent with this possibility (R. Hagan and H. Hess, unpublished).

To understand the significance of CMT2 kinetochore localization it will be critical to ask by FRAP or other methods whether CMT2 binds statically to kinetochore Mad2 or cycles dynamically between the kinetochore and the cytosol. We detect CMT2 in the cytosol as well as at kinetochores and provide evidence that CMT2 inhibits Mad2 at both sites, making it likely that CMT2 transits with Mad2. While it remains possible that other factors than Mad2 are necessary for CMT2 to bind kinetochores, testing this

experimentally is complicated by the fact that Mad2 sits atop the kinetochore localization hierarchy, and RNAi of many kinetochore and checkpoint proteins displaces Mad2 and, hence, CMT2.

How do Mad2, CMT2, and other checkpoint proteins leave the kinetochore in metaphase? In PtK1 cells the minus-end directed motor dynein transports Mad2 onto the spindle, and dynein inhibition leads to mitotic arrest (Howell et al., 2001). However, dynein also forms complexes with Zw10 and ROD, which are required for spindle checkpoint function, and dynein may play multiple roles in establishment of tension and chromosome segregation (Hunter and Wordeman, 2000; Starr et al., 1998; Wojcik et al., 2001). For Mad2 to be completely removed from kinetochores, the stable Mad1-Mad2 complex must either be removed or disassembled by Mad2 tail opening. An attractive possibility is that microtubule attachment displaces checkpoint complexes from kinetochores, either by competing for a common binding site or by leading to colocalization of checkpoint-removing complexes such as dynein/dynactin. Finally, we cannot exclude the possibility that capping of Mad2 complexes by CMT2 not only silences them but tags them for removal.

#### **3.4.4 CMT2 and chromosome segregation**

Intense work has focused on finding ways in which spindle checkpoint dysfunction might lead to genomic instability, aneuploidy, and cancer. Mutations in human spindle checkpoint genes are rare in humans, though functional mutation of Bub1, BubR1, and the Zw10-ROD-Zwilch complex have been detected in human cancers (Cahill et al., 1998; Hanks et al., 2004; Wang et al., 2004). Targeted deletion of Mad2,

BubR1, CENPE, and Bub3 in mice has proven embryonic lethal in all cases with little common evidence pointing to tumor promotion as a result of checkpoint failure. One explanation for these results is that loss of an essential checkpoint gene yields massive chromosome loss that is lethal in most mitoses. We observed that weak overexpression of CMT2 causes an accelerated mitosis with obvious but not catastrophic chromosome loss (Figure 3.2A). The majority of chromosomes congress and attach to the spindle in GFP-CMT2 cells, and depletion of CMT2 does not alter attachment or spindle function. Thus, we believe that these chromosomes missegregate not because of an attachment defect but because CMT2 inhibition of Mad2 shortens prometaphase and metaphase and overcomes the checkpoint. This phenotype requires only mild overexpression of GFP-CMT2, as strong overexpression leads to the formation of GFP-CMT2 aggregates in interphase, resulting in apoptosis (data not shown). Thus, we suggest that dysregulated CMT2 expression might impair checkpoint activity sufficiently to induce mild chromosome missegregation but not cell death. As discussed in Chapter 4, the CMT2 genomic locus is frequently amplified or translocated in human cancers, and careful experimentation will be required to determine if this contributes to genomic instability early in tumorigenesis.

### **3.4.5 Summary and conclusions**

In summary, we show that CMT2 is a potent inhibitor of the human Mad2 spindle checkpoint protein and is required for proper completion of mitosis. CMT2 colocalizes with spindle checkpoint proteins in the cytosol and on unattached kinetochores and forms complexes with Mad1-Mad2 and Cdc20-Mad2 *in vivo*. Our data help to resolve the

question of how multiple active pools of Mad2 can be efficiently regulated at different cellular locations. More broadly, the work presented here highlights the essential nature of checkpoint regulation in mitosis and questions the classic model of the spindle checkpoint as a surveillance mechanism that is inactive in normal mitoses. Negative regulation of the checkpoint is an unexplored avenue that promises to yield insight into both the workings of the eukaryotic cell cycle and, perhaps, the early steps of tumor progression.

### **3.5 Materials and methods**

#### **Generation of plasmids**

Mad2 (EST Genbank ID R10991) was subcloned by PCR into pGEX-6P-2 (Amersham Biosciences) and pEGFPC1 (Clontech). CMT2 (IMAGE clone 321778, ATCC) was subcloned into pEGFPC1, pET28A, and pFBnHis10HA. CMT2<sup>1-138</sup> was subcloned by PCR into pGEX-6P-2. The cDNA for mRFP, a kind gift of R. Tsien, was fused to histone H2B in pCDNA3.1 (Invitrogen). All plasmids were confirmed by sequencing.

#### **Cell culture and antibodies**

Polyclonal antibodies were raised in NZW rabbits against human CMT2 and CMT2<sup>1-138</sup> expressed in *E. coli* (Covance). A column of immobilized CMT2<sup>1-138</sup> was made with the SulfoLink kit (Pierce) for affinity purification of anti-CMT2<sup>1-138</sup> immune sera. Antibody dilutions for immunoblotting, immunofluorescence, and immunoprecipitation are in Supplementary Table 3.1.

HeLa, Histone 2B-GFP HeLa , HeLa Histone 2B-mRFP, and HeLa CENPB-GFP cells were generated and cultured as described (Meraldi et al, 2004). All siRNA oligos were purchased from Dharmacon Research. The sequences for the CMT2 siRNA duplexes are CMT2-1 (GGAGUUCUAUGAACUGGAC) and CMT2-3 (CUGUAAUCAUCGCUGAACAA). Duplexes and RNAi for Lamin A (Elbashir *et al.*, 2001), Mad1 and Mad2 (Martin-Lluesma et al., 2002) and hNuf2R and BubR1(Meraldi et al., 2004) have been described. HeLa cells were transfected with siRNA as described (Elbashir *et al.*, 2001) and analyzed 48 hours after transfection. GFP-CMT2 and GFP-Mad2 were transiently expressed in HeLa Histone 2B-mRFP cells using Fugene 6 (Roche Diagnostics) and cells analyzed 16 hours after transfection.

### **Immunoprecipitation and Immunoblotting**

HeLa cells were arrested overnight in 200ng/mL nocodazole (Sigma), harvested in lysis buffer (150mM NaCl, 0.5% NP-40, 1mM DTT, 10% glycerol, complete phosphatase and protease inhibitors, 50mM Hepes pH 7.6, 100μM ATP, 2mM EDTA) and clarified by centrifugation. Approximately 5-10 mg of cellular protein was pre-cleared with protein A beads (Pharmacia) and incubated with antibody for 1 hour at 4°C before addition of 20μL protein A beads and incubation for 2-3 hours. Beads were pelleted, washed in cold IP buffer, and boiled in 2x SDS sample buffer before SDS-PAGE. Whole cell extracts were prepared by boiling cells in 2x SDS sample buffer with 15% β-ME before SDS-PAGE.

### **Microscopy**



Cells were fixed, permeabilized and blocked as described (Kapoor *et al.*, 2000). Cross-adsorbed secondary antibodies were used (Molecular Probes). Images were acquired as described (Martinez-Exposito *et al.*, 1999) and kinetochore fluorescence intensities were calculated as described (Meraldi *et al.*, 2004) .

Live cell imaging was performed in  $\Delta T$  0.15 mm-dishes (Biopetechs) in CO<sub>2</sub>-independent medium (GibcoBRL) at 37°C. 0.2s exposures were acquired every 3 min for 6 hr using a 20x NA0.75 objective on a Nikon Applied Precision Deltavision microscope equipped with a Mercury 100W lamp, GFP-long pass filter set (for Histone 2B-GFP-Hela cells) or a Sedat filter set (to follow GFP-proteins in Histone 2B-Red-Hela cells; Chroma) and Coolsnap HQ camera. Point visitation was used to follow cells in multiple fields. Interkinetochore distances were measured in unfixed HeLa GFP-CENP-B expressing cells as described (Meraldi *et al.*, 2004).

### **Estimation of anaphase entry half-lives**

Anaphase entry half-lives were calculated by fitting cumulative frequency data from live cell imaging by nonlinear least squares regression in the nlintool of Matlab 7.0 (The Mathworks). Observed half-lives were considered to be the sum of the observed lag and the calculated  $t_{1/2}$ .

**Table 3.1**  
Antibodies used in this study

Antibody	Source	Organism	Antigen	IF dilution	WB dilution	IP dilution
anti-CMT2-N	this study	Rabbit	hCMT2 <sup>1-138</sup>	1-2µg/mL	2µg/mL	1:500
anti-CMT2-FL	this study	Rabbit	hCMT2	1:500	1:500	
anti-Bub1	S. Taylor	Sheep		0.3-1µg/mL	0.5-1µg/mL	
anti-BubR1	S. Taylor	Sheep		1:1000	1:1000	
anti-Mad2	Covance	Rabbit		1:250		
anti-Mad2	A. Burds	Rabbit			1:500	
anti-Mad1	P. Meraldi	Rabbit		1:1500	1:1000	
anti-actin	Sigma, A2066	Rabbit			1:1000	
anti-β-tubulin	Sigma, Tub 2.1	Mouse		1:1000	1:1000	
anti-cyclin A	Santa Cruz, H-432	Rabbit		1:500		
anti-cyclin B1	Santa Cruz, GNS1	Mouse		1:500		
anti-Cdc20	Santa Cruz, E-7	Mouse		1:1000	1:500	
CREST	Antibodies, Inc	Human		1:200		

### Supplemental Material

Supplemental Figure 3.1 depicts cumulative frequency data for anaphase entry times of cells overexpressing GFP, GFP-Mad2, and GFP-CMT2. Supplemental Figure 3.2 summarizes checkpoint protein localization in control and CMT2 RNAi and presents evidence that CENPE localization does not require CMT2. Supplemental Figure 3.3 demonstrates that CMT2 colocalizes with Bub1 and that the siRNA duplex CMT2-3 abrogates CMT2 kinetochore localization.

### **3.6 Acknowledgements**

We thank S. Taylor (Univ. of Manchester) and R. Tsien (UC San Diego) for the kind gift of reagents and members of the Sorger Lab for critical reading of this manuscript. This work was funded by NIH grant CA84179 to P.K.S. Patrick Meraldi contributed a portion of the data in Figures 3.2, 3.3, and 3.7.

### 3.7 References

- Cahill, D. P., Lengauer, C., Yu, J., Riggins, G. J., Willson, J. K., Markowitz, S. D., Kinzler, K. W., and Vogelstein, B. (1998). Mutations of mitotic checkpoint genes in human cancers. *Nature* *392*, 300-303.
- Chan, G. K., and Yen, T. J. (2003). The mitotic checkpoint: a signaling pathway that allows a single unattached kinetochore to inhibit mitotic exit. *Prog Cell Cycle Res* *5*, 431-439.
- Chen, R. H. (2002). BubR1 is essential for kinetochore localization of other spindle checkpoint proteins and its phosphorylation requires Mad1. *J Cell Biol* *158*, 487-496.
- Cleveland, D. W., Mao, Y., and Sullivan, K. F. (2003). Centromeres and kinetochores: from epigenetics to mitotic checkpoint signaling. *Cell* *112*, 407-421.
- Dawson, I. A., Roth, S., and Artavanis-Tsakonas, S. (1995). The *Drosophila* cell cycle gene *fizzy* is required for normal degradation of cyclins A and B during mitosis and has homology to the *CDC20* gene of *Saccharomyces cerevisiae*. *J Cell Biol* *129*, 725-737.
- De Antoni, A., Pearson, C. G., Cimini, D., Canman, J. C., Sala, V., Nezi, L., Mapelli, M., Sironi, L., Faretta, M., Salmon, E. D., and Musacchio, A. (2005). The Mad1/Mad2 complex as a template for Mad2 activation in the spindle assembly checkpoint. *Curr Biol* *15*, 214-225.
- Dobles, M., Liberal, V., Scott, M. L., Benezra, R., and Sorger, P. K. (2000). Chromosome missegregation and apoptosis in mice lacking the mitotic checkpoint protein Mad2. *Cell* *101*, 635-645.
- Elbashir, S. M., Harborth, J., Lendeckel, W., Yalcin, A., Weber, K., and Tuschl, T. (2001). Duplexes of 21-nucleotide RNAs mediate RNA interference in cultured mammalian cells. *Nature* *411*, 494-498.
- Fang, G. (2002). Checkpoint protein BubR1 acts synergistically with Mad2 to inhibit anaphase-promoting complex. *Mol Biol Cell* *13*, 755-766.
- Geley, S., Kramer, E., Gieffers, C., Gannon, J., Peters, J. M., and Hunt, T. (2001). Anaphase-promoting complex/cyclosome-dependent proteolysis of human cyclin A starts at the beginning of mitosis and is not subject to the spindle assembly checkpoint. *J Cell Biol* *153*, 137-148.
- Gillett, E. S., Espelin, C. W., and Sorger, P. K. (2004). Spindle checkpoint proteins and chromosome-microtubule attachment in budding yeast. *J Cell Biol* *164*, 535-546.
- Gupta, A., Inaba, S., Wong, O. K., Fang, G., and Liu, J. (2003). Breast cancer-specific gene 1 interacts with the mitotic checkpoint kinase BubR1. *Oncogene* *22*, 7593-7599.

- Habu, T., Kim, S. H., Weinstein, J., and Matsumoto, T. (2002). Identification of a MAD2-binding protein, CMT2, and its role in mitosis. *Embo J* 21, 6419-6428.
- Hagan, R. S., and Sorger, P. K. (2005). Cell biology: the more MAD, the merrier. *Nature* 434, 575-577.
- Hanks, S., Coleman, K., Reid, S., Plaja, A., Firth, H., Fitzpatrick, D., Kidd, A., Mehes, K., Nash, R., Robin, N., *et al.* (2004). Constitutional aneuploidy and cancer predisposition caused by biallelic mutations in BUB1B. *Nat Genet* 36, 1159-1161.
- Hartwell, L. H., and Weinert, T. A. (1989). Checkpoints: controls that ensure the order of cell cycle events. *Science* 246, 629-634.
- Hoffman, D. B., Pearson, C. G., Yen, T. J., Howell, B. J., and Salmon, E. D. (2001). Microtubule-dependent changes in assembly of microtubule motor proteins and mitotic spindle checkpoint proteins at PtK1 kinetochores. *Mol Biol Cell* 12, 1995-2009.
- Howell, B. J., Hoffman, D. B., Fang, G., Murray, A. W., and Salmon, E. D. (2000). Visualization of Mad2 dynamics at kinetochores, along spindle fibers, and at spindle poles in living cells. *J Cell Biol* 150, 1233-1250.
- Howell, B. J., McEwen, B. F., Canman, J. C., Hoffman, D. B., Farrar, E. M., Rieder, C. L., and Salmon, E. D. (2001). Cytoplasmic dynein/dynactin drives kinetochore protein transport to the spindle poles and has a role in mitotic spindle checkpoint inactivation. *J Cell Biol* 155, 1159-1172.
- Howell, B. J., Moree, B., Farrar, E. M., Stewart, S., Fang, G., and Salmon, E. D. (2004). Spindle checkpoint protein dynamics at kinetochores in living cells. *Curr Biol* 14, 953-964.
- Hoyt, M. A. (2001). A new view of the spindle checkpoint. *J Cell Biol* 154, 909-911.
- Hoyt, M. A., Totis, L., and Roberts, B. T. (1991). *S. cerevisiae* genes required for cell cycle arrest in response to loss of microtubule function. *Cell* 66, 507-517.
- Hunter, A. W., and Wordeman, L. (2000). How motor proteins influence microtubule polymerization dynamics. *J Cell Sci* 113 Pt 24, 4379-4389.
- Kalitsis, P., Earle, E., Fowler, K. J., and Choo, K. H. (2000). Bub3 gene disruption in mice reveals essential mitotic spindle checkpoint function during early embryogenesis. *Genes Dev* 14, 2277-2282.
- Kallio, M., Weinstein, J., Daum, J. R., Burke, D. J., and Gorbsky, G. J. (1998). Mammalian p55CDC mediates association of the spindle checkpoint protein Mad2 with the cyclosome/anaphase-promoting complex, and is involved in regulating anaphase onset and late mitotic events. *J Cell Biol* 141, 1393-1406.

- Kapoor, T. M., Mayer, T. U., Coughlin, M. L., and Mitchison, T. J. (2000). Probing spindle assembly mechanisms with monastrol, a small molecule inhibitor of the mitotic kinesin, Eg5. *J Cell Biol* 150, 975-988.
- Kops, G. J., Foltz, D. R., and Cleveland, D. W. (2004). Lethality to human cancer cells through massive chromosome loss by inhibition of the mitotic checkpoint. *Proc Natl Acad Sci U S A* 101, 8699-8704.
- Kotani, S., Tanaka, H., Yasuda, H., and Todokoro, K. (1999). Regulation of APC activity by phosphorylation and regulatory factors. *J Cell Biol* 146, 791-800.
- Kraft, C., Herzog, F., Gieffers, C., Mechtler, K., Hagting, A., Pines, J., and Peters, J. M. (2003). Mitotic regulation of the human anaphase-promoting complex by phosphorylation. *Embo J* 22, 6598-6609.
- Lew, D. J., and Burke, D. J. (2003). The spindle assembly and spindle position checkpoints. *Annu Rev Genet* 37, 251-282.
- Li, R., and Murray, A. W. (1991). Feedback control of mitosis in budding yeast. *Cell* 66, 519-531.
- Martinez-Exposito, M. J., Kaplan, K. B., Copeland, J., and Sorger, P. K. (1999). Retention of the BUB3 checkpoint protein on lagging chromosomes. *Proc Natl Acad Sci U S A* 96, 8493-8498.
- Martin-Lluesma, S., Stucke, V. M., and Nigg, E. A. (2002). Role of Hec1 in spindle checkpoint signaling and kinetochore recruitment of Mad1/Mad2. *Science* 297, 2267-2270.
- Meraldi, P., Draviam, V. M., and Sorger, P. K. (2004). Timing and checkpoints in the regulation of mitotic progression. *Dev Cell* 7, 45-60.
- Michel, L. S., Liberal, V., Chatterjee, A., Kirchwegger, R., Pasche, B., Gerald, W., Dobles, M., Sorger, P. K., Murty, V. V., and Benezra, R. (2001). MAD2 haplo-insufficiency causes premature anaphase and chromosome instability in mammalian cells. *Nature* 409, 355-359.
- Millband, D. N., and Hardwick, K. G. (2002). Fission yeast Mad3p is required for Mad2p to inhibit the anaphase-promoting complex and localizes to kinetochores in a Bub1p-, Bub3p-, and Mph1p-dependent manner. *Mol Cell Biol* 22, 2728-2742.
- Minshull, J., Straight, A., Rudner, A. D., Dernburg, A. F., Belmont, A., and Murray, A. W. (1996). Protein phosphatase 2A regulates MPF activity and sister chromatid cohesion in budding yeast. *Curr Biol* 6, 1609-1620.
- Musacchio, A., and Hardwick, K. G. (2002). The spindle checkpoint: structural insights into dynamic signalling. *Nat Rev Mol Cell Biol* 3, 731-741.

Poddar, A., Stukenberg, P. T., and Burke, D. J. (2005). Two complexes of spindle checkpoint proteins containing Cdc20 and Mad2 assemble during mitosis independently of the kinetochore in *Saccharomyces cerevisiae*. *Eukaryot Cell* *4*, 867-878.

Rieder, C. L., Schultz, A., Cole, R., and Sluder, G. (1994). Anaphase onset in vertebrate somatic cells is controlled by a checkpoint that monitors sister kinetochore attachment to the spindle. *J Cell Biol* *127*, 1301-1310.

Rudner, A. D., and Murray, A. W. (2000). Phosphorylation by Cdc28 activates the Cdc20-dependent activity of the anaphase-promoting complex. *J Cell Biol* *149*, 1377-1390.

Shah, J. V., Botvinick, E., Bonday, Z., Furnari, F., Berns, M., and Cleveland, D. W. (2004). Dynamics of centromere and kinetochore proteins; implications for checkpoint signaling and silencing. *Curr Biol* *14*, 942-952.

Shelby, R. D., Hahn, K. M., and Sullivan, K. F. (1996). Dynamic elastic behavior of alpha-satellite DNA domains visualized in situ in living human cells. *J Cell Biol* *135*, 545-557.

Sigrist, S., Jacobs, H., Stratmann, R., and Lehner, C. F. (1995). Exit from mitosis is regulated by *Drosophila* fizzy and the sequential destruction of cyclins A, B and B3. *Embo J* *14*, 4827-4838.

Starr, D. A., Williams, B. C., Hays, T. S., and Goldberg, M. L. (1998). ZW10 helps recruit dynactin and dynein to the kinetochore. *J Cell Biol* *142*, 763-774.

Sudakin, V., Chan, G. K., and Yen, T. J. (2001). Checkpoint inhibition of the APC/C in HeLa cells is mediated by a complex of BUBR1, BUB3, CDC20, and MAD2. *J Cell Biol* *154*, 925-936.

Tang, Z., Bharadwaj, R., Li, B., and Yu, H. (2001). Mad2-Independent inhibition of APCCdc20 by the mitotic checkpoint protein BubR1. *Dev Cell* *1*, 227-237.

Tang, Z., Shu, H., Oncel, D., Chen, S., and Yu, H. (2004). Phosphorylation of Cdc20 by Bub1 provides a catalytic mechanism for APC/C inhibition by the spindle checkpoint. *Mol Cell* *16*, 387-397.

Taylor, S. S., Ha, E., and McKeon, F. (1998). The human homologue of Bub3 is required for kinetochore localization of Bub1 and a Mad3/Bub1-related protein kinase. *J Cell Biol* *142*, 1-11.

Vigneron, S., Prieto, S., Bernis, C., Labbe, J. C., Castro, A., and Lorca, T. (2004). Kinetochore localization of spindle checkpoint proteins: who controls whom? *Mol Biol Cell* *15*, 4584-4596.

Wang, Z., Cummins, J. M., Shen, D., Cahill, D. P., Jallepalli, P. V., Wang, T. L., Parsons, D. W., Traverso, G., Awad, M., Silliman, N., *et al.* (2004). Three classes of genes mutated in colorectal cancers with chromosomal instability. *Cancer Res* 64, 2998-3001.

Waters, J. C., Chen, R. H., Murray, A. W., and Salmon, E. D. (1998). Localization of Mad2 to kinetochores depends on microtubule attachment, not tension. *J Cell Biol* 141, 1181-1191.

Weaver, B. A., Bonday, Z. Q., Putkey, F. R., Kops, G. J., Silk, A. D., and Cleveland, D. W. (2003). Centromere-associated protein-E is essential for the mammalian mitotic checkpoint to prevent aneuploidy due to single chromosome loss. *J Cell Biol* 162, 551-563.

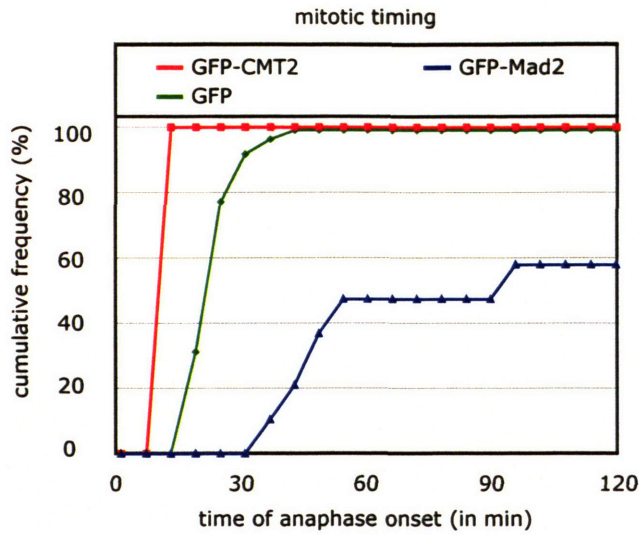
Wojcik, E., Basto, R., Serr, M., Scaerou, F., Karess, R., and Hays, T. (2001). Kinetochores dynein: its dynamics and role in the transport of the Rough deal checkpoint protein. *Nat Cell Biol* 3, 1001-1007.

Xia, G., Luo, X., Habu, T., Rizo, J., Matsumoto, T., and Yu, H. (2004). Conformation-specific binding of p31(comet) antagonizes the function of Mad2 in the spindle checkpoint. *Embo J* 23, 3133-3143.

Yudkovsky, Y., Shteinberg, M., Listovsky, T., Brandeis, M., and Hershko, A. (2000). Phosphorylation of Cdc20/fizzy negatively regulates the mammalian cyclosome/APC in the mitotic checkpoint. *Biochem Biophys Res Commun* 271, 299-304.



## Supplemental Figure 3.1

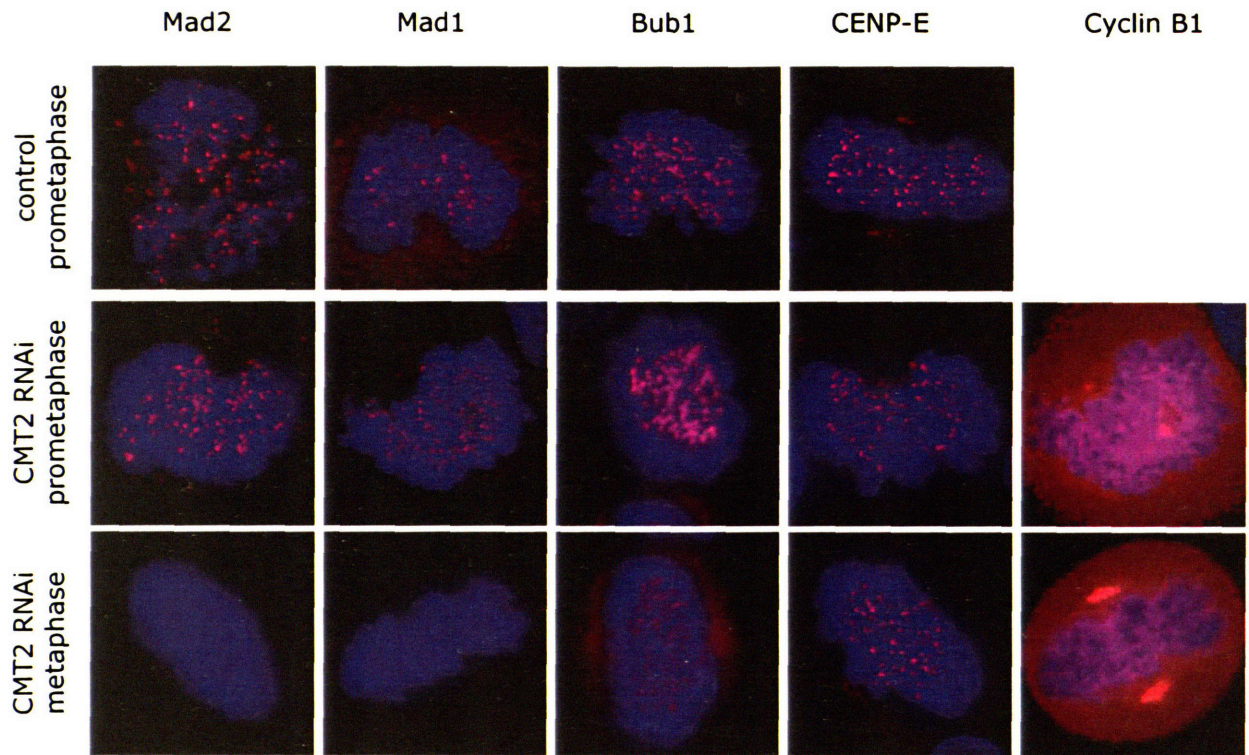


### Supplemental Figure 3.1: Anaphase entry kinetics of CMT2 and Mad2

#### overexpressing cells

HeLa Histone 2B-mRFP cells were transfected with GFP, GFP-CMT2, or GFP-Mad2 and the time from NBD to anaphase A was measured by fluorescence videomicroscopy as in Figure 3.7.

## Supplemental Figure 3.2



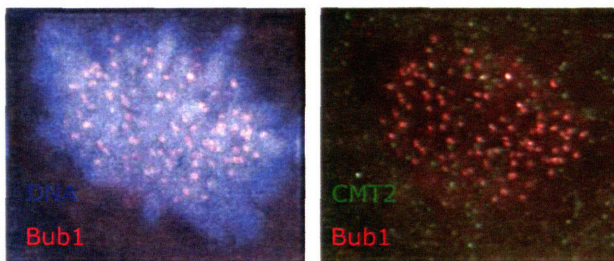
	Mad2	Mad1	Bub1	BubR1	Bub3	Mps1	CENP-E	CENP-F
control prometaphase	++	++	++	++	++	++	++	++
control metaphase	-	-	+	+	+	+	++	++
CMT-2 RNAi prometaphase	++	++	++	++	++	++	++	++
CMT-2 metaphase	-	-	+	+	+	+	++	++

### Supplemental Figure 3.2: Localization of checkpoint proteins in CMT2 RNAi

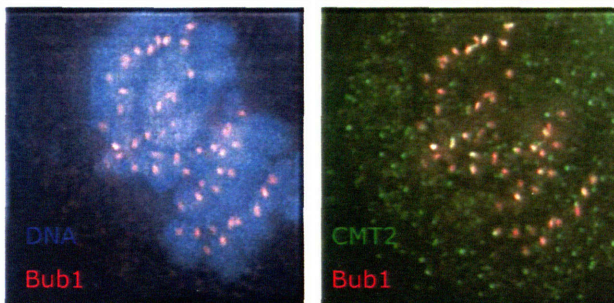
HeLa cells transfected with control or CMT2 siRNA were fixed and stained with antibodies for checkpoint proteins as shown. Cell cycle phase was determined by DNA and spindle morphology. Presence or absence of checkpoint proteins in Figure 3.3 and Supplemental Figure 3.2 is summarized in the table. Images for CENP-F are not shown.

### Supplemental Figure 3.3

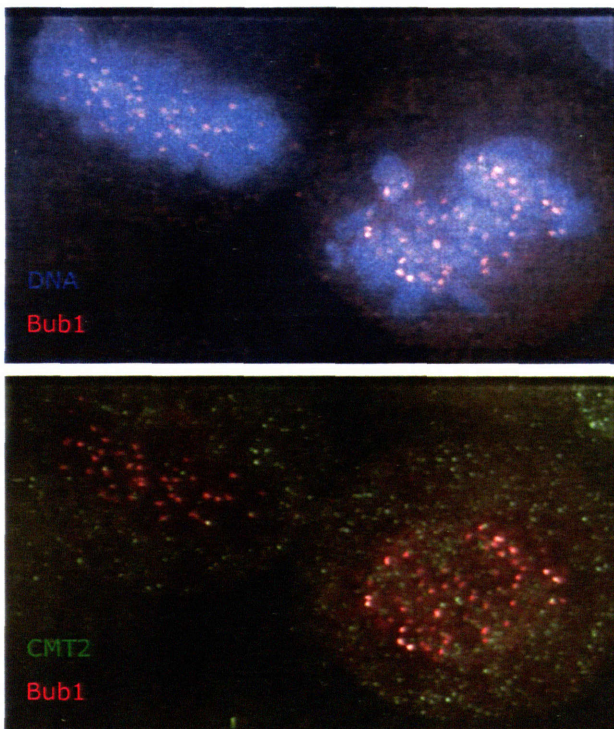
Prometaphase  
Lamin A RNAi



Prometaphase  
CMT2-1 RNAi



CMT2-3 RNAi



#### Supplemental Figure 3.3: Specificity of CMT2 kinetochore localization

To demonstrate that loss of CMT2 from kinetochores after CMT2 RNAi is not a specific effect of the CMT2-1 siRNA, cells were transfected with control or CMT2-3 siRNA, fixed, and stained for CMT2, Bub1, and DNA as in Figure 3. 4. CMT2 colocalizes with Bub1 in prometaphase.

## **Chapter 4**

### **Conclusions and Future Directions**

Analysis of spindle checkpoint combines many of the most interesting elements of studying mitosis: elegant cell biology, challenging biochemistry, and the possibility of linking basic processes with disease development. When I started my graduate work, the connections between checkpoint proteins and their functions were just beginning to be made. Few of the relevant proteins had been expressed or characterized and the lethality of checkpoint gene deletion made it difficult, if not impossible, to probe a protein's function by removing it from the cell. The basic question of how the checkpoint is inactivated in higher eukaryotes remained largely unaddressed. Since then, many interactions between checkpoint proteins have been discovered by indirect methods, though few of them have been reconstituted *in vitro* or analyzed structurally. New genes have been added to the spindle checkpoint, and the advent of RNAi has made it possible for us to test the function of these genes in mammalian cells without gene targeting by homologous recombination. At the same time, better imaging tools and software have allowed us to probe protein function in single cells by watching the detailed movements of mitotic chromosomes, giving us a far better understanding of mitosis than population-based assays had yielded previously.

The work that I have presented in the preceding chapters answers basic questions regarding the biochemistry and cell biology of the checkpoint protein Mad2 and its regulator, CMT2. My findings serve to confirm certain notions of checkpoint signaling, but also to call into question the idea of the spindle checkpoint as a passive surveillance system. In this chapter I discuss these findings in the context of the field and propose new models for checkpoint activation and inactivation. I also discuss the relevance of

this work to genomic instability and tumorigenesis and propose future experiments for understanding the spindle checkpoint.

#### **4.1 Mad2 conformation and checkpoint signaling**

The spindle checkpoint must sense either the structural state of kinetochore-microtubule occupancy or a mechanical property of this interaction such as the tension produced by microtubule pulling forces. Because of the short time span of mitosis and the high cost of missegregation, the checkpoint must also be able to arrest the cell cycle rapidly. As a result of these two facts, it was reasoned that conformational changes, rather than post-translational modification, might provide a checkpoint signal that is both rapid and coupled to changes in a kinetochore's mechanical properties. An early NMR study of Mad2 implicated the C-terminal tail in ligand binding but was unable to resolve the tail structure (Luo et al., 2000). Upon the discovery that Mad2 binds to Mad1 and Cdc20, a critical question became how Mad2 binds upstream and downstream checkpoint proteins. I mapped in detail the interactions of Mad2 with Mad1 and, identified a minimal 9aa binding region, and explored the constraints on binding at each amino acid position. My findings represent a refinement of earlier mapping efforts and allowed us to construct an optimal Mad2-binding motif that is present not only in checkpoint proteins but in experimentally validated non-checkpoint Mad2 interactors such as TACE, ER $\beta$ , and IR. In addition, I tested at the residue level predictions made by the Mad1-Mad2 co-crystal structure and extended them to Mad2-Cdc20 binding. These structural studies posed two important questions: first, does Mad2 bind to its targets weakly, as suggested by its dynamic localization and rapid activation, or tightly? Second, do Mad1 and Cdc20

cooperate for Mad2 binding, as suggested by yeast genetics, or do they compete for a common binding site? I next measured Mad1-Mad2 and Cdc20-Mad2 interactions by multiple biophysical assays and found them to be of higher affinity than previously reported. I also demonstrated that these ligands compete for the same binding site on Mad2 and their binding behavior is similarly affected by mutations in Mad2. In agreement with later NMR studies, I found at low resolution that Mad1 and Cdc20 peptides induce similar conformations in Mad2.

Mad2 clearly switches conformations in the process of inhibiting Cdc20. The finding that Mad1 and Cdc20 compete for Mad2 appears to contradict the requirement of Mad1 for Cdc20-Mad2 formation in yeast and frogs (Chung and Chen, 2002; Hwang et al., 1998). This paradox may be partially resolved by the *in vitro* finding that O-Mad2 can dimerize with Mad1-bound C-Mad2, potentially positioning O-Mad2 for association with Cdc20 at kinetochores (De Antoni et al., 2005; Hagan and Sorger, 2005). As discussed in Chapter 2, this model does not make clear how switching between open and closed states is regulated or how the interaction of Mad2 and Cdc20 is made sensitive to the status of the kinetochore. It will be critical to test dimerization-defective mutants in both yeast and tissue culture cells, as well as to determine the structure of the O-Mad2-C-Mad2-Mad1 complex.

Mad1 binds Mad2 with high affinity, and Mad1 is saturated with Mad2 throughout the cell cycle. How is the Mad2-Mad1 complex assembled in interphase? Interconversion between the open and closed Mad2 conformers in isolation is extremely slow (Luo et al., 2004), suggesting that Mad2 tail opening may require other factors such as chaperones or a specific tail-regulating protein. Cdc20 is a conformationally unstable

protein that requires a specific chaperone, CCT, for stable expression and function (Camasses et al., 2003). Mad1 is similarly difficult to express and purify and thus may be a target for assisted folding and conformational regulation as well. It is notable that the majority of studies, including those presented here, resort to the use of short Mad1 and Cdc20 fragments. The Mad1 fragment in the Mad1-Mad2 crystal structure homodimerizes, and this dimerization imposes asymmetry on the two bound, closed Mad2 molecules in the unit cell, but it is not known whether this is a crystal artifact, as other domains of Mad1 that are predicted to be near Mad2 could not be crystallized (Sironi et al., 2002). A critical question for understanding Mad2 interactions *in vivo* is whether other domains of Mad1 or Cdc20 contribute to or affect Mad2 without being part of the minimal binding motif.

While the conformational aspect of checkpoint signaling requires further structural study, there is currently no way to assay Mad2 conformation *in vivo*. A major advance in the field came with the first observation of dynamic Mad2 localization in cells (Howell et al., 2000), and real-time measurements of Mad2 conformation would prove equally illuminating. Fusion of fluorescent proteins at both termini has allowed intramolecular FRET sensing of conformational changes in living cells and presents an attractive method (Miyawaki and Tsien, 2000; Zhang et al., 2001). However, it remains an open question whether fusion of a bulky fluorescent protein to the Mad2 C terminus impairs tail closure. Real-time *in vivo* measurements of Mad2 conformation and the dynamic interactions between spindle checkpoint proteins will be necessary to extend the biochemical observations made here and by other groups.



## 4.2 Checkpoint inactivation

Does checkpoint inactivation occur by an active process, by extinguishing generation of checkpoint signal, or by sidestepping the requirement for Cdc20 activation? Each of these theoretical models existed when I began this work, but there was no experimental evidence for active silencing of the checkpoint or the idea that such inactivation would be necessary in an unperturbed mitosis free of microtubule poisons. The study of CMT2 presented here suggests not only that active inhibition is necessary for checkpoint silencing but also that every mammalian mitosis depends on a proper balance between simultaneous positive and negative regulation of the checkpoint. Supporting this idea are recent findings that overexpression of checkpoint proteins such as Mad2 in mammals and Bub1p or Mad3p in yeast can induce the very chromosome instability against which these proteins are supposed to protect (Hernando et al., 2004; Warren et al., 2002).

At a mechanistic level, previous models of checkpoint inactivation focused on either sidestepping the spindle checkpoint by direct APC/C activation or removing Mad1-Mad2 complexes from the kinetochore by trafficking them onto the spindle or displacing them with microtubules. Because closed Mad2 was presumed to be the activated state of Mad2 in all cases, Mad2 inhibition might occur either by active tail opening or by binding of a competitive ligand such as TACE that would sequester Mad2 and liberate Cdc20. By focusing on simple inhibition of the closed Mad2 conformer, these mechanisms fail to account for the dynamic localization of Mad2, the finding that both kinetochore and cytosolic Mad2 function in the checkpoint (Chung and Chen, 2002), and the heterodimerization of open and closed Mad2.

Our work proposes that CMT2 is a versatile and potent Mad2 inhibitor that halts generation of active Mad2 at kinetochores by inhibiting Mad2 dimerization on C-Mad2-Mad1 complexes *and* inhibits cytosolic, Mad1-free Mad2. This model rests initially on our findings that CMT2 localizes to kinetochores and the cytosol and forms ternary complexes with both Mad1-Mad2 and Cdc20-Mad2 *in vitro* and *in vivo*. However, how can we maintain that CMT2 is functional and not merely resident at both locations? Our assertion that CMT2 inhibits Mad2 in the cytosol stems from the finding that CMT2 RNAi is sufficient to arrest cells in contexts where Mad2 does not localize to kinetochores, i.e. Mad1 or Nuf2R RNAi. This result complements the discovery of a Mad1- and kinetochore-independent role for Mad2 in inhibiting Cdc20 early in metaphase (Meraldi et al., 2004). It is not clear if this early Mad2 function involves dimerization either at non-kinetochore sites such, as the nuclear pore, or on Cdc20-Mad2 complexes in the cytosol. De Antoni et al suggest that Mad2 dimerization may be nucleated by Cdc20-Mad2 complexes, but this phenomenon has not been demonstrated *in vivo* or *in vitro* (De Antoni et al., 2005). If C-Mad2 inhibits Cdc20 in the cytosol without recruiting additional O-Mad2, how can CMT2 be proposed to inhibit this activity? Central to this idea is a single experiment by Xia et al showing that a ternary CMT2-Mad2-Cdc20 complex can activate APC/C<sup>Cdc20</sup> without disrupting Cdc20-Mad2 binding (Xia et al., 2004). These *in vitro* APC/C activation assays have been simultaneously illuminating and confusing for the field, given that they were the basis of the now-disproven idea that higher order oligomers of Mad2 – which are now known to be aggregates – represent the active state (Fang et al., 1998). While APC/C activation assays have improved with time, our reliance on them highlights the need for *in vivo* and

single-cell APC/C activity assays. Also, while a low resolution APC/C structure exists, it has not revealed the basis of APC/C activation by Cdc20 and Cdh1 and thus we cannot envision a biochemical mechanism for how CMT2 reactivates inhibited Cdc20 (Gieffers et al., 2001). Extensive work has shown that APC/C itself is the target of multiple modifications, and its sensitivity to inhibition varies throughout the cell cycle (Kraft et al., 2003; Sudakin et al., 2001). One possibility is that CMT2 recruits accessory proteins that modify either Cdc20, Mad2, or core APC/C units, thus relieving inhibition without displacing Mad2.

A basic feature of proteins required for checkpoint activation is their localization to kinetochores and, in many cases, their dynamic shuttling between kinetochores and the cytosol. In contrast with previous studies, we show for the first time that CMT2 resides at kinetochores. We find that CMT2 is unique among examined proteins in that its kinetochore localization requires Mad2. In chapter 3 we discuss the surprising result that CMT2 is recruited to kinetochores in nocodazole-treated cells, which have an active spindle checkpoint, and propose that pro- and anti-checkpoint signals are simultaneously assembled at kinetochores to allow for rapid and tightly coupled checkpoint signaling. At present, it is difficult to dissect apart kinetochore and cytosolic functions for many proteins in mammalian cells. We examine cells depleted of CMT2 and other checkpoints and infer the amount of Mad2 activity – and hence CMT2 activity – based on population kinetics of anaphase entry. Confirming a function for CMT2 and other proteins at the kinetochore will require more direct means of manipulating checkpoint protein localization. It is currently possible to induce protein localization to a specific site such as mitochondria or the cell membrane by attachment of minimal localization tags such as

a CAAX motif (Bear et al., 2000), but no such kinetochore-localizing motifs are currently known in either yeast or mammals. Forcing CMT2 onto kinetochores by fusion with such a motif and then assaying for cell cycle progression in both unperturbed and nocodazole-treated cells could provide a convincing test of whether kinetochore localization contributes to Mad2 inhibition. Indeed, such an experiment would also illuminate requirements for checkpoint *activation*. It remains an open question whether the kinetochore localization of proteins such as BubR1, Bub1, and Bub3 suffices for their activation. Induced localization of wildtype and mutant checkpoint proteins would constitute a useful tool for determining the requirements for checkpoint signaling.

Our data provide the first framework for understanding how Mad2 can be inhibited at multiple sites by a single protein. It will be critical to determine if CMT2, like Mad2, BubR1, and Cdc20, cycles through the kinetochore or if kinetochore and cytosolic CMT2 are kept separate. Preliminary biochemical data exist to show that CMT2 does, in fact, prevent the association of O-Mad2 with C-Mad2-Mad1 (M. Mapelli, personal communication). There is now a pressing need to demonstrate this behavior *in vivo* and to understand its structural basis. Are other components of the checkpoint such as BubR1 or Bub1 inhibited by proteins analogous to CMT2? BubR1 presents a special problem in that it may require inactivation of both the Mad3-like N terminus and, ostensibly, the kinase domain. Kinase inactivation may be modulated by CENP-E conformation or displacement (Mao et al., 2003). Overexpression of BCSG1 protein decreases BubR1 levels in tissue culture cells, but it remains to be shown whether BubR1 degradation occurs and whether the kinetics of BubR1 destruction are consistent with the onset of anaphase (Gupta et al., 2003). Because low levels of BubR1 remain at

kinetochores in metaphase and anaphase, BubR1 inactivation likely involves multiple steps.

### **4.3 Checkpoint activation and conformational inhibition of Cdc20**

There are at least seven documented mechanisms by which cells inhibit Cdc20 directly to delay the metaphase-anaphase transition. Mad2, BubR1, the MCC complex, and RASSF1A each inhibit Cdc20 by binding to it (Fang, 2002; Hwang et al., 1998; Song et al., 2004; Sudakin et al., 2001). Bub1, PKA, and Cdk1/cyclin B all phosphorylate Cdc20 and impair its ability to activate APC/C (Searle et al., 2004; Tang et al., 2004; Yudkovsky et al., 2000). Cdc20 thus integrates signals from at least two checkpoints (spindle assembly and DNA damage) and the core cell cycle machinery. Because Cdc20 has proven difficult to purify and characterize *in vitro*, little is known at the residue or atomic levels about the mechanisms by which it activates APC/C, specifies substrates for ubiquitination, or is inhibited by checkpoint protein binding. Structural and biophysical studies have not yet identified conformational changes in Cdc20, and NMR analysis has been limited to the N terminal domain (Luo et al., 2000).

While it is known that the spindle checkpoint inhibits Cdc20, multiple active checkpoint complexes have been identified and their relative contributions to checkpoint activation *in vivo* remain unknown. Direct Cdc20-inhibitory activity has been demonstrated *in vitro* for Mad2, BubR1, Bub1, and MCC and is suspected for Mps1, but depletion of single proteins inactivates the checkpoint, suggesting that each protein is necessary but no one protein or complex is sufficient for Cdc20 inhibition *in vivo*. In addition, it has long been suspected that successful checkpoint arrest by a single

unattached kinetochore must involve amplification of the signal generated at that kinetochore. Recent mathematical models suggest that on-kinetochore signal generation without amplification cannot explain the kinetics of cell cycle arrest and progression (Doncic et al., 2005). Despite fifteen years of spindle checkpoint research, two major questions still loom: what is the active “wait anaphase” signal and how does it inactivate Cdc20? Below, I propose a model of allosteric, conformational Cdc20 inhibition that synthesizes work in this laboratory and others as well as ways of validating this model.

#### **4.4 Cooperative inhibition of Cdc20**

Despite the difficulty of working with Cdc20, important details of its structure and biochemical behavior have emerged. (1) Cdc20 has two domains, a C-terminal WD domain that is responsible for substrate specificity and an N-terminal domain (Cdc20<sup>1-165</sup>). (2) Cdc20 is conformationally labile and requires a chaperone for proper expression and function (Camasses et al., 2003). (3) Mad2 binds Cdc20 in a portion of the N terminus that is adjacent to the WD domain boundary, which we will term the “neck” between domains. (4) BubR1/Mad3p binds Cdc20 but the binding region has not been identified. (5) Bub1 phosphorylates Cdc20 at up to six positions in the N terminal domain, and these phosphorylations are inhibitory for APC/C activation (Tang et al., 2004). (6) Cdc20 phosphorylation by several possible kinases is required for spindle checkpoint activity (Chung and Chen, 2003). (7) As observed in this and other labs, full length Cdc20 binds Mad2 *in vitro* with lower affinity than isolated Cdc20<sup>1-165</sup> (R. Hagan, data not shown, Tang et al., 2001; Zhang and Lees, 2001).

Cdc20 is an unstable and often insoluble protein. Observation (7) suggests that the C-terminal WD domain partially inhibits binding of the N-terminal domain to ligands such as Mad2. The WD domain may impair Mad2 binding either directly by steric occlusion of the Mad2-binding motif or indirectly by inducing a binding-incompetent conformation without actually masking the site. On the basis of these observations, I propose a model in which Cdc20 inhibition involves four steps, each of which is cooperative with the others: phosphorylation of the Cdc20 N terminus by Bub1 or other kinases; binding of Mad2 to the “neck” between Cdc20’s two domains; binding of BubR1/Mad3p to either the WD or N-terminal domain of Cdc20; and dissociation of the Cdc20 N terminal and WD domains (Figure 4.1). This model is reliant upon the unproven idea that the Cdc20 N-terminal and C-terminal domains undergo intramolecular association; each inhibitory event serves to prop open the closed Cdc20 structure, thus promoting each of the other inhibitory events.

How might this model explain spindle checkpoint activation at kinetochores? Mad2, Cdc20, and BubR1 cycle through kinetochores with nearly equal kinetics, but it is not known whether they cycle as monomers or a complex. The fast phases of Cdc20 and BubR1 flux are close to the rate of diffusion, suggesting that the rapidly fluxing pool of each either is not binding the other during its short transit time on the kinetochore or is already bound in the cytosol (Howell et al., 2004). As a result, some additional regulatory step or steps must promote association of Cdc20 and BubR1 as they pass through unattached kinetochores. As for Mad2, it is clear that simple co-localization of O-Mad2 and Cdc20 at kinetochores is not sufficient to render Cdc20-Mad2 binding

Figure 4.1

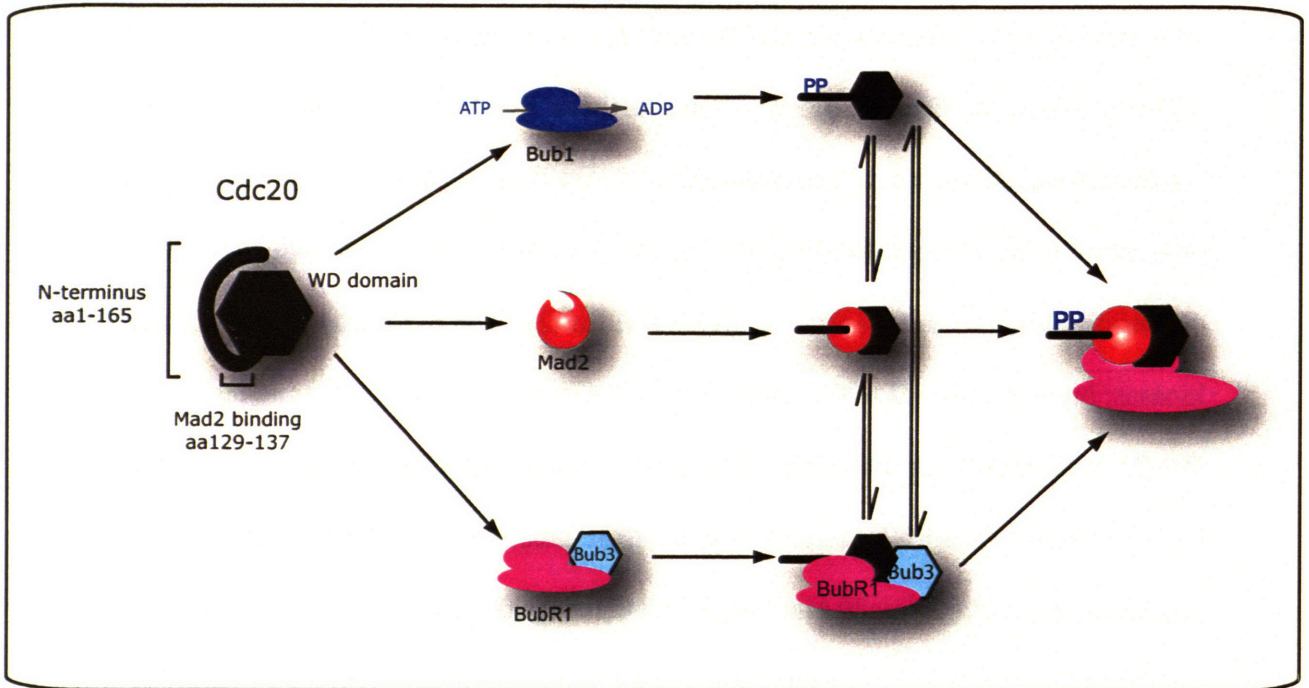


**Figure 4.1: A cooperative model for spindle checkpoint activation**

The N-terminal and WD domains of Cdc20 may undergo intramolecular association. Phosphorylation by Bub1 (top), binding of Mad2, or binding of BubR1/Mad3 disrupts the interdomain interaction. Dissociation of the domains by any one event promotes the other two events by making their target surfaces more accessible. Complete inhibition of Cdc20 is the sum of catalytic phosphorylation and stoichiometric binding.



sensitive to kinetochore-microtubule status, as these pools colocalize in the cytosol regardless of the state of the checkpoint. While it remains possible that each checkpoint protein occupies a distinct site on the kinetochore surface, there is evidence at least in fission yeast that the two scaffolding complexes, Mad1 and Bub1, exist in a single complex that is required for checkpoint activation (Brady and Hardwick, 2000). This suggests that the loci of Cdc20 phosphorylation by Bub1 and Cdc20 binding by Mad2 are closely apposed on the kinetochore and thus these events may be spatially coupled.

This conformational model of Cdc20 inhibition predicts first that the Cdc20 N- and C-terminal domains associate and, second, that phosphorylation of the N-terminus inhibits this association. Cdc20 phosphorylation sites are closely bunched and distributed across the N-terminal domain, but they do not conform to a discernible consensus (Chung and Chen, 2003; Tang et al., 2004). This suggests that these phosphorylations “paint” the N-terminus with negative charge rather than causing a local alteration of the surface that directs specific protein-protein interactions. The immediate predictions of this model regarding intramolecular Cdc20 interactions can be tested *in vitro* using recombinant Cdc20<sup>1-165</sup> and Cdc20<sup>WD</sup>. An equally important task is determining the binding site on Cdc20 for BubR1, though binding to either domain or a region near the Mad2-binding motif fits within the model. As mentioned previously, understanding the dynamics of Cdc20 conformation *in vivo* requires the development of better tools for probing protein conformation in living cells. Like Mad2, Cdc20 is a prime candidate for intramolecular FRET analysis (Miyawaki and Tsien, 2000). Of particular interest will be the role of the chaperonin CCT, which is required for Cdc20 function in budding yeast. CCT, also

known as TRiC or TCP1, is conserved in humans but its role in mammalian mitosis has not been examined. Cdc20 is positioned as the node for integrating multiple signals that drive and dampen cell cycle progression, and I propose that it does this by a conformational plasticity that mirrors that of its inhibitor Mad2.

#### **4.5 CMT2 regulation**

In chapters 2 and 3, I propose and test the idea that by opposing Mad2 activity, CMT2 acts to switch off the spindle checkpoint. CMT2 is positioned at kinetochores in prometaphase when the spindle checkpoint is active, as well as when cells are treated with nocodazole. What flips this CMT2 switch upon kinetochore-MT binding? We are only beginning to explore CMT2 regulation, but several possibilities are immediately evident. Cell synchrony experiments suggested that CMT2 expression is cell cycle-regulated, with levels rising as cells enter mitosis and then falling during telophase (Habu et al., 2002). However, CMT2 protein remains detectable throughout the cell cycle, and Northern blot analysis detected CMT2 mRNA in almost all tissues regardless of proliferative status (Figure 1.4). A general observation of cell cycle research is that inhibitors of cell cycle progression such as Cdk inhibitors (CDKIs) or checkpoint proteins are often expressed throughout the cell cycle, while promoters of progression such as cyclins, Cdc20, or Cdh1 are only expressed during a narrow window of time. Regulation of the spindle checkpoint by controlled expression of CMT2 would thus fit with our understanding of cell cycle progression, and it will be necessary to determine the transcriptional program of CMT2 expression. However, simply controlling the levels of

CMT2 in the cell does not seem sufficient to create a rapid and sensitive “go anaphase” signal.

The other common themes of mitotic regulation are post-translational modification and regulated protein-protein binding. CMT2 interactors other than Mad2 have not been identified. Modification of CMT2 is not necessary for Mad2 binding or reactivation of APC/C<sup>Cdc20</sup>, as shown by the activity of bacterially-expressed recombinant CMT2. I have begun searching for modifications of CMT2. As presented in Appendix 1, CMT2 undergoes a phosphatase-sensitive shift in electrophoretic mobility when HeLa cells are treated with nocodazole. I have since found that CMT2 is an extremely efficient substrate of Bub1 but not Mps1, and CMT2 phosphorylation by recombinant Bub1 exceeds that of the sole published substrate, Cdc20. With the help of Mustafa Ünlü, I have mapped the Bub1 phosphorylation site on human CMT2 by mass spectrometry to a highly conserved threonine, T211. CMT2 pT211 phosphopeptides have been detected in checkpoint-arrested cells (data not shown). On the basis of these preliminary results, I propose that Bub1 inactivates CMT2 under conditions of checkpoint activity by phosphorylating it. This is the first evidence that checkpoint activation in higher eukaryotes involves simultaneous inactivation of a negative signal. This idea fits well with our finding that CMT2 associates with kinetochores in prophase, positioning it near both its substrate (Mad2) and regulatory inputs (Bub1). This model also fits neatly with the long-held observation that kinetochore phosphorylation corresponds with cell cycle arrest while phosphatase activity is required for anaphase entry (Campbell and Gorbsky, 1995; Gorbsky and Ricketts, 1993; Nicklas et al., 1995).

How might phosphorylation inhibit CMT2 function? At least two obvious models must be tested. First, phosphorylation by Bub1 may inhibit CMT2-Mad2 binding. While this is possible, the strong Mad2-dependent localization of CMT2 to kinetochores in nocodazole arrest suggests that it is not the case. The CMT2-Mad2-Cdc20 ternary complex activates APC/C even though CMT2 alone does not (Xia et al., 2004), and a second model is that phosphorylation of CMT2 blocks this activation. In addition to searching for modification at sites other than T211, I have constructed mutants that mimic the unphosphorylated and phosphorylated states of CMT2 and plan to test them for Mad2 binding, kinetochore localization, and cell cycle progression effects. The regulation of CMT2 is an extremely exciting area that will illustrate the complexity of mitotic regulation in higher eukaryotes.

#### **4.6 Spindle checkpoint dysfunction and cancer**

Aneuploidy has been known as a common characteristic of solid tumors since the observations of Theodor Boveri (Boveri, 1914). Tumor aneuploidy may reflect a causal role for chromosome missegregation in genomic instability or it may result from dysregulation of the cell cycle after cellular transformation. A large body of work has been dedicated to determining a causal role for spindle checkpoint dysfunction in tumorigenesis but the link between aneuploidy and cancer is still mysterious. After initial reports of spindle checkpoint gene mutation in human cancers (Cahill et al., 1998), further studies have found that such mutations are in fact quite rare (Draviam et al., 2004; Musacchio and Hardwick, 2002). Familial biallelic mutations in BubR1 give rise to

mosaic variegated aneuploidy, a pleiotropic disease that is associated with strong cancer predisposition much like inherited mutations in DNA checkpoint proteins (D'Andrea and Grompe, 2003; Hanks et al., 2004). In all cases reported thus far, targeted deletion of checkpoint genes causes embryonic lethality, as the massive chromosome loss observed leads invariably to widescale mitotic catastrophe and apoptosis (Dobles et al., 2000; Kalitsis et al., 2000; Wang et al., 2004a; Weaver et al., 2003). Mice heterozygous for Mad2 deletion develop lung papillary adenocarcinoma late in life (Michel et al., 2001). This tumor is extremely rare in humans and it is not clear how decreased Mad2 expression specifically primes tumorigenesis in the lungs. Bub3 heterozygotes exhibit chromosome instability but do not develop tumors, though this may simply reflect the suspected redundancy of Bub3 with the protein Rael (Babu et al., 2003; Kalitsis et al., 2005). Very strikingly, mice carrying a hypomorphic BubR1 allele exhibit an accelerated ageing phenotype but do not develop cancer (Baker et al., 2004). When combined with cell biological data, these studies suggest that successful mitosis in mammals depends on accurate checkpoint signaling, and frank loss of a checkpoint protein is rarely, if ever, permissive for survival. How then might spindle checkpoint dysfunction contribute to cancer development?

One way in which the spindle checkpoint might fail is by altered expression of checkpoint genes. The transcriptional control of most checkpoint genes is not known, but genes such as p53, BRCA1, FoxM1 and E2F family members have been implicated in controlling both basal checkpoint gene expression and upregulation of some checkpoint genes following upstream stress or DNA damage (Hernando et al., 2004; Laoukili et al., 2005; Oikawa et al., 2005; Ren et al., 2002; Seike et al., 2002; Wang et al., 2004b). The

simplest hypothesis is that transcriptional dysregulation or epigenetic silencing would lower expression of a critical checkpoint gene below the threshold required for checkpoint function but perhaps above the threshold required for cell viability. Intriguingly, evidence has begun to accumulate that some human cancers overexpress spindle checkpoint proteins (Li and Zhang, 2004; Wu et al., 2004). This phenotype may be secondary to unrestrained proliferation. However, experiments in yeast and some mammalian systems suggest that the mitotic arrest caused by Mad2 or Mad3p overexpression is impermanent and leads ultimately to genomic instability. In this case, either under- or overexpression of checkpoint proteins may drive chromosome instability.

It is also possible that spindle checkpoint dysfunction occurs only transiently in the life of a cell undergoing transformation. This little-considered hypothesis is supported by the finding that overexpression of the CDKI p21 represses the expression of BubR1, Mad2, and CENP-F (Chang et al., 2000). Although several other critical checkpoint genes were not examined, the authors found that p21 overexpression decreases transcript levels for both checkpoint genes and genes controlling mitotic progression, such as Cdc2 and cyclin B1. The cell cycle arrest imposed by p21 is dependent on the tumor suppressor p16 for its maintenance (Stein et al., 1999). Mutations of p21 are extremely rare in human cancers, but p16 is frequently inactivated by mutation or deletion and such cells slip through p21-induced arrest. After release from p21 arrest, expression of mitosis-promoting genes such as cyclin B1 and Cdc2 recovers before checkpoint gene expression. These cells accumulate mitotic abnormalities and missegregate their chromosomes with high frequency and a high incidence of aneuploidy, suggesting that their spindle checkpoints are compromised. Confirmation of the idea that p21 arrest

transiently impairs the checkpoint while still allowing mitotic progression requires further experimentation and careful analysis.

A third way in which cells may lose their spindle checkpoint on the road to cancer is viral inhibition. At least two transforming viruses have been shown to interact with the spindle checkpoint. Human Mad1 was initially cloned as a binding partner of the viral oncoprotein Tax from human T cell leukemia virus type I (Jin et al., 1998). Expression of Tax leads to multinucleation and polyploidy, but the contribution of Mad1 to adult T cell leukemogenesis has not been examined. In addition, the large T antigen of simian virus 40 binds Bub1, and large T expression overrides the spindle checkpoint (Cotsiki et al., 2004). These findings are consistent with the well-established idea that tumor-promoting viruses such as SV40 and HPV are known to target multiple cell cycle control pathways simultaneously.

A fourth way in which the spindle checkpoint can fail without mutation of its components is by overexpression or overactivity of a negative regulator. I demonstrate in chapter 3 that even mild overexpression of CMT2 causes errors of chromosome segregation. Human CMT2 is expressed from a locus on chromosome 6p21.1 (Chapter 1, Figure 1.4). This locus is a frequent site of translocation and both high- and low-level amplification in many human tumors across a wide spectrum of tumor types (Bergsagel and Kuehl, 2001; Furge et al., 2005; Man et al., 2004; Rigaud et al., 2001). Previous investigation of the role of 6p21 in tumorigenesis has focused on neighbors that flank CMT2 on either side: cyclin D3, VEGF, and the slightly more distant MHC cluster. Because CMT2 was only recently identified as a spindle checkpoint regulator, its expression in 6p21-amplified or translocated tumors has not been examined. The

possibility of CMT2's involvement in tumorigenesis is particularly intriguing when a historical analogy is drawn between the spindle checkpoint and cyclin/Cdk signaling. Upon the discovery that cyclins and Cdks controlled entry into mitosis, there was widespread suspicion mutation in cyclin/Cdk genes might cause cancer. Intense search efforts found that mutation or amplification of these genes is quite rare, with a few notable exceptions such as cyclin D3. Subsequent research uncovered a second level of cyclin regulation by the CDKI proteins such as p16 and p21. A major breakthrough came with the realization that CDKI genes are frequently mutated in human cancers and these mutations are critical steps in the pathway towards genomic instability and malignancy (Kamb et al., 1994; Liggett and Sidransky, 1998; Lloyd et al., 1999). Discovery of a second level of spindle checkpoint regulation has just begun with the identification of BCSG1 and CMT2, negative regulators of BubR1 and Mad2, respectively. BCSG1 was first identified as a gene that is overexpressed in breast tumors (Gupta et al., 2003). These proteins and the mechanism by which they function in checkpoint regulation provide a promising route to understanding the causes of chromosome instability.

#### **4.7 Conclusions**

The work I present here synthesizes biochemical and cell biological analysis to reveal a central role for negative regulation of the spindle checkpoint in mammalian mitosis. I argue that silencing of the checkpoint by proteins such as CMT2 is required for mitotic progression and examine the mechanism by which CMT2 opposes Mad2. My work raises questions concerning the molecular nature of the "wait anaphase" checkpoint signal and provides a way forward in determining how such signals are transmitted and



modulated. However, the work here also points to problems that currently afflict the field. Checkpoint components are often expressed in low abundance, and proteins such as Bub1, BubR1, Cdc20, and even CMT2 have proven extremely difficult to characterize biochemically. Checkpoint genes in higher eukaryotes do not yield easily to genetic analysis, and there is a paucity of structural information in the field. Progress in understanding the spindle checkpoint will require the identification of checkpoint kinase substrates, dynamic analysis of the many complexes involved in checkpoint signaling, a better understanding of the lesions detected by the checkpoint, and the development of tools to follow checkpoint activity in individual living cells.

## 4.8 References

- Babu, J. R., Jeganathan, K. B., Baker, D. J., Wu, X., Kang-Decker, N., and van Deursen, J. M. (2003). Rae1 is an essential mitotic checkpoint regulator that cooperates with Bub3 to prevent chromosome missegregation. *J Cell Biol* 160, 341-353.
- Baker, D. J., Jeganathan, K. B., Cameron, J. D., Thompson, M., Juneja, S., Kopecka, A., Kumar, R., Jenkins, R. B., de Groen, P. C., Roche, P., and van Deursen, J. M. (2004). BubR1 insufficiency causes early onset of aging-associated phenotypes and infertility in mice. *Nat Genet* 36, 744-749.
- Bear, J. E., Loureiro, J. J., Libova, I., Fassler, R., Wehland, J., and Gertler, F. B. (2000). Negative regulation of fibroblast motility by Ena/VASP proteins. *Cell* 101, 717-728.
- Bergsagel, P. L., and Kuehl, W. M. (2001). Chromosome translocations in multiple myeloma. *Oncogene* 20, 5611-5622.
- Boveri, T. (1914). *Zur Frage der Entstehung maligner Tumoren*, Vol. 1.
- Brady, D. M., and Hardwick, K. G. (2000). Complex formation between Mad1p, Bub1p and Bub3p is crucial for spindle checkpoint function. *Curr Biol* 10, 675-678.
- Cahill, D. P., Lengauer, C., Yu, J., Riggins, G. J., Willson, J. K., Markowitz, S. D., Kinzler, K. W., and Vogelstein, B. (1998). Mutations of mitotic checkpoint genes in human cancers. *Nature* 392, 300-303.
- Camasses, A., Bogdanova, A., Shevchenko, A., and Zachariae, W. (2003). The CCT chaperonin promotes activation of the anaphase-promoting complex through the generation of functional Cdc20. *Mol Cell* 12, 87-100.
- Campbell, M. S., and Gorbsky, G. J. (1995). Microinjection of mitotic cells with the 3F3/2 anti-phosphoepitope antibody delays the onset of anaphase. *J Cell Biol* 129, 1195-1204.
- Chang, B. D., Broude, E. V., Fang, J., Kalinichenko, T. V., Abdryashitov, R., Poole, J. C., and Roninson, I. B. (2000). p21Waf1/Cip1/Sdi1-induced growth arrest is associated with depletion of mitosis-control proteins and leads to abnormal mitosis and endoreduplication in recovering cells. *Oncogene* 19, 2165-2170.
- Chung, E., and Chen, R. H. (2002). Spindle checkpoint requires Mad1-bound and Mad1-free Mad2. *Mol Biol Cell* 13, 1501-1511.
- Chung, E., and Chen, R. H. (2003). Phosphorylation of Cdc20 is required for its inhibition by the spindle checkpoint. *Nat Cell Biol* 5, 748-753.
- Cotsiki, M., Lock, R. L., Cheng, Y., Williams, G. L., Zhao, J., Perera, D., Freire, R., Entwistle, A., Golemis, E. A., Roberts, T. M., *et al.* (2004). Simian virus 40 large T

antigen targets the spindle assembly checkpoint protein Bub1. *Proc Natl Acad Sci U S A* *101*, 947-952.

D'Andrea, A. D., and Grompe, M. (2003). The Fanconi anaemia/BRCA pathway. *Nat Rev Cancer* *3*, 23-34.

De Antoni, A., Pearson, C. G., Cimini, D., Canman, J. C., Sala, V., Nezi, L., Mapelli, M., Sironi, L., Faretta, M., Salmon, E. D., and Musacchio, A. (2005). The Mad1/Mad2 complex as a template for Mad2 activation in the spindle assembly checkpoint. *Curr Biol* *15*, 214-225.

Dobles, M., Liberal, V., Scott, M. L., Benezra, R., and Sorger, P. K. (2000). Chromosome missegregation and apoptosis in mice lacking the mitotic checkpoint protein Mad2. *Cell* *101*, 635-645.

Doncic, A., Ben-Jacob, E., and Barkai, N. (2005). Evaluating putative mechanisms of the mitotic spindle checkpoint. *Proc Natl Acad Sci U S A* *102*, 6332-6337.

Draviam, V. M., Xie, S., and Sorger, P. K. (2004). Chromosome segregation and genomic stability. *Curr Opin Genet Dev* *14*, 120-125.

Fang, G. (2002). Checkpoint protein BubR1 acts synergistically with Mad2 to inhibit anaphase-promoting complex. *Mol Biol Cell* *13*, 755-766.

Fang, G., Yu, H., and Kirschner, M. W. (1998). The checkpoint protein MAD2 and the mitotic regulator CDC20 form a ternary complex with the anaphase-promoting complex to control anaphase initiation. *Genes Dev* *12*, 1871-1883.

Furge, K. A., Dykema, K. J., Ho, C., and Chen, X. (2005). Comparison of array-based comparative genomic hybridization with gene expression-based regional expression biases to identify genetic abnormalities in hepatocellular carcinoma. *BMC Genomics* *6*, 67.

Gieffers, C., Dube, P., Harris, J. R., Stark, H., and Peters, J. M. (2001). Three-dimensional structure of the anaphase-promoting complex. *Mol Cell* *7*, 907-913.

Gorbsky, G. J., and Ricketts, W. A. (1993). Differential expression of a phosphoepitope at the kinetochores of moving chromosomes. *J Cell Biol* *122*, 1311-1321.

Gupta, A., Inaba, S., Wong, O. K., Fang, G., and Liu, J. (2003). Breast cancer-specific gene 1 interacts with the mitotic checkpoint kinase BubR1. *Oncogene* *22*, 7593-7599.

Habu, T., Kim, S. H., Weinstein, J., and Matsumoto, T. (2002). Identification of a MAD2-binding protein, CMT2, and its role in mitosis. *Embo J* *21*, 6419-6428.

Hagan, R. S., and Sorger, P. K. (2005). Cell biology: the more MAD, the merrier. *Nature* *434*, 575-577.

- Hanks, S., Coleman, K., Reid, S., Plaja, A., Firth, H., Fitzpatrick, D., Kidd, A., Mehes, K., Nash, R., Robin, N., *et al.* (2004). Constitutional aneuploidy and cancer predisposition caused by biallelic mutations in BUB1B. *Nat Genet* 36, 1159-1161.
- Hernando, E., Nahle, Z., Juan, G., Diaz-Rodriguez, E., Alaminos, M., Hemann, M., Michel, L., Mittal, V., Gerald, W., Benezra, R., *et al.* (2004). Rb inactivation promotes genomic instability by uncoupling cell cycle progression from mitotic control. *Nature* 430, 797-802.
- Howell, B. J., Hoffman, D. B., Fang, G., Murray, A. W., and Salmon, E. D. (2000). Visualization of Mad2 dynamics at kinetochores, along spindle fibers, and at spindle poles in living cells. *J Cell Biol* 150, 1233-1250.
- Howell, B. J., Moree, B., Farrar, E. M., Stewart, S., Fang, G., and Salmon, E. D. (2004). Spindle checkpoint protein dynamics at kinetochores in living cells. *Curr Biol* 14, 953-964.
- Hwang, L. H., Lau, L. F., Smith, D. L., Mistrot, C. A., Hardwick, K. G., Hwang, E. S., Amon, A., and Murray, A. W. (1998). Budding yeast Cdc20: a target of the spindle checkpoint. *Science* 279, 1041-1044.
- Jin, D. Y., Spencer, F., and Jeang, K. T. (1998). Human T cell leukemia virus type 1 oncoprotein Tax targets the human mitotic checkpoint protein MAD1. *Cell* 93, 81-91.
- Kalitsis, P., Earle, E., Fowler, K. J., and Choo, K. H. (2000). Bub3 gene disruption in mice reveals essential mitotic spindle checkpoint function during early embryogenesis. *Genes Dev* 14, 2277-2282.
- Kalitsis, P., Fowler, K. J., Griffiths, B., Earle, E., Chow, C. W., Jansen, K., and Choo, K. H. (2005). Increased chromosome instability but not cancer predisposition in haploinsufficient Bub3 mice. *Genes Chromosomes Cancer*.
- Kamb, A., Gruis, N. A., Weaver-Feldhaus, J., Liu, Q., Harshman, K., Tavitgian, S. V., Stockert, E., Day, R. S., 3rd, Johnson, B. E., and Skolnick, M. H. (1994). A cell cycle regulator potentially involved in genesis of many tumor types. *Science* 264, 436-440.
- Kraft, C., Herzog, F., Gieffers, C., Mechtler, K., Hagting, A., Pines, J., and Peters, J. M. (2003). Mitotic regulation of the human anaphase-promoting complex by phosphorylation. *Embo J* 22, 6598-6609.
- Laoukili, J., Kooistra, M. R., Bras, A., Kauw, J., Kerkhoven, R. M., Morrison, A., Clevers, H., and Medema, R. H. (2005). FoxM1 is required for execution of the mitotic programme and chromosome stability. *Nat Cell Biol* 7, 126-136.
- Li, G. Q., and Zhang, H. F. (2004). Mad2 and p27 expression profiles in colorectal cancer and its clinical significance. *World J Gastroenterol* 10, 3218-3220.

Liggett, W. H., Jr., and Sidransky, D. (1998). Role of the p16 tumor suppressor gene in cancer. *J Clin Oncol* 16, 1197-1206.

Lloyd, R. V., Erickson, L. A., Jin, L., Kulig, E., Qian, X., Cheville, J. C., and Scheithauer, B. W. (1999). p27kip1: a multifunctional cyclin-dependent kinase inhibitor with prognostic significance in human cancers. *Am J Pathol* 154, 313-323.

Luo, X., Fang, G., Coldiron, M., Lin, Y., Yu, H., Kirschner, M. W., and Wagner, G. (2000). Structure of the Mad2 spindle assembly checkpoint protein and its interaction with Cdc20. *Nat Struct Biol* 7, 224-229.

Luo, X., Tang, Z., Xia, G., Wassmann, K., Matsumoto, T., Rizo, J., and Yu, H. (2004). The Mad2 spindle checkpoint protein has two distinct natively folded states. *Nat Struct Mol Biol* 11, 338-345.

Man, T. K., Lu, X. Y., Jaeweon, K., Perlaky, L., Harris, C. P., Shah, S., Ladanyi, M., Gorlick, R., Lau, C. C., and Rao, P. H. (2004). Genome-wide array comparative genomic hybridization analysis reveals distinct amplifications in osteosarcoma. *BMC Cancer* 4, 45.

Mao, Y., Abrieu, A., and Cleveland, D. W. (2003). Activating and silencing the mitotic checkpoint through CENP-E-dependent activation/inactivation of BubR1. *Cell* 114, 87-98.

Meraldi, P., Draviam, V. M., and Sorger, P. K. (2004). Timing and checkpoints in the regulation of mitotic progression. *Dev Cell* 7, 45-60.

Michel, L. S., Liberal, V., Chatterjee, A., Kirchwegger, R., Pasche, B., Gerald, W., Dobles, M., Sorger, P. K., Murty, V. V., and Benezra, R. (2001). MAD2 haplo-insufficiency causes premature anaphase and chromosome instability in mammalian cells. *Nature* 409, 355-359.

Miyawaki, A., and Tsien, R. Y. (2000). Monitoring protein conformations and interactions by fluorescence resonance energy transfer between mutants of green fluorescent protein. *Methods Enzymol* 327, 472-500.

Musacchio, A., and Hardwick, K. G. (2002). The spindle checkpoint: structural insights into dynamic signalling. *Nat Rev Mol Cell Biol* 3, 731-741.

Nicklas, R. B., Ward, S. C., and Gorbsky, G. J. (1995). Kinetochores are sensitive to tension and may link mitotic forces to a cell cycle checkpoint. *J Cell Biol* 130, 929-939.

Oikawa, T., Okuda, M., Ma, Z., Goorha, R., Tsujimoto, H., Inokuma, H., and Fukasawa, K. (2005). Transcriptional control of BubR1 by p53 and suppression of centrosome amplification by BubR1. *Mol Cell Biol* 25, 4046-4061.

Ren, B., Cam, H., Takahashi, Y., Volkert, T., Terragni, J., Young, R. A., and Dynlacht, B. D. (2002). E2F integrates cell cycle progression with DNA repair, replication, and G(2)/M checkpoints. *Genes Dev* 16, 245-256.

Rigaud, G., Moore, P. S., Taruscio, D., Scardoni, M., Montresor, M., Menestrina, F., and Scarpa, A. (2001). Alteration of chromosome arm 6p is characteristic of primary mediastinal B-cell lymphoma, as identified by genome-wide allelotyping. *Genes Chromosomes Cancer* 31, 191-195.

Searle, J. S., Schollaert, K. L., Wilkins, B. J., and Sanchez, Y. (2004). The DNA damage checkpoint and PKA pathways converge on APC substrates and Cdc20 to regulate mitotic progression. *Nat Cell Biol* 6, 138-145.

Seike, M., Gemma, A., Hosoya, Y., Hosomi, Y., Okano, T., Kurimoto, F., Uematsu, K., Takenaka, K., Yoshimura, A., Shibuya, M., *et al.* (2002). The promoter region of the human BUBR1 gene and its expression analysis in lung cancer. *Lung Cancer* 38, 229-234.

Sironi, L., Mapelli, M., Knapp, S., De Antoni, A., Jeang, K. T., and Musacchio, A. (2002). Crystal structure of the tetrameric Mad1-Mad2 core complex: implications of a 'safety belt' binding mechanism for the spindle checkpoint. *Embo J* 21, 2496-2506.

Song, M. S., Song, S. J., Ayad, N. G., Chang, J. S., Lee, J. H., Hong, H. K., Lee, H., Choi, N., Kim, J., Kim, H., *et al.* (2004). The tumour suppressor RASSF1A regulates mitosis by inhibiting the APC-Cdc20 complex. *Nat Cell Biol* 6, 129-137.

Stein, G. H., Drullinger, L. F., Soulard, A., and Dulic, V. (1999). Differential roles for cyclin-dependent kinase inhibitors p21 and p16 in the mechanisms of senescence and differentiation in human fibroblasts. *Mol Cell Biol* 19, 2109-2117.

Sudakin, V., Chan, G. K., and Yen, T. J. (2001). Checkpoint inhibition of the APC/C in HeLa cells is mediated by a complex of BUBR1, BUB3, CDC20, and MAD2. *J Cell Biol* 154, 925-936.

Tang, Z., Bharadwaj, R., Li, B., and Yu, H. (2001). Mad2-Independent inhibition of APCCdc20 by the mitotic checkpoint protein BubR1. *Dev Cell* 1, 227-237.

Tang, Z., Shu, H., Oncel, D., Chen, S., and Yu, H. (2004). Phosphorylation of Cdc20 by Bub1 provides a catalytic mechanism for APC/C inhibition by the spindle checkpoint. *Mol Cell* 16, 387-397.

Wang, Q., Liu, T., Fang, Y., Xie, S., Huang, X., Mahmood, R., Ramaswamy, G., Sakamoto, K. M., Darzynkiewicz, Z., Xu, M., and Dai, W. (2004a). BUBR1 deficiency results in abnormal megakaryopoiesis. *Blood* 103, 1278-1285.

Wang, R. H., Yu, H., and Deng, C. X. (2004b). A requirement for breast-cancer-associated gene 1 (BRCA1) in the spindle checkpoint. *Proc Natl Acad Sci U S A* 101, 17108-17113.

Warren, C. D., Brady, D. M., Johnston, R. C., Hanna, J. S., Hardwick, K. G., and Spencer, F. A. (2002). Distinct chromosome segregation roles for spindle checkpoint proteins. *Mol Biol Cell* *13*, 3029-3041.

Weaver, B. A., Bonday, Z. Q., Putkey, F. R., Kops, G. J., Silk, A. D., and Cleveland, D. W. (2003). Centromere-associated protein-E is essential for the mammalian mitotic checkpoint to prevent aneuploidy due to single chromosome loss. *J Cell Biol* *162*, 551-563.

Wu, C. W., Chi, C. W., and Huang, T. S. (2004). Elevated level of spindle checkpoint protein MAD2 correlates with cellular mitotic arrest, but not with aneuploidy and clinicopathological characteristics in gastric cancer. *World J Gastroenterol* *10*, 3240-3244.

Xia, G., Luo, X., Habu, T., Rizo, J., Matsumoto, T., and Yu, H. (2004). Conformation-specific binding of p31(comet) antagonizes the function of Mad2 in the spindle checkpoint. *Embo J* *23*, 3133-3143.

Yudkovsky, Y., Shteinberg, M., Listovsky, T., Brandeis, M., and Hershko, A. (2000). Phosphorylation of Cdc20/fizzy negatively regulates the mammalian cyclosome/APC in the mitotic checkpoint. *Biochem Biophys Res Commun* *271*, 299-304.

Zhang, J., Ma, Y., Taylor, S. S., and Tsien, R. Y. (2001). Genetically encoded reporters of protein kinase A activity reveal impact of substrate tethering. *Proc Natl Acad Sci U S A* *98*, 14997-15002.

Zhang, Y., and Lees, E. (2001). Identification of an overlapping binding domain on Cdc20 for Mad2 and anaphase-promoting complex: model for spindle checkpoint regulation. *Mol Cell Biol* *21*, 5190-5199.

## **Appendix**



## **Hagan and Sorger, 2005**

The following review is reprinted, pending permission, from R.S. Hagan and P.K. Sorger, 2005. The more MAD, the merrier. *Nature* **434**: 575-7

### **Cell biology: The more MAD, the merrier**

ROBERT S. HAGAN AND PETER K. SORGER

Cells must pass the correct number of chromosomes to their progeny through the complex ballet of cell division. An unusual conformation-sensitive switch seems to maintain accurate chromosome segregation.

The maintenance of normal chromosome number during cell division requires the precise separation of duplicated sister chromosomes into two equal sets. Andrea Mussachio and colleagues<sup>1</sup>, writing in *Current Biology*, shed light on how a protein called Mad2 ensures the fidelity of this process. The authors propose that two different structural forms of Mad2 collaborate to change one of the partners from an inactive to an active state. Such 'self-templated' changes in protein conformation are a characteristic of prions, but represent a new mechanism for cell signalling.

To achieve the correct separation, each chromosome is attached through the multi-protein 'kinetochore' complex to an intracellular scaffold called the spindle. In the 'anaphase' stage of cell division, this structure pulls the sister chromosomes apart to form

two groups at opposite ends of the cell, each with one sister from each chromosome pair. The two groups will be surrounded by membranes to become the nuclei of the daughter cells. The onset of anaphase is blocked until all chromosomes are bound correctly to the spindle. Defects in the proteins that make up this blockade (or 'spindle checkpoint') lead to abnormal chromosome numbers in the daughter cells, with potentially disastrous consequences — many tumour cells, for example, have abnormal chromosome complements. The spindle checkpoint activates a cascade of signals that converge on Cdc20, a protein that regulates the anaphase-promoting complex (APC)<sup>2</sup>. If even a single kinetochore remains unattached to the spindle, a diffusible signal is generated that is sufficient to restrain Cdc20 and block cell division at the start of anaphase for many hours<sup>3</sup>. But the nature of the signal and the mechanism by which it is propagated remain elusive.

Two highly conserved Cdc20-binding proteins, Mad2 and BubR1, are essential to inhibit APC (and therefore anaphase). These attach to kinetochores early in cell division, and dissociate as the kinetochore attaches to the spindle, but they persist on the kinetochores of misoriented or unattached chromosomes (reviewed in ref.2). Cdc20, Mad2 and BubR1 cycle rapidly on and off kinetochores, suggesting that they might be part of the diffusible checkpoint signal<sup>3,4</sup>.

Previous studies have focused on the ability of Mad2 to bind to Cdc20 and the checkpoint protein Mad1. The Mad1–Mad2 interaction localizes Mad2 to kinetochores and seems to occur early in the checkpoint pathway, whereas the binding of Mad2 to Cdc20 blocks APC activation and happens later in the checkpoint cascade (for review see

ref. 2). Upon associating with Mad1 or Cdc20, the carboxy-terminal tail of Mad2 rearranges from a disordered 'open' conformation (OMad2) to a closed conformation (CMad2), thereby encircling Mad1 or Cdc20 peptides like a safety belt<sup>5,6</sup>. Mad1 and Cdc20 compete for the same binding site on Mad2 but, paradoxically, Mad1 is required for the formation of Cdc20–Mad2 complexes *in vivo*. The high stability of Mad1–Mad2 complexes and the slow spontaneous interconversion of OMad2 and CMad2 seem at odds with the rapid kinetics of checkpoint signalling.

De Antoni *et al.*<sup>1</sup> use Mad2 mutants locked into open and closed conformations to show that two Mad2 molecules participate in this complicated dance. Mad2 variants lacking ten amino acids at the carboxy terminus cannot close the safety belt, are stuck in the open state and do not bind to Mad1 or Cdc20. However, the authors show that 'always-open' Mad2 can bind stably to Mad1–CMad2 complexes. Strikingly, OMad2 and CMad2 can partner each other, but two molecules of the same conformation cannot associate. In cells, the always-open OMad2 localizes to kinetochores when normal Mad2 is present, but it cannot engage the checkpoint, presumably because it cannot bind directly to Cdc20. Importantly, Mad2 mutants that cannot form partnerships with other Mad2 molecules do not bind to Mad1–CMad2, localize to kinetochores or support checkpoint function.

From these data, the authors propose a model in which 'core' complexes of Mad1–CMad2 increase the concentration and stability of OMad2 at kinetochores (Fig. 1). When the checkpoint is activated, the OMad2 in Mad1–CMad2–OMad2 complexes can be transferred to Cdc20, closing up to form Cdc20–CMad2. Such complexes prevent APC

## Appendix Figure 1

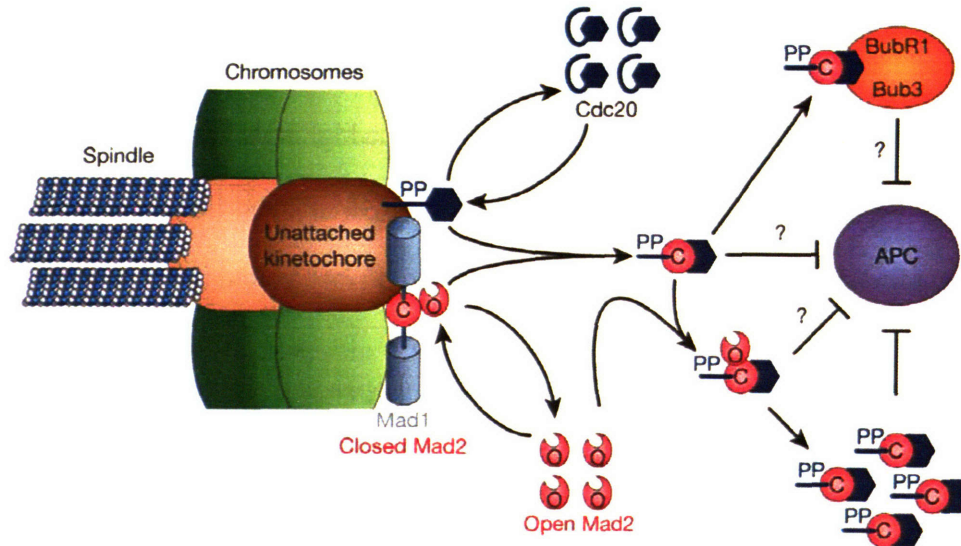


**Figure 1**

Mad2 encloses Mad1 to form a stable complex. Open-conformation Mad2 (OMad2) molecules bind to and are released from the Mad1-Mad2 complex in a cyclic fashion. At kinetochores (brown) that lack microtubule attachment, the OMad2 molecule encloses and binds activated Cdc20 (black), a step that may be promoted by the phosphorylation (PP) of Cdc20. The resulting closed Mad2 (CMad2)-Cdc20 complex inhibits anaphase-promoting complex (APC) and may bind BubR1 and Bub3. This complex may also act as a template for the formation of more CMad2-Cdc20 complexes from the cytosolic pool of OMad2, amplifying the checkpoint signal. Multiple protein complexes may be responsible for APC inhibition; their exact composition remains unknown.

activation and thus arrest cell division. This is a striking shift from previous models in which just a single CMad2 molecule bound to Mad1 before unfolding its safety belt and transferring to Cdc20. This new model fits neatly with data showing that two distinct pools of Mad2 associate with kinetochores: one that remains stably bound throughout cell division, and one that continuously binds and dissociates with a half-life of about 20 seconds<sup>3,7</sup>. As predicted by the model, Cdc20 also cycles on and off kinetochores with similar kinetics, whereas Mad1 does not.

Despite the elegance of De Antoni and colleagues' model, many questions remain unanswered. It is not clear how kinetochore–spindle attachment regulates Mad2-mediated checkpoint signalling. Also unknown is the molecular nature of the diffusible signal; De Antoni *et al.* suggest that Cdc20–CMad2 may constitute this signal and may act as an amplifier by binding to and activating other OMad2 molecules. Finally, the notion that Mad2 can inhibit Cdc20 only after being activated by Mad1 does not explain how cytosolic Mad2 regulates Cdc20 early in the cell cycle in a Mad1-independent manner<sup>8</sup>.

One promising approach to tackling these issues is to focus on Cdc20. Cdc20 is found in cells in association with Mad2, and two other proteins, BubR1 and Bub3 (ref. 9), and is phosphorylated at multiple sites. Intriguingly, Mad2 binds tightly *in vitro* to Cdc20 in the absence of any other proteins (most notably Mad1). *In vivo*, however, Mad2 requires kinetochores that are not attached to the spindle to bind to Cdc20, implying that access to the Mad2-binding site on Cdc20 is regulated. One possible regulator is BubR1, which is required for both the kinetochore-dependent and kinetochore-independent functions of Mad2. An attractive possibility is that all of these inputs regulate a transition in Cdc20

between conformations that are susceptible to Mad2-dependent inhibition and those that are resistant. Although much remains to be learned about Cdc20 and the spindle checkpoint in general, the work of De Antoni *et al.* highlights the central role of Mad2 in guiding a cell through cell division with all of its chromosomes in order.

1. De Antoni, A. *et al. Curr. Biol.* **15**, 214–225 (2005).
2. Rieder, C. L., Cole, R. W., Khodjakov, A. & Sluder, G. *J. Cell Biol.* **130**, 941–948 (1995).
3. Howell, B. J., Hoffman, D. B., Fang, G., Murray, A. W. & Salmon, E. D. *J. Cell Biol.* **150**, 1233–1250 (2000).
4. Musacchio, A. & Hardwick, K. G. *Nature Rev. Mol. Cell Biol.* **3**, 731–741 (2002).
5. Luo, X., Tang, Z., Rizo, J. & Yu, H. *Mol. Cell* **9**, 59–71 (2002).
6. Sironi, L. *et al. EMBO J.* **21**, 2496–2506 (2002).
7. Shah, J. V. *et al. Curr. Biol.* **14**, 942–952 (2004).
8. Meraldi, P., Draviam, V. M. & Sorger, P. K. *Dev. Cell* **7**, 46–60 (2004).
9. Sudakin, V., Chan., G. K. & Yen, T. J. *J. Cell Biol.* **154**, 925–936 (2001).